RELATING STRUCTURAL PROPERTIES TO SALTINESS PERCEPTION OF MODEL LIPOPROTEIC GELS

BY

WAN-YUAN KUO

DISSERTATION

Submitted in partial fulfillment of the requirements
for the degree of Doctor of Philosophy in Food Science and Human Nutrition
with a concentration in Food Science
in the Graduate College of the
University of Illinois at Urbana-Champaign, 2016

Urbana, Illinois

Doctoral Committee:

Professor Soo-Yeun Lee, Chair
Assistant Professor Youngsoo Lee, Director of Research
Professor Shelly Schmidt
Associate Professor Pawan Takhar

ABSTRACT

Sodium reduction in processed foods is an urgent mission to tackle sodium overconsumption. Eighty-nine percent of US adults consume more than the recommended amount of sodium, leading to the high prevalence of hypertension. Lipoproteic foods including cheese and processed meats are potential targets for sodium reduction, as they form the major source of sodium in modern diets. Structural engineering to enhance sodium release and saltiness perception is promising for sodium reduction in lipoproteic foods, which release as low as only 5% of sodium during mastication.

The goal of this research is to relate structural properties, including porosity and particle size of fat, to the saltiness perception of a mode lipoproteic gel system. The outcome of this research can imply strategies for structural engineering to enhance the saltiness perception of lipoproteic foods.

Solid lipoproteic colloid (SLC), a solid matrix made of lipid and protein in the oil-in-water emulsion structure, was used as the model food in this study. The SLCs were made with varying contents of protein, fat, and NaCl. Two levels of homogenization pressure were applied to the emulsion before the heat-induced gelation to form the SLCs. The images of the SLC microstructure was captured using environmental scanning electron microscopy (ESEM), and the porosity was quantified using an image analysis of the ESEM observations. The gyration radius of fat ($R_{g,f}$) in the SLCs was quantified using ultra-small-angle X-ray scattering with a synchrotron-source. Serum release, which is the amount of liquid compressed out from the SLCs, and textural properties were measured using a texture analyzer. A conductivity meter was used to measure the *in vitro* sodium release during the compression of the SLCs in water by a texture analyzer. Sensory evaluations were carried out on the SLCs with 1.5% NaCl. A quantitative descriptive analysis (QDA) method was used to characterize the saltines and textural properties of the SLCs. A time-intensity (TI) method was used to evaluate the temporal saltiness perception properties of the SLCs.

The saltiness of the SLCs correlated positively with the porosity, but did not correlate with the $R_{g,f}$. The increased saltiness with increasing porosity was due to the greater serum release which enabled rapid sodium release. The lack of the effect of $R_{g,f}$ on the SLC saltiness was due to the counteracting impacts of the $R_{g,f}$ on the sodium release. Lowering the $R_{g,f}$ led to more extensive breakdown but less serum release of the SLCs. The increased sodium

release with increased sample breakdown was counteracted by the decreased sodium release due to decreased serum release.

This study revealed the structural influences focused with porosity and particle size of fat on the saltiness perception of lipoproteic model foods. The results implied the potential to enhance the saltiness of lipoproteic products with optimized porosity and particle size of fat. Future studies can aim at modulating the structure toward higher saltiness while maintaining the sensory acceptance of the lipoproteic products. Also, future evaluation of the in-mouth sodium release can provide more fundamental information in the saltiness perception of SLC foods.

ACKNOWLEDGEMENTS

I would like to express my most sincere appreciation to my advisor, Dr. Youngsoo Lee, who has supported me throughout my doctoral research. He has challenged and guided me during the development of my research through assistant in lab work and many academic discussions. His understanding and positive attitude toward his students is the model I wish to follow for my future career.

I would also like to express my gratefulness to Dr. Soo-Yeun Lee, who graciously gave her time to discuss my project and guide me on the sensory studies. Her challenging questions help me reflect and solidify the core concept of my study. Also, I'm grateful to have the precious opportunity to work with Dr. Jan Ilavsky. His kind offer and exceptional knowledge in material science has helped advance my research by using frontier technologies.

Furthermore I would like to thank my committee members, Dr. Shelly Schmidt and Dr. Pawan Takhar. The valuable advice they have provided throughout the discussions have helped me identify the strengths and weaknesses of my study. It has been a pleasure to learn from their expertise and also share in their passion for research.

I would like to say thank you to my labmates – the Youngsoo Lee lab and the Soo Lee lab. At times the grueling experiment schedule threatened to overtake me. However, there is a group of people that are always there when I need them, and I never feel alone. I would not have been able to complete the experiments without their support.

Lastly, I would want to thank my family and friends Their relentless love has sustained me through the tough days over the past years. My boyfriend, Joshua Gottemoller, whose understanding and love has empowered me to embrace the life difficulties in the last and most stressful year of my thesis research. I am truly blessed.

Table of Contents

CHAPTER 1

Introduction

1.1 Significance

Ninety-nine percent of the world adult population consumed more than the recommended intake of sodium (2,000 g sodium/day by WHO) (Powles and others 2013). Eighty-nine percent of US adults have sodium intake excessing the recommended limit of 2,300 mg per day (Cogswell and others 2012; Jackson and others 2016). Diet high in sodium is the second highest dietary risk factors to the global burden of disease (Lim and others 2012). The significant contribution of dietary sodium intake to high blood pressure has been extensively reviewed by the Dietary Guidelines Advisory Committee in 2005 and 2010 (DGAC 2005; DGAC 2010). Although the latest DGAC called for reexamination of the evidence for the past guidelines on sodium intake, it still addressed the overconsumption of sodium as the main health risk to Americans (DGAC 2015). From 1999-2010, the prevalence of hypertension and pre-hypertension of Americans have been reported to be alarmingly high (Guo and others 2012). About one third of American adults have hypertension, and about another one third are pre-hypertensive (Wang and Wang 2004; Cutler and others 2008). The cumulative lifetime risk for developing hypertension of middle aged Americans is 90% (Vasan and others 2002). The benefits of sodium reduction extend to hypertensive and non-hypertensive individuals. It is estimated that annual savings of up to 7 billion USD in health care can be achieved by reducing the average dietary sodium intake by 400 mg/day (DGAC 2005; DGAC 2010).

However, the efforts from past 40 years to reduce sodium consumption have not made significant reduction in Americans' sodium intake (Henney and others 2010a). From 1988 to 2012, the mean dietary sodium intake by the US males and females stayed stable at more than 4,000 and 3,000 mg per day, respectively (Henney and others 2010b; USDA 2014). This is significantly higher than the Upper Intake Level (UL) of sodium for young adults, 2,300 mg per day (IOM 2015). It is worth notice that debates continue on the overall health benefits led by population-wide sodium reduction targeting at 1,500 mg/day. In fact, the latest Institute of medicine (IOM) report called for more data to validate the health outcome of the general population by further lowering the sodium intake from 2,300 mg to 1,500 mg (Institute of

Medicine (IOM) 2013). Nevertheless, the report still emphasized the importance of reducing the excess intake of sodium from the current 3,400 mg/day to 2,300 mg/day.

Several strategies of sodium reduction have been proposed, but often limited by the extent of reduction or the range of applications. For example, the stealth reduction may eventually get adverse reaction when the gradual decrease of sodium accumulates to a noticeable level (Phelps and others 2006). Salt replacers such as potassium chloride often have off-tastes that restrict the substitution to a maximum of 50% (Eoin 2006). Likewise, the saltiness potentiation by ingredients such as ribonucleotides and amino acids may not be useful in mildly tasted products due to strong flavors of these compounds (Heidolph and others 2011). Saltiness compensation by tastes other than saltiness from yeast extracts, spices, herbs, aroma compounds are practical only when their attributes are congruent with salty taste (Djordjevic and others 2004). Smaller size or specific crystallography of salt crystal which dissolves faster may enhance the saltiness perception, but works mostly for surface-salted foods such as French fries and chips (Heidolph and others 2011).

Processed foods contribute more than 70% of sodium in modern American diet (Mattes and Donnelly 1991; Anderson and others 2010). Among the processed foods, solid lipoproteic colloid (SLC) foods such as cheese and sausage exist frequently in the top 10 sources of dietary sodium (National Cancer Institute Jan 24th 2013). Hence, the SLC foods in total contribute a significant portion of dietary sodium (DGAC 2010), and is a potential target for sodium reduction.

The SLC foods are the solid foods with oil-in-water emulsion structure made of lipid and protein. The effects of formulation and processing treatment on the saltiness perception of the SLC foods have been widely studied. Nonetheless, our extensive literature review showed that there are conflicting findings of the treatment effects on saltiness across studies. For example, nearly equal amount of studies reported the effects of increasing fat content on sodium release or saltiness perception to be positive (Shamil and others 1991–1992; Ruusunen and others 2001; Colmenero and others 2005; Phan and others 2008; Lauverjat and others 2009a; Ventanas and others 2010; Panouille and others 2011), negative (Eymery and Pangborn 1988; Wirth 1988; Paneras and others 1996; Hughes and others 1997; Romeih and others 2002; Phan and others 2008; Panouille and others 2011), or neutral (Stampanoni and Noble 1991; Kähkönen and Tuorila 1998; Ruusunen and others 2001; Lteif and others 2009; Saint-Eve and others 2009). These conflicting findings reflect the multiple mechanisms, through which food matrix could affect saltiness, while treatment effects on these

mechanisms differ by systems. Hence processing and formulation treatment variables, though used mostly by current studies, are not universal variables to adjust saltiness perception.

Previous research showed that 70 - 95% of sodium is not released from SLC foods before being swallowed (Phan and others 2008). Therefore, engineering the matrix structure to enhance sodium release and saltiness perception is promising for sodium reduction in the SLC foods. Several structural modification to enhance saltiness perception has recently been demonstrated in simple systems. By adjusting the formulation of gellan/WPI gel while maintaining the large deformation property, serum release and hence sodium release was increased (Stieger 2011). By incorporating air phase into agar gels, the apparent concentrate sodium in the liquid phase was increased (Goh and others 2010). The saltiness enhancement in the above two studies both led to 40% reduction on required sodium. By creating spatial contrast in sodium concentration within bread slices, the removal of taste adaptation to enhance saltiness led to 25% cut down on required sodium (Noort and others 2010).

Porosity (Stieger 2011; Stieger and van de Velde 2013) and particle size of fat (Kuo and others 2014) are two structural properties identified as potential target for structural engineering to enhance saltiness. Previous literature also demonstrated the feasibility of adjusting the above two structural properties via formulation and processing (Sala and others 2010; Stieger 2011; Sala and Stieger 2013; Stieger and van de Velde 2013). In order for the outcome to be compatible with the practical industrial processing, this study chose porosity and particle size of fat as the two structural factors for investigating their effect on saltiness perception. The findings from this study will provide insights for engineering SLC structures to enhance the saltiness perception, and will provide more knowledge to the fundamentals in saltiness perception of SLC food. In long term, this study will accelerate the sodium reduction research to tackle sodium overconsumption.

1.2 Overall Hypothesis and Goal

We *hypothesize* that the saltiness perception increases with increasing porosity and with decreasing particle size of fat in the SLC matrix. The *goal* of this study is to quantify the structural properties, including porosity and particle size of fat, and relate these structural properties to saltiness perception of the model food SLC.

Figure 1.1 illustrates the conceptual diagram of the impact of structural properties on saltiness perception in SLC foods. The structural properties including porosity and particle

size of fat are results of varying formulation and processing treatments. Different structural properties lead to the changes in various SLC secondary properties including texture and sodium release. Variations in these SLC secondary properties eventually cause the differences in saltiness perception. The treatment effects on structural properties depend on the formulation and processing of each food system, but the impact of the structural properties on saltiness perception of SLCs may be universal across different SLC products.

1.3 Specific Objectives

The *specific objectives* of this research:

1) **Relating porosity to sodium release of the SLCs**

The hypothesis of this objective is that increase in porosity leads to increasing serum release which results in faster sodium release. The porosity was quantified by an image analysis of the SLC microstructure. The SLC microstructure was imaged by the environmental scanning electron microscopy (ESEM). The SLCs with varying porosity were then compared for their serum release and sodium release to validate the hypothesis.

2) **Relating particle size of fat to sodium release of the SLCs**

The hypothesis of this objective is that decrease in particle size of fat leads to increased extent of gel breakdown, which enhances sodium release. Ultra-small-angle X-ray scattering was used as a novel technique to quantify the particle size of fat in the SLCs. The particle size of fat of the SLCs was then correlated to the texture and the sodium release properties to validate the hypothesis.

3) **Correlating structural properties to sodium release of the SLCs**

The hypothesis of this objective is that both increasing porosity and decreasing particle size of fat lead to increased sodium release of an SLC. The SLCs varied in porosity and particle size of fat were created by varying levels of protein, fat and NaCl, and by varying homogenization pressures. The structural properties, including the porosity and particle size of fat, were correlated with the sodium release to validate the hypothesis.

4) **Correlating structural properties to saltiness perception of the SLCs**

The hypotheses of this objective are 1) saltiness perception of the SLCs increases with increasing porosity due to the increased serum release, and 2) saltiness perception of the

SLCs increases with decreasing particle size of fat due to the increased extent of gel breakdown. The saltiness perception and textural properties of the SLCs were evaluated using the quantitative descriptive analysis (QDA). The temporal saltiness perception properties of the SLCs were evaluated using the time-intensity (TI) method. The sensory properties (QDA saltiness and texture, and the TI properties) were correlated with the instrumental properties (structure, texture, and sodium release) to validate the above hypotheses.

1.4 References

Anderson CAM, Appel LJ, Okuda N, Brown IJ, Chan Q, Zhao L, Ueshima H, Kesteloot H, Miura K, Curb JD, Yoshita K, Elliott P, Yamamoto ME, Stamler J. 2010. Dietary Sources of Sodium in China, Japan, the United Kingdom, and the United States, Women and Men Aged 40 to 59 Years: The INTERMAP Study. J.Am.Diet.Assoc. 110(5):736-45.

Atlan S, Trelea IC, Saint-Eve A, Souchon I, Latrille E. 2006. Processing gas chromatographic data and confidence interval calculation for partition coefficients determined by the phase ratio variation method. J Chromatogr A 1110(1–2):146-55.

Awad S. 2007. Effect of sodium chloride and pH on the rennet coagulation and gel firmness. LWT - Food Sci Tech 40(2):220-4.

Barbut S. 1995. Effect of sodium level on the microstructure and texture of whey protein isolate gels. Food Res Int 28(5):437-43.

Clariana M, Guerrero L, Sárraga C, Díaz I, Valero Á, García-Regueiro JA. 2011. Influence of high pressure application on the nutritional, sensory and microbiological characteristics of sliced skin vacuum packed dry-cured ham. Effects along the storage period. Innovat Food Sci Emerg Tech 12(4):456-65.

Clariana M, Guerrero L, Sarraga C, Garcia-Regueiro JA. 2012. Effects of high pressure application (400 and 900 MPa) and refrigerated storage time on the oxidative stability of sliced skin vacuum packed dry-cured ham. Meat Sci 90(2):323-9.

Cogswell ME, Zhang Z, Carriquiry AL, Gunn JP, Kuklina EV, Saydah SH, Yang Q, Moshfegh AJ 2012. Sodium and potassium intakes among US adults: NHANES 2003-2008. Am J Clin Nutr 96(3):647-57.

Colmenero FJ, Ayo MJ, Carballo J. 2005. Physicochemical properties of low sodium frankfurter with added walnut: effect of transglutaminase combined with caseinate, KCl and dietary fibre as salt replacers. Meat Sci. 69(4):781-8.

Cutler JA, Sorlie PD, Wolz M, Thom T, Fields LE, Roccella EJ. 2008. Trends in hypertension prevalence, awareness, treatment, and control rates in united states adults between 1988-1994 and 1999-2004. Hypertension 52(5):818-27.

de Loubens C, Panouillé M, Saint-Eve A, Déléris I, Tréléa IC, Souchon I. 2011. Mechanistic model of in vitro salt release from model dairy gels based on standardized breakdown test simulating mastication. J Food Eng. 105(1):161-8.

DGAC. 2005. Report of the Dietary Guidelines Advisory Committee on the Dietary Guidelines for Americans, 2005, to the Secretary of Agriculture and the Secretary of Health and Human Services. U.S. Department of Agriculture, Agricultural Research Service, Washington, DC.

DGAC. 2010. Report of the Dietary Guidelines Advisory Committee on the Dietary Guidelines for Americans, 2010, to the Secretary of Agriculture and the Secretary of Health and Human Services. U.S. Department of Agriculture, Agricultural Research Service, Washington, DC.

DGAC. 2015. Scientific Report of the 2015 Dietary Guidelines Advisory Committee, to the Secretary of Agriculture and the Secretary of Health and Human Services. U.S. Department of Agriculture, Agricultural Research Service, Washington, DC.

Djordjevic J, Zatorre RJ, Jones-Gotman M. 2004. Odor-induced changes in taste perception. Experimental Brain Research 159(3):405-8.

Eoin D. 2006. Reducing salt: A challenge for the meat industry. Meat Sci. 74(1):188-96.

Epstein N. 1989. On Tortuosity and the tortuosity factor in flow and diffusion through porous-media. Chem Eng Sci 44(3): 777-9.

Eymery O, Pangborn RM. 1988. Influence of fat, citric-acid and sodium-chloride on texture and taste of a cheese analog. Sci.Aliments 8(1): 15-32.
Floury J, Rouaud O, Le Poullennec M, Famelart M. 2009. Reducing salt level in food: Part 2. Modelling salt diffusion in model cheese systems with regards to their composition. LWT - Food Sci Tech 42(10):1621-8.
Foster TP, Parrott EL. 1990. Release of highly water-soluble medicinal compounds from inert, heterogeneous matrices.1. Physical Mixture. J Pharm Sci 79(9):806-10.
Fulladosa E, Sala X, Gou P, Garriga M, Arnau J. 2012. K-lactate and high pressure effects on the safety and quality of restructured hams. Meat Sci 91(1):56-61.
Fulladosa E, Serra X, Gou P, Arnau J. 2009. Effects of potassium lactate and high pressure on transglutaminase restructured dry-cured hams with reduced salt content. Meat Sci 82(2):213-8.
Goh SM, Leroux B, Groeneschild CAG, Busch JLHC. 2010. On the effect of tastant excluded fillers on sweetness and saltiness of a model food. J Food Sci. 75(4):S245-9.
Guo F, He D, Zhang W, Walton RG. 2012. Trends in prevalence, awareness, management, and control of hypertension among United States adults, 1999 to 2010. J Am Coll Cardiol 60(7):599-606.
Heidolph BB, Ray DK, Roller S, Koehler P, Weber J, Slocum S, Noort MWJ. 2011. Looking for my lost shaker of salt... replacer: flavor, function, future. Cereal foods world 565-19.
Henney JE, Taylor CL, Boon CS. 2010a. Preface. In: Committee on Strategies to Reduce Sodium Intake, Institute of Medicine, editor. Strategies to reduce sodium intake in the United States. Washington, D.C.: The National Academies Press. p ix.
Henney JE, Taylor CL, Boon CS. 2010b. Sodium Intake Reduction: An Important But Elusive Public Health Goal. In: Committee on Strategies to Reduce Sodium Intake, Institute of Medicine, editor. Strategies to reduce sodium intake in the United States. Washington, D.C.: The National Academies Press. p 29-66.
Hughes E, Cofrades S, Troy DJ. 1997. Effects of fat level, oat fibre and carrageenan on frankfurters formulated with 5, 12 and 30% fat. Meat Sci 45(3):273-81.
Ilavsky J, Jemian PR, Allen AJ, Zhang F, Levine LE, Long GG. 2009. Ultra-small-angle X-ray scattering at the Advanced Photon Source. J App Crystallogr 42469-79.
Ilavsky J, Jemian PR. 2009. Irena: tool suite for modeling and analysis of small-angle scattering. J App Crystallogr 42: 347-53.
Institute of Medicine (IOM). 2013. Sodium Intake in Poplations: Assessment of Evidence.
IOM. 2005. Sodium and Chloride. In: IOM, editor. Dietary Reference Intakes for Water, Potassium, Sodium, Chloride, and Sulfate. Washington, D.C: Natl. Academies Press. p 269-423.
Jackson SL, King SMC, Zhao L, Cogswell ME. 2016. Prevalence of Excess Sodium Intake in the United States — NHANES, 2009–2012. Morbidity and Mortality Weekly Report January 8, 64: 1393-7. Centers for Disease Control and Prevention. Retrieved from http://www.cdc.gov/mmwr/preview/mmwrhtml/mm6452a1.htm
Kähkönen P, Tuorila H. 1998. Effect of reduced-fat information on expected and actual hedonic and sensory ratings of sausage. Appetite 30(1):13-23.
Kirk SE, Skepper JN, Donald AM. 2009. Application of environmental scanning electron microscopy to determine biological surface structure. J Microscopy-Oxford 233(2): 205-24.
Koliandris A, Lee A, Ferry A, Hill S, Mitchell J. 2008. Relationship between structure of hydrocolloid gels and solutions and flavour release. Food Hydrocoll. 22(4):623-30.
Kuo W, Ilavsky J, Lee Y. 2014. Ultra-small-angle X-ray-scattering (USAXS) quantification of structural properties related to sodium release of solid lipoproteic colloid gel –

implications for sodium reduction. 12th IHC (International Hydrocolloids Conference), May 2014, Taipei, Taiwan.
Lauverjat C, Deleris I, Trelea IC, Salles C, Souchon I. 2009a. Salt and aroma compound release in model cheeses in relation to their mobility. J Agric Food Chem 57(21):9878-87.
Lauverjat C, Loubens Cd, Déléris I, Tréléa IC, Souchon I. 2009b. Rapid determination of partition and diffusion properties for salt and aroma compounds in complex food matrices. J Food Eng 93(4):407-15.
Lemyre J, Lamarre S, Beaupre A, Ritcey AM. 2010. A new approach for the characterization of reverse micellar systems by dynamic light scattering. Langmuir 26(13): 10524-31.
Lim SS, Vos T, Flaxman AD, Danaei G, Shibuya K, Adair-Rohani H, AlMazroa MA, Amann M, Anderson HR, Andrews KG, Aryee M, Atkinson C, Bacchus LJ, Bahalim AN, Balakrishnan K, Balmes J, Barker-Collo S, Baxter A, Bell ML, Blore JD, Blyth F, Bonner C, Borges G, Bourne R, Boussinesq M, Brauer M, Brooks P, Bruce NG, Brunekreef B, Bryan-Hancock C, Bucello C, Buchbinder R, Bull F, Burnett RT, Byers TE, Calabria B, Carapetis J, Carnahan E, Chafe Z, Charlson F, Chen H, Chen JS, Cheng AT, Child JC, Cohen A, Colson KE, Cowie BC, Darby S, Darling S, Davis A, Degenhardt L, Dentener F, Des Jarlais DC, Devries K, Dherani M, Ding EL, Dorsey ER, Driscoll T, Edmond K, Ali SE, Engell RE, Erwin PJ, Fahimi S, Falder G, Farzadfar F, Ferrari A, Finucane MM, Flaxman S, Fowkes FGR, Freedman G, Freeman MK, Gakidou E, Ghosh S, Giovannucci E, Gmel G, Graham K, Grainger R, Grant B, Gunnell D, Gutierrez HR, Hall W, Hoek HW, Hogan A, Hosgood III HD, Hoy D, Hu H, Hubbell BJ, Hutchings SJ, Ibeanusi SE, Jacklyn GL, Jasrasaria R, Jonas JB, Kan H, Kanis JA, Kassebaum N, Kawakami N, Khang Y, Khatibzadeh S, Khoo J, Kok C, Laden F, Lalloo R, Lan Q, Lathlean T, Leasher JL, Leigh J, Li Y, Lin JK, Lipshultz SE, London S, Lozano R, Lu Y, Mak J, Malekzadeh R, Mallinger L, Marcenes W, March L, Marks R, Martin R, McGale P, McGrath J, Mehta S, Memish ZA, Mensah GA, Merriman TR, Micha R, Michaud C, Mishra V, Hanafiah KM, Mokdad AA, Morawska L, Mozaffarian D, Murphy T, Naghavi M, Neal B, Nelson PK, Nolla JM, Norman R, Olives C, Omer SB, Orchard J, Osborne R, Ostro B, Page A, Pandey KD, Parry CD, Passmore E, Patra J, Pearce N, Pelizzari PM, Petzold M, Phillips MR, Pope D, Pope III CA, Powles J, Rao M, Razavi H, Rehfuess EA, Rehm JT, Ritz B, Rivara FP, Roberts T, Robinson C, Rodriguez-Portales JA, Romieu I, Room R, Rosenfeld LC, Roy A, Rushton L, Salomon JA, Sampson U, Sanchez-Riera L, Sanman E, Sapkota A, Seedat S, Shi P, Shield K, Shivakoti R, Singh GM, Sleet DA, Smith E, Smith KR, Stapelberg NJ, Steenland K, Stöckl H, Stovner LJ, Straif K, Straney L, Thurston GD, Tran JH, Van Dingenen R, van Donkelaar A, Veerman JL, Vijayakumar L, Weintraub R, Weissman MM, White RA, Whiteford H, Wiersma ST, Wilkinson JD, Williams HC, Williams W, Wilson N, Woolf AD, Yip P, Zielinski JM, Lopez AD, Murray CJ, Ezzati M. 2012. A comparative risk assessment of burden of disease and injury attributable to 67 risk factors and risk factor clusters in 21 regions, 1990–2010: a systematic analysis for the Global Burden of Disease Study 2010. The Lancet 380(9859):2224-60.
Lteif L, Olabi A, Baghdadi OK, Toufeili I. 2009. The characterization of the physicochemical and sensory properties of full-fat, reduced-fat, and low-fat ovine and bovine Halloumi. J Dairy Sci 92(9):4135-45.
Mattes RD, Donnelly D. 1991. Relative Contributions of Dietary-Sodium Sources. J.Am.Coll.Nutr. 10(4):383-93.
Noort MWJ, Bult JHF, Stieger M, Hamer RJ. 2010. Saltiness enhancement in bread by inhomogeneous spatial distribution of sodium chloride. J Cereal Sci 52(3):378-86.
Noronha N, Duggan E, Ziegler GR, Stapleton JJ, O'Riordan ED, O'Sullivan M. 2008. Comparison of microscopy techniques for the examination of the microstructure of starch-containing imitation cheeses. Food Res Int 41(5): 472-9.

Paneras ED, Bloukas JG, Papadima SN. 1996. Effect of meat source and fat level on processing and quality characteristics of frankfurters. LWT - Food Sci Tech 29(5–6):507-14.
Panouille M, Saint-Eve A, de Loubens C, Deleris I, Souchon I. 2011. Understanding of the influence of composition, structure and texture on salty perception in model dairy products. Food Hydrocoll. 25(4):716-23.
Papadokostaki KG, Amarantos SG, Petropoulos JH. 1998. Kinetics of release of particulate solutes incorporated in cellulosic polymer matrices as a function of solute solubility and polymer swellability .1. Sparingly soluble solutes. J Appl Polym Sci 67(2):277-87.
Phan VA, Yven C, Lawrence G, Chabanet C, Reparet JM, Salles C. 2008. *in vivo* sodium release related to salty perception during eating model cheeses of different textures. Int Dairy J 18(9):956-63.
Phelps T, Angus F, Clegg S, Kilcast D, Narain C, den Ridder C. 2006. Sensory issues in salt reduction. Food Quality and Preference 17(7-8):633-4.
Pons M, Fiszman SM. 1996. Instrumental texture profile analysis with particular reference to gelled systems. J Texture Stud 27(6):597-624.
Powles J, Fahimi S, Micha R, Khatibzadeh S, Shi P, Ezzati M, Engell RE, Lim SS, Danaei G, Mozaffarian D, on behalf of the Global Burden of Diseases Nutrition and Chronic Diseases Expert Group (NutriCoDE). 2013. Global, regional and national sodium intakes in 1990 and 2010: a systematic analysis of 24 h urinary sodium excretion and dietary surveys worldwide. BMJ Open 3(12):e003733.
Ramaswamy S, Gupta M, Goel A, Aaltosalmi U, Kataja M, Koponen A, Ramarao BV. 2004. The 3D structure of fabric and its relationship to liquid and vapor transport. Colloids Surf Physicochem Eng Aspects 241(1–3):323-33.
Richards JJ, Weigandt KM, Pozzo DC. 2011. Aqueous dispersions of colloidal poly(3-hexylthiophene) gel particles with high internal porosity. J Colloid Interface Sci 364(2):341-50.
Romeih E, Michaelidou A, Biliaderis C, Zerfiridis G. 2002. Low-fat white-brined cheese made from bovine milk and two commercial fat mimetics: chemical, physical and sensory attributes. Int Dairy J 12(6):525-40.
Ruusunen M, Simolin M, Puolanne E. 2001. The effect of fat content and flavor enhancers on the perceived saltiness of cooked 'bologna-type' sausages. J Muscle Foods 12(2):107-20.
Saint-Eve A, Lauverjat C, Magnan C, Deleris I, Souchon I. 2009. Reducing salt and fat content: Impact of composition, texture and cognitive interactions on the perception of flavoured model cheeses. Food Chem 116(1):167-75.
Sala G, Stieger M, van de Velde F. 2010. Serum release boosts sweetness intensity in gels. Food Hydrocoll. 24(5):494-501.
Sala G, Stieger M. 2013. Time to first fracture affects sweetness of gels. Food Hydrocoll 30(1):73-81.
Shamil S, Wyeth LJ, Kilcast D. 1991–1992. Flavour release and perception in reduced-fat foods. Food Qual Prefer 3(1):51-60.
Silva EJ, Zaniquelli MED, Loh W. 2007. Light-scattering investigation on microemulsion formation in mixtures of diesel oil (or hydrocarbons) plus ethanol plus additives. Energy Fuels 21(1): 222-6.
Sources of Sodium Among the US Population, 2005-06. Risk Factor Monitoring and Methods Branch Website. Applied Research Program. [Internet]. ; Jan 24th, 2013 [Accessed]. Available from: http://riskfactor.cancer.gov/diet/foodsources/sodium/.
Stampanoni CR, Noble AC. 1991. The influence of fat, acid, and salt on the perception of selected taste and texture attributes of cheese analogs - a Scalar Study. J Texture Stud 22(4): 367-80.

Stieger M, van de Velde F. 2013. Microstructure, texture and oral processing: New ways to reduce sugar and salt in foods. Curr. Opin. Colloid. In. 18(4):334-48.
Stieger M. 2011. Texture-taste interactions: Enhancement of taste intensity by structural modifications of the food matrix. Procedia Food Sci 1(0):521-7.
Svergun DI, Shtykova EV, Volkov VV, Feigin LA. 2011. Small-angle X-Ray scattering, synchrotron radiation, and the structure of bio- and nanosystems. Crystallogr Rep 56(5):725-50.
USDA (US Department of Agriculture). 2014. What we eat in America. NHANES 2011–2012, individuals 2 years and over (excluding breast-fed children), day 1. Retrieved from http://www.ars.usda.gov/SP2UserFiles/Place/80400530/pdf/1112/Table_1_NIN_GEN_11.pd
Vasan RS, Beiser A, Seshadri S, Larson MG, Kannel WB, D'Agostino RB, Levy D. 2002. Residual lifetime risk for developing hypertension in middle-aged women and men - The Framingham Heart Study. Jama-J Am Med Assoc 287(8):1003-10.
Ventanas S, Puolanne E, Tuorila H. 2010. Temporal changes of flavour and texture in cooked bologna type sausages as affected by fat and salt content. Meat Sci 85(3):410-9.
Verbeek PW, Verwer BJH. 1990. Shading from shape, the eikonal equation solved by grey-weighted distance transform. Pattern Recog Lett 11(10):681-90.
Wang YF, Wang QJ. 2004. The prevalence of prehypertension and hypertension among US adults according to the new Joint National Committee guidelines. Arch Intern Med 164(19):2126-34.
Wirth F. 1988. [Reduction of the NaCl content and the action of salt substitutes in meat products.]. Mitteilungsblatt der Bundesanstalt fuer Fleischforschung, Kulmbach (No. 100):7940-5.
Wu YS, van Vliet LJ, Frijlink HW, van der Voort Maarschalk K. 2006. The determination of relative path length as a measure for tortuosity in compacts using image analysis. Europ J Pharm Sci 28(5):433-40.
Xiong R, Meullenet JF, Hankins JA, Chung WK. 2002. Relationship between sensory and instrumental hardness of commercial cheeses. J Food Sci 67(2):877-83.
Zhi YJ, Navam H, Kilara A. 1999. Thermal properties of whey protein aggregates. J Dairy Sci 82(9):1882-9.

1.5 Tables and Figures

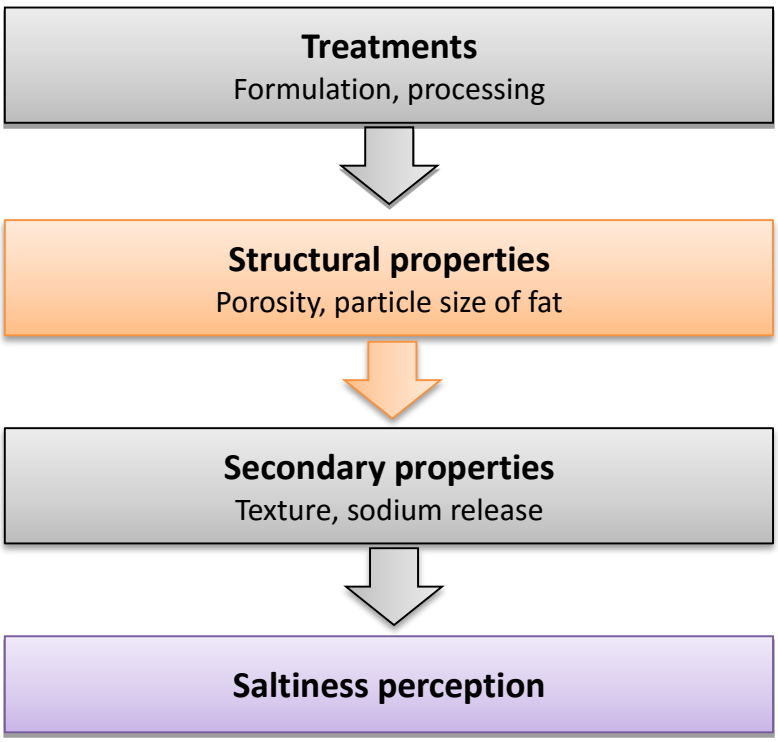

Figure 1.1. Schematic diagram from treatment to structural properties to saltiness perception of the SLCs.

CHAPTER 2

Literature Review

2.1 Effect of Food Matrix on Saltiness Perception[1]

2.1.1 The process of saltiness perception

The process of saltiness perception can be described by three distinct consecutive stages (Figure 2.1). The 1st stage designates the migration of sodium from the solid foods to surroundings, from the moment when food is placed in the mouth until sodium is released into oral cavity. Following the 1st stage, the 2nd stage covers the traveling of sodium in the oral cavity, from the moment when it is released from food matrix, till it reaches the surface of tongue. The 3rd stage refers to the influx of sodium from the tongue surface into the Taste receptor cells (TRCs) and subsequent cognitive transduction of signal responsible for saltiness generation. For solid foods such as cheeses and sausages, sodium must first be released from the matrix during masticatory breakdown. Hence, the saltiness perception includes the overall three-stage process. In contrast, for liquid-like foods such as sauces and soups, sodium is relatively mobile and more readily mixed with saliva as compared to sodium in solid foods. Hence, the saltiness perception would be primarily determined by the last two stages.

We hypothesize that saltiness perception is governed by sodium migration during oral processing of food. And two main factors affecting sodium migration are the concentration gradient of sodium and the resistance to sodium migration. For the 1st and the 2nd stages, the role of the two factors affecting sodium migration is based on the principles of mass transfer (Geankoplis 2003). For the 3rd stage, the role of the two factors affecting sodium migration is based on the principles of ion transport across the ion channel (Gilbertson and Zhang 1998). This study focuses on the saltiness perception as affected by the matrix structure and hence sodium release. This focus corresponds primarily to the first stage as described above. Thus,

[1] ***The contents of this section have been published in: Kuo W, Lee Y. 2014. Effect of food matrix on saltiness perception-implications for sodium reduction. Comprehensive Reviews in Food Science and Food Safety 13(5):906-23. See appendix A-1 for the reprint permission and the reprint.***

the matrix effects during the first stage of saltiness perception are further elaborated in the following sections.

2.1.2 Mechanisms for sodium release from the food matrix

The sodium release from the food matrix in the 1st stage is via diffusive and/or convective transports. The diffusive transport is driven by the difference in sodium concentration across the matrix boundary. The convective transport is driven by the outward liquid flow during the matrix compression. Both diffusive and convective transports depend on the concentration gradient of sodium and the resistance to sodium migration. At given sodium contents of the food, the concentration gradient of sodium is affected by the sodium availability as a result of ionic interaction (Section 2.1.3.1). The resistance to sodium diffusion is governed by the tortuosity and sieving effects of the matrix (Section 2.1.4.1), whereas the resistance to the convective transport of sodium is reflected by the velocity of the serum flow during the matrix compression (Section 2.1.5.1). In addition, the rate of both diffusive and convective transport increase with increased surface area, as a result of the matrix fragmentation during the mastication (Section 2.1.5.2). Furthermore, the oral processing parameters may vary in response to different matrix properties. This may additionally modify the food breakdown and thus sodium release (Section 2.1.6).

2.1.3 Matrix effect on sodium availability

2.1.3.1 Sodium – polymer interaction in the matrix

The frequent use of NaCl to adjust texture of many food products reflects its nature to interact with ionic polymers such as protein and polysaccharides. Such interaction, though is favored for processing, usually lowers the availability of sodium ion for perception (Rosett and others 1995; Doyle and Glass 2010). NaCl is commonly added to processed meat to enhance water-binding capacity, and thus tenderness and juiciness of the product. The actual process includes swelling of the myofilaments, as a result of Cl^- penetration, and surrounding the filaments with Na^+Cl^- (Ruusunen and Puolanne 2005). In addition to meat protein, NaCl is often used to interact with gluten and milk proteins to achieve the desired texture of bakery and dairy products.

Table 2.1 summarizes the studies of the effects of sodium-polymer interaction on sodium release or saltiness perception of some solid food systems. Ruusunen and others (2001) studied the effect of replacing 71% (w/w) of fat content on the saltiness of 'Bologna-type' sausages. When the fat was replaced with lean meat, the saltiness of the sausage was significantly reduced ($p < 0.05$), but when the fat was replaced with water, the saltiness did not change. They, thus, concluded that the ionic interaction between sodium and the lean meat limited the availability of sodium for saltiness perception. Clariana and others (2011) studied the effects of high-pressure processing (HPP) on the saltiness of dry-cured ham. The saltiness of the sample treated at 600 MPa for 360 s was higher than that of the control sample. They explained that the HPP weakened the sodium-protein interaction and, thus, led to a higher concentration of free sodium in the product than in the control. Similar results were reported in other studies of dry-cured ham but translated differently. Saccani and others (2004), Serra and others (2007), and Fulladosa and others (2009, 2012) suggested that the poorer water-holding capacity (WHC) after HPP treatment facilitated sodium release with the liquid from the matrix (see Section 2.1.5.1 for more discussion). These findings suggested that sodium-polymer interaction apparently is not the only factor that determines saltiness. Indeed, altering formulation or processing parameters often leads to multiple changes in product properties such as moisture content and texture (Ruusunen and others 2001). These changes could affect saltiness through physical (sodium diffusion in matrix, see Section 2.1.4 for more discussion) or perceptual (texture-taste interaction) mechanisms. Therefore, controlled model food systems, coupled with instrumental analyses of sodium release, would also be needed to study the impact of sodium-polymer interaction on saltiness perception.

Lauverjat and others (2009) measured sodium release from the model cheese to the surrounding water and obtained the partition coefficient of NaCl (K_{NaCl}). The K_{NaCl} values of all of their cheese samples were below 1, implying a significant portion of NaCl was retained in the model cheese than in the water. This was ascribed to the ionic interaction between sodium ions and the phosphoserine residues of casein. The ionic interaction between sodium and protein was evaluated in terms of sodium mobility in model cheese by measuring the bound fraction and the longitudinal relaxation time (T_1) of sodium with ^{23}Na-NMR (Boisard and others 2014). The cheeses with higher weight ratios of fat/protein had lower bound fractions of sodium and greater T_1, indicating greater sodium mobility. This was attributed to the lower protein content in these cheeses which rendered lower ionic interaction between

sodium and casein molecules. The resulting higher sodium mobility thus led to higher sodium availability in these cheeses, which also presented greater degree of in-mouth sodium release.

It should be noted that during oral processing, the structure and texture of the matrix may change instantaneously. Hence, the sodium availability and migration rate may also change dynamically with the evolution of the matrix properties. However, since the chewing period is relatively short compared to the time required to reach partition equilibrium, the K_{NaCl} of a matrix could be considered constant throughout oral processing (de Loubens and others 2011b).

2.1.4 Matrix effect on spontaneous diffusion of sodium

2.1.4.1 Tortuosity and sieving effects

The tortuosity and sieving effect are the intrinsic structural properties of the matrix that predominantly lower the rate of the spontaneous diffusion of sodium. These properties were studied initially for cheese-salting, where sodium migrates from brine into unsalted cheese. More recently these properties have been used to explain sodium release from matrices made of lipid and protein. The tortuosity refers to the obstruction by fat globules or protein aggregates which make the ions travel tortuously with extra length. The sieving effect refers to the friction the ions encounter when passing through the matrix with the lowest pore size comparable to that of the ions (Guinee 2004). Geurts (1974) had reported that the diffusion coefficient of NaCl (D_{NaCl}) in the liquid phase of cheese ($1.2*10^{-10}$-$3*10^{-10}$ m^2/s) was much lower than in water at 12.5°C (about $1.2*10^{-9}$ m^2/s). Indeed, the D_{NaCl} in cheese products was mainly determined by the volume fractions of fat and protein due to the tortuosity and sieving effects. First, the presence of fat and protein in cheese directly forms a physical barrier which accounts for the tortuosity. Second, the network formed via protein-protein interaction presents small pores which directly exert a sieving effect. Third, the water-binding property of protein indirectly contributes to the sieving effect by increased friction. Besides, the water bound to protein also indirectly contributes to tortuosity by increased occupation of available pore space.

Table 2.2 lists the studies of the tortuosity or sieving effects on the spontaneous diffusion of sodium in food systems. Hughes and others (1997) observed increased saltiness in frankfurters when the fat content was reduced from 0.3 to 0.05 kg/kg sample by replacing it with water. The authors related this saltiness increase to the removal of the hydrophobic

barrier, fat, which impeded sodium diffusion. Phan and others (2008) measured the in-mouth sodium release from model cheese by sampling the saliva of subjects during their chewing processes. It was also claimed that the NaCl diffusion was boosted with a decreased amount of fat working as the hydrophobic barrier. The barrier property in the above 2 studies could indeed be considered as the tortuosity effect of fat. Instrumental analyses would be preferred to evaluate the extent of sodium diffusion as a more direct evidence of the matrix effects.

Lauverjat and others (2009), Floury and others (2009), and Panouille and others (2011) examined the effects of composition on the apparent diffusion coefficient of NaCl ($*D_{NaCl}$) in model cheese. The $*D_{NaCl}$ was obtained by measuring sodium release with a conductivity probe and calculating the mass transfer based on Fick's second law. Overall, all 3 studies observed a decrease in $*D_{NaCl}$ with increased dry matter content, which was explained by the increase in viscoelasticity and decrease in void volume. At constant dry matter content, the $*D_{NaCl}$ was lower in the sample with higher protein content, suggesting that protein is more influential than fat in restricting sodium diffusion (Lauverjat and others 2009). It was explained by the contributions of protein to tortuosity and sieving effect via multiple routes as previously discussed. By contrast, fat only contributed to tortuosity. Furthermore, with given sample composition, the $*D_{NaCl}$ dropped with renneting of the sample (Panouille and others 2011), decreased NaCl content (Floury and others 2009; Lauverjat and others 2009), or decreased pH (Floury and others 2009), which was mainly due to the alteration of casein arrangement and thus the network structure formed with the protein by these treatments. It also implies that the effective volume fraction of protein, which varies with the network structure, is more indicative than the protein content in determining sodium diffusion.

It should be noticed that most solid or gel-like foods undergo deformation during oral processing. Since the matrix structure may be changed simultaneously during the deformation, the tortuosity and sieving effects, and hence, the apparent diffusion coefficient of NaCl ($*D_{NaCl}$) may also change dynamically. However, the changes in geometry and surface area due to matrix deformation and breakdown should have more significant impacts on sodium release. Thus, the $*D_{NaCl}$ could still be considered constant regardless of the product deformation (de Loubens and others 2011b).

2.1.5 Matrix effect on sodium migration during deformation

2.1.5.1 Serum release of the matrix

Table 2.3 lists the studies on the effects of serum release on the migration of sodium under matrix deformation. As mentioned in Section 2.1.3.1, both Clariana and others (2011) and Fulladosa and others (2009) observed increased saltiness of the dry-cured ham after high-pressure treatments, and attributed this to a decrease in sodium-protein interaction and poorer water holding capacity (WHC), respectively. In the study by Fulladosa and others (2009), the transglutaminase-restructured dry-cured hams were treated with 600 MPa for 360 s. The high pressure-treated samples showed a higher percentage of water loss, implying poorer WHC than the control. Therefore, it was concluded that the high-pressure processing (HPP) boosted the sodium release by creating more expressible water that efficiently carried sodium out from the food matrix during oral processing. This hypothesis was also proposed in similar studies by Fulladosa and others (2012) and Clariana and others (2012). Still, without measuring the sodium-polymer interaction, it was not clear whether the saltiness increment was partly due to dissociation of the bound sodium after HPP treatments.

The serum release of fruits, vegetables, and meat products could be related to their juiciness perception (Stieger 2011). While saltiness was positively related with sensory juiciness in some meat products (Ruusunen and Puolanne 2005; Ventanas and others 2010), such relationship was not observed by Matulis and others (1995), Crehan and others (2000), or Moeller and others (2010). This inconsistency again reflects the multiple matrix effects on saltiness perception. Thus, it is necessary to obtain a sodium release profile as the baseline to study saltiness perception.

Jack and others (1995) examined the effects of texture in terms of hardness on sodium release of commercial cheeses using in-mouth conductivity probes. The cheese samples showed a positive correlation between the rate of sodium release and the hardness of cheese. The authors postulated that the cheese with higher hardness had lower moisture content and consequently higher NaCl concentration in the aqueous phase. Thus, the concentrated NaCl solution, when being expressed during oral processing, resulted in a higher release rate of sodium. Nevertheless, as the sodium release was measured in-mouth, the effects of oral processing on the matrix breakdown could not be excluded. The authors indeed mentioned that the greater chewing force required for the harder gel could also contribute to the higher release rate of sodium. Stieger (2011) studied the effects of microstructure on serum release

and sodium release of model gels made by acid-induced cold-gelation of gellan/whey protein isolate mixtures. By adjusting the total solid content and the gellan amount, they prepared a series of gels with identical large deformation properties but different serum release under instrumental compression. With the increased gellan ratio, the gel microstructure changed from a protein -continuous to a bi-continuous structure. The change from a protein -continuous to a bi-continuous structure increased the amount of serum release and, consequently, resulted in higher juiciness and saltiness in sensory evaluation. More convincing conclusion could have been drawn if the sodium release during the instrumental compression was also measured and compared with the serum release and saltiness.

During the mastication process, the serum release behavior may change momentarily with the evolution of food microstructure (van den Berg and others 2007). However, it is still assumed that the differences in original structures between samples are much greater than the differences in structures generated during oral processing. Hence, only the changes in surface area would need to be discussed for the effect of fragmentation on serum release.

2.1.5.2 Matrix fragmentation

Oral processing of solid foods typically includes mastication that breaks down food into pieces smaller than 2 mm, the particle size threshold for swallowing (Prinz and Lucas 1995). Table 2.4 lists the studies on the effects of fragmentation tendency on the migration of sodium during matrix deformation. In the study with commercial cheeses (Jack and others 1995), the half-fat Cheddar, which presented slow sodium release, was found to be more rubbery by the sensory test. It was hypothesized that the rubbery nature of the sample lowered the extent of disintegration on each chew stroke, which disfavored sodium release. Instrumental analyses for texture and sodium release using model food systems would be a great addition to support the above statement.

Koliandris and others (2008) investigated the effect of matrix texture on sodium release of two model gels consisting of low-/high-acetyl gellan and κ-carrageenan/locust bean gum. When the concentration of low-acetyl gellan or κ-carrageenan was increased, the instrumental brittleness and the rate of *in vitro* sodium release increased correspondingly. Thus, they suggested that brittle samples yielded higher surface area after compression, and released more sodium in a given time period. However, the surface area was not measured to confirm this statement.

The research group of Souchon I. (Saint-Eve and others 2009; de Loubens and others 2011a; Panouille and others 2011) has also investigated the dependency of sodium release or saltiness on breakdown properties of model cheeses. Their earlier study concluded that texture had no effect on saltiness, despite the "fragmentable" score by sensory evaluation increased with the fat content (Saint-Eve and others 2009). The lack of saltiness-texture correlation might be due to the comparatively narrow range of variations in the formulation of cheese samples, where the dry matter (DM) was 0.37-0.44 kg/kg cheese and the fat content was 0.2-0.4 kg/kg DM. In 2 of their later studies (de Loubens and others 2011a; Panouille and others 2011), the DM and fat contents varied in greater ranges of 0.15-0.43 kg/kg sample and 0-0.4 kg/kg DM, respectively. Panouille and others (2011) observed decreased saltiness with increased protein content, and attributed this to the densely formed protein network with more rubbery and less brittle texture. However, their instrumental texture analysis did not confirm this trend. de Loubens and others (2011a) established a real-time measurement of sodium release during gel compression using a texture analyzer. Based on a mass transfer model that includes the surface area of the broken gel as the main parameter, they fitted the release data to obtain the surface area. By comparing with their sensory evaluation results, they hypothesized that the gel with higher fat content was fragmented faster due to the disruption of the protein network by fat. This could be evidenced by the larger breakdown surface area, earlier perception of crumbliness, and longer perception of saltiness of the high-fat sample. Nonetheless, this hypothesis only applied to the samples with milk retentate of 0.25 kg/kg gel. Their previous study (Panouille and others 2011) showed that the saltiest sample (retentate 0.15 kg/kg gel, fat 0.4 kg/kg DM) had a fairly small breakdown surface area. In addition, the high saltiness was not attributed to the high fragmentation tendency, but to the partitioning effect (Panouille and others 2011). The partitioning effect refers to the concentrating of sodium in the aqueous phase upon incorporation of fat due to the stronger partitioning of sodium in the aqueous versus the fat phase in the emulsion. The discrepancy between the above 2 parallel studies implies that the fragmentation tendency, expressed by the surface area, may not be the universal predictor for sodium release and saltiness. Other variables such as tortuosity and serum release may need to be incorporated when explaining the saltiness of a product.

In the study of in-mouth sodium release by Phan and others (2008), the sodium release at 20 s and 60 s of chewing increased, respectively, with increased water-to-protein ratio and fat-to-protein ratio. This means that the matrix effects dominating sodium release

depended on the duration of mastication. For the initial 20 s of chewing, the authors suggested that water in the matrix was most helpful for sodium release, which indeed was a consequence of serum release. By contrast, when the chewing was prolonged to 60 s, the effect of fragmentation might become prominent. Thus high fat content would make the matrix more fragmentable and lead to greater sodium release. Yet, none of the studies in Section 2.1.5 considered both serum release and fragmentation in the design of the experiments and the interpretation of the results. In fact, when 2 samples bear the similar fragmentation tendency, but different amounts of serum release, then the sodium release would still be different. This means that to describe sodium release accurately, a more comprehensive model incorporating individual matrix effects may be required.

2.1.6 Interactions between matrix properties and oral processing

So far, the discussions about the matrix effects on sodium release or saltiness perception only include the direct impact from the matrix. In fact, the matrix properties and the oral processing could be interactive. In other words, the mastication and/or salivary functions during oral processing may vary from product to product. Such interaction between matrix and oral processing may lead to a different sodium release profile which could not be revealed by instrumental analyses. Ideally, it will provide a more comprehensive picture of saltiness perception by incorporating all the interactions between matrix properties and oral processing. However, the variety and complexity of such interactions may require another article for discussion. Hence, only limited studies from the literature are discussed in this section to illustrate the concept of such interaction and its potential influences on saltiness perception.

During typical oral processing, mastication and salivary properties are the major 2 oral parameters related to flavor release (Salles and others 2011; Lawrence and others 2012). Tarrega and others (2011) studied the relationship between compositional/textural properties of model cheeses and panelists' mastication activities. The samples with lower fat content had more hardness and required greater chewing work per cycle, number of chewing strokes, and higher amount of total incorporated saliva. However, chewing rate was independent of the fat content or texture of the samples. Similar results were also reported by Mioche and others (2002) and Gaviao and others (2004).

Apart from eating foods, salivary flow may be modulated by certain medicines (Mattes and others 1994), physiological activity (such as chewing paraffin film (Mackie and Pangborn 1990), wax, or rubber (Kerr 1961)), environment (temperature, illumination, and sound), or higher-order cognitive factors (attention, mental imagery, and labeling (Spence 2011)). During eating, saliva flow rate can be elevated from $5*10^{-9}$ m^3/s (Christensen and others 1984) to beyond $1.67*10^{-8}$ m^3/s (Navazesh and Christensen 1982) by chemosensory (taste, smell, and chemical irritancy) (Neyraud and others 2003; Harthoorn and others 2009) or tactile factors (Mattes 1997). Among the different chemosensory and tactile factors taste is the most dominating stimulus. Among the different tastes, sourness increases salivary flow rate the most, followed by umami, salty, sweet, and bitter tastes (Froehlich and others 1987; Hodson and Linden 2006). In addition, certain fatty acids were also shown to stimulate saliva secretion (Koriyama and others 2002; Hodson and Linden 2004). Chewing foods with different physicochemical features could also change saliva flow (Mackie and Pangborn 1990).

The matrix effects on oral processing have been widely investigated. However, effects of the consequently altered oral processing on sodium release have been rarely studied, and discussions found in the literature provide only limited valid evidence. Lawrence and others (2012) discovered that, for the model cheese with highest sodium level in their study, the in-mouth sodium release increased with the moisture content of the cheese. This was attributed partly to the facilitated sodium extraction from the matrix due to high moisture content of the sample and high salivation induced by the high sodium concentration (Chabanet and others 2013). Still, as discussed in their article, other factors such as higher amount of non-complexed sodium might also contribute to sodium release in the mouth, and thus this need further investigation. Phan and others (2008) observed that individuals with higher salivary flow rate or masticatory performance produced a bolus with higher sodium release from model cheeses. They ascribed this to high efficiency of sodium extraction by saliva and more extensive food breakdown. Interestingly, saltiness remained the same, and this was hypothesized to be due to receptor saturation or adaption. Pionnier and others (2004) observed that the in-mouth sodium release, expressed by area under the curve of concentration versus time plot, was correlated positively with chewing time but negatively with salivary flow rates, chewing rates, masticatory performances, and swallowing rates. While the findings from Phan and others (2008) and Pionnier and others (2004) were based

on inter-individual differences, their implications on the interaction between the matrix properties and oral processing are limited.

An overview of the studies in the 1st stage implies that future research on sodium release from the food matrix should address the followings. First, direct measures of sodium-polymer interaction such as ^{23}Na-NMR relaxation time should be evaluated. This will help to identify whether a change in sodium release is due to its change in concentration gradient and/or the change in resistance to sodium migration. Second, model food gels with well-controlled emulsion structures should be used. Both serum release and fragmentation degree should be examined and correlated to the *in vitro* sodium release parameters. This will help to identify the matrix effects on the diffusive and/or convective transport of sodium, and the corresponding changes in the temporal sodium release. Third, the comparison between the *in vitro* and in-mouth sodium release should be conducted. This will help to identify the interactions between the matrix and the oral processing properties.

2.2 X-ray Scattering to Characterize Food Structure

Food microstructure has a profound impact on the sodium release and saltiness perception of foods (Kuo and Lee 2014). Conventional characterizations of food microstructures rely heavily on electron microscopy (EM) for its suitable characterization range (Dudkiewicz and others 2012). However, the need of sample pre-treatment for EM eliminates the possibility of real-time analysis, and increases the chance to damage the original structures. The limited imaging based on the 2-dimentional vicinity of a thin layer (Harada and Matsuoka 2004) and the arbitrary selection of the imaging field also makes the sample representation prone to bias.

X-ray scattering is a promising technology to study food microstructures. While X-ray scattering has been extensively utilized to explore the microstructures of synthetic and inorganic materials, their applications in food research are still emerging (Väänänen and others 2003; Peyronel and others 2014a; Peyronel and others 2014b). The strength of X-ray scattering resides in its abilities for the multiple structural characterization (chemical composition, crystallography, size, shape and association of particles (Dudkiewicz and others 2012)) in the wide range of structure size (angstrom to micrometer (Ilavsky and others 2002; Ilavsky and others 2009; Ilavsky and others 2013)), the ensemble-averaged signal collection from the 3-D structure, the minimum or no sample pretreatment, and the compatibility with

highly concentrated or opaque samples (Harada and Matsuoka 2004; Peyronel and others 2014a). Furthermore, X-ray scattering with the high flux of the synchrotron-source enables short time data collection (Harada and Matsuoka 2004), providing options for real-time analysis of microstructure during food digestion. The synchrotron X-ray scattering also provides the data with higher signal-to-noise ratio, which is critical to observe the structures in biomaterials which have weaker scattering contrast and lower uniformity than inorganic materials.

Among the synchrotron radiation facilities worldwide, the Advanced Photon Source (APS) at the Argonne National Laboratory (Argonne, IL) equipped with the brightest X-ray in the western hemisphere. Combined with pinhole small-angle X-ray scattering (SAXS), the ultra-small angle X-ray scattering (USAXS) facility at APS offers structural characterization at the scale from nanometer to micrometer (Ilavsky and others 2013). This scale range is ideal to the present study, since it covers the particle sizes of the protein aggregates and fat globules in the SLCs. Given the promising feature of X-ray scattering, very rare amount of study had utilized USAXS to characterize food structures (Peyronel and others 2014a). Hence, it is beneficial to explore the use of USAXS in understanding food structure as a mean to improve the physicochemical, sensory, and nutritional quality of foods.

2.3 Sensory Evaluations for Saltiness Perception Properties of Lipoproteic Foods

Sensory methods including quantitative descriptive analysis (QDA) (Saint-Eve and others 2009), temporal dominance of sensation (TDS) (de Loubens and others 2011a) and time-intensity (TI) (Phan and others 2008; de Loubens and others 2011b) are commonly used to evaluate saltiness perception properties of lipoproteic foods. In addition, in-mouth sodium release during chewing was also assessed for a comparison with the TI data of saltiness perception (Phan and others 2008; de Loubens and others 2011b).

Saint-Eve and others (2009) used QDA to study the sensory properties of model cheese. The model cheese was made by renneting the mixture of milk retentate and anhydrous milk fat (AMF). The terms of attribute used included taste (salty and sweet), texture by mouth (crumbly, firm, fragmentable, and sticky), tactile texture (springy and firm), and several odor and aroma terms. The results showed that the level of NaCl affected the texture of the model cheese, particularly in the low fat samples. When the NaCl concentration of the model cheese was decreased from 1.5% to 0.5% (w/w), the sample became firmer,

more fragmentable and crumbly. However, the variation in texture of the model cheese had no effects on the saltiness perception.

In contrast to the QDA which evaluates the overall intensity of given attributes of the products, TDS and TI evaluates temporal perception properties of the products. In a TDS test, a panelist selects the most dominating sensory attribute from a given number of attributes along the evaluation time. The total count of a single attribute at different time along the evaluation is then summarized across all the panelists in the panel. The temporal perception of up to 10 attributes can be collected in a single evaluation (Pineau and others 2009). While TDS records the "dominance rate" of multiple attributes per evaluation, TI method quantitatively records the intensity of only one attribute per evaluation. In a TI test, the panelist rates the intensity score of a given attribute along the evaluation time (Lee and Pangborn 1986).

de Loubens and others used TDS (de Loubens and others 2011a) and TI (de Loubens and others 2011b) to study the temporal perception properties of a model cheese. The model cheese was made by renneting the mixture of milk retentate and AMF. It is particularly interesting to compare the saltiness perception properties of the model cheese evaluated by the TDS and the TI methods across the two studies. In the TDS study (de Loubens and others 2011a), the attributes evaluated included saltiness, moistness, softness, firmness, crumbliness, stickiness, and fattiness. The TDS results showed that the fat-containing model cheese displayed earlier domination of crumbliness during the sample chewing than the non-fat sample. This implied faster breakdown of the fat-containing sample, which explained the earlier and longer dominance of saltiness observed from such sample. However, the TI evaluating on the same set of samples showed that the fat containing sample took longer time to reach maximum saltiness than the non-fat samples (de Loubens and others 2011b). Further studies comparing the QDA, TDS and TI evaluations on the same sets of samples may be helpful to identify the temporal parameters that determine the overall saltiness perception of lipoproteic foods.

The temporal saltiness perception of lipoproteic foods can be further compared with in-mouth sodium release. Phan and others (2008) studied the in-mouth sodium release during chewing of a model cheese. The model cheese was made of rennet casein, AMF, and phosphate salts. The saliva was sampled using cotton buds at given intervals during the 120 seconds of chewing. The temporal saltiness perception was also recorded using the TI method. Sodium release was found to decrease with increasing fat content. This trend was

ascribed to the hydrophobic barrier effect of fat. However, saltiness was found to increase with increasing fat content. This trend was ascribed to the emulsification which concentrated the water phase. The difference between the trends of in-mouth sodium release and saltiness perception suggested that saltiness perception is a complex process involving multiple factors. de Loubens and others (2011b) correlated the parameters between in-mouth sodium release and TI. Total sodium release was not correlated with the area under the curve of TI ($R^2 < 0.1$). The maximum rate of sodium release in mouth was found to positively correlate with the maximum saltiness in the TI curve ($R^2 = 0.6$). More studies comparing the parameters between in-mouth sodium release, TI, TDS and overall saltiness are need to further understand the process and mechanisms of saltiness perception.

2.4 References

Boisard L, Andriot I, Martin C, Septier C, Boissard V, Salles C, Guichard E. 2014. The salt and lipid composition of model cheeses modifies in-mouth flavour release and perception related to the free sodium ion content. Food Chem. 145(0):437-44.

Chabanet C, Tarrega A, Septier C, Siret F, Salles C. 2013. Fat and salt contents affect the in-mouth temporal sodium release and saltiness perception of chicken sausages. Meat Sci. 94(2):253-61.

Christensen CM, Navazesh M, Brightman VJ. 1984. Effects of pharmacologic reductions in salivary flow on taste thresholds in man. Arch.Oral Biol. 29(1):17-23.

Clariana M, Guerrero L, Sarraga C, Garcia-Regueiro JA. 2012. Effects of high pressure application (400 and 900 MPa) and refrigerated storage time on the oxidative stability of sliced skin vacuum packed dry-cured ham. Meat Sci. 90(2):323-9.

Clariana M, Guerrero L, Sárraga C, Díaz I, Valero Á, García-Regueiro JA. 2011. Influence of high pressure application on the nutritional, sensory and microbiological characteristics of sliced skin vacuum packed dry-cured ham. Effects along the storage period. Innovative Food Science & Emerging Technologies 12(4):456-65.

Crehan CM, Hughes E, Troy DJ, Buckley DJ. 2000. Effects of fat level and maltodextrin on the functional properties of frankfurters formulated with 5, 12 and 30% fat. Meat Sci. 55(4):463-9.

de Loubens C, Panouillé M, Saint-Eve A, Déléris I, Tréléa IC, Souchon I. 2011a. Mechanistic model of in vitro salt release from model dairy gels based on standardized breakdown test simulating mastication. J.Food Eng. 105(1):161-8.

de Loubens C, Saint-Eve A, Deleris I, Panouille M, Doyennette M, Trelea IC, Souchon I. 2011b. Mechanistic model to understand in vivo salt release and perception during the consumption of dairy gels. J.Agric.Food Chem. 59(6):2534-42.

Doyle ME, Glass KA. 2010. Sodium reduction and its effect on food safety, food quality, and human health. Comprehensive Reviews in Food Science and Food Safety 9(1):44-56.

Dudkiewicz A, Luo P, Tiede K, Boxall A. 2012. Detecting and characterizing nanoparticles in food, beverages and nutraceuticals. Woodhead Publ.Food Sci.Technol.Nutr. (218):53-81.

Floury J, Rouaud O, Le Poullennec M, Famelart M. 2009. Reducing salt level in food: Part 2. Modelling salt diffusion in model cheese systems with regards to their composition. LWT - Food Science and Technology 42(10):1621-8.

Froehlich DA, Pangborn RM, Whitaker JR. 1987. The effect of oral stimulation on human parotid salivary flow rate and alpha-amylase secretion. Physiol.Behav. 41(3):209-17.

Fulladosa E, Serra X, Gou P, Arnau J. 2009. Effects of potassium lactate and high pressure on transglutaminase restructured dry-cured hams with reduced salt content. Meat Sci. 82(2):213-8.

Fulladosa E, Sala X, Gou P, Garriga M, Arnau J. 2012. K-lactate and high pressure effects on the safety and quality of restructured hams. Meat Sci. 91(1):56-61.

Gaviao MBD, Engelen L, van der Bilt A. 2004. Chewing behavior and salivary secretion. Eur.J.Oral Sci. 112(1):19-24.

Geankoplis CJ. 2003. Principles of Unsteady-State and Convective Mass Transfer. In: Christie J. Geankoplis, editor. Transport Processes and Separation Process Principles. 4th ed. Upper Saddle River, New Jersey: Prentice Hall. p 459-512.

Geurts TJ. 1974. Transport of salt and water during salting of cheese. I. Analysis of the processes involved. Nederlands melk- en zuiveltijdschrift 28(2):102-29.

Gilbertson T, Zhang H. 1998. Characterization of sodium transport in gustatory epithelia from the hamster and rat. Chem.Senses 23(3):283-93.

Guinee TP. 2004. Salting and the role of salt in cheese. International Journal of Dairy Technology 57(2-3):99-109.
Harada T, Matsuoka H. 2004. Ultra-small-angle X-ray and neutron scattering study of colloidal dispersions. Current Opinion in Colloid & Interface Science 8(6):501-6.
Harthoorn LF, Brattinga C, Van Kekem K, Neyraud E, Dransfield E. 2009. Effects of sucrose on salivary flow and composition: differences between real and sham intake. Int.J.Food Sci.Nutr. 60(8):637-46.
Hodson NA, Linden RWA. 2006. The effect of monosodium glutamate on parotid salivary flow in comparison to the response to representatives of the other four basic tastes. Physiol.Behav. 89(5):711-7.
Hodson NA, Linden RWA. 2004. Is there a parotid-salivary reflex response to fat stimulation in humans? Physiol.Behav. 82(5):805-13.
Hughes E, Cofrades S, Troy DJ. 1997. Effects of fat level, oat fibre and carrageenan on frankfurters formulated with 5, 12 and 30% fat. Meat Sci. 45(3):273-81.
Ilavsky J, Allen AJ, Long GG, Jemian PR. 2002. Effective pinhole-collimated ultrasmall-angle x-ray scattering instrument for measuring anisotropic microstructures. Rev.Sci.Instrum. 73(3):1660-2.
Ilavsky J, Zhang F, Allen AJ, Levine LE, Jemian PR, Long GG. 2013. Ultra-Small-Angle X-ray Scattering Instrument at the Advanced Photon Source: History, Recent Development, and Current Status. Metallurgical and Materials Transactions A-Physical Metallurgy and Materials Science 44A(1):68-76.
Ilavsky J, Jemian PR, Allen AJ, Zhang F, Levine LE, Long GG. 2009. Ultra-small-angle X-ray scattering at the Advanced Photon Source. Journal of Applied Crystallography 42469-79.
Jack FR, Piggott JR, Paterson A. 1995. Cheddar Cheese Texture Related to Salt Release during Chewing, Measured by Conductivity - Preliminary-Study. J.Food Sci. 60(2):213-7.
Kerr AC. 1961. In: A. C. Kerr, editor. The physiological regulation of salivary secretion in man. New York: Pergamon Press. p 24-27; 48-59.
Koliandris A, Lee A, Ferry A, Hill S, Mitchell J. 2008. Relationship between structure of hydrocolloid gels and solutions and flavour release. Food Hydrocoll. 22(4):623-30.
Koriyama T, Wongso S, Watanabe K, Abe H. 2002. Fatty acid compositions of oil species affect the 5 basic taste perceptions. J.Food Sci. 67(2):868-73.
Kuo W, Lee Y. 2014. Effect of food matrix on saltiness perception-implications for sodium reduction. Comprehensive Reviews in Food Science and Food Safety 13(5):906-23.
Lauverjat C, Deleris I, Trelea IC, Salles C, Souchon I. 2009. Salt and aroma compound release in model cheeses in relation to their mobility. J.Agric.Food Chem. 57(21):9878-87.
Lawrence G, Buchin S, Achilleos C, Berodier F, Septier C, Courcoux P, Salles C. 2012a. in vivo sodium release and saltiness perception in solid lipoprotein matrices. 1. Effect of composition and texture. J.Agric.Food Chem. 60(21):5287-98.
Lee WE, Pangborn RM. 1986. Time-Intensity - the Temporal Aspects of Sensory Perception. Food Technol. 40(11):71.
Mackie DA, Pangborn RM. 1990. Mastication and its influence on human salivary flow and alpha-amylase secretion. Physiol.Behav. 47(3):593-5.
Mattes RD. 1997. Physiologic responses to sensory stimulation by food: Nutritional implications. J.Am.Diet.Assoc. 97(4):406-13.
Mattes RD, Shaw LM, Engelman K. 1994. Effects of Cannabinoids (Marijuana) on Taste Intensity and Hedonic Ratings and Salivary Flow of Adults. Chem.Senses 19(2):125-40.
Matulis RJ, Mckeith FK, Sutherland JW, Brewer MS. 1995. Sensory Characteristics of Frankfurters as Affected by Fat, Salt, and Ph. J.Food Sci. 60(1):42-7.

Mioche L, Bourdiol P, Monier S, Martin J. 2002. The relationship between chewing activity and food bolus properties obtained from different meat textures. Food Quality and Preference 13(7–8):583-8.
Moeller SJ, Miller RK, Aldredge TL, Logan KE, Edwards KK, Zerby HN, Boggess M, Box-Steffensmeier JM, Stahl CA. 2010. Trained sensory perception of pork eating quality as affected by fresh and cooked pork quality attributes and end-point cooked temperature. Meat Sci. 85(1):96-103.
Navazesh M, Christensen CM. 1982. A Comparison of whole mouth resting and stimulated salivary measurement procedures. J.Dent.Res. 61(10):1158-62.
Neyraud E, Prinz J, Dransfield E. 2003. NaCl and sugar release, salivation and taste during mastication of salted chewing gum. Physiol.Behav. 79(4-5):731-7.
Panouille M, Saint-Eve A, de Loubens C, Deleris I, Souchon I. 2011. Understanding of the influence of composition, structure and texture on salty perception in model dairy products. Food Hydrocoll. 25(4):716-23.
Peyronel F, Pink DA, Marangoni AG. 2014a. Triglyceride nanocrystal aggregation into polycrystalline colloidal networks: Ultra-small angle X-ray scattering, models and computer simulation. Current Opinion in Colloid & Interface Science 19(5):459-70.
Peyronel F, Quinn B, Marangoni AG, Pink DA. 2014b. Ultra Small Angle X-Ray Scattering for Pure Tristearin and Tripalmitin: Model Predictions and Experimental Results. Food Biophysics 9(4):304-13.
Phan VA, Yven C, Lawrence G, Chabanet C, Reparet JM, Salles C. 2008. *in vivo* sodium release related to salty perception during eating model cheeses of different textures. Int.Dairy J. 18(9):956-63.
Pineau N, Schlich P, Cordelle S, Mathonnière C, Issanchou S, Imbert A, Rogeaux M, Etiévant P, Köster E. 2009. Temporal Dominance of Sensations: Construction of the TDS curves and comparison with time–intensity. Food Quality and Preference 20(6):450-5.
Pionnier E, Chabanet C, Mioche L, Taylor AJ, Le Quere JL, Salles C. 2004. 2. *in vivo* nonvolatile release during eating of a model cheese: Relationships with oral parameters. J.Agric.Food Chem. 52(3):565-71.
Prinz JF, Lucas PW. 1995. Swallow thresholds in human mastication. Arch.Oral Biol. 40(5):401-3.
Rosett T, Wu Z, Schmidt S, Ennis D, Klein B. 1995. Kcl, Cacl2, Na+ Binding, and Salt Taste of Gum Systems. J.Food Sci. 60(4):849.
Ruusunen M, Simolin M, Puolanne E. 2001. The effect of fat content and flavor enhancers on the perceived saltiness of cooked 'bologna-type' sausages. Journal of Muscle Foods 12(2):107-20.
Ruusunen M, Puolanne E. 2005. Reducing sodium intake from meat products. Meat Sci. 70(3):531-41.
Saccani G, Parolari G, Tanzi E, Rabbuti S. 2004. Sensory and microbiological properties of dried hams treated with high hydrostatic pressure. Proceedings of 50th international congress of meat science and technology 726–729.
Saint-Eve A, Lauverjat C, Magnan C, Deleris I, Souchon I. 2009. Reducing salt and fat content: Impact of composition, texture and cognitive interactions on the perception of flavoured model cheeses. Food Chem. 116(1):167-75.
Salles C, Chagnon M, Feron G, Guichard E, Laboure H, Morzel M, Semon E, Tarrega A, Yven C. 2011. In-mouth mechanisms leading to flavor release and perception. Crit.Rev.Food Sci.Nutr. 51(1):67-90.
Serra X, Grèbol N, Guàrdia MD, Guerrero L, Gou P, Masoliver P, Gassiot M, Sárraga C, Monfort JM, Arnau J. 2007. High pressure applied to frozen ham at different process

stages. 2. Effect on the sensory attributes and on the colour characteristics of dry-cured ham. Meat Sci. 75(1):21-8.
Spence C. 2011. Mouth-watering: the influence of environmental and cognitive factors on salivation and gustatory/flavor perception. J.Texture Stud. 42(2):157-71.
Stieger M. 2011. Texture-taste interactions: Enhancement of taste intensity by structural modifications of the food matrix. Procedia Food Sci. 1(0):521-7.
Tarrega A, Yven C, Sémon E, Salles C. 2011. In-mouth aroma compound release during cheese consumption: Relationship with food bolus formation. Int.Dairy J. 21(5):358-64.
Väänänen T, Ikonen T, Jokela K, Serimaa R, Pietilä L, Pehu E. 2003. X-ray scattering study on potato (Solanum tuberosum L.) cultivars during winter storage. Carbohydr.Polym. 54(4):499-507.
van den Berg L, van Vliet T, van der Linden E, van Boekel MAJS, van de Velde F. 2007. Serum release: The hidden quality in fracturing composites. Food Hydrocoll. 21(3):420-32.
Ventanas S, Puolanne E, Tuorila H. 2010. Temporal changes of flavour and texture in cooked bologna type sausages as affected by fat and salt content. Meat Sci. 85(3):410-9.

2.5 Tables and Figures

Table 2.1. Effects of sodium-protein interaction on the initial availability of sodium in the 1st stage of saltiness perception (release from food matrix)[a].

System	Treatment	Result	Explanation	Source
Model cheese[b]	Content variation: F ↑ (0.07 - 0.15 kg/kg; DM fixed; P ↓ accordingly) or DM ↑ (0.25 - 0.37 or 0.37 - 0.44 kg/kg; F/P mass ratio fixed)	For all samples, $K_{NaCl} < 1$	Sodium-casein (phosphoserine residue) electrostatic interaction reduced amount of sodium available for outward migration.	(Lauverjat and others 2009)
Model cheese[c]	F/P mass ratio ↑ (20/28 - 28/20; DM content fixed)	In-mouth sodium release and saltiness ↑; ^{23}Na-NMR determined bound fraction of sodium ↓; transverse relaxation time ↑	Cations were retained mainly by proteins via electrostatic interactions with its phosphoserine and carboxyl residues.	(Boisard and others 2014)
'Bologna-type' sausage	F content ↓ (0.28 - 0.08 kg/kg; replaced with H_2O or lean meat)	Total NaCl content unchanged; saltiness ↓ only in lean-meat replacing sample	Sodium-meat protein interaction reduced amount of sodium available for perception.	(Ruusunen and others 2001)
Dry-cured ham	High-pressure processing (HPP, 600 MPa, 360 s)	Total NaCl content unchanged; saltiness ↑	HPP weakened the sodium-meat protein interaction, thus yielded more sodium available for perception.	(Clariana and others 2011)

a. DM: dry matter, F: fat, K_{NaCl}: partition coefficient of NaCl, P: protein.
b. Made by renneting the mixtures of anhydrous milk fat (AMF), ultrafiltered skim milk retentate powder, NaCl, and water.
c. Made with AMF, rennet casein, acid casein, melting salts, NaCl, and water.

Table 2.2. Effects of tortuosity or sieving on the spontaneous diffusion of sodium in the 1st stage of saltiness perception (release from food matrix)[a].

System	Treatment	Result	Explanation	Source
Chicken sausage	F/P mass ratio ↓ (2.5 - 1)	Sodium release and saltiness ↑	Lowering F content led to less masking to sodium release.	(Chabanet and others 2013)
Franks	F content ↓ (0.3 - 0.05 kg/kg; replaced with H_2O)	Saltines ↑	Lowering fat content decreased hydrophobic barriers that impeded sodium migration in the gel, and thus enhanced sodium release.	(Hughes and others 1997)
Model cheese[b]	F content ↓ (0.3 - 0.2 kg/kg; DM content ↓ accordingly)	Sodium release rate ↑		(Phan and others 2008)
Model cheese[c]	Renneting	$*D_{NaCl}$ ↓	Renneting induced network development by protein, resulting in gelation.	(Panouille and others 2011)
	DM content ↑ (0.26 - 0.43 kg/kg)	$*D_{NaCl}$ ↓	Increased DM content gave higher volume occupation by protein and fat, and higher viscoelasticity (in renneted samples).	
Model cheese[c]	DM content ↑ (0.25 - 0.37 or 0.37 - 0.4 kg/kg) or F content ↓ (0.15 - 0.07 kg/kg; replaced with P)	$*D_{NaCl}$ ↓	Higher DM content led to higher firmness, lower amount of available water and a more pronounced sieving effect of protein network; protein impeded sodium more effectively than fat did.	(Lauverjat and others 2009)
	NaCl content ↓ (0.015 - 0.005 kg/kg)	$*D_{NaCl}$ ↓	NaCl content reduction limited the modification of gel structure, and in turn altered the sodium migration.	
Model cheese[c]	DM content ↑ (0.37 - 0.44 kg/kg)	$*D_{NaCl}$ ↓	DM content increment resulted in a more crosslinked, less fluffier network, and thus generated higher friction against sodium migration.	(Floury and others 2009)
	NaCl content ↓ (0.005 - 0.015 kg/kg)	$*D_{NaCl}$ ↓	Sodium content reduction led to tighter casein network structure, and thus impeded sodium migration.	
	pH ↓ (6.5 - 6.2)	$*D_{NaCl}$ ↓	pH reduction led to poorer hydration of casein micelle, and hence lower solubility of the protein, disfavoring sodium migration.	

a. DM: dry matter, F: fat, P: protein, $*D_{NaCl}$: apparent diffusion coefficient of sodium.
b. Made with anhydrous milk fat, rennet casein, melting salts, and water.
c. Made by renneting mixtures of anhydrous milk fat, ultrafiltered skim milk retentate powder, NaCl, and water.

Table 2.3. Effects of serum release on the migration of sodium under matrix deformation in the 1st stage of saltiness perception (release from food matrix).

System	Treatment	Result	Explanation	Source
Transglutaminase restructured dry-cured hams with reduced sodium	High-pressure processing (HPP, 600 MPa, 360 s)	Poorer water holding capacity (WHC), and saltiness ↑, but sodium content unchanged	HPP led to poorer WHC of muscle proteins, resulting in higher serum release during sample deformation, which carried out more sodium available for perception.	(Fulladosa and others 2009)
Restructured dry-cured ham	HPP (600 MPa, 360 s)	Saltiness ↑		(Fulladosa and others 2012)
Sliced and vacuum-packaged commercial dry-cured ham	HPP (400 MPa, 360 s)	Saltiness ↑		(Clariana and others 2012)
Gellan/whey protein isolate gel made by acid-induced cold gelation	Gellan content ↑ (dry matter content adjusted to reach similar large-scale deformation property)	Serum release ↑ Sensory juiciness↑ Saltiness ↑	Gellan increment changed the gel morphology from protein-continuous to bi-continuous, leading to higher gel permeability which carried out sodium faster.	(Stieger 2011)

Table 2.4. Effects of fragmentation tendency on the migration of sodium under matrix deformation in the 1st stage of saltiness perception (release from food matrix)[a].

System	Treatment[a]	Result	Explanation[a]	Source
Commercial cheeses	Varying textural characteristics	Sensory rubbery ↑, in-mouth sodium release rate ↓	Rubbery samples disintegrated less extensively on each chew stroke, and thus gave slower sodium release.	(Jack and others 1995)
Gels made of LAG, HAG, KC, LBG	LAG or KC content ↑ (DM content fixed)	Fracture strain ↓; textural brittleness and sodium release rate ↑	Increase in LAG or KC content resulted in more brittle gels, yielding larger surface area after chewing, and thus boosted sodium release.	(Koliandris and others 2008)
Model cheese[b]	F content↑ (0 - 0.17 kg/kg; DM content ↑ accordingly)	Breakdown surface area and sodium release rate ↑; start time ↓ and duration of saltiness dominance ↑	Increased F content weakened the protein network of the gel, which broke down more easily and generated larger surface area beneficial to sodium release.	(de Loubens and others 2011a)
Model cheese[b]	P content ↓ (0.15 - 0.09 kg/kg; DM content fixed or ↓ accordingly)	Saltiness ↑	P content decrement led to higher brittleness and lower rubbery of the gel, which fragmented more easily and yield larger surface area.	(Panouille and others 2011)

a. DM: dry matter, F: fat, LAG: low acetyl-gellan, HAG: high acetyl-gellan, KC: κ-carrageenan, LBG: locust bean gum, P: protein.
b. Made by renneting mixtures of anhydrous milk fat, ultrafiltered skim milk retentate powder, sodium, and water.

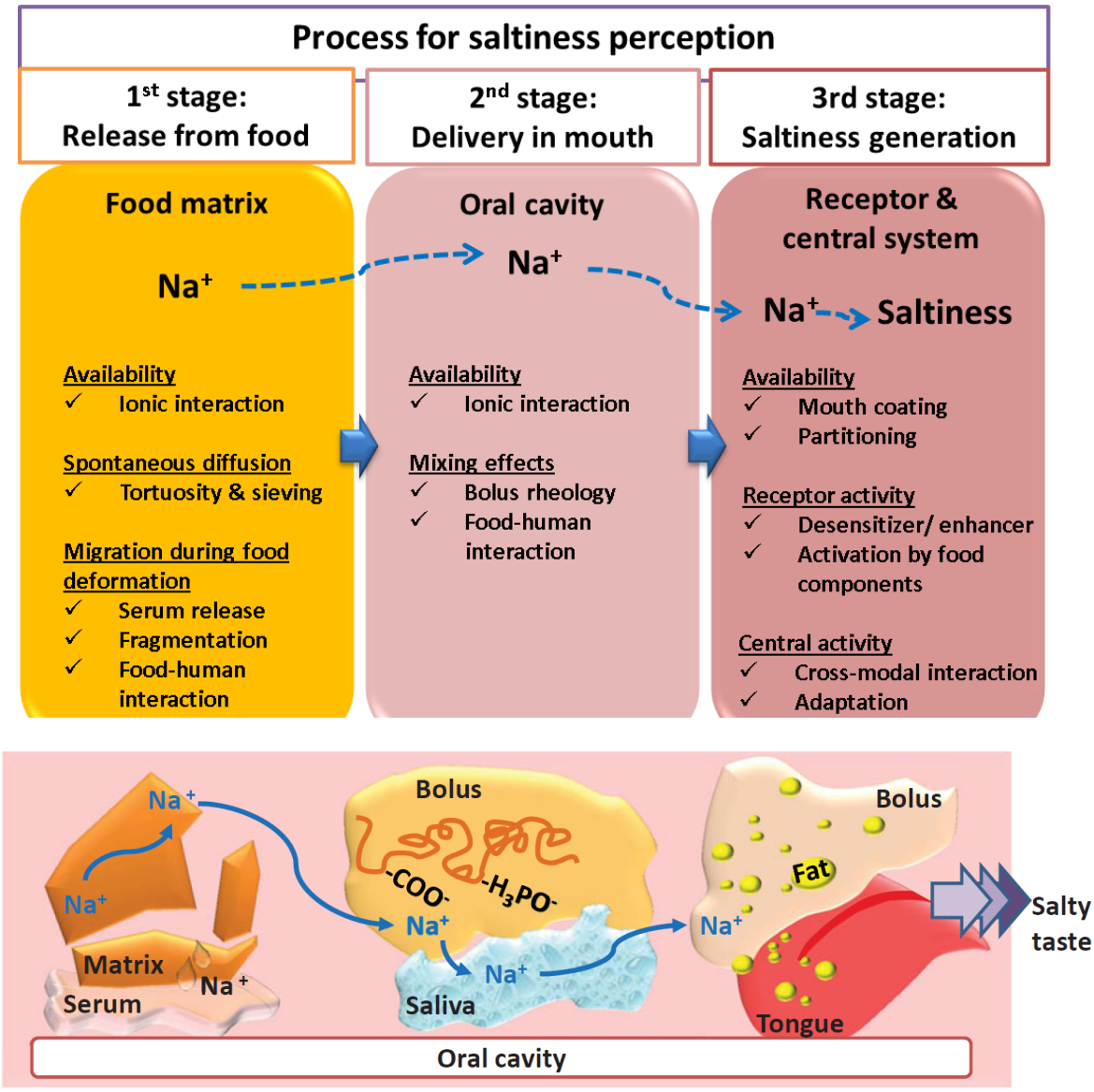

Figure 2.1. Schematic illustration of the matrix effects during the three stages of saltiness perception (Kuo and Lee 2014).

CHAPTER 3

Relating Porosity to Sodium Release of the Solid Lipoproteic Colloids[1]

3.1 Abstract

The microstructure of food can be engineered to enhance sodium release during mastication, which may be used as a strategy to reduce sodium content in foods. This study aimed to relate sodium release to microstructural properties of solid lipoproteic colloid (SLC) foods. The SLC gels with 1.5% (w/w) NaCl were prepared by homogenization of whey protein isolate and anhydrous milk fat, followed by heat-induced gelation. The gels varied in protein content (8 or 16%), fat content (0, 11, 22 or 33%), and homogenization pressures (14 or 55 MPa). The maximum rate of sodium release during the initial gel compression increased with increasing gel porosity and pore size. This was due to more releasable serum in the gels with larger pore volume and larger pores. The maximum concentration of sodium at the end of sodium release increased with reduced size of the fat particles in the gels. The smaller fat particles were dispersed more uniformly and interrupted the protein network more, and facilitated the gel breakdown. The above findings suggested that, during the breakdown of the SLC gels, the major mechanisms of sodium release are via serum release followed by sodium diffusion, which are governed by the gel porosity and the particle size of fat, respectively. This study demonstrated the dependence of temporal sodium release properties on the microstructural properties of an SLC food system. The findings from this study could lay the foundation for further investigation of the dependence of saltiness perception on SLC microstructure, which can provide insight for sodium reduction in SLC products.

Keywords

sodium reduction, sodium release, serum release, particle size, porosity

[1] ***The contents of this chapter has been published in: Kuo W, Lee Y. 2014. Temporal sodium release related to gel microstructural properties - implications for sodium reduction. J.Food Sci. 79(11):E2245-52. See Appendix A-2 for the reprint permission and the reprint.***

3.2 Introduction

Sodium overconsumption is an alarming health problem around the world. The global mean sodium intake in 2010 was 3,950 mg/day, nearly doubling the limit of 2,000 mg/day recommended by the World Health Organization (WHO) (Powles and others 2013). Diet high in sodium is the second highest dietary risk factor attributable to the global burden of disease in 2010 (Lim and others 2012). Evidences from multiple randomized trials have indicated the positive relationship between sodium intake and blood pressure (Aaron and Sanders 2013). Overconsumption of sodium has been associated with the development or severity of several chronic diseases such as cardiovascular diseases (Cook and others 2014), bone diseases, kidney stones, gastric cancer, and asthma (Doyle and Glass 2010). Though there have been mixed findings on the association between health and sodium reduction at further lower level (2,300 mg/day to 1,500 mg/day), the health benefits of lowering excessive sodium intake to 2,300 mg/day are widely agreed and advised by the most recent report of the Institute of Medicine (Committee on the Consequences of Sodium Reduction in Populations 2013). Based on the US *National Health and Nutrition Examination* Survey (*NHANES*) 2003-2008, 91% of US adults consume more than 2,300 mg of sodium per day, (Cogswell and others 2012). Overconsumption of sodium is believed to be a major cause of the 65% incidence rate of hypertension or pre-hypertension of the US adults, leading to 100,000 annual deaths and $73.4 billion medical costs in 2009 (Danaei and others 2009; Henney and others 2010a). An estimate of $7 billion annual savings in health care can be achieved by reducing the average dietary sodium intake by 400 mg/day (DGAC 2005; DGAC 2010). Nevertheless, given the initiation of sodium reduction act early in the 1960s, from 1988 to 2010, the mean dietary sodium intake by the US males and females stayed stable around 4,000 and 3,000 mg per day, respectively (Henney and others 2010a; Henney and others 2010b; Anand, J., Goldman, J.D., Steinfeldt, L.C., Montville, J.B., Heendeniya, K.Y., Omolewa-Tomobi, G., Enns, C.W., Ahuja, J.K., Martin, C.L., LaComb, R.P., Moshfegh, A.J. 2012; Cogswell and others 2012).

More than 70% of dietary sodium comes from processed foods (Mattes and Donnelly 1991; Anderson and others 2010). Among the processed foods, solid lipoproteic colloid (SLC) foods such as cheese and sausage, which bear fat/protein emulsion structure, are significant sources of sodium (DGAC 2010). A recent study on SLC model foods revealed that, depending on the chewing behavior of individuals, 70-95% sodium is not released before swallowing (Phan and others 2008). Thus, engineering the matrix microstructure to enhance sodium release is a promising solution for sodium reduction in processed SLC foods

(Stieger and van de Velde 2013). The reduction of sodium content in SLC foods may cause safety issues or alter the product quality such as flavor and texture attributes. Nevertheless, with combined techniques, the microbiological and sensory properties of reduced-sodium foods can be ensured to meet the standards (Grummer and others 2013; Juneja and others 2013).

Previous studies showed that sodium release is affected by several microstructural properties of the food matrix (Stieger and van de Velde 2013). The porosity, which is defined as the volume fraction of voids occupied with fluids in the gel, is positively correlated with serum release during the gel compression (van den Berg and others 2007a). Besides, the gels with bi-continuous network structure yielded higher serum release than the gels with homogeneous structure (van den Berg and others 2008). Increase in serum release of food products can boost the release and perception intensity of tastants such as sucrose (Sala and others 2010) or sodium chloride (Stieger 2011; van de Velde and Adamse 2013). Nevertheless, the above studies were based on protein/polysaccharide mixture systems without the incorporation of emulsion structures, and thus the implications may not be extended to the SLC foods.

In another series of studies, the effects of emulsion structures on sodium release of SLC model gels were assessed. Increase in fat content or decrease in particle size of fat was found to cause greater extent of gel breakdown and thus more sodium release (Boisard and others 2013, 2014; de Loubens and others 2011a; de Loubens and others 2011b; Panouille and others 2011). However, little is known regarding the dependence of sodium release on serum release in SLC gels with varying emulsion structures. Lawrence and others (2012a) reported a positive correlation between the in-mouth sodium release and the water content of the SLC gels. Phan and others (2008) observed that the factors dominating the in-mouth sodium release of model SLC gels changed with chewing time. In the initial 20 sec of chewing, the samples with higher water content had higher sodium release, while after 60 sec of chewing, the samples with higher fat content had higher sodium release. This could infer that the sodium release depends more on serum release in the initial stage of chewing, but depends more on gel fragmentation with prolonged chewing. However, the suggested hypothesis above was not confirmed by the instrumental analyses of serum release and sodium release. To construct a more comprehensive picture of temporal sodium release as a function of the SLC gel microstructures, studies with standardized measurements of sodium release and sufficient characterization of gel microstructures and textures are needed.

To the best of our knowledge, there has not yet been any study that examined the relationship between sodium release and multiple microstructural properties in the same SLC system. The objective of this study is to relate temporal sodium release to critical microstructural properties, including porosity, pore size and particle size of fat of the SLC gels. Effects of these microstructural properties on the temporal sodium release properties, including the maximum rate of sodium release, the maximum concentration of released sodium, and the area under the sodium concentration-time curve, are discussed. To help explain the microstructural influences on sodium release, the serum release and textural properties related to the microstructures and sodium release of the SLC gels were also analyzed.

3.3 Materials and Methods

3.3.1 Preparation of the SLC gels

Table 1 lists the formulas and homogenization pressures of the SLC gels. Whey protein isolate (WPI, Hilmar 9000, Hilmar Ingredients, Hilmar, CA) and anhydrous milk fat (AMF, Berkshire Dairy & Food Products, LLC, Wyomissing, PA) were used to prepare the 6 SLC gels. The SLC gels in this study contained 1.5% (w/w) NaCl and 2 levels of protein (8 and 16%, w/w). For the gels with 8% protein, the fat levels varied from 0, 22 to 33% (w/w) to evaluate the effects of direct increment of fat contents on the gel microstructures and sodium release. For the gels with 16% protein, the fat level was 11% so as the solid content to be similar to the gels of 8% protein and 22% fat. In addition, for the gels with the highest fat content (33%) and the gels with highest protein content (16%), two different homogenization pressures (14 and 55 MPa) were used to observe the effects of pressure on the structures in the gels. The SLC gel codes represent their formulas and homogenization pressures as follows: protein (%)-fat (%)-NaCl (%)-pressure (MPa). When making the SLC gels, WPI was first suspended in the NaCl solution by stirring for 10 min at room temperature. Then, the WPI suspension was incubated at 45˚C for 20 min, followed by storage at 6-8˚C for 16 hr to ensure complete hydration of the WPI powder. Before the pre-homogenization, the WPI suspension was incubated at 45˚C for 20 min. The WPI suspension was pre-homogenized with the 45˚C pre-warmed AMF at 11,600 rpm for 3 min using an IKA T-25 Digital High-Speed Homogenizer (IKA Works Inc., NC). The pre-homogenized emulsion was then incubated at 45˚C for 40 min. Afterward, the pre-homogenized emulsion was pressure

homogenized for 3 min using the APV two stage homogenizer (SPX Flow Technology, Denmark) with first stage at 14 or 55 MPa and second stage at 3.4 MPa. The pressure-homogenized emulsion was then subjected to 170 mmHg vacuum at room temperature for 20 min to eliminate air bubbles. To make the SLC gel, the emulsion was filled into a Teflon tube (150 mm length, 25.4 mm inner diameter) with both ends sealed with rubber stoppers. The Teflon tube was then heated in 90˚C water bath for 30 min, followed by 16 hr storage at 6-8˚C. Three to five batches were made for each SLC gel sample.

3.3.2 Characterization of structural properties

3.3.2.1 Particle size

For the dynamic light scattering (DLS) measurement, the freshly prepared emulsion after vacuum treatment was examined at 25°C by ZetaPALS zeta potential analyzer (Brookhaven Instruments Co., Holtsville, NY). Intensity-weighted particle size distribution was collected from the average of three readings, and the D_{90} values were obtained for each distribution of particle sizes in the intensity profiles. Three to five measurements on the DLS were completed for each sample.

3.3.2.2 ESEM images

Environmental scanning electron microscopy (ESEM) with a field-emission electron gun (FEI Company, Hillsboro, OR) was used to characterize the microstructures of the SLC gels. A 3 x 3 x 7 mm^3 sample stick cut from the cylindrical gel was frozen fractured in liquid N_2, mounted on the stage, immediately put into ESEM to allow ice sublimation at 1 Torr wet mode, and then, observed with accelerating voltage of 20 kV. The gel micrographs were processed using Matlab (Version 7.0.4.356 R14, The Mathworks Inc., Natick, Massachusetts). A series of functions available in the Matlab Image Processing Toolbox (MathWorks 2014) was used to process the grayscale images of the gel micrographs. The Matlab code for the process described below is attached in Appendix B1. First, the ‘tophat’ and the ‘wiener2’ filters were applied to even the background and to smooth the pore morphology, respectively. An improved grayscale thresholding method including the application of two thresholds was developed to accurately analyze the porosity and pore size of the samples. The first threshold was applied to separate the pore from the matrix. The grayscale intensity of the threshold at which the maximum number of pore could be identified was used (Salvador and others 2009). The second threshold was then applied to remove the

foreground regions that protruded from the major plane of the matrix. These foreground regions were believed to be the artifacts made during the freeze-fracture step prior to the ESEM observation. The grayscale intensity of second threshold was determined by multiplying 1.25 to the grayscale intensity of the first threshold. At this ratio, the grayscale intensity of the second threshold was approximately the same as that determined by the triangle method (Zack and others 1977) used in previous literature. The binary image obtained after the thresholding was then further processed with the 'imclose' filter to dilate narrow breaks and to erode small objects. Then the watershed segmentation was used to separate the connected objects. The porosity was calculated as the percent area with black pixel (pores) versus the total area analyzed. The pore size was expressed as equivalent diameter of a circle. The ESEM characterization and image analysis for each batch preparation of the sample were made triplicates.

3.3.2.3 Measurement of *in vitro* sodium release

The *in vitro* sodium release was determined by combining a compression test using a texture analyzer (TA-XT2i, Texture Technologies Corp., Scarsdale, N.Y.) with a conductivity measurement (de Loubens and others 2011a) at room temperature (23°C). As shown in Figure 1(A), a cylindrical SLC gel (25.4 mm diameter, 25.4 mm length) was placed in a 500 mL jar, under a TA-25 cylinder probe (50 mm diameter, aluminum) of the texture analyzer. Also sitting in the jar was a mechanical stirrer and a conductivity probe (Orion DuraProbe 4-Electrode Conductivity Cells 013005MD) connected with an Orion VERSA STAR Multiparameter Benchtop Meter (Thermo Fisher Scientific Inc. Waltham, MA). The measurement was initiated by addition of 400 mL DI water into the jar at time 0 s, and followed by the gel compression at time 25 s. The sample was compressed at the crosshead speed of 1.0 mm/s till 80% of strain. The conductivity was read every 5 s for a total of 365 s, during which the water was stirred at 200 rpm to ensure constant concentration of sodium within the jar. Three parameters were extracted from the concentration-time profiles of the *in vitro* sodium release measurement (Figure 1B). The maximum rate of sodium release, R_{max}, is the greatest slope calculated from any three continuous data points alone the concentration-time curve. The maximum concentration of released sodium, I_{max}, is the sodium concentration at the end of the measurement. The area under the curve of sodium release, AUC, is the integrated area under the concentration-time curve.

3.3.2.4 Serum release and texture analysis

The SLC gels cut into 25.4 mm long cylinders were hermetically stored at room temperature for 3 hr before the texture analysis by the TA-XT2i Texture Analyzer (Texture Technologies Corp., Scarsdale, N.Y.). A combined compression test and serum release measurement was performed with a TA-25 cylinder probe (50 mm diameter, aluminum) at room temperature (23°C). A thin layer of mineral oil (Sigma 330779, Sigma-Aldrich, St. Louis, MO), was spread on top of the gel. The gel sample was then placed on the Whatman 42 filter paper (Maidstone, Kent, UK) right before the test. The force was measured during compression with the crosshead speed of 1.0 mm/s with the maximum strain of 80%. These compression conditions have been identified to well reflect the sensory texture properties (Xiong and others 2002). To quantify the serum release, the filter paper was removed and weighed right after the compression test.

3.3.3 Statistical analysis

The means across the measurement replications for each sample batch were taken, and the results were analyzed using the SAS Software (SAS 9.3, SAS Institute Inc., Cary, NC). The proc glm and the LSMEANS with the adjusted Tukey test were used to analyze the difference between the means of the samples.

3.4 Results and Discussion

3.4.1 Microstructural difference between the SLC gels

Figure 2 shows the ESEM images of the frozen fractured SLC gels. Differences in porosity and pore size can be observed between the SLC gels with varying formula and homogenization pressures. These visual differences shown in Figure 2 can be further confirmed by the image analysis results presented in Table 2. The particle sizes of protein aggregates and fat in different SLC emulsions are included in Table 2. For the protein particles, the non-fat sample 8-0-1.5-55 had three distributions, whereas the other samples had only one. The distribution of the smallest protein found in the sample 8-0-1.5-55 was not detected in the fat-containing samples, probably due to its relatively low scattering intensity compared to the fat particles (data not shown). The distribution of the largest protein in the sample 8-0-1.5-55 was not found in the fat-containing samples. It may be due to the presence

of fat which used a portion of the protein as the emulsifier, and also interfered with the protein aggregation.

The microstructure of the non-fat sample (8-0-1.5-55, Figure 2A) was especially different from the other five samples (Figure 2B-F). The non-fat sample 8-0-1.5-55 was comprised of coarsely aggregated protein particles and had large pores. Whereas the other samples were formed by tightly linked, continuous network with relatively lower porosities and pore sizes (Table 2). For the SLC gels with the same protein content (samples 8-0-1.5-55, 8-22-1.5-55 and 8-33-1.5-55; Figure 2A, B and C), both the porosity and pore size decreased with increasing fat content (Table 2). This was due to the lower moisture contents with increasing amounts of fat. For the SLC gels with similar dry matter contents (samples 8-22-1.5-55 and 16-11-1.5-55; Figure 2B and E), the gel with higher protein but lower fat content (sample 16-11-1.5-55) had lower porosity and smaller pore size (Table 2). This is believed to be caused by the greater structure forming capacity of protein than fat. Both protein and fat occupy the space in the gels and hence reduce the void volume. However, protein can be hydrated and thus entrap water molecules as part of its structure (Geurts 1974). Also, protein can form 3-D network which may embed small voids within its network. Therefore, at similar dry matter contents, the sample with higher fraction of protein showed lower porosity and pore size. When comparing the SLC gels with the same formulation but different homogenization pressures (16-11-1.5-14 vs. 16-11-1.5-55 and 8-33-1.5-14 vs. 8-33-1.5-55), the samples prepared using higher pressure showed lower sizes of the fat globules (Table 2). This was due to more extensive homogenization at higher pressures, and the similar results were reported in a previous study (Huppertz 2011).

3.4.2 *in vitro* sodium release properties of the SLC gels

The representative sodium concentration–time curves of the *in vitro* sodium release are illustrated in Figure 1(B). Table 3 shows the 3 parameters extracted from the sodium concentration-time curves. During the compression and breakdown of a gel matrix in aqueous media, sodium is released from the gel into the surroundings via either convective or diffusive transfer (Kuo and Lee, in press). In the beginning of the uniaxial compression, the SLC gels dilated along the radial direction and expelled considerable amount of releasable serum. The same manner of gel deformation was also observed by van den Berg and others (2007a) from protein/polysaccharide gels. This fast release of serum transferred relatively

large amount of the dissolved sodium from the gel to the surrounding. The sudden release of sodium resulted in the initial abrupt increment of sodium concentration in the surrounding liquid, which accounted for the R_{max}. Therefore, the sodium migration during the gel compression can be considered as primarily through the convective transfer by the serum. After the compression, sodium continued to migrate from the gel into the aqueous phase via diffusion along the concentration gradient between the gel and the aqueous phase. This accounted for the continuing increment of the sodium concentration in the sodium release profile. The total amount of sodium released at the end of measurement was reflected by the I_{max} value, and the cumulative concentration of sodium along the release time was reflected by the AUC.

The profiles of the *in vitro* sodium release of the SLC gels varied with the gel formula and homogenization pressures. The sample 8-0-1.5-55 showed the fastest sodium release (greatest R_{max} value, Table 3) during the gel compression, but the concentration increment reached a plateau earlier than any other gels. Comparing those fat-containing samples, the samples with relatively lower protein but higher fat contents (8-22-1.5-55, 8-33-1.5-55 and 8-33-1.5-14) released more sodium (greater I_{max} and AUC, Table 3) than those gels with relatively higher protein content (16-11-1.5-55 and 16-11-1.5-14). At the same formula, sample 16-11-1.5-55 released more sodium (Table 3) than sample 16-11-1.5-14. The microstructural factors that led to different texture, serum release, and, thus, the different sodium release properties of the SLC gels are discussed further in the following sections.

3.4.3 Effect of fat content on sodium release

Comparing the formula in Table 1 and the sodium release properties in Table 3 implied that the fat content has significant impact on the sodium release of the SLC gels. At constant protein concentration (samples 8-0-1.5-55, 8-22-1.5-55 and 8-33-1.5-55), the increase in the fat content led to increased I_{max} values. This may be attributed to the lowered values of strain at maximum stress (Table 4) with increased fat content. Although for these three samples, the maximum stress increased with increasing fat content due to elevated dry matter contents, the decreased values of strain at maximum stress suggested earlier fracture of the gels. The earlier fracture could result in greater extent of gel breakdown and hence create larger surface area of the gel for sodium release (Koliandris and others 2008). The differences in deformation of the gels due to the compression can be seen in Figure 3. The sample 8-0-

1.5-55 (Figure 3A) was only compressed but not fractured throughout the tests, whereas the samples 8-22-1.5-55 and 8-33-1.5-55 (Figure 3B and C, respectively) broke into multiple pieces associated with various sizes of small debris. Figure 3(G) shows the internal structure of a representative fat-containing sample (8-22-1.5-55) at higher magnification. Many globular fat particles are embedded in the protein network, and some of the fat particles are indicated by the arrows in Figure 3(G). The embedded fat could interfere with the network structure of protein, generating more points of fracture upon compression. This could explain the increased degree of breakdown with increasing fat contents among samples 8-0-1.5-55, 8-22-1.5-55 and 8-33-1.5-55. As a result, the gels with higher fat content yielded greater surface area after fracture, which could lead to greater sodium release. The reduced fracture strain and enhanced sodium release with increasing fat content were also reported by previous literature of model dairy gel made of renneted milk powder (de Loubens and others 2011a; Panouillé and others 2011).

van den Berg and others (2007a, b) corrected the fracture properties of protein/polysaccharide gels for the effect of serum release. In this study, when the textural properties were also corrected for the serum release according to the calculations of van den Berg and others (2007a, b) (data not shown), the trends of textural properties among different gels discussed above remain valid.

The effects of fat content on sodium release is more pronounced when comparing the SLC gels with similar dry matter contents (samples 8-22-1.5-55 and 16-11-1.5-55). The sample 8-22-1.5-55 with higher fat content has significantly lower values of maximum stress and strain at maximum stress (Table 4), and significantly higher I_{max} and AUC (Table 3). In addition, the higher I_{max} and AUC values of the samples 8-22-1.5-55 compared to the sample 16-11-1.5-55 could be partly due to the difference in ionic interaction. Previous literature has identified that the sodium-protein interaction in the lipoproteic foods reduces the amount of free sodium available for release (Ruusunen and others 2001; Lauverjat and others 2009; Boisard and others 2013). Thus, the increased interaction between sodium and protein might have decreased the sodium mobility for the sample 16-11-1.5-55, and led to lower sodium release. Boisard and others (2013, 2014) also studied the effects of fat content in model cheese with constant dry matter contents. The *in vitro* sodium release rate, in-mouth sodium release, and saltiness perception increased with increased fat/protein ratio. They ascribed it to the weaker structure of the cheese and higher sodium mobility, evidenced by the lower stress at maximal deformation and the higher NMR relaxation times of sodium, respectively.

However, Lawrence and others (2012a) reported that the maximum sodium concentration released from the lipoproteic matrices in mouth was negatively related with the ratio between fat and dry matter content. They hypothesized that the fat served as the barrier which retarded sodium release. The sample breakdown in their study was done by multiple chews in mouth, and should be more extensive than that in the present study. Also, for the sample with higher fat content and thus lower fracture stress, the panelists may use less work and time to chew (Lawrence and others 2012b). This could ultimately result in similar breakdown degree between the samples with varying fat contents. Hence, it is possible that, in their study, the barrier effect of fat is more pronounced than the gel breakdown effect of fat, and led to the results opposite from our findings.

3.4.4 Effects of emulsion particle sizes on sodium release

In addition to compositional properties such as fat content, emulsion particle size also affected the I_{max} of the SLC gels. When comparing the two SLC gels with same formula but different homogenization pressures (16-11-1.5-14 and 16-11-1.5-55), sample 16-11-1.5-55 has lower size of the fat globules (Table 2) and higher I_{max} (Table 3). This is again related to the lower value of strain at maximum stress (Table 4) of sample 16-11-1.5-55, which implied greater surface area of the broken pieces and thus enhanced sodium release. The similar relationship in particle size, I_{max}, and strain at maximum stress was noticed from the samples 8-33-1.5-55 and 8-33-1.5-14, although statistically not significant. At constant fat content, the SLC gel with smaller fat globules has a higher number of fat globules randomly dispersed in the protein network. These highly dispersed fat globules interfere with the formation of protein network, and thus accounted for earlier and greater extent of breakdown upon compression. The greater extent of breakdown of the sample 16-11-1.5-55 (Figure 3E) than sample 16-11-1.5-14 (Figure 3F) can also be identified from the images of the broken gels. The side view image of the sample 16-11-1.5-55 (Figure 3E) shows more broken pieces than that of the sample 16-11-1.5-14 (Figure 3F). A previous study on the model cheese made of rennet casein also found that lower size of fat globules was associated with reduced fracture stress and fracture energy and higher concentration of sodium release (Phan and others 2008). The relationship described above, however, was not significant between the samples 8-33-1.5-55 and 8-33-1.5-14. This is possibly because of the high fat content relative to protein leading to weak gels. Thus, the size of fat globules showed less impact on the I_{max} and the

strain at maximum stress for the samples 8-33-1.5-55 and 8-33-1.5-14 than for the samples 16-11-1.5-55 and 16-11-1.5-14.

3.4.5 Effect of porosity and pore size on sodium release

While the I_{max} values of the sodium release were closely associated with the fat content and the size of the fat globules, the maximum rate of sodium release, R_{max}, depended primarily on the porosity and pore size of the SLC gels.

The sample 8-0-1.5-55 has the highest porosity and pore size (Table 2) and highest R_{max} value among the samples (Table 3). This was attributed to the greatest serum release of this sample (Table 4). As discussed in the previous section, the serum release during gel compression is accounted for the R_{max} values of the *in vitro* sodium release. According to previous studies (van den Berg and others 2007b; Stieger and van de Velde 2013), serum release had a strong positive correlation to gel porosity, and coarse stranded gels had higher serum release. In addition, the hydraulic permeability, which describes the ease of fluid transport through pore spaces, is proportional to the square of pore radius (Sakai 1994). As discussed in the previous section, the sample 8-0-1.5-55 had coarsely aggregated protein particles and considerable void space and large pore size. Therefore, the highest R_{max} and serum release of the sample 8-0-1.5-55 can be attributed to the high porosity and large pore size of this sample. In a study on gellan/whey protein isolate (WPI) gel made by acid induced cold gelation (Stieger 2011), sodium release was boosted by engineering the microstructure of food matrix to enhance serum release. The authors showed that, with the increment in gellan content and the adjustment of dry matter content, the microstructure of the gel changed from protein-continuous to bi-continuous, while large deformation properties remained relatively close. The increase in permeability led to higher saltiness perception of the gel.

When comparing the two samples with similar dry matter contents but different fat content, the impacts of porosity and pore size on the R_{max} values could also be observed. As discussed in previous sections, the porosity and pore size were both significantly lower in sample 16-11-1.5-55 than in sample 8-22-1.5-55 (Table 2), due to the greater structure forming capacity of protein than fat. The serum release (Table 4) and R_{max} (Table 3) values of the sample 16-11-1.5-55 were accordingly lower than those of the sample 8-22-1.5-55. The differences, though, are not significant at $\alpha = 0.05$. Such lack of significance could result from the lower gel integrity of the sample 8-22-1.5-55 due to the greater structural

interference by fat. During the compression, the sample 8-22-1.5-55 broke earlier than the sample 16-11-1.5-55.

The earlier fracture could release the formal pressure on the gel, and thus lower the chance for the serum to be compressed out. In addition to the formal pressure, the serum release rate also depends on the gel porosity (van den Berg and others 2007a). Loss of porosity during the gel deformation could lead to levelling-off of the serum release. Future studies on the microstructural changes of the SLC gels after compression would help to identify the impact of porosity alteration during the compression on serum release. On the other hand, the lack of significant difference in the R_{max} values may partly be due to the comparatively high R_{max} value of the sample 8-0-1.5-55 than the other samples. In fact, when the adjusted Tukey test was performed on the five samples excluding the sample 8-0-1.5-55, the R_{max} value of the sample 8-22-1.5-55 was significantly higher than that of 16-11-1.5-55.

The effect of homogenization pressure on structural properties showed clear trends. The sample 16-11-1.5-55 has significantly lower porosity and pore size as compared to the sample 16-11-1.5-14 (Table 2). This difference can also be observed from Figure 2(E and F). The sample 16-11-1.5-55 displays finer network structure with smaller and more evenly-distributed pore size than that of the sample 16-11-1.5-14. This indicated that increased pressure of homogenization induced effective dispersion of protein particles and formation of a finer, more crosslinked gel network. The serum release of the sample 16-11-1.5-55 was significantly lower than that of the sample 16-11-1.5-14 (Table 4). This complies with the previous discussion about the impacts of porosity and pore size on serum release. The trend of porosity, pore size, serum release, R_{max} values and I_{max} values between the samples 8-33-1.5-55 and 8-33-1.5-14 were similar to those between the samples 16-11-1.5-55 and 16-11-1.5-14. However, the differences in porosity and pore size are not significant at $\alpha = 0.05$. This may indicate that the change of homogenization pressure is more effective in creating structural variations of protein-rich gels than in fat-rich gels.

In the study of Lawrence and others (2012a) on the lipoproteic matrices, the maximum sodium concentration during the in-mouth sodium release assessment was positively correlated with the water content of the samples. They related this to the higher solvating capacity of sodium with enhanced water content. If the serum release and sensory juiciness were evaluated, it would help to identify the mechanisms behind the positive relationship between sodium release and water content of the samples in their study.

3.5 Conclusions

This study explored the dependence of sodium release on multiple structural properties of the SLC gels using quantitative analyses of *in vitro* sodium release, gel microstructures, and textures. The parameters from the *in vitro* sodium release curves, describing the temporal sodium release properties, were closely related with various microstructural properties and the associated textural properties of the SLC gels. Generally, the R_{max}, maximum rate of sodium release during the gel compression, increased with increasing porosity and pore size of the gels owning to greater serum release. The I_{max}, maximum concentration of sodium released, increased with increasing fat content or decreasing particle size of fat owning to more extensive gel breakdown. The findings from this study provided insights for engineering the microstructure of SLC-based products to modify the temporal properties of sodium release. Optimized food structure can effectively amplify saltiness and achieve the sodium reduction in the SLC-based products with a further understanding of the correlation between the sodium release and saltiness perception.

3.6 References

Aaron KJ, Sanders PW. 2013. Role of dietary salt and potassium intake in cardiovascular health and disease: A review of the evidence. Mayo Clin Proc 88(9):987-95.

Anand, J, Goldman, JD, Steinfeldt, LC, Montville, JB, Heendeniya, KY, Omolewa-Tomobi, G, Enns, CW, Ahuja, JK, Martin, CL, LaComb, RP, Moshfegh, AJ. 2012. What We Eat In America, NHANES 2009-2010: Documentation and Data Files. FASEB Journal 27.

Anderson CAM, Appel LJ, Okuda N, Brown IJ, Chan Q, Zhao L, Ueshima H, Kesteloot H, Miura K, Curb JD, Yoshita K, Elliott P, Yamamoto ME, Stamler J. 2010. Dietary sources of sodium in China, Japan, the United Kingdom, and the United States, women and men aged 40 to 59 years: The INTERMAP Study. J Am Diet Assoc 110(5):736-45.

Boisard L, Andriot I, Arnould C, Achilleos C, Salles C, Guichard E. 2013. Structure and composition of model cheeses influence sodium NMR mobility, kinetics of sodium release and sodium partition coefficients. Food Chem 136(2):1070-7.

Boisard L, Andriot I, Martin C, Septier C, Boissard V, Salles C, Guichard E. 2014. The salt and lipid composition of model cheeses modifies in-mouth flavour release and perception related to the free sodium ion content. Food Chem. 145(0):437-44.

Cogswell ME, Zhang Z, Carriquiry AL, Gunn JP, Kuklina EV, Saydah SH, Yang Q, Moshfegh AJ. 2012. Sodium and potassium intakes among US adults: NHANES 2003-2008. Am J Clin Nutr 96(3):647-57.

Committee on the Consequences of Sodium Reduction in Populations. 2013. Findings and conclusions. In: Brian L. Strom, Ann L. Yaktine, and Maria Oria, editors. Sodium intake in populations: assessment of evidence. Washington, D.C.: The National Academies Press. p 119-126.

Cook NR, Appel LJ, Whelton PK. 2014. Lower Levels of Sodium Intake and Reduced Cardiovascular Risk. Circulation 129(9):981-9.

Danaei G, Ding EL, Mozaffarian D, Taylor B, Rehm J, Murray CJL, Ezzati M. 2009. The preventable causes of death in the United States: Comparative risk assessment of dietary, lifestyle, and metabolic risk factors. Plos Medicine 6(4):e1000058.

de Loubens C, Panouillé M, Saint-Eve A, Déléris I, Tréléa IC, Souchon I. 2011a. Mechanistic model of in vitro salt release from model dairy gels based on standardized breakdown test simulating mastication. J Food Eng 105(1):161-8.

de Loubens C, Saint-Eve A, Deleris I, Panouille M, Doyennette M, Trelea IC, Souchon I. 2011b. Mechanistic model to understand in vivo salt release and perception during the consumption of dairy gels. J Agric Food Chem 59(6):2534-42.

DGAC. 2010. Report of the Dietary Guidelines Advisory Committee on the Dietary Guidelines for Americans, 2010, to the Secretary of Agriculture and the Secretary of Health and Human Services. U.S. Department of Agriculture, Agricultural Research Service, Washington, DC.

DGAC. 2005. Report of the Dietary Guidelines Advisory Committee on the Dietary Guidelines for Americans, 2005, to the Secretary of Agriculture and the Secretary of Health and Human Services. U.S. Department of Agriculture, Agricultural Research Service, Washington, DC.

Doyle ME, Glass KA. 2010. Sodium reduction and its effect on food safety, food quality, and human health. Compr Rev Food Sci F 9(1):44-56.

Geurts TJ. 1974. Transport of salt and water during salting of cheese. I. Analysis of the processes involved. Nederlands melk- en zuiveltijdschrift 28(2):102-29.

Grummer J, Bobowski N, Karalus M, Vickers Z, Schoenfuss T. 2013. Use of potassium chloride and flavor enhancers in low sodium Cheddar cheese. J Dairy Sci 96(3):1401-18.

Henney JE, Taylor CL, Boon CS. 2010a. Preface. In: Committee on Strategies to Reduce Sodium Intake, Institute of Medicine, editor. Strategies to reduce sodium intake in the United States. Washington, D.C.: The National Academies Press. p ix.
Henney JE, Taylor CL, Boon CS. 2010b. Sodium intake reduction: an important but elusive public health goal. In: Committee on Strategies to Reduce Sodium Intake, Institute of Medicine, editor. Strategies to reduce sodium intake in the United States. Washington, D.C.: The National Academies Press. p 29-66.
Huppertz T. 2011. Homogenization of Milk | High-Pressure Homogenizers. In: John W. Fuquay, editor. Encyclopedia of Dairy Sciences (Second Edition). San Diego: Academic Press. p 755-60.
Juneja VK, Altuntaş EG, Ayhan K, Hwang C, Sheen S, Friedman M. 2013. Predictive model for the reduction of heat resistance of Listeria monocytogenes in ground beef by the combined effect of sodium chloride and apple polyphenols. Int J Food Microbiol 164(1):54-9.
Koliandris A, Lee A, Ferry A, Hill S, Mitchell J. 2008. Relationship between structure of hydrocolloid gels and solutions and flavour release. Food Hydrocoll 22(4):623-30.
Kuo W, Lee Y. 2014. Effect of food matrix on saltiness perception – implications for sodium reduction. Compr Rev Food Sci F 13:906-923.
Lawrence G, Buchin S, Achilleos C, Berodier F, Septier C, Courcoux P, Salles C. 2012a. *in vivo* sodium release and saltiness perception in solid lipoprotein matrices. 1. Effect of composition and texture. J Agric Food Chem 60(21):5287-98.
Lawrence G, Septier C, Achilleos C, Courcoux P, Salles C. 2012b. *in vivo* sodium release and saltiness perception in solid lipoprotein matrices. 2. Impact of oral parameters. J Agric Food Chem 60(21):5299-306.
Lauverjat C, Deleris I, Trelea IC, Salles C, Souchon I. 2009. Salt and aroma compound release in model cheeses in relation to their mobility. J Agric Food Chem 57(21):9878-87.
Lim SS, Vos T, Flaxman AD, Danaei G, Shibuya K, Adair-Rohani H, AlMazroa MA, Amann M, Anderson HR, Andrews KG, Aryee M, Atkinson C, Bacchus LJ, Bahalim AN, Balakrishnan K, Balmes J, Barker-Collo S, Baxter A, Bell ML, Blore JD, Blyth F, Bonner C, Borges G, Bourne R, Boussinesq M, Brauer M, Brooks P, Bruce NG, Brunekreef B, Bryan-Hancock C, Bucello C, Buchbinder R, Bull F, Burnett RT, Byers TE, Calabria B, Carapetis J, Carnahan E, Chafe Z, Charlson F, Chen H, Chen JS, Cheng AT, Child JC, Cohen A, Colson KE, Cowie BC, Darby S, Darling S, Davis A, Degenhardt L, Dentener F, Des Jarlais DC, Devries K, Dherani M, Ding EL, Dorsey ER, Driscoll T, Edmond K, Ali SE, Engell RE, Erwin PJ, Fahimi S, Falder G, Farzadfar F, Ferrari A, Finucane MM, Flaxman S, Fowkes FGR, Freedman G, Freeman MK, Gakidou E, Ghosh S, Giovannucci E, Gmel G, Graham K, Grainger R, Grant B, Gunnell D, Gutierrez HR, Hall W, Hoek HW, Hogan A, Hosgood III HD, Hoy D, Hu H, Hubbell BJ, Hutchings SJ, Ibeanusi SE, Jacklyn GL, Jasrasaria R, Jonas JB, Kan H, Kanis JA, Kassebaum N, Kawakami N, Khang Y, Khatibzadeh S, Khoo J, Kok C, Laden F, Lalloo R, Lan Q, Lathlean T, Leasher JL, Leigh J, Li Y, Lin JK, Lipshultz SE, London S, Lozano R, Lu Y, Mak J, Malekzadeh R, Mallinger L, Marcenes W, March L, Marks R, Martin R, McGale P, McGrath J, Mehta S, Memish ZA, Mensah GA, Merriman TR, Micha R, Michaud C, Mishra V, Hanafiah KM, Mokdad AA, Morawska L, Mozaffarian D, Murphy T, Naghavi M, Neal B, Nelson PK, Nolla JM, Norman R, Olives C, Omer SB, Orchard J, Osborne R, Ostro B, Page A, Pandey KD, Parry CD, Passmore E, Patra J, Pearce N, Pelizzari PM, Petzold M, Phillips MR, Pope D, Pope III CA, Powles J, Rao M, Razavi H, Rehfuess EA, Rehm JT, Ritz B, Rivara FP, Roberts T, Robinson C, Rodriguez-Portales JA, Romieu I, Room R, Rosenfeld LC, Roy A, Rushton L, Salomon JA, Sampson U, Sanchez-Riera L, Sanman E, Sapkota A, Seedat S, Shi P, Shield K, Shivakoti R, Singh GM, Sleet DA, Smith E, Smith KR,

Stapelberg NJ, Steenland K, Stöckl H, Stovner LJ, Straif K, Straney L, Thurston GD, Tran JH, Van Dingenen R, van Donkelaar A, Veerman JL, Vijayakumar L, Weintraub R, Weissman MM, White RA, Whiteford H, Wiersma ST, Wilkinson JD, Williams HC, Williams W, Wilson N, Woolf AD, Yip P, Zielinski JM, Lopez AD, Murray CJ, Ezzati M. 2012. A comparative risk assessment of burden of disease and injury attributable to 67 risk factors and risk factor clusters in 21 regions, 1990–2010: a systematic analysis for the Global Burden of Disease Study 2010. The Lancet 380(9859):2224-60.

Functions in image processing toolbox [Internet]. : MathWorks; 2014 [Accessed 2014 March 17]. Available from: http://www.mathworks.com/help/images/functionlist.html

Mattes RD, Donnelly D. 1991. Relative contributions of dietary-sodium sources. J Am Coll Nutr 10(4):383-93.

Panouille M, Saint-Eve A, de Loubens C, Deleris I, Souchon I. 2011. Understanding of the influence of composition, structure and texture on salty perception in model dairy products. Food Hydrocoll 25(4):716-23.

Phan VA, Yven C, Lawrence G, Chabanet C, Reparet JM, Salles C. 2008. *in vivo* sodium release related to salty perception during eating model cheeses of different textures. Int Dairy J 18(9):956-63.

Powles J, Fahimi S, Micha R, Khatibzadeh S, Shi P, Ezzati M, Engell RE, Lim SS, Danaei G, Mozaffarian D, on behalf of the Global Burden of Diseases Nutrition and Chronic Diseases Expert Group (NutriCoDE). 2013. Global, regional and national sodium intakes in 1990 and 2010: a systematic analysis of 24 h urinary sodium excretion and dietary surveys worldwide. BMJ Open 3(12):e003733.

Ruusunen M, Simolin M, Puolanne E. 2001. The effect of fat content and flavor enhancers on the perceived saltiness of cooked 'bologna-type' sausages. Journal of Muscle Foods 12(2):107-20.

Sakai K. 1994. Determination of pore size and pore size distribution: 2. Dialysis membranes. J Membr Sci 96(1–2):91-130.

Sala G, Stieger M, van de Velde F. 2010. Serum release boosts sweetness intensity in gels. Food Hydrocoll 24(5):494-501.

Salvador P, Toldrà M, Saguer E, Carretero C, Parés D. 2009. Microstructure–function relationships of heat-induced gels of porcine haemoglobin. Food Hydrocoll 23(7):1654-9.

Stieger M. 2011. Texture-taste interactions: Enhancement of taste intensity by structural modifications of the food matrix. Procedia Food Sci 1(0):521-7.

Stieger M, van de Velde F. 2013. Microstructure, texture and oral processing: New ways to reduce sugar and salt in foods. Curr Opin Colloid In 18(4):334-48.

van de Velde F, Adamse M. 2013. Juiciness enhances the perceived saltiness of meat products. New Food 2.

van den Berg L, van Vliet T, van der Linden E, van Boekel MAJS, van de Velde F. 2007a. Serum release: The hidden quality in fracturing composites. Food Hydrocoll 21(3):420-32.

van den Berg L, van Vliet T, van der Linden E, van Boekel MAJS, van de Velde F. 2007b. Breakdown properties and sensory perception of whey proteins/polysaccharide mixed gels as a function of microstructure. Food Hydrocoll 21(5–6):961-76.

van den Berg L, van Vliet T, van der Linden E, van Boekel MAJS, van de Velde F. 2008. Physical properties giving the sensory perception of whey proteins/polysaccharide gels. Food Biophys 3(2):198-206.

Xiong R, Meullenet JF, Hankins JA, Chung WK. 2002. Relationship between sensory and instrumental hardness of commercial cheeses. J Food Sci 67(2):877-83.

Zack G, Rogers W, Latt S. 1977. Automatic-measurement of sister chromatid exchange frequency. J Histochem Cytochem 25(7):741-53.

3.7 Tables and Figures

Table 3.1. Formula, homogenization pressure of the solid lipoproteic colloid gels and their compositional properties.

Sample name	Content (% w/w)			Homogenization pressure (MPa)	Dry matter (% w/w)
	Protein	Fat	NaCl		
8-0-1.5-55	8	0	1.5	55	11
8-22-1.5-55	8	22	1.5	55	32
8-33-1.5-55	8	33	1.5	55	45
8-33-1.5-14	8	33	1.5	14	45
16-11-1.5-55	16	11	1.5	55	30
16-11-1.5-14	16	11	1.5	14	30

Table 3.2. Structural properties of the solid lipoproteic colloid gels[a].

Sample	Particle size ± SD (nm)		Porosity ± SD (%)	Pore size ± SD (μm)
	Protein aggregates	Fat globules		
8-0-1.5-55	5.1 ± 0.4d 59.6 ± 15.2cd 240.5 ± 2.4a	-	83.1 ± 1.5a	1.953 ± 0.263a
8-22-1.5-55	84.9 ± 25.7c	289.9 ± 31.2b	67.7 ± 2.2b	0.978 ± 0.194b
8-33-1.5-55	60.5 ± 10.4cd	247.8 ± 18.2b	61.7 ± 1.5bc	0.955 ± 0.082b
8-33-1.5-14	195.4 ± 29.6ab	640.3 ± 69.3a	65.6 ± 1.4b	1.022 ± 0.114b
16-11-1.5-55	94.4 ± 13.3c	254.7 ± 3.7b	57.1 ± 5.7c	0.428 ± 0.060c
16-11-1.5-14	167.6 ± 16.9b	568.7 ± 22.3a	67.2 ± 2.0b	1.150 ± 0.111b

a. Means within the columns followed by the same letters are not significantly different ($P < 0.05$).

Table 3.3. Sodium release properties of the solid lipoproteic colloid gels[a].

Sample	R_{max}± SD[b] (ppm/s)	I_{max}± SD (ppm)	AUC ± SD (10^3 ppm.s)
8-0-1.5-55	2.99 ± 0.73a	50.32 ± 2.95b	15.728 ± 1.14a
8-22-1.5-55	0.74 ± 0.18b	75.90 ± 3.82a	16.584 ± 1.36a
8-33-1.5-55	0.82 ± 0.20b	79.13 ± 3.86a	17.72 ± 0.98a
8-33-1.5-14	0.73 ± 0.10b	76.20 ± 6.49a	16.80 ± 1.54a
16-11-1.5-55	0.36 ± 0.11b	43.23 ± 7.03b	9.676 ± 1.81b
16-11-1.5-14	0.34 ± 0.10b	33.83 ± 4.40c	8.024 ± 0.94b

a. Means within the columns followed by the same letters are not significantly different ($P < 0.05$).

b. R_{max}, maximum rate of sodium release; I_{max}, maximum concentration of released sodium; AUC, area under the curve of sodium release. See Materials and Method section for the complete description of the three sodium release parameters.

Table 3.4. Textural properties of the solid lipoproteic colloid gels[a].

Sample	Serum release ± SD (g)	Maximum stress ± SD (KPa)	Strain at maximum stress ± SD (%)
8-0-1.5-55	2.471 ± 0.166a	56.13 ± 9.39d	79.85 ± 0.32a
8-22-1.5-55	0.524 ± 0.035c	93.07 ± 9.37cd	55.08 ± 1.86c
8-33-1.5-55	0.301 ± 0.015d	169.72 ± 21.45b	55.87 ± 3.19c
8-33-1.5-14	0.485 ± 0.043c	100.92 ± 17.97c	59.79 ± 3.42c
16-11-1.5-55	0.449 ± 0.060cd	214.72 ± 51.01ab	67.80 ± 1.95b
16-11-1.5-14	0.767 ± 0.093b	236.21 ± 20.60a	78.06 ± 3.58a

a. Means within the columns followed by the same letters are not significantly different ($P < 0.05$).

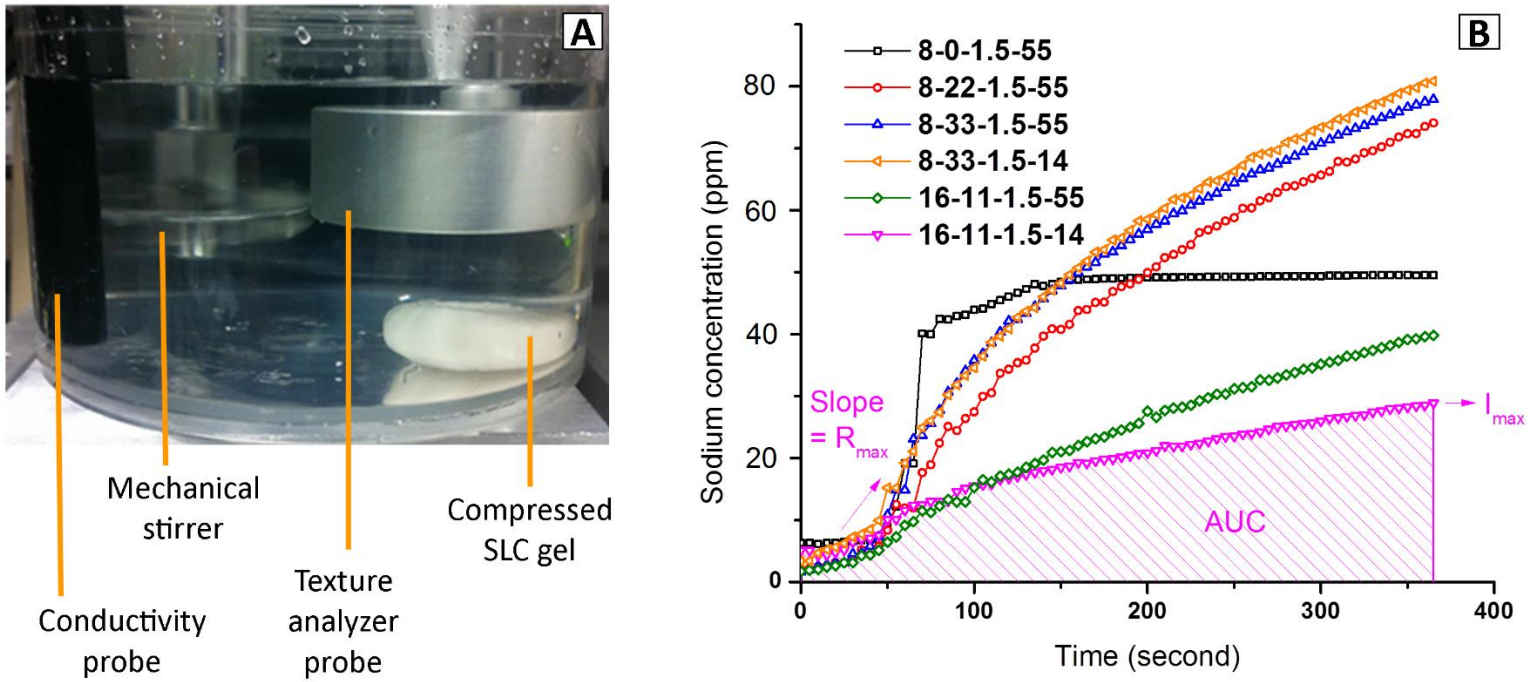

Figure 3.1. The measurement setting (A) and the representative curves (B) of the *in vitro* sodium release of the solid lipoproteic colloid gels. The maximum rate of sodium release, R_{max}, the maximum concentration of released sodium, I_{max}, and the area under the curve of sodium release, AUC were derived from each curve as indicated in the graph. Sample code represents protein (%,w/w)-fat (%,w/w)-NaCl (%,w/w)-homogenization pressure (MPa).

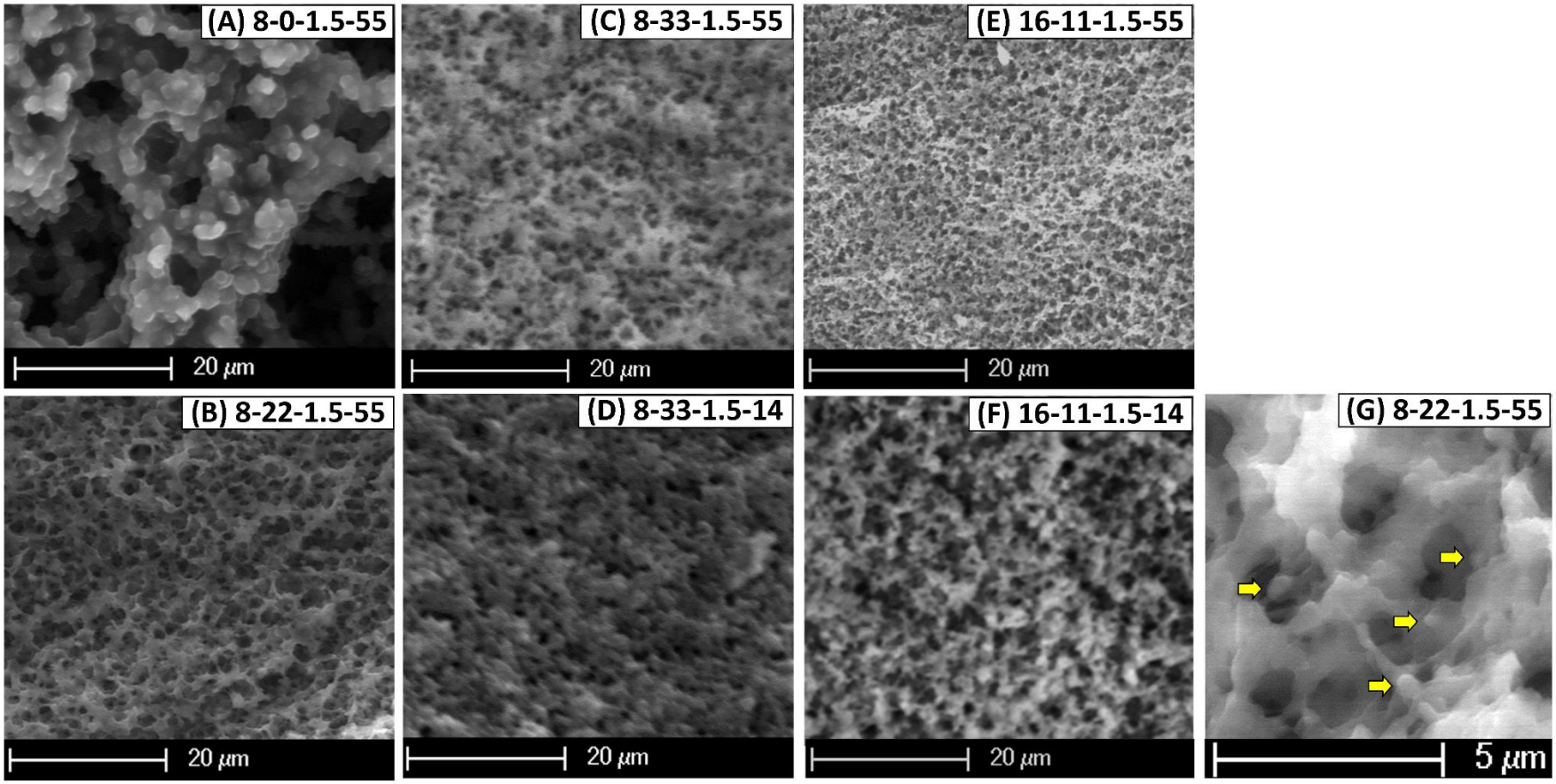

Figure 3.2. Environmental scanning electron microscopy (ESEM) images of the cross-sections of frozen-fractured lipoproteic emulsion gels. (A) 8-0-1.5-55, (B) 8-22-1.5-55, (C) 8-33-1.5-55, (D) 8-33-1.5-14, (E) 16-11-1.5-55, (F) 16-11-1.5-14, (G) 8-22-1.5-55 at higher magnification, showing the protein network embedded with fat particles (some pointed by the arrows). Sample code represents protein (%,w/w)-fat (%,w/w)-NaCl (%,w/w)-homogenization pressure (MPa).

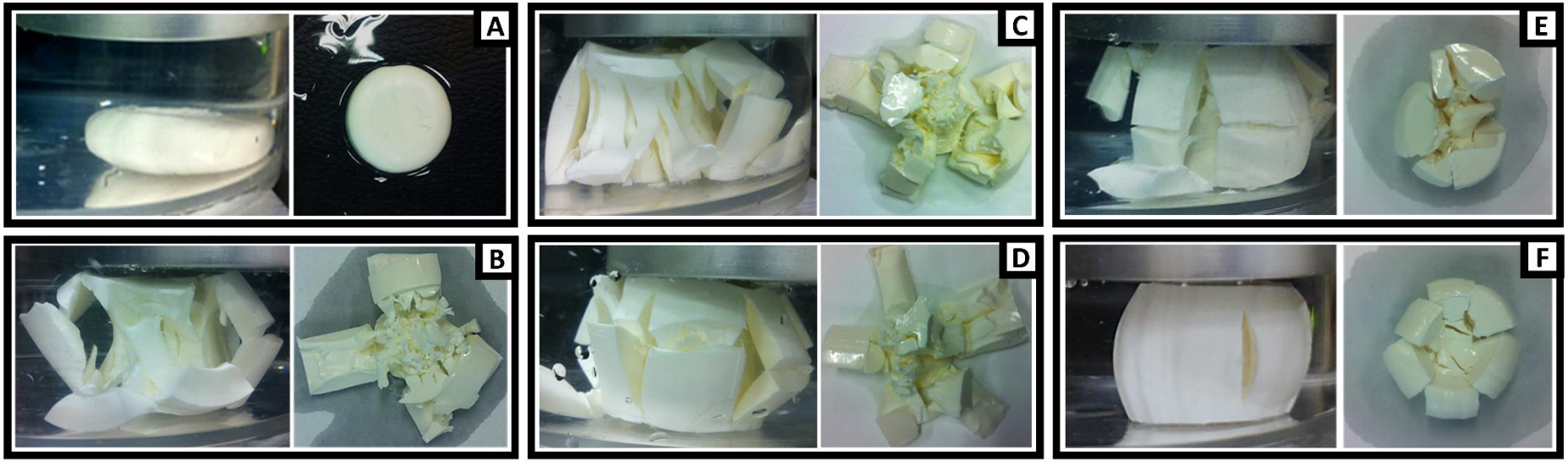

Figure 3.3. The solid lipoproteic colloid gels during the *in vitro* sodium release measurement (left of each graph) and after texture analysis (right of each graph). (A) 8-0-1.5-55, (B) 8-22-1.5-55, (C) 8-33-1.5-55, (D) 8-33-1.5-14, (E) 16-11-1.5-55, (F) 16-11-1.5-14. Sample code represents protein (%,w/w)-fat (%,w/w)-NaCl (%,w/w)-homogenization pressure (MPa).

CHAPTER 4

Relating Particle Size of Fat to Sodium Release of the Solid Lipoproteic Colloids[1]

4.1 Abstract

Sodium reduction in protein/lipid-based products such as cheese is becoming increasingly important to the food industry. Understanding the structure critical to sodium release is one of the keys to effectively controlling the sensory quality of the product while lowering the sodium content. In this study, ultra-small-angle X-ray scattering (USAXS), novel to food research, was used to characterize the structure of solid lipoproteic colloid (SLC) gels as a model food. The SLC gels were made via heat-induced gelation of emulsions of whey protein isolate and anhydrous milk fat. The gels varied in the contents of protein, fat, and NaCl and homogenization pressures. The gyration radii of the protein aggregates ($R_{g,p}$) and the fat globules ($R_{g,f}$) of the samples before and after the gelation were obtained via fitting the USAXS profiles to inspect the structure formation of the SLC gels. The effects of formulation and processing on the gel $R_{g,p}$ and the gel $R_{g,f}$ were analyzed. In addition, the gel $R_{g,f}$ and the hydrodynamic radius of the droplets ($R_{h,e}$) in the emulsions were correlated with sodium release. The correlation suggested that gel $R_{g,f}$ is a better indicator of sodium release than the emulsion $R_{h,e}$. The findings from this study indicated that USAXS is feasible for the structural investigation of protein/lipid-based foods.

Keywords

ultra-small-angle X-ray scattering (USAXS), solid lipoproteic colloid gel, sodium release, sodium reduction, whey protein isolate, structure

[1] ***The contents of this chapter has been published in: Kuo W, Ilavsky J, Lee Y. 2016. Structural characterization of solid lipoproteic colloid gels by ultra-small-angle X-ray scattering and the relation with sodium release. Food Hydrocoll. 56: 325-33. See Appendix A-3 for the reprint permission and the reprint.***

4.2 Introduction

Reducing the sodium content of food products based on lipid/protein emulsion structures such as cheese and processed meat has gained increasing attention in the food industry (Desmond 2006; Desmond 2007; Johnson and others 2009). Currently, industrial and experimental strategies for sodium reduction include stealth reduction (Phelps and others 2006), sodium replacement (Eoin 2006; Sinopoli and Lawless 2012), saltiness potentiation (Yamaguchi and Takahashi 1984; Brewer and others 1995; Heidolph and others 2011), multisensory application (Djordjevic and others 2004; Dotsch and others 2009), and physical modification of salt crystals (Heidolph and others 2011). More recently, the new concept of structural engineering has been proposed to enhance the sodium release and/or saltiness perception of the food matrix (Busch and others 2013; Stieger and van de Velde 2013; Jiménez-Colmenero 2013). The hypothesis underlying this strategy is that the structure of the food matrix dominates the physicochemical properties of the foods and hence the sodium release and saltiness perception of the food products (Kuo and Lee 2014a). Therefore, at a given salt level, the sodium release and saltiness perception of the food matrix can potentially be maximized by an optimized food structure.

Various mechanisms have been proposed in the literature to enhance sodium release via food structure modification. Sodium release is greater in foods with more available sodium, with a higher diffusion coefficient of sodium, with more serum release (i.e., the amount of squeezable liquid), or with a higher degree of fragmentation (Kuo and Lee 2014a). In lipoproteic foods, the availability of sodium has been increased by lowering the protein contents (Boisard and others 2014; Lauverjat and others 2009; Ruusunen and others 2005). Additionally, the diffusion coefficient of sodium in lipoproteic foods has been increased by lowering the fat or dry matter content (Chabanet and others 2013; Floury and others 2009; Hughes and others 1997; Lauverjat and others 2009; Panouille and others 2011; Phan and others 2008). In addition, lowering the degree of protein crosslinking lowered the diffusion coefficient of sodium (Panouille and others 2011). In a model polysaccharide/protein gel, the serum release was found to be higher in a bi-continuous microstructure than in a protein-continuous one (Stieger 2011). Lastly, the fragmentation degree of lipoproteic foods is greater with higher fat content (de Loubens and others 2011), lower protein content (Panouille and others 2011), or smaller particle size of the emulsion droplets (Kuo and Lee 2014b).

The increased sodium release in lipoproteic foods associated with smaller emulsion droplets was ascribed to the higher surface area after the food breakdown (Kuo and Lee 2014b). When emulsion gels undergo deformation, the initiation of fracture more likely starts at the interface between fat and protein than between protein and protein. This tendency is because the fat droplets are structural defects, and defects increase the stress concentration of the gel matrix (Sala and others 2009; van Vliet and others 1993). This property has been further demonstrated by reductions in the gel fracture strain, stress or energy and by increases in sodium release with higher fat contents or lower emulsion droplet particle sizes in lipoproteic gels (de Loubens and others 2011; Kuo and Lee 2014b; Panouille and others 2011; Phan and others 2008). Our previous study on model solid lipoproteic colloid (SLC) gels revealed that a higher homogenization pressure led to a lower hydrodynamic radius of the emulsion droplets ($R_{h,e}$), which implied an SLC gel network with more randomly dispersed structural defects. More structural defects thus led to easier fracture and higher surface area of the fractured debris. However, the increase in sodium release with reduced $R_{h,e}$ was not universally significant (Kuo and Lee 2014b). Because the $R_{h,e}$ was obtained from dynamic light scattering (DLS) of the emulsions prior to the heat-induced gelation, we hypothesized that the particle size of the actual fat globules within the lipoproteic gel correlates better than the emulsion $R_{h,e}$ to the fragmentation degree and thus the release of sodium. An ideal analytical tool to obtain the particle size of fat globules in solid gels is necessary to validate the hypothesis.

Currently, microscopy is the most relevant tool for analyzing the nano- and microstructures of solid foods, and electron microscopy has been extensively used for its suitable characterization range (Dudkiewicz and others 2012; Kalab and others 1995). However, electron microscopy usually requires sample pre-treatment, which can take several days and potentially damage the original food structure. In addition, electron microscopy is limited to 2-D imaging a thin layer or a surface (Harada and Matsuoka 2004) and thus may not represent the bulk sample well.

A small but increasing number of studies have been reported on using ultra-small-angle X-ray scattering (USAXS) to characterize biomaterials (Agrawal and others 2007; Nave and others 1986). Even fewer studies have used USAXS to study food systems (Peyronel and others 2014; Peyronel and others 2014; Väänänen and others 2003). Depending on the scattering angle, the family of X-ray scattering, including wide-, small-, and ultra-small-angle X-ray scattering, can provide structural information such as chemical

composition, crystallography, size, shape and association of particles at different scales (Dudkiewicz and others 2012). Typical pinhole small-angle X-ray scattering (SAXS) characterizes structures at 1 - 100 nm. With advanced USAXS instruments, the range can be extended to 1 nm - 1 μm (Ilavsky and others 2002; Ilavsky and others 2013; Ilavsky and others 2009). This range ideally covers the wide size range of individual components in foods and the associated structures of the components. Requiring minimal or no pre-treatment, USAXS provides ensemble 3-D structural information from a bulk sample while minimizing the damage of the structure. In addition, USAXS can be applied to turbid systems, such as solid fat and denatured protein, that light scattering is unable to characterize (Harada and Matsuoka 2004; Peyronel and others 2014). Using a synchrotron X-ray radiation source rather than a conventional source provides higher flux and thus higher contrast, so that normally low-contrast biomaterials or foods can be studied more effectively (Harada and Matsuoka 2004).

The objective of the present study is to use USAXS/pinhole SAXS to investigate the structure of SLC gels and to correlate the USAXS-derived structural properties in the gel with sodium release. The structure formation during the heat-induced gelation of the samples and the effects of formulation and treatment on the gyration radii of the protein aggregates ($R_{g,p}$) and the fat globules ($R_{g,f}$) are discussed. Two radius values, the USAXS-derived gel $R_{g,f}$ and the DLS-derived emulsion $R_{h,e}$, are compared for how well each correlates to sodium release from the SLC gels.

4.3 Materials and Methods

4.3.1 Materials and sample preparation

Whey protein isolate (WPI, Hilmar 9000, Hilmar Ingredients, Hilmar, CA, USA) and anhydrous milk fat (AMF, Berkshire Dairy & Food Products, LLC, Wyomissing, PA) were used to prepare the SLC gels. The SLC gels are coded according to their formula and homogenization pressure as Protein(%)-Fat(%)-NaCl(%)-pressure (MPa) (Table 1). The SLC gels in this study contained 2 levels of protein (8 and 16%, w/w), 4 levels of fat (0, 11, 22 and 33%, w/w), and 2 levels of NaCl (1.5 and 3.5%, w/w), and they were prepared under 2 different homogenization pressures (14 or 55 MPa). The formula of the samples in this study was chosen to approximate the contents and texture of commercial lipoproteic foods. The two homogenization pressures can result in significantly different emulsion $R_{h,e}$ values (Kuo and

Lee 2014b), which enables investigating the effects of fat globule particle size on the sodium released from the SLC gel. The SLC gel preparation was previously described in detail (Kuo and Lee 2014b). Briefly, WPI was suspended in a NaCl aqueous solution at 45°C and incubated at 6-8°C overnight. Then, the WPI suspension was pre-homogenized with pre-melted AMF at 45°C using an IKA T-25 Digital High-Speed Homogenizer (IKAWorks Inc., Wilmington, NC, USA). The pre-emulsion was pressure homogenized using an APV 2-stage homogenizer (15 MR, SPX Flow Technology, Soeborg, Denmark) and then heated at 90°C for 30 min to form the SLC gels. Three to five batches were made for each SLC gel sample.

4.3.2 USAXS measurement

The USAXS combined with pinhole SAXS was carried out using the Bonse-Hart double-crystal USAXS instrument at beamline 15-ID-D operated by ChemMatCARS at the Advanced Photon Source, Argonne National Laboratory, Argonne, IL, USA (Ilavsky and others 2009). The 1 mm thick gel sample was sealed in a silicone isolator (JTR20R-A2-1.0-Press-To-Seal, Grace Bio-Labs, Inc., Bend, Oregon, USA). After temperature equilibration for 3 h, the specimen was measured at the scattering vector range Q = 0.0001 to 1.35 $Å^{-1}$ at 20°C, where Q is equal to $4\pi\sin(\theta/2)/\lambda$, and θ and λ are the scattering angle and beam wavelength, respectively. The USAXS measurement was carried out for all samples listed in Table 1 except for one sample due to instrument operational error. Background and absorption corrections for the 1-D profile and subsequent data analyses were performed by IGOR Pro v6.12 with the Irena package (Ilavsky and Jemian 2009)**.** The Modeling II macro of the Irena package was used to fit the profile of the slit-smeared data (slit length 0.02677 and 0.028503 $Å^{-1}$ for the samples with 1.5% and 3.5% NaCl, respectively). A spheroid with an aspect ratio of one was used as the structure for the fittings of both $R_{g,p}$ and $R_{g,f}$ in this study. Selected SLC emulsions (Figure 4.1) were also measured prior to the heating to compare the structural change before and after the gelation.

4.3.3 Hydrodynamic radius, gel morphology, sodium release and textural properties

To investigate the correlations of the gel $R_{g,f}$ and the emulsion $R_{h,e}$ with sodium release from the gel, ten SLC samples (8-22-1.5-55, 8-33-1.5-55, 8-33-1.5-14, 16-11-1.5-55, 16-11-1.5-14 and their five counterparts with 3.5% NaCl) were selected for characterizations of the emulsion $R_{h,e}$, gel morphology, sodium release and textural properties. Our previous

study (Kuo and Lee 2014b) showed wide variations in sodium release across the SLC gels with 1.5% NaCl listed above. The samples with 3.5% NaCl were also selected to compare the effects of the gel $R_{g,f}$ and the emulsion $R_{h,e}$ at different levels of sodium.

The emulsion $R_{h,e}$ was observed via DLS using a ZetaPALS Zeta potential analyzer (Brookhaven Instruments Co., Holtsville, N.Y., U.S.A.) at 25˚C. After the vacuum procedure, the freshly made emulsions were diluted with DI water to reach the appropriate intensity for the DLS measurement. The $R_{h,e}$ values were collected from the intensity-weighted particle size distribution, which was averaged from 3 instrumental readings. Three to five DLS measurements were completed for each sample.

The internal morphology of the SLC gels was examined using environmental scanning electron microscopy with a field emission electron gun (ESEM, FEI Co., Hillsboro, Oreg., U.S.A.). The gels were cut into $3 \times 3 \times 7$ mm^3 sticks and then freeze fractured in liquid nitrogen. The freeze-fractured gels were immediately mounted on the stage, and ice in the samples was allowed to sublime (i.e., freeze etching) at 1 Torr using the wet mode in the ESEM chamber. The fractured face was then observed with an accelerating voltage of 20 kV.

The sodium release from the SLC gels was measured by simultaneously compressing the gel in DI water and measuring the conductivity of the water at room temperature (23 °C) (de Loubens and others 2011a). The samples were compressed using a texture analyzer (TA-XT2i, Texture Technologies Corp., Scarsdale, N.Y., U.S.A.). The conductivity was measured using a conductivity probe (Orion DuraProbe 4-Electrode Conductivity Cells 013005MD) connected with an Orion VERSA STAR Multiparameter Benchtop Meter (Thermo Fisher Scientific Inc., Waltham, Mass, U.S.A.). A cylindrical sample of SLC gel (25.4-mm dia., 25.4-mm length) was placed in a 500 mL jar under a TA-25 cylinder probe (50-mm dia., aluminum) of the texture analyzer. First, 400 mL of DI water was added into the jar. After 25 seconds, the texture analyzer began compressing the gel at a crosshead speed of 1.0 mm/s until 80% strain. The conductivity of the DI water was read every 5 s for a total of 365 s while the water was stirred at 200 rpm by a mechanical stirrer. Three parameters were extracted from the curves of the *in vitro* sodium release (Figure 4.2). The maximum rate of sodium release, R_{max}, is the greatest slope calculated from any 3 continuous data points along the concentration–time curve. The maximum concentration of released sodium, C_{max}, is the sodium concentration at the end of the measurement. The area under the curve of sodium release, AUC, is the integrated area under the concentration–time curve.

The textural properties of the SLC gels were measured via a compression test using the texture analyzer (TA-XT2i, Texture Technologies Corp., Scarsdale, N.Y., U.S.A.) at room temperature (23 °C). A thin layer of mineral oil (Sigma 330779, Sigma-Aldrich, St. Louis, Mo., U.S.A.) was spread on top of the gel. The gels were then compressed under the TA-25 cylinder probe (50-mm dia., aluminum) at a speed of 1 mm/s to a maximum strain of 80%. The serum release from the gels during the compression test was collected by a pre-weighed filter paper (Whatman 42, Maidstone, Kent, U.K.) placed underneath the gel. The serum release is the difference in the weight of the filter paper before and after the compression of the gel.

4.3.4 Statistical analyses

Pearson correlation was used for all the correlation analyses in this study. For all the SLC gels, the gel $R_{g,p}$ and the gel $R_{g,f}$ were correlated with the gel formula and treatment. For the ten further characterized samples (listed in Section 4.3.3), the USAXS-derived gel $R_{g,f}$ and the DLS-derived emulsion $R_{h,e}$ were correlated with the sodium release and textural properties of the SLC gels.

4.4 Results and Discussion

4.4.1 Structure of the SLC gels formed via heat-induced gelation

4.4.1.1 Structural formation of the non-fat gels

Figure 1A shows the USAXS profiles of the non-fat dispersions before the heat gelation process and their corresponding gels. The non-fat dispersions (Figure 4.1A, 8-0-1.5-14, 8-0-1.5-55, and 16-0-1.5-55 dispersions) presented knee-like patterns, with the knee at approximately 0.06 $Å^{-1}$. Based on the Guinier approximation, these curves represented the particles with the gyration radius (R_g) between 1.7 – 2.2 nm. These sizes corresponded to the R_gs of the native beta-lactoglobulin (bLG) monomers or dimers (1.4-1.7 and 2.1-2.3 nm, respectively) (Barteri and others 2000; Gottschalk and others 2003; Moitzi and others 2011; Verheul and others 1999; Witz and others 1964). These sizes also corresponded to the R_g of the native alpha-lactalbumin (aLA) (1.6 nm) (Arai and others 2002). In WPI, bLG is the most abundant component, followed by aLA (typically ranging from 44–70% w/w and 14–22% w/w, respectively) (Farrell Jr. and others 2004; Foegeding and others 2011; Lucey 2014).

Therefore, the $R_{g,p}$s of the above non-fat dispersions may be an average of the R_gs of the bLG and the aLA present in the sample.

The USAXS profiles of the non-fat gels (Figure 4.1A, 8-0-1.5-14, 8-0-1.5-55, and 16-0-1.5-55 gels) also displayed the knee-like patterns, but they were shifted toward the lower Q range compared with those of their corresponding dispersions. The Guinier approximation resulted in the $R_{g,p}$s of the gels ranging between 7.2 and 9.2 nm, much higher than the corresponding $R_{g,p}$s of the dispersions. These particles in the gels could be aggregates consisting of bLG and aLA. Previous research revealed that bLG formed aggregates with aLA via disulfide bonds and hydrophobic interactions when heated in an aqueous solution (Dalgleish and others 1997). Protein aggregates with a radius of 29 nm were reported when a WPI solution (3% w/w protein, 54 mM NaCl) was heated at 90°C for 5 min (Ryan and others 2012). The much smaller WPI aggregates found in this study as compared with those in previous studies could be due to the homogenization treatment prior to heating. The shearing force of the homogenization may have dispersed the protein particles, disrupting the inter-particle interactions and thus reducing the degree of aggregation. Our previous work has shown that the particle size of protein aggregates decreases with increasing homogenization pressure (Kuo and Lee 2014b). Additionally, differences in the concentrations of protein and NaCl and in the heating conditions could also lead to the varying particle size of the protein aggregates.

At the lower Q range ($Q < 0.005$ Å^{-1}), the non-fat dispersions (Figure 4.1A, 8-0-1.5-14, 8-0-1.5-55, and 16-0-1.5-55 dispersions) did not show any scattering signals, indicating a lack of larger structures at this scale (approximately 100 nm to 5 μm). The non-fat gels (Figure 4.1A, 8-0-1.5-14, 8-0-1.5-55, and 16-0-1.5-55 gels) showed a linear log-log decay in the Q range of 0.0002 – 0.002 Å^{-1}. A power law fitting in this Q range on the de-smeared data provided exponents of approximately 4. This power law decay is attributed to Porod scattering by the smooth surfaces of larger scatterers (Feigin and Svergun 1987; Yoshida and others 2014). The Guinier regions of these larger scatterers are beyond the lowest Q (corresponding to 2 μm) in the USAXS measurement in this study. These larger scatterers are believed to be the protein particulates in the SLC gels. These protein particulates, with sizes above 2 μm and smooth surfaces, can be identified in the ESEM image of the SLC gel 8-0-1.5-14 (Figure 4.3A).

4.4.1.2 Structure formation of the fat-containing SLC gels

Figure 4.1B shows the USAXS profiles of the fat–containing SLC emulsions before the heat gelation process and their corresponding gels. At Q = 0.15 $Å^{-1}$, a peak was observed in the patterns of the fat-containing samples. This peak is the diffraction of the 2L (bilayered stacking) form of the crystalline AMF within the fat globules in the emulsion structure (Lopez and others 2001). Similar to the non-fat dispersions (Figure 4.1A), the fat-containing emulsions (Figure 4.1B, 8-33-1.5-14, 8-33-1.5-55, 16-33-1.5-14 and 16-33-1.5-55 emulsions) exhibited scattering at approximately Q = 0.06 $Å^{-1}$, suggesting that this pattern was from the protein scattering. The $R_{g,p}$s of these particles, however, range between 2.4 and 4.6 nm, slightly higher than those in the non-fat emulsions (1.7 – 2.2 nm). The higher emulsion $R_{g,p}$s suggests more aggregation of the bLG or the aLA into oligomers. For example, the bLG octamer has an R_g of 3.4 nm (Timasheff and Townend 1964; Witz and others 1964). The higher degree of protein aggregation could be attributed to the relatively higher proportion of protein to water in the fat-containing emulsions than in the non-fat dispersions. For example, the proportion of protein to water in the emulsion 8-33-1.5-14 and the dispersion 8-0-1.5-14 are 0.12 and 0.09, respectively.

As in the non-fat samples (Figure 4.1A), the protein scattering patterns of the fat-containing samples shifted toward lower Qs after the gelation process (Figure 4.1B, 8-33-1.5-14, 8-33-1.5-55, 16-33-1.5-14 and 16-33-1.5-55 gels). The $R_{g,p}$s are again higher than their non-fat counterparts, ranging between 23 and 67 nm. This difference could be the net result from higher concentrations of NaCl and protein in the aqueous phase of the fat-containing samples. Previous studies on heating WPI and bLG solutions showed that the aggregate diameters increased with increasing NaCl concentrations due to lower intermolecular repulsion, enhanced chemical and physical aggregation, and lower protein solubility (Ryan and others 2012; Verheul and others 1998). Additionally, the aggregate association rate increased with increasing concentrations of either NaCl or protein (Bryant and McClements 2000; Marangoni and others 2000; Ryan and others 2012; Wu and others 2005).

At a Q of approximately 0.001 $Å^{-1}$, all the fat-containing samples (Figure 4.1B) showed clear knees in the scattering profiles, which were used to calculate the $R_{g,f}$. This pattern was attributed to the fat globules for the following reasons. First, this pattern was not observed in the profiles of the non-fat samples. Second, compared with $R_{g,p}$, this pattern

showed relatively moderate changes in size after the gelation, which better reflected the status of the fat globules rather than the protein aggregates during heating. Third, as will be discussed in section 4.4.3.1, ESEM observation of the cross-sectional area of the SLC gels revealed fat particles with a radius of approximately 500 nm, corresponding to the $R_{g,f}$ range between 77 and 711 nm (Table 2).

4.4.2 Effect of formulation and treatments on the SLC gel structure

Figure 4.4 shows the USAXS profiles of the SLC gels made with different formulas and at different homogenizations pressures. All the non-fat gels in Figure 4.4 shared similar profile features, including knee-like scattering from the protein aggregates and a power law decay representing the 3-D networking of the aggregates. Likewise, all the fat-containing gels in Figure 4.4 shared similar profile features, including an AMF diffraction peak and two knee-like scatterings from the protein aggregates and the fat globules. The AMF peak intensity increased with the increasing fat content in the formula, implying a successful incorporation of fat into the SLC gels. Additionally, the AMF peaks are broader in the gels made with higher homogenization pressure (Figure 4.4, C vs. A and D vs. B, 55 vs. 14 MPa). According to the Scherrer formula, wider diffraction peaks imply smaller crystallites (Patterson 1939). Hence the broader AMF peaks indicated smaller fat crystals in the fat globules. This finding confirmed that the higher pressure effectively dispersed the emulsion structure. Table 2 lists the values of the gel $R_{g,p}$ and $R_{g,f}$ derived from the Guinier approximation of the USAXS profiles. Overall, both the gel $R_{g,p}$ and $R_{g,f}$ decreased with increasing homogenization pressure ($p < 0.01$). This correlation is much stronger when only the fat-containing gels were analyzed ($p < 0.001$). Higher homogenization pressures have been shown to induce partial denaturation of proteins, improving protein adsorption on the fat globules and thus resulting in a more stable emulsion system (Lee and others 2009). Within the group of fat-containing gels made at the low homogenization pressure, the $R_{g,p}$ was positively correlated ($p < 0.01$) with the protein content and negatively correlated ($p < 0.05$) with fat content. A similar positive correlation between the gel $R_{g,p}$ and the protein content was found within the group of fat-containing gels made with the high homogenization pressure ($p < 0.05$). These correlations between the $R_{g,p}$s and the protein and fat contents indicated the counteracting behaviors between the protein and fat during the emulsification and gel formation. A higher protein content may promote the probability of protein-protein interaction, leading to larger protein aggregates. A higher fat content may interfere with the

protein association, preventing the growth of the protein aggregates. On the other hand, a higher fat content may require a greater fraction of protein for emulsification, reducing the available amount of protein for protein-protein interaction. In the group of fat-containing samples made with the higher homogenization pressure, the gel $R_{g,p}$ did not significantly depend on the fat content. This lack of dependence may be due to the more thorough dispersion of the protein at the higher pressure, which overcame the effect of fat content on the gel $R_{g,p}$.

4.4.3 Dependence of sodium release on the gel $R_{g,f}$ or emulsion $R_{h,e}$

4.4.3.1 Correlations between the gel $R_{g,f}$ and sodium release

To understand the influence of the gel $R_{g,f}$ and the emulsion $R_{h,e}$ on sodium release from the SLC gels, ten fat-containing SLC samples (listed in Section 4.3.3) were further characterized for sodium release, the texture and morphology of the gels, and the emulsion size, $R_{h,e}$. The sodium release by the gel as it was compressed by the texture analyzer was measured in water. However, the behavior of the textural properties of the samples acquired during the sodium release measurements was found to be consistent with the behavior observed in the actual textural analysis (data not shown). Hence, the breakdown properties of the gels observed from the textural analysis can be used to explain the differences in their sodium release properties. Table 3 shows the sodium release and textural properties of the SLC gels with 3.5% NaCl and the $R_{h,e}$ values of the corresponding emulsions. The properties of the SLC samples with 1.5% NaCl can be found in our previous study (Kuo and Lee 2014b). Table 4 shows some of the correlation coefficients between the above properties and the gel $R_{g,f}$ derived from USAXS. For the SLC gels with 3.5% NaCl, the gel $R_{g,f}$ was negatively correlated with the C_{max} (the maximum concentration of released sodium) and the AUC (area under the curve of sodium release vs. time plot) at a highly significant level ($p < 0.005$). These correlations can be attributed to the effect of fat on the breakdown properties of the SLC gels. Previous studies on SLC gels showed that, at the same total fat content, smaller fat globules implied a gel network with a higher number of randomly dispersed fat particles (Kuo and Lee 2014b; Phan and others 2008). As fat interfered with the integrity of the protein network, the higher number of dispersed fat particles could lead to a greater extent of breakdown and more debris when compressed. This hypothesis can be supported by the positive correlation found between the gel $R_{g,f}$ and the strain at the maximum stress of the

SLC gels with 3.5% NaCl (Table 4). In other words, the required strain to break the gels decreased as the gel $R_{g,f}$ decreased. The greater extent of breakdown and more debris, which results in more total surface area for the broken gels, would favor the enhanced release of sodium from the gel in a given period of time (de Loubens and others 2011). This hypothesis can be supported by the negative correlations of the strain at maximum stress with the C_{max} and with the AUC in the SLC gels with 3.5% NaCl (Table 4). The negative correlation between the gel $R_{g,f}$ and the sodium release, however, was not significant in the SLC gels with 1.5% NaCl. This lack of significance may be due to a difference in the force of inter-protein interaction among the SLC gels with varying NaCl contents. A higher amount of NaCl in the SLC gels implied greater charge screening on the repulsive force between protein molecules. Previous studies showed that this improved screening favored the aggregation, branching, and densification of whey protein particles (Langton and Hermansson 1996; Pouzot and others 2004; Verheul and others 1998). Hence, an overall stronger protein-protein interaction was expected in the protein networks with higher NaCl contents (Hussain and others 2012; Lorenzen and Schrader 2006). As a result, the SLC gels with 3.5% NaCl exhibited relatively stronger inter-protein interaction than the SLC gels with 1.5% NaCl, and this stronger interaction made the initiation of break upon compression more likely to occur at the protein-fat interface. In other words, the properties of the protein-fat interface dominated the breakdown properties of the SLC gels with 3.5% NaCl. Decreased gel $R_{g,f}$ led to higher sodium release due to increases in the surface area, the probability of break initiation, and the extent of breakdown. In contrast, the protein-protein interaction in the SLC gels with 1.5% NaCl was weaker than that with 3.5% NaCl, and thus the breakdown at the protein-fat interface might not have been dominant. This difference explained the lack of correlation between the gel $R_{g,f}$, the strain at maximum stress, and the sodium release in the SLC gels with 1.5% NaCl. The above hypothesis can be supported by the ESEM images of the SLC gels shown in Figure 4.3. The SLC gels with 3.5% NaCl displayed a denser and more aggregated network morphology than that of the SLC gels with 1.5% NaCl, which suggested greater protein-protein interaction at higher NaCl contents. Furthermore, for the two SLC gels with 3.5% NaCl made with the lower homogenization pressure (8-33-3.5-14 and 16-11-3.5-14, Figures 4.3J and L), some bright spherical fat particles stood out from the protein network. In the images of the corresponding 1.5% NaCl gels (8-33-1.5-14 and 16-11-1.5-14, Figures 4.3D and F), these fat globules were less visible and more embedded within the protein network. This difference in the appearance of the fat globules among the protein

matrix indicated a possibly stronger protein-protein interaction and weaker protein-fat interaction in the SLC gels with the higher NaCl content.

4.4.3.2 Correlations between the emulsion $R_{h,e}$ and sodium release during compression

No significant correlation was found between the emulsion $R_{h,e}$ and the sodium release from the SLC gels with either 1.5 or 3.5% NaCl (Table 4). This lack of correlation could be because the emulsion $R_{h,e}$ was measured in the SLC emulsions before the heat-induced gelation. Among the 10 samples that underwent the correlation analysis, most of them showed less than ±10% difference between the gel $R_{g,f}$ and the emulsion $R_{h,e}$ values. This consistency implied that the emulsion droplets were relatively stable during the heating process. However, for the samples 16-11-1.5-14 and 16-11-3.5-14, the gel $R_{g,f}$ values were 61% and 101% greater than the emulsion $R_{h,e}$ values. This increase suggested that the emulsion droplets in these two samples were less stable and might have coalesced more drastically during the heating.

According to Figure 4.1B showing some selected SLC samples with 1.5% NaCl, the $R_{g,f}$s grew by 10 to 50% after the gelation. Hence, the fat globules in both SLC gels made with 1.5% and 3.5% NaCl exhibited inconsistent degrees of coalescence as a result of the heating. In the case of 3.5% NaCl, because the gel breakdown and accordingly the sodium release were directly related to the size of the fat globules in the gel, the USAXS-derived gel $R_{g,f}$ proved to be more predictive of sodium release than the DLS-based emulsion $R_{h,e}$.

4.5 Conclusions

In this study, USAXS was successfully used as a novel technique to investigate the structure of SLC gels and as a demonstration of its potential to predict the sodium release properties of the gels. The protein in the SLC emulsions underwent heat-induced aggregation during the gelation process, resulting in significant increases in the particle sizes of the protein aggregates. Additionally, the fat-containing gels had much larger protein aggregates compared with those in the non-fat gels. The sizes of the fat globules were comparatively more stable than those of the protein aggregates throughout the gelation. The gel $R_{g,p}$ and the gel $R_{g,f}$ were negatively correlated with the homogenization pressure, and the protein and fat contents counteractively affected the protein aggregation. For the SLC gels made with the higher NaCl content, the USAXS-derived gel $R_{g,f}$ predicted the sodium release better than the DLS-based emulsion $R_{h,e}$ did. With sodium being the primary chemical for salty stimuli, present findings in the literature do not agree on whether saltiness perception depends primarily on the maximum rate (de Loubens and others 2011), maximum intensity or area under the curve (Morris and others 2009) of sodium delivery. Future studies evaluating the saltiness perception of the SLC gels with respect to sodium release and gel structures may help identify the governing parameters for saltiness perception. This approach can provide industrial insights and practical strategies for sodium reduction via engineering the structure of lipoproteic foods.

4.6 References

Agrawal SK, Sanabria-DeLong N, Jemian PR, Tew GN, Bhatia SR. 2007. Micro- to nanoscale structure of biocompatible PLA-PEO-PLA hydrogels. Langmuir 23(9):5039-44.

Arai M, Ito K, Inobe T, Nakao M, Maki K, Kamagata K, Kihara H, Amemiya Y, Kuwajima K. 2002. Fast compaction of α-lactalbumin during folding studied by stopped-flow X-ray scattering. J.Mol.Biol. 321(1):121-32.

Barteri M, Gaudiano MC, Rotella S, Benagiano G, Pala A. 2000. Effect of pH on the structure and aggregation of human glycodelin A. A comparison with beta-lactoglobulin A. Biochimica Et Biophysica Acta-Protein Structure and Molecular Enzymology 1479(1-2):255-64.

Boisard L, Andriot I, Martin C, Septier C, Boissard V, Salles C, Guichard E. 2014. The salt and lipid composition of model cheeses modifies in-mouth flavour release and perception related to the free sodium ion content. Food Chem. 145(0):437-44.

Brewer MS, Gills LA, Vega JD. 1995. Sensory characteristics of potassium lactate and sodium chloride in a model system. J.Sens.Stud. 10(1):73-87.

Bryant CM, McClements DJ. 2000. Influence of NaCl and CaCl2 on cold-set gelation of heat-denatured whey protein. J.Food Sci. 65(5):801-4.

Busch JLHC, Yong FYS, Goh SM. 2013. Sodium reduction: Optimizing product composition and structure towards increasing saltiness perception. Trends Food Sci.Technol. 29(1):21-34.

Chabanet C, Tarrega A, Septier C, Siret F, Salles C. 2013. Fat and salt contents affect the in-mouth temporal sodium release and saltiness perception of chicken sausages. Meat Sci. 94(2):253-61.

Dalgleish DG, Senaratne V, Francois S. 1997. Interactions between alpha-lactalbumin and beta-lactoglobulin in the early stages of heat denaturation. J.Agric.Food Chem. 45(9):3459-64.

de Loubens C, Panouillé M, Saint-Eve A, Déléris I, Tréléa IC, Souchon I. 2011. Mechanistic model of in vitro salt release from model dairy gels based on standardized breakdown test simulating mastication. J.Food Eng. 105(1):161-8.

Desmond E. 2007. Reducing salt in meat and poultry products. In: D. Kilcast, F. Angus, editors. Reducing salt in foods - practical strategies. Cambridge, UK: Woodhead Publishing. p 233-55.

Desmond E. 2006. Reducing salt: A challenge for the meat industry. Meat Sci. 74(1):188-96.

Djordjevic J, Zatorre RJ, Jones-Gotman M. 2004. Odor-induced changes in taste perception. Experimental Brain Research 159(3):405-8.

Dotsch M, Busch J, Batenburg M, Liem G, Tareilus E, Mueller R, Meijer G. 2009. Strategies to Reduce Sodium Consumption: A Food Industry Perspective. Crit.Rev.Food Sci.Nutr. 49(10):841-51.

Dudkiewicz A, Luo P, Tiede K, Boxall A. 2012. Detecting and characterizing nanoparticles in food, beverages and nutraceuticals. Woodhead Publ.Food Sci.Technol.Nutr. (218):53-81.

Eoin D. 2006. Reducing salt: A challenge for the meat industry. Meat Sci. 74(1):188-96.

Farrell Jr. HM, Jimenez-Flores R, Bleck GT, Brown EM, Butler JE, Creamer LK, Hicks CL, Hollar CM, Ng-Kwai-Hang KF, Swaisgood HE. 2004. Nomenclature of the Proteins of Cows' Milk—Sixth Revision. J.Dairy Sci. 87(6):1641-74.

Feigin LA, Svergun DI. 1987. Structure Analysis by Small-angle X-ray and Neutron Scattering. New York: Plenum Press.

Floury J, Rouaud O, Le Poullennec M, Famelart M. 2009. Reducing salt level in food: Part 2. Modelling salt diffusion in model cheese systems with regards to their composition. LWT - Food Science and Technology 42(10):1621-8.
Foegeding EA, Luck P, Vardhanabhuti B. 2011. Milk Protein Products | Whey Protein Products. In: John W. Fuquay, editor. Encyclopedia of Dairy Sciences (Second Edition). San Diego: Academic Press. p 873-8.
Gottschalk M, Nilsson H, Roos H, Halle B. 2003. Protein self-association in solution: The bovine beta-lactoglobulin dimer and octamer. Protein Science 12(11):2404-11.
Harada T, Matsuoka H. 2004. Ultra-small-angle X-ray and neutron scattering study of colloidal dispersions. Current Opinion in Colloid & Interface Science 8(6):501-6.
Heidolph BB, Ray DK, Roller S, Koehler P, Weber J, Slocum S, Noort MWJ. 2011. Looking for my lost shaker of salt... replacer: flavor, function, future. Cereal Foods World 56(1):5-19.
Hughes E, Cofrades S, Troy DJ. 1997. Effects of fat level, oat fibre and carrageenan on frankfurters formulated with 5, 12 and 30% fat. Meat Sci 45(3):273-81.
Hussain R, Gaiani C, Jeandel C, Ghanbaja J, Scher J. 2012. Combined effect of heat treatment and ionic strength on the functionality of whey proteins. J.Dairy Sci. 95(11):6260-73.
Ilavsky J, Allen AJ, Long GG, Jemian PR. 2002. Effective pinhole-collimated ultrasmall-angle x-ray scattering instrument for measuring anisotropic microstructures. Rev.Sci.Instrum. 73(3):1660-2.
Ilavsky J, Zhang F, Allen AJ, Levine LE, Jemian PR, Long GG. 2013. Ultra-Small-Angle X-ray Scattering Instrument at the Advanced Photon Source: History, Recent Development, and Current Status. Metallurgical and Materials Transactions A-Physical Metallurgy and Materials Science 44A(1):68-76.
Ilavsky J, Jemian PR. 2009. Irena: tool suite for modeling and analysis of small-angle scattering. Journal of Applied Crystallography 42: 347-53.
Ilavsky J, Jemian PR, Allen AJ, Zhang F, Levine LE, Long GG. 2009. Ultra-small-angle X-ray scattering at the Advanced Photon Source. Journal of Applied Crystallography 42469-79.
Jiménez-Colmenero F. 2013. Potential applications of multiple emulsions in the development of healthy and functional foods. Food Res.Int. 52(1):64-74.
Johnson ME, Kapoor R, McMahon DJ, McCoy DR, Narasimmon RG. 2009. Reduction of Sodium and Fat Levels in Natural and Processed Cheeses: Scientific and Technological Aspects. Comprehensive Reviews in Food Science and Food Safety 8(3):252-68.
Kalab M, Allanwojtas P, Miller SS. 1995. Microscopy and Other Imaging Techniques in Food Structure-Analysis. Trends Food Sci.Technol. 6(6):177-86.
Kuo W, Lee Y. 2014a. Effect of food matrix on saltiness perception-implications for sodium reduction. Comprehensive Reviews in Food Science and Food Safety 13(5):906-23.
Kuo W, Lee Y. 2014b. Temporal sodium release related to gel microstructural properties-implications for sodium reduction. J.Food Sci. 79(11):E2245-52.
Langton M, Hermansson A. 1996. Image analysis of particulate whey protein gels. Food Hydrocoll. 10(2):179-91.
Lauverjat C, Deleris I, Trelea IC, Salles C, Souchon I. 2009. Salt and aroma compound release in model cheeses in relation to their mobility. J Agric Food Chem 57(21):9878-87.
Lee S, Lefèvre T, Subirade M, Paquin P. 2009. Effects of ultra-high pressure homogenization on the properties and structure of interfacial protein layer in whey protein-stabilized emulsion. Food Chem. 113(1):191-5.
Lopez C, Lavigne F, Lesieur P, Bourgaux C, Ollivon M. 2001. Thermal and structural behavior of milk fat. 1. Unstable species of anhydrous milk fat. J.Dairy Sci. 84(4):756-66.

Lorenzen PC, Schrader K. 2006. A comparative study of the gelation properties of whey protein concentrate and whey protein isolate. Lait 86(4):259-71.
Lucey JA. 2014. Chapter 17 - Milk Protein Gels. In: Harjinder Singh, Mike Boland, Abby Thompson, editors. Milk Proteins (Second edition). San Diego: Academic Press. p 493-523.
Marangoni AG, Barbut S, McGauley SE, Marcone M, Narine SS. 2000. On the structure of particulate gels - the case of salt-induced cold gelation of heat-denatured whey protein isolate. Food Hydrocoll. 14(1):61-74.
Moitzi C, Donato L, Schmitt C, Bovetto L, Gillies G, Stradner A. 2011. Structure of beta-lactoglobulin microgels formed during heating as revealed by small-angle X-ray scattering and light scattering. Food Hydrocoll. 25(7):1766-74.
Morris C, Koliandris A, Wolf B, Hort J, Taylor AJ. 2009. Effect of pulsed or continuous delivery of salt on sensory perception over short time intervals. Chemosens Percep. 2(1): 1-8.
Nave C, Diakun GP, Bordas J. 1986. Ultra-small angle X-ray diffraction from muscle. Nuclear Instruments and Methods in Physics Research Section A: Accelerators, Spectrometers, Detectors and Associated Equipment 246(1–3):609-12.
Panouille M, Saint-Eve A, de Loubens C, Deleris I, Souchon I. 2011. Understanding of the influence of composition, structure and texture on salty perception in model dairy products. Food Hydrocoll. 25(4):716-23.
Patterson AL. 1939. The Scherrer formula for x-ray particle size determination. Physic Rev. 56(10): 978-982.
Peyronel F, Pink DA, Marangoni AG. 2014a. Triglyceride nanocrystal aggregation into polycrystalline colloidal networks: Ultra-small angle X-ray scattering, models and computer simulation. Current Opinion in Colloid & Interface Science 19(5):459-70.
Peyronel F, Quinn B, Marangoni AG, Pink DA. 2014b. Ultra Small Angle X-Ray Scattering for Pure Tristearin and Tripalmitin: Model Predictions and Experimental Results. Food Biophysics 9(4):304-13.
Phan VA, Yven C, Lawrence G, Chabanet C, Reparet JM, Salles C. 2008. *in vivo* sodium release related to salty perception during eating model cheeses of different textures. Int.Dairy J. 18(9):956-63.
Phelps T, Angus F, Clegg S, Kilcast D, Narain C, den Ridder C. 2006. Sensory issues in salt reduction. Food Quality and Preference 17(7-8):633-4.
Pouzot M, Nicolai T, Durand D, Benyahia L. 2004. Structure factor and elasticity of a heat-set globular protein gel. Macromolecules 37(2):614-20.
Ruusunen M, Vainionpää J, Lyly M, Lähteenmäki L, Niemistö M, Ahvenainen R, Puolanne E. 2005. Reducing the sodium content in meat products: The effect of the formulation in low-sodium ground meat patties. Meat Science, 69(1): 53-60.
Ryan KN, Vardhanabhuti B, Jaramillo DP, van Zanten JH, Coupland JN, Foegeding EA. 2012. Stability and mechanism of whey protein soluble aggregates thermally treated with salts. Food Hydrocoll. 27(2):411-20.
Sala G, van Vliet T, Cohen Stuart MA, Aken GAv, van de Velde F. 2009. Deformation and fracture of emulsion-filled gels: Effect of oil content and deformation speed. Food Hydrocoll. 23(5):1381-93.
Sinopoli DA, Lawless HT. 2012. Taste properties of potassium chloride alone and in mixtures with sodium chloride using a check-all-that-apply method. J.Food Sci. 77(9):S319-22.
Stieger M, van de Velde F. 2013. Microstructure, texture and oral processing: New ways to reduce sugar and salt in foods. Curr. Opin. Colloid. In. 18(4):334-48.

Timasheff S, Townend R. 1964. Structure of the beta-Lactoglobulin Tetramer. Nature 203(494):517-9.
Väänänen T, Ikonen T, Jokela K, Serimaa R, Pietilä L, Pehu E. 2003. X-ray scattering study on potato (Solanum tuberosum L.) cultivars during winter storage. Carbohydr.Polym. 54(4):499-507.
van Vliet T, Luyten H, Walstra P. 1993. Time-Dependent Fracture-Behavior of Food. Food Colloids and Polymers : Stability and Mechanical Properties 113: 175-90.
Verheul M, Roefs SPFM, de Kruif KG. 1998. Kinetics of heat-induced aggregation of beta-lactoglobulin. J.Agric.Food Chem. 46(3):896-903.
Verheul M, Pedersen JS, Roefs SPFM, de Kruif KG. 1999. Association behavior of native beta-lactoglobulin. Biopolymers 49(1):11-20.
Witz J, Luzzati V, Timasheff SN. 1964. Molecular Interactions in Beta-Lactoglobulin .8. Small-Angle X-Ray Scattering Investigation of Geometry of Beta-Lactoglobulin a Tetramerization. J.Am.Chem.Soc. 86(2):168.
Wu H, Xie JJ, Morbidelli M. 2005. Kinetics of cold-set diffusion-limited aggregations of denatured whey protein isolate colloids. Biomacromolecules 6(6):3189-97.
Yamaguchi S, Takahashi C. 1984. Interactions of Monosodium Glutamate and Sodium Chloride on Saltiness and Palatability of a Clear Soup. J.Food Sci. 49(1):82-5.
Yoshida K, Fukushima Y, Yamaguchi T. 2014. A study of alcohol and temperature effects on aggregation of β-lactoglobulin by viscosity and small-angle X-ray scattering measurements. Journal of Molecular Liquids 189(0):1-8.

4.7 Tables and Figures

Table 4.1. Formula and homogenization pressure of the solid lipoproteic colloid (SLC) gels. Sample code represents protein(%,w/w)-fat(%,w/w)-NaCl(%,w/w)-homogenization pressure(MPa).

Protein (%, w/w)	Fat (%, w/w)	Sample code			
		1.5 % (w/w) NaCl		3.5% (w/w) NaCl	
		Homogenization at 14 MPa	Homogenization at 14 MPa	Homogenization at 14 MPa	Homogenization at 55 MPa
8	0	8-0-1.5-14	8-0-1.5-55	8-0-3.5-14	8-0-3.5-55
8	11	8-11-1.5-14	8-11-1.5-55	8-11-3.5-14	8-11-3.5-55
8	22	8-22-1.5-14	8-22-1.5-55	8-22-3.5-14	8-22-3.5-55
8	33	8-33-1.5-14	8-33-1.5-55	8-33-3.5-14	8-33-3.5-55
16	0	16-0-1.5-14	16-0-1.5-55	16-0-3.5-14	16-0-3.5-55
16	11	16-11-1.5-14	16-11-1.5-55	16-11-3.5-14	16-11-3.5-55
16	22	16-22-1.5-14	16-22-1.5-55	16-22-3.5-14	16-22-3.5-55
16	33	16-33-1.5-14	16-33-1.5-55	16-33-3.5-14	16-33-3.5-55

Table 4.2. Radii of gyration of the protein aggregates ($R_{g,p}$) and the fat globules ($R_{g,f}$) in the SLC gels derived from USAXS measurement. Sample code represents protein(%,w/w)-fat(%,w/w)-NaCl(%,w/w)-homogenization pressure(MPa).

Sample (n for NaCl%)	$R_{g,p}$ (nm)		$R_{g,f}$ (nm)	
	n = 1.5	n = 3.5	n = 1.5	n = 3.5
8-0-n-14	9.2	3.1	-	-
8-11-n-14	87.0	59.8	449.3	371.5
8-22-n-14	54.9	53.6	484.6	387.3
8-33-n-14	40.0	37.6	319.3	291.2
16-0-n-14	8.8	2.8	-	-
16-11-n-14	125.1	155.5	457.5	711.0
16-22-n-14	91.5	103.0	325.2	407.8
16-33-n-14	67.0	N.D.[a]	274.0	N.D.[a]
8-0-n-55	7.2	7.5	-	-
8-11-n-55	27.5	24.4	120.5	125.2
8-22-n-55	22.2	21.6	125.8	121.6
8-33-n-55	22.5	31.7	121.2	110.1
16-0-n-55	8.2	20.7	-	-
16-11-n-55	45.5	35.5	153.6	91.2
16-22-n-55	35.0	24.3	113.6	77.4
16-33-n-55	33.5	30.2	101.0	66.3

a. Sample not measured due to operation error.

Table 4.3. Sodium release and textural properties of the SLC gels with 3.5% NaCl, and the hydrodynamic radius of the droplets in the corresponding emulsions[a].

Sample	R_{max} ± SD [b] (ppm Na/s)	C_{max} ± SD (ppm Na)	AUC ± SD (10^3 ppm Na.s)	Serum release ± SD (g)	Max stress ± SD (KPa)	Strain at maximum stress ± SD (%)	Emulsion $R_{h,e}$ ± SD (nm)
8-22-3.5-55	2.38 ± 0.77ab[c]	181.21 ± 5.88a	43.13 ± 1.52a	0.49 ± 0.08b	112.25 ± 15.80ab	54.08 ± 3.42c	127.88 ± 22.42b
8-33-3.5-55	2.59 ± 0.49ab	166.53 ± 10.15ab	39.54 ± 2.54ab	0.30 ± 0.07c	166.29 ± 29.46ab	56.41 ± 1.12c	134.62 ± 10.40b
8-33-3.5-14	1.76 ± 0.30b	150.44 ± 9.70b	35.51 ± 2.44b	0.47 ± 0.01b	101.22 ± 3.89b	60.28 ± 1.98b	329.18 ± 13.17a
16-11-3.5-55	2.90 ± 0.12a	178.09 ± 17.75a	43.39 ± 4.50a	0.47 ± 0.07b	179.14 ± 16.04a	46.30 ± 2.00d	296.16 ± 3.34b
16-11-3.5-14	2.09 ± 0.31ab	95.18 ± 20.13c	24.41 ± 5.66c	0.90 ± 0.04a	172.75 ± 83.98a	69.61 ± 2.72a	352.12 ± 33.19a

a. See Kuo and Lee (2014b) for the properties of the SLC gels with 1.5% NaCl.
b. R_{max}, maximum rate of sodium release; C_{max}, maximum concentration of released sodium; AUC, area under the curve of sodium release. Serum release, amount of liquid expelled from the sample during the compression test. $R_{h,e}$, hydrodynamic radius of the emulsions particles measured using dynamic light scattering (DLS).
c. The numbers followed by the same letters are not significantly different.

Table 4.4. Correlation coefficients between sodium release, textural properties and particle sizes of fat globules of the SLC gels at constant NaCl contents[a].

	C_{max} (ppm Na)		AUC (10^3 ppm Na.s)		Strain at maximum stress (%)		Emulsion $R_{h,e}$ from DLS (nm)		Gel $R_{g,f}$ from USAXS (nm)	
NaCl % in SLC gels	1.5	3.5	1.5	3.5	1.5	3.5	1.5	3.5	1.5	3.5
R_{max}[b] (ppm Na/s)	0.989 *** [c]	0.553	0.994 ****	0.610	-0.924 *	-0.749	-0.151	-0.412	-0.498	-0.578
C_{max} (ppm Na)			0.999 ****	0.996 ****	-0.957 *	-0.913 *	-0.170	-0.652	-0.551	-0.987 ***
AUC (10^3 ppm Na.s)					-0.948 *	-0.940 *	-0.163	-0.632	-0.537	-0.979 ***
Serum release (g)					0.773	0.705	0.599	0.642	0.821	0.923 *
Strain at maximum stress (%)							0.415	0.399	0.761	0.902 *
Emulsion $R_{h,e}$ from DLS (nm)									0.883 *	0.660

a. Refer to Section 4.3.3 for the list of the samples. The correlation was carried on each of the five samples with the same NaCl contents.
b. R_{max}, maximum rate of sodium release; C_{max}, maximum concentration of released sodium; AUC, area under the curve of sodium release. Serum release, amount of liquid expelled from the sample during the compression test. $R_{h,e}$, hydrodynamic radius of the emulsions particles measured using dynamic light scattering (DLS).
c. The numbers with the superscripts of one, two, three or four asterisks indicate significant correlations for $P < 0.05$, 0.01, 0.005 and 0.001, respectively.

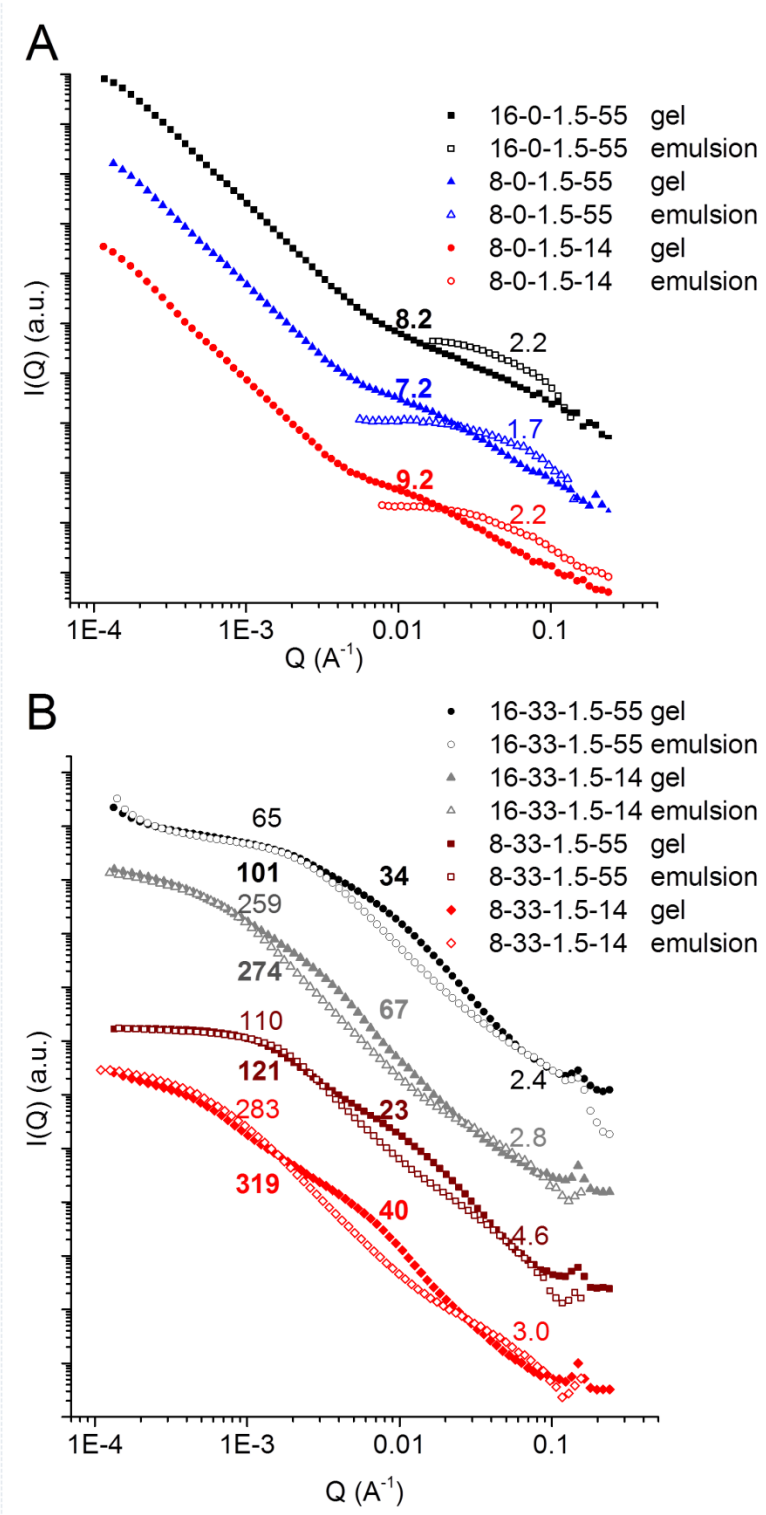

Figure 4.1. Slit smeared USAXS profiles of the SLC emulsions and their counterpart gels. A. Non-fat samples and B. Fat- containing samples. The curves are vertically shifted to avoid overlap. The positive numbers are the R_g values of the particles in nanometer, with bolded numbers being those of the gels. The negative numbers are the slope of the power law decay exponents. Sample code represents protein(%,w/w)-fat(%,w/w)-NaCl(%,w/w)-homogenization pressure(MPa).

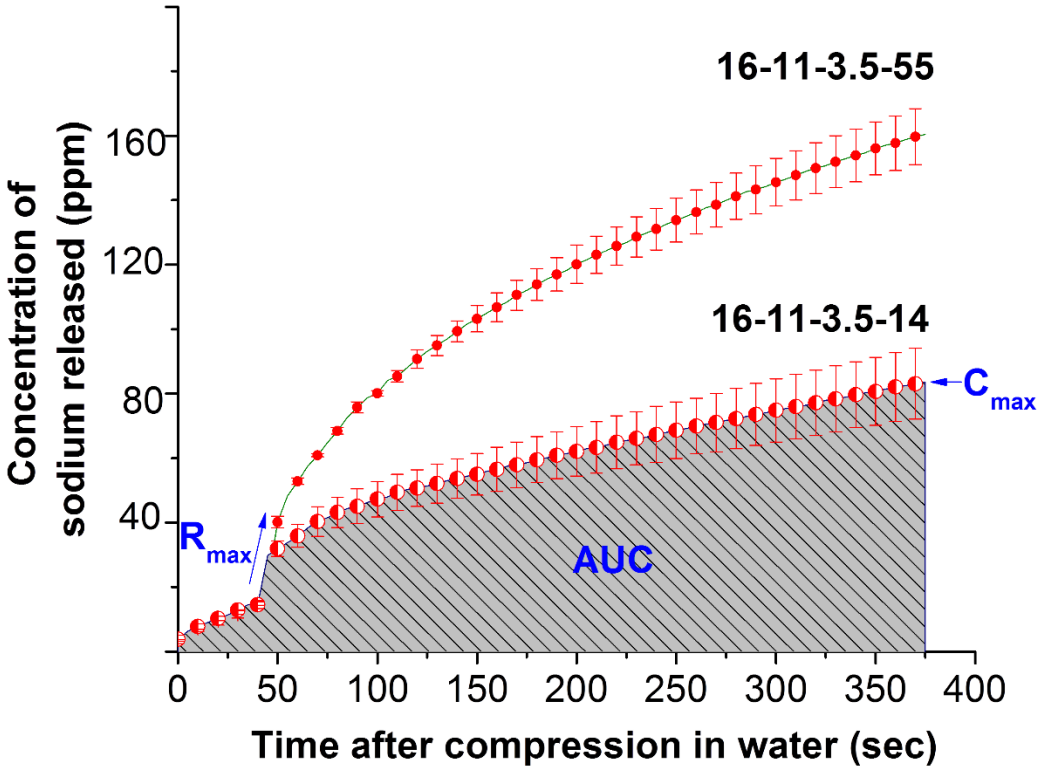

Figure 4.2. Representative curves of the *in vitro* sodium release of two SLC gels. The maximum rate of sodium release, R_{max}, the maximum concentration of released sodium, C_{max}, and the area under the curve of sodium release, AUC were derived from each curve as indicated in the graph. Sample code represents protein (%,w/w)–fat (%,w/w)–NaCl (%,w/w)–homogenization pressure (MPa).

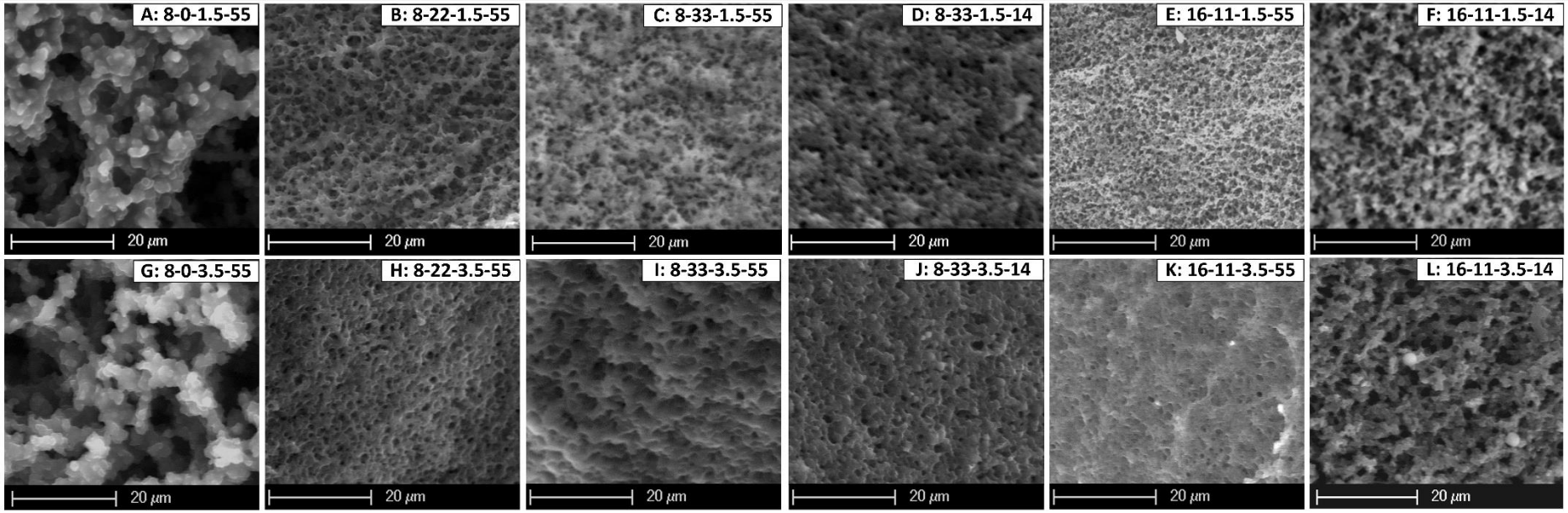

Figure 4.3. Environmental scanning electron microscopy (ESEM) images of the cross-sections of frozen-fractured lipoproteic emulsion gels. Sample code represents protein(%,w/w)-fat(%,w/w)-NaCl(%,w/w)-homogenization pressure(MPa).

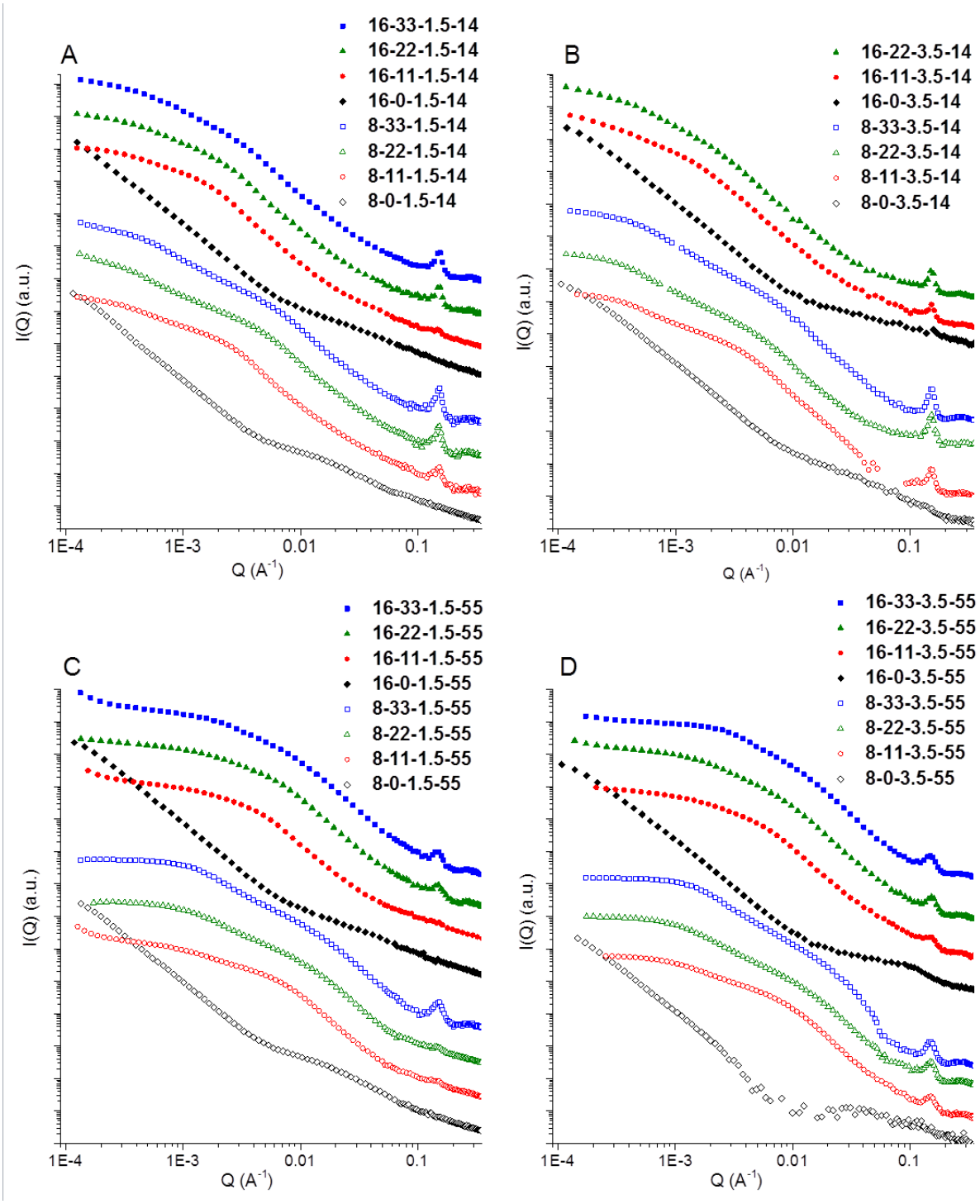

Figure 4.4. Slit smeared USAXS profiles of the SLC gels made with 1.5% (A, C) or 3.5% (B, D) NaCl at homogenization pressures of 14 (A, B) or 55 (C, D) MPa. The curves are vertically shifted to avoid overlap. Sample code represents protein(%,w/w)-fat(%,w/w)-NaCl(%,w/w)-homogenization pressure(MPa).

CHAPTER 5

Correlating Structural Properties to Sodium Release of the Solid Lipoproteic Colloids

5.1 Abstract

Effect of porosity and particle size of fat on the sodium release properties of model solid lipoproteic colloids (SLCs) were investigated. The treatment variables for the SLCs were the levels of protein (8 and 16 %, w/w), fat (0, 11, 22, and 33%, w/w) and NaCl (1.5% and 3.5%, w/w) as well as the pressure of homogenization (14 and 55 MPa). Sodium release was measured by compressing the SLCs in water using a texture analyzer while recording the conductivity of the water. Correlation analyses between the porosity, particle size of fat, the treatment variables, the textural and the sodium release properties were performed separately on the two groups of SLCs with 1.5% and 3.5% NaCl. For both groups of the SLCs, the porosity correlated positively with the serum release and the maximum rate of sodium release. However, when only the fat-containing SLCs were analyzed, the particle size of fat, instead of the porosity, correlated positively with the serum release. For the SLCs with 3.5% NaCl, the particle size of fat correlated positively with the strain at maximum stress, and negatively with the maximum concentration of released sodium and the area under the curve of sodium release. The above correlations suggested that sodium is mainly released via convective transport with serum during the gel compression, and then via diffusive transport after the gel fracture.

Keywords

Solid lipoproteic colloid (SLC), Porosity, Gyration radius of fat ($R_{g,f}$), Serum release, Texture, Sodium release

5.2 Introduction

Engineering food structure to improve the sensory and nutritional qualities of the products has become one of the featuring areas in food science and food industry (Aguilera 2005; Stieger 2011; Knoop and others 2013; Norton and others 2014). Enhancing sodium release via engineering food structure has been proposed as one key strategy to allow reduction in sodium content in processed foods (Stieger and van de Velde 2013; van de Velde F, Adamse M. 2013). Understanding the structural effects on the transport mechanisms of sodium can help tailoring the product processing for a designed and efficient sodium delivery.

Transport of sodium from porous food systems to the oral cavity can be via convective and/or diffusive transfer (Geankoplis 2003; Kuo and Lee 2014b). In convective transfer, sodium migrates with the fluid flow from the food matrix into surroundings. Deformation of the food matrix due to oral processing can initiate outward fluid flow from the pores, resulting in serum release (van den Berg and others 2007a). Sodium ions that are free of charge interaction with the matrix molecules are readily carried out by the serum. Previous studies showed the serum release of gels can be enhanced by increasing porosity, by forming coarse-stranded network, or by forming bi-continuous network of gels (van den Berg and others 2007a; van den Berg and others 2007b; van den Berg and others 2008). Moreover, increasing serum release has been shown to enhance sodium release and saltiness perception (Stieger 2011). However, the study by Stieger (2011) used model gels composed of proteins and polysaccharides. While many food products such as cheese and sausages contain emulsified fat, it has not been studied how the presence of fat can alter the serum release and sodium release. It has been demonstrated in meat products that by increasing the juiciness, a reduction of sodium by at least 15% did not change the saltiness perception (van de Velde F, Adamse M. 2013). Still, the roles of fat particles in the meat products were not examined in the above study.

While the driving force of convective transfer for sodium is the serum flow, the driving force for spontaneous diffusion of sodium is the concentration gradient of sodium across the food matrix and the surrounding oral cavity (Geankoplis 2003; Kuo and Lee 2014b). In model lipoproteic gel systems, decrease in particle size of fat caused greater extent of gel fragmentation and thus greater surface area, allowing more sodium release (de Loubens and others 2011a; de Loubens and others 2011b; Panouille and others 2011; Boisard and others 2013; Boisard and others 2014). However, the above studies did not measure serum

release of the gels. In another study on model lipoproteic gels, in-mouth sodium release correlated positively with the water content of the gel (Phan and others 2008; Lawrence and others 2012).

Considering that the effect of porosity and particle size of fat on sodium release have only been separately investigated in model food systems, it is essential to understand the effect of both structural properties in determining the sodium release in the same system. The objective of this study is to correlate the structural properties, including porosity and particle size of fat, to the *in vitro* sodium release properties during the compression of solid lipoproteic colloids (SLC). We hypothesize that both increasing porosity and decreasing particle size of fat can lead to increased sodium release of an SLC. The correlation of the structural properties to the temporal properties of sodium release further will reveal the time-wise variation of sodium transport mechanisms throughout the gel compression process. The results will be important for understanding the saltiness perception of lipoproteic products such as cheese and sausages, as well as developing prototypes for sodium reduction.

5.3 Materials and Methods

5.3.1 Preparation of solid lipoproteic colloids (SLCs)

The protocol for the preparation of the SLCs is detailed in previous literatures (Kuo and Lee 2014a; Kuo and others 2016). Briefly, NaCl solutions containing whey protein isolate were homogenized with anhydrous milk fat using the APV 2-stage homogenizer (15 MR, SPX Flow Technology, Soeborg, Denmark), followed by heat induced gelation to form the SLCs. The SLCs varied by the contents of protein (8 and 16 %, w/w), fat (0, 11, 22, and 33%, w/w), NaCl (1.5 and 3.5%, w/w), and homogenization pressures (14 and 55 MPa).

5.3.2 Structural, textural and sodium release properties of the SLCs

The protocols for acquiring the structural, textural and sodium release properties of the SLCs are detailed in previous literatures (Kuo and Lee 2014a; Kuo and others 2016) unless additionally specified.

The images of the SLC internal structure were captured using environmental scanning electron microscopy (ESEM) with a field emission electron gun (FEI Co., Hillsboro, Oreg., U.S.A.)(Kuo and Lee 2014a). The pores of the gel on the ESEM photos were identified using

image analysis with the method described by Kuo and Lee (Kuo and Lee 2014a). The porosity was calculated as the volume fraction of the pores relative to the total volume of the gel, assuming the pores are spherical. The gyration radius of fat particles ($R_{g,f}$) in the SLCs was determined using the Bonse-Hart double-crystal ultra-small-angle X-ray scattering (USAXS) instrument operated by ChemMatCARS at the Advanced Photon Source, Argonne National Laboratory (Argonne, IL, USA) (Kuo and others 2016).

The textural properties, including serum release, maximum stress ($stress_{max}$), and strain at maximum stress ($strain_{max}$) were measured by a compression test using a texture analyzer (TA-XT2i, Texture Technologies Corp., Scarsdale, N.Y., U.S.A.) (Kuo and Lee 2014a).

The *in vitro* sodium release properties of the SLCs were determined by compressing the SLC in water using a texture analyzer (TA-XT2i, Texture Technologies Corp., Scarsdale, N.Y., U.S.A.), while recording the conductivity of the water by a conductivity probe (Orion DuraProbe 4-Electrode Conductivity Cells 013005MD) connected with an Orion VERSA STAR Multiparameter Benchtop Meter (Thermo Fisher Scientific Inc., Waltham, Mass, U.S.A.). The parameters extracted from the curve of sodium release included the maximum rate of sodium release (R_{max}), the maximum concentration of released sodium (C_{max}), and the area under the curve (AUC) of sodium release (Kuo and Lee 2014a).

5.3.3 Statistical analyses

Linear correlation was performed using OriginPro 2015 (OriginLab Corporation, Northampton, MA, USA). The correlation coefficients between the treatment factors, the structural, textural and the sodium release properties were calculated for the two groups of SLCs with 1.5 and 3.5% NaCl. Analysis of variance was performed using SAS Software (SAS 9.3, SAS Inst., Inc., Cary, N.C., U.S.A.). The proc glm and the LSMEANS with the adjusted Tukey test were used to analyze the difference between the means of the samples.

5.4 Results and Discussion

Table 5.1, 5.2, and 5.3 shows the structural, textural, and sodium release properties of the SLCs made with 1.5 and 3.5% NaCl. Linear correlation analysis was performed between the treatments and the measured variables of the SLCs within the same level of NaCl (Table

5.4). The treatment variables used in the linear correlation included the contents (w/w) of protein (P%), fat (F%) and water (W%), the weight ratios of fat to protein (F/P), fat to water (F/W), fat to solids (F/S), and protein to water (P/W) in the SLCs. Among protein content related terms, P% was presented in Table 5.4 instead of P/W for the following reason. The P% and P/W showed the same trend of correlations with all the measured variables. However, P% correlated better supported by the greater values of correlation coefficients and higher level of significance (data not shown) than P/W. Likewise, for the fat content related terms, F/S instead of F%, F/P or F/W was presented in Table 5.4 for the following reason. F/S, F%, F/P and F/W showed same trend of correlations with the measured variables, but F/S showed better correlations with the measured variables (data now shown) than F%, F/P or F/W.

5.4.1 Effect of the treatments on the porosity of the SLCs

For the SLCs with 1.5% NaCl, the porosity correlated positively with the W% and negatively with the F/S (Table 5.4). Similar trends were found in the SLCs with 3.5% NaCl, with higher levels of significance and greater values of the correlation coefficients than the SLCs with 1.5% NaCl. The positive correlation between the porosity and the W% reflected the nature of porosity – originating from the voids filled with fluids in water-based gel network (van den Berg and others 2007b). Hence, in general higher water content of the gel leads to higher porosity (Kuo and Lee 2014a). However, in the SLC systems the porosity correlated stronger with the F/S ratio than with the water content. When comparing some selected samples with similar water contents, the effect of F/S ratio on porosity can be clearly seen. For example, the water contents of samples 8-33-1.5-14 and 16-22-1.5-14 are 57 and 59% (w/w), respectively, and the F/S of the above two samples are 0.77 and 0.54, respectively. The porosity of the former (53%) is significantly lower than the porosity of the latter (71%) (Table 5.1). This difference can be attributed to the more thorough dispersing of the protein network by the higher amount of emulsion particles in the gel with higher F/S. Based on the ESEM images of the gel cross-sections, sample 8-33-1.5-14 (Figure 5.1A) contained finer and more homogeneous network with smaller pores compared to sample 16-22-1.5-14 (Figure 5.1B). This relatively dispersed structure implied that the protein-protein interaction in sample 8-33-1.5-14 is more frequently interrupted by the emulsion particles. In contrast to sample 8-33-1.5-14, sample 16-22-1.5-14 contained coarser networks formed by larger aggregates of proteins. This coarser structure implied great extent of protein-protein

interaction, which was due to lower F/S. Hence, increasing in fat content of lipoproteic gels could lead to more dispersed network structure which occupied more space, and ultimately yield lower porosity of the gel. The similar effect of the F/S on the porosity can also been found between samples 8-33-1.5-55 and 16-22-1.5-55 (Table 5.1, Figure 5.1C and D). The lower porosity of the samples with smaller pores may be partially due to the detection limit of the ESEM. Based on the image resolution, the lowest pore diameter distinguishable in this study was 97.4 nm. Pores with diameters below this limit could not be identified. Hence, the low porosity of the sample 8-33-1.5-14 may be partially due to its greater portion of smaller pores that were undetectable.

5.4.2 Effect of porosity on the textural properties of the SLCs

Table 5.2 shows the textural properties of the SLCs. Linear correlation revealed the effect of the porosity on the textural and sodium release properties of the SLCs (Table 5.4). For both SLC groups with 1.5% and 3.5% NaCl, the porosity correlated positively with the serum release during the gel compression. This correlation has been previously discovered in polysaccharide/protein hybrid gels (van den Berg and others 2007a; van den Berg and others 2007b; Stieger and van de Velde 2013) and SLCs with 1.5% NaCl (Kuo and Lee 2014a). As the pores in the water-based gels are the void spaces occupied with fluid, the gels with greater porosity store higher amount of liquid. When the gels are subjected to external force, deformation of the pore microstructure leads to rapid loss of the contained fluid, yielding serum release (van den Berg and others 2007a).

However, for the SLCs with both levels of NaCl, the correlation between porosity and serum release originated mainly from the significantly greater porosity and serum release of the non-fat samples than those of the fat-containing samples. In fact, the porosity did not show a significant correlation with the serum release among only the fat-containing samples ($P = 0.80$ and 0.07 for SLCs with 1.5 and 3.5% NaCl, respectively). This lack of correlation may be due to the other factor, $R_{g,f}$, which counteracted the effect of porosity in determining serum release. The presence of fat particles leads to earlier fracture of the fat-containing gels than the non-fat gels. Once the gel is fractured the applied stress is released and the potential for serum release decreases (see section 5.4.5. for more discussion). Compared to the fat-containing SLCs, the non-fat SLCs showed relatively high values of $strain_{max}$ (Table 5.2). In fact, these non-fat SLCs only deformed without a fracture throughout the compression test.

The serum was able to continuously migrate out from the non-fat SLCs during the compression, and yielded in considerably higher serum release compared to the fat-containing SLCs.

The present study showed that the correlation between porosity and serum release is weaker in the SLCs with 1.5% NaCl, compared to the SLCs with 3.5% NaCl (Table 5.4). The poorer correlation in the SLCs with 1.5% NaCl was because that the samples with the highest porosity (8-0-1.5-14 and 8-0-1.5-55) did not show the greatest serum release (Table 5.1 and 5.2). This discrepancy was due to the poorer stability of the non-fat SLCs with lower NaCl content. The samples moved out from the fridge sit at room temperature for 3 hours prior to the measurement of serum release. Syneresis was observed from the non-fat SLCs, while the leaching was greater in the SLCs with 1.5% NaCl, compared to those with 3.5% NaCl (data not shown). The greater stability against syneresis of the SLCs with more NaCl may be due to the enhanced protein bridging under greater charge screening. Greater screening effect occurs at elevated NaCl amount, which helps neutralize the surface charge and lessens the electrostatic repulsion between protein molecules. This improved screening can promote aggregation, branching and densification of whey protein particles (Langton and Hermansson 1996; Pouzot and others 2004), yielding a stronger network structure (Lorenzen and Schrader 2006; Hussain and others 2012). The comparatively stronger and more stable structure of the SLCs with 3.5% NaCl thus was able to retain more liquid prior to the measurement of serum release.

5.4.3 Effect of the porosity on the sodium release properties of the SLCs

Among the three parameters extracted from the sodium release profiles, R_{max} correlated positively with the porosity and the serum release, for the SLCs with both levels of NaCl (Table 5.4). These correlations implied that the initial sodium release from the gel is mainly driven by the serum release during the gel compression. In the sodium release curve, R_{max} reflects the fastest increment of sodium concentration in the beginning of the measurement. During this period the gel is undergoing the compression during which the most serum is compressed out. Sodium thus is convectively transported by the serum flowing from the gel to the surrounding water. The rapid flow of serum from the gel thus results in the dramatic raise of sodium concentration in the surrounding water. It is worth noticing that the

correlations between porosity and R_{max} are as strong as the correlations between W% and R_{max}, as shown by the similar correlation coefficients and significance levels (Table 5.4).

It has been shown that the perceived saltiness could be boosted by adding polysaccharide into sausages to increase the serum release (Stieger 2011; van de Velde F, Adamse M. 2013). Alternatively, saltiness can be enhanced via high-pressure processing which yielded dry-cured hams with greater serum release (Fulladosa and others 2009; Clariana and others 2012; Fulladosa and others 2012). The sensory assessments in the above studies can be complemented by the instrumental evaluation of sodium release in the present study. Together, these studies supported that increasing porosity increases serum release, leading to faster sodium release during the initial gel deformation, and eventually boost saltiness perception.

Although in this study the serum release and sodium release were measured separately, the force-distance curves recorded by the texture analyzer during the two types of measurements are not significantly different from each other. This consistency suggested that the texture of the samples did not differ between the regular compression test (for serum release) and the compression in water (for the sodium release). In addition to R_{max}, AUC also correlated positively to serum release. Since serum release did not correlate to C_{max}, it is hypothesized that the higher R_{max} contributed to the higher AUC during initial sodium release, and in turn, to the overall AUC.

There were no correlations between the porosity, serum release and the R_{max} among only the fat-containing SLCs, for the SLCs with both NaCl levels. The lack of correlation again indicated that it was the significant difference between the non-fat and fat-containing SLC that resulted in the correlation between the porosity, serum release and the R_{max}.

The image analysis to quantify the SLC porosity performed in this study may have two limitations. First, the image analysis used in this study does not distinguish the closed pores from the open pores. Indeed, at the same level of porosity, the samples with higher fraction of open pores may yield in faster transport of sodium than the samples with lower fraction of open pores. Modifying the image analysis code to quantify the close-pore porosity and the open-pore porosity may improve the prediction of sodium release by porosity. Second, the image analysis used in this study has the detection limit of 97 nm based on the image resolution. Hence, the porosity might be underestimated especially for the samples with greater fraction of pores below 97 nm. Quantifying porosity using a pycnometer may

improve the detection limit compared to the image analysis, and, thus give more accurate porosity values.

5.4.4 Effect of the treatment on $R_{g,f}$ of SLCs

The treatment effect on $R_{g,f}$ of the SLCs has been thoroughly elaborated in Chapters 3 and 4 (Kuo and Lee 2014a; Kuo and others 2016). Overall, the $R_{g,f}$ correlated negatively with the homogenization pressure (Table 5.4). Higher pressure during the homogenization provides greater shear which breaks down the fat particles more (Huppertz 2011). At the same time, higher pressure induces higher degree of protein denaturation, improving the protein adsorption on the fat particles, making the emulsion system more stable (Lee and others 2009).

5.4.5 Effect of the $R_{g,f}$ on the textural properties of the SLCs

For the SLCs with both levels of NaCl, the $R_{g,f}$ correlated positively with the serum release (Table 5.4). This correlation is due to the earlier fracture of the gels with smaller fat particles. Fat particles are structural defects that increase the stress concentration of the gel matrix (van Vliet and others 1993; Sala and others 2009), and, thus initiate fracture when the gel is subjected to external force. At the same level of fat content, the gels with smaller particle size of fat indicated that the network is dispersed with greater number of the structural defects. The gels with smaller fat particles are thus more likely to fracture earlier during the compression (Sala and Stieger 2013). According to the Darcy relation (Walstra 2003), the volume flow rate of serum through the permeable area of a porous media is proportional to the pressure difference acting on the liquid over a given distance. The gel fracture would release the external pressure, which disfavors the serum release. The earlier fracture of the SLCs with smaller $R_{g,f}$ thus results in lower serum release. The contribution of fat particle on texture and sodium release can be supported by the positive correlation between the $R_{g,f}$, $strain_{max}$, and the serum release in the SLCs with 3.5% NaCl (Table 5.4).

5.4.6 Effect of the $R_{g,f}$ on the sodium release properties of the SLCs

In the measurement of the sodium release, the rapid release of sodium via convective transfer by the serum may be more reflected by the R_{max}. Compare to the convective transfer,

the slower sodium release via diffusion may be more reflected by the C_{max} and AUC. The above difference is because that the R_{max} represents the initial increment of sodium concentration following right after the gel compression. In contrast, the C_{max} and AUC represent respectively the final and cumulative concentration of sodium release into the surrounding water at the end of the measurement.

Among the sodium release parameters extracted, C_{max} and AUC both correlated negatively with the $R_{g,f}$. However, these correlations only exist in the SLCs with 3.5% NaCl (Table 5.4). These correlation can be linked to the correlation between the $R_{g,f}$ and the $strain_{max}$ for the SLCs with 3.5% NaCl. As mentioned in section 5.4.5, the SLCs with smaller $R_{g,f}$ fracture earlier during the compression. Earlier gel fracture could lead to more fragmented debris, and, hence greater total surface area of emulsion-filled gels (Sala and Stieger 2013). In the measurement of sodium release, the earlier and more extensive the gel breaks down, the more sodium can diffuse out from the newly formed surface area of the debris (Koliandris and others 2008; de Loubens and others 2011a; Panouille and others 2011). The greater total area after the fracture of the SLCs would therefore enhance the diffusive sodium release and yield higher C_{max} and AUC. It is worth noticing that for the SLCs with 3.5% NaCl, C_{max} correlated positively with the homogenization pressure (Table 5.4). However, the correlation between the C_{max} and the $R_{g,f}$ was stronger than the correlation between the C_{max} and the homogenization pressure. Besides, the correlation between the AUC and the $R_{g,f}$ was stronger than the correlation between the AUC and F/S.

The lack of the correlation between the $R_{g,f}$, $strain_{max}$, C_{max} and AUC in the SLCs with 1.5% NaCl may be attributed to the lower inter-protein interaction at lower NaCl content. As discussed in section 5.4.2 and in previous literatures (Langton and Hermansson 1996; Pouzot and others 2004), the protein-protein interaction is stronger in the gel networks with higher NaCl level, due to the screening effect of NaCl. The stronger inter-protein interaction in the SLCs with 3.5% NaCl could therefore yield a network where the initiation of fracture more likely occurs at the protein-fat interface (Kuo and others 2016). Hence the effect of the $R_{g,f}$ on the gel fracture, and thus, the sodium release, is more evident in the SLCs with 3.5% NaCl compared to the SLCs with 1.5% NaCl.

The present study revealed two potential structural adjustments to enhance sodium release. The maximum rate of sodium release can be boosted via increasing the porosity and thus serum release. The maximum concentration and the cumulative concentration of the released sodium can be boosted via reducing the particle size of fat and hence facilitating the

gel fracture. Nevertheless, the counteracting effect on the serum release and the gel fragmentation by the $R_{g,f}$ requires further investigation. Indeed, sensory method will be required to answer whether greater serum release led by larger fat particles, or more fragmentation led by smaller fat particles in the gel, is more critical to enhancing the perceived saltiness. In addition, effective strategies for sodium reduction require consideration of the food categories. For example, serum release, or juiciness, is positive attribute for meat quality (Brown and others 1996), but regarded as defect in pudding or dairy products (van den Berg and others 2007a).

5.5 Conclusions

In this study, effect of the treatment on the structural properties of the solid lipoproteic colloids (SLCs) was evaluated. Also, effect of the structural properties on the textural and sodium release properties of the SLCs was investigated. For both SLCs with 1.5% and 3.5% NaCl, water content (W%) and the weight ratio of fat to solid (F/S) correlated positively and negatively with the porosity, respectively. The porosity correlated positively with serum release and the maximum rate of sodium release (R_{max}). These correlations indicated that convective transport via serum flow is the main driving force of sodium release during the gel compression. For both SLCs with 1.5% and 3.5% NaCl, the gyration radius of fat particles ($R_{g,f}$) correlated negatively with the homogenization pressure. For the SLCs with 3.5% NaCl, the $R_{g,f}$ correlated positively with the strain at maximum stress ($strain_{max}$) and negatively with the maximum concentration of released sodium (C_{max}) and the area under the curve of sodium release (AUC). These correlations indicated that, after the gel fracture, the diffusive transport of sodium release via the new surfaces is the main driving force of sodium release. The lack of such correlations in the SLCs with 1.5% NaCl suggested the stronger inter-protein interaction in the SLCs with 3.5% NaCl. The present study revealed the rules of porosity and particle size of fat in governing the convective and diffusive transport for sodium release during different stages of gel breakdown. The findings are essential for understanding the temporal saltiness perception of the SLCs. Combining this study with future sensory evaluations on the SLCs will deliver more clear messages for a potential sodium reduction in lipoproteic products via effective sodium release.

5.6 References

Aguilera JM. 2005. Why food microstructure? J.Food Eng. 67(1–2):3-11.

Boisard L, Andriot I, Arnould C, Achilleos C, Salles C, Guichard E. 2013. Structure and composition of model cheeses influence sodium NMR mobility, kinetics of sodium release and sodium partition coefficients. Food Chem. 136(2):1070-7.

Boisard L, Andriot I, Martin C, Septier C, Boissard V, Salles C, Guichard E. 2014. The salt and lipid composition of model cheeses modifies in-mouth flavour release and perception related to the free sodium ion content. Food Chem. 145(0):437-44.

Brown W, Gerault S, Wakeling I. 1996. Diversity of perceptions of meat tenderness and juiciness by consumers: A time-intensity study. J.Texture Stud. 27(5):475-92.

Clariana M, Guerrero L, Sarraga C, Garcia-Regueiro JA. 2012. Effects of high pressure application (400 and 900 MPa) and refrigerated storage time on the oxidative stability of sliced skin vacuum packed dry-cured ham. Meat Sci. 90(2):323-9.

de Loubens C, Panouillé M, Saint-Eve A, Déléris I, Tréléa IC, Souchon I. 2011a. Mechanistic model of in vitro salt release from model dairy gels based on standardized breakdown test simulating mastication. J.Food Eng. 105(1):161-8.

de Loubens C, Saint-Eve A, Deleris I, Panouille M, Doyennette M, Trelea IC, Souchon I. 2011b. Mechanistic model to understand in vivo salt release and perception during the consumption of dairy gels. J.Agric.Food Chem. 59(6):2534-42.

Fulladosa E, Serra X, Gou P, Arnau J. 2009. Effects of potassium lactate and high pressure on transglutaminase restructured dry-cured hams with reduced salt content. Meat Sci. 82(2):213-8.

Fulladosa E, Sala X, Gou P, Garriga M, Arnau J. 2012. K-lactate and high pressure effects on the safety and quality of restructured hams. Meat Sci. 91(1):56-61.

Geankoplis CJ. 2003. Principles of Unsteady-State and Convective Mass Transfer. In: Christie J. Geankoplis, editor. Transport Processes and Separation Process Principles. 4th ed. Upper Saddle River, New Jersey: Prentice Hall. p 459-512.

Huppertz T. 2011. Homogenization of Milk | High-Pressure Homogenizers. In: John W. Fuquay, editor. Encyclopedia of Dairy Sciences (Second Edition). San Diego: Academic Press. p 755-60.

Hussain R, Gaiani C, Jeandel C, Ghanbaja J, Scher J. 2012. Combined effect of heat treatment and ionic strength on the functionality of whey proteins. J.Dairy Sci. 95(11):6260-73.

Knoop JE, Sala G, Smit G, Stieger M. 2013. Combinatory effects of texture and aroma modification on taste perception of model gels. Chemosens.Percept. 6(2):60-9.

Koliandris A, Lee A, Ferry A, Hill S, Mitchell J. 2008. Relationship between structure of hydrocolloid gels and solutions and flavour release. Food Hydrocoll. 22(4):623-30.

Kuo W, Lee Y. 2014a. Temporal sodium release related to gel microstructural properties-implications for sodium reduction. J.Food Sci. 79(11):E2245-52.

Kuo W, Lee Y. 2014b. Effect of food matrix on saltiness perception-implications for sodium reduction. Comprehensive Reviews in Food Science and Food Safety 13(5):906-23.

Kuo W, Ilavsky J, Lee Y. 2016. Structural characterization of solid lipoproteic colloid gels by ultra-small-angle X-ray scattering and the relation with sodium release. Food Hydrocoll. 56: 325-33.

Langton M, Hermansson A. 1996. Image analysis of particulate whey protein gels. Food Hydrocoll. 10(2):179-91.

Lawrence G, Buchin S, Achilleos C, Berodier F, Septier C, Courcoux P, Salles C. 2012. *in vivo* sodium release and saltiness perception in solid lipoprotein matrices. 1. Effect of composition and texture. J.Agric.Food Chem. 60(21):5287-98.
Lee S, Lefèvre T, Subirade M, Paquin P. 2009. Effects of ultra-high pressure homogenization on the properties and structure of interfacial protein layer in whey protein-stabilized emulsion. Food Chem. 113(1):191-5.
Lorenzen PC, Schrader K. 2006. A comparative study of the gelation properties of whey protein concentrate and whey protein isolate. Lait 86(4):259-71.
Norton JE, Wallis GA, Spyropoulos F, Lillford PJ, Norton IT. 2014. Designing food structures for nutrition and health benefits. Annual Review of Food Science and Technology 5: 5177-95.
Panouille M, Saint-Eve A, de Loubens C, Deleris I, Souchon I. 2011. Understanding of the influence of composition, structure and texture on salty perception in model dairy products. Food Hydrocoll. 25(4):716-23.
Phan VA, Yven C, Lawrence G, Chabanet C, Reparet JM, Salles C. 2008. *in vivo* sodium release related to salty perception during eating model cheeses of different textures. Int.Dairy J. 18(9):956-63.
Pouzot M, Durand D, Nicolai T. 2004. Influence of the ionic strength on the structure of heat-set globular protein gels at pH 7. beta-lactoglobulin. Macromolecules 37(23):8703-8.
Sala G, Stieger M. 2013. Time to first fracture affects sweetness of gels. Food Hydrocoll. 30(1):73-81.
Sala G, van Vliet T, Cohen Stuart MA, Aken GAv, van de Velde F. 2009. Deformation and fracture of emulsion-filled gels: Effect of oil content and deformation speed. Food Hydrocoll. 23(5):1381-93.
Stieger M. 2011. Texture-taste interactions: Enhancement of taste intensity by structural modifications of the food matrix. Procedia Food Sci. 1(0):521-7.
Stieger M, van de Velde F. 2013. Microstructure, texture and oral processing: New ways to reduce sugar and salt in foods. Curr. Opin. Colloid. In. 18(4):334-48.
van de Velde F, Adamse M. 2013. Juiciness enhances the perceived saltiness of meat products. New Food 2.
van den Berg L, van Vliet T, van der Linden E, van Boekel MAJS, van de Velde F. 2007a. Serum release: The hidden quality in fracturing composites. Food Hydrocoll. 21(3):420-32.
van den Berg L, van Vliet T, van der Linden E, van Boekel MAJS, van de Velde F. 2007b. Breakdown properties and sensory perception of whey proteins/polysaccharide mixed gels as a function of microstructure. Food Hydrocoll. 21(5–6):961-76.
van den Berg L, van Vliet T, van der Linden E, van Boekel MAJS, van de Velde F. 2008. Physical properties giving the sensory perception of whey proteins/polysaccharide gels. Food Biophys. 3(2):198-206.
van Vliet T, Luyten H, Walstra P. 1993. Time-dependent fracture-behavior of food. Food Colloids and Polymers : Stability and Mechanical Properties 113: 175-90.
Walstra P. 2003. Physical chemistry of foods. New York, NY: Marcel Dekker Inc.

5.7 Tables and Figures

Table 5.1. Porosity and the gyration radius of fat ($R_{g,f}$) of the SLCs[a].

Sample	Porosity ± SD (%)	$R_{g,f}$ (nm)
8-0-1.5-14	71.84 ± 5.16 ab	-
8-0-1.5-55	75.77 ± 2.02 a	-
8-11-1.5-14	54.80 ± 4.38 cdef	449.3
8-11-1.5-55	65.47 ± 2.57 abcd	120.5
8-22-1.5-14	62.34 ± 7.14 abcde	484.6
8-22-1.5-55	56.02 ± 0.64 bcdef	125.8
8-33-1.5-14	53.38 ± 1.20 def	319.3
8-33-1.5-55	48.48 ± 1.76 f	121.2
16-0-1.5-14	61.05 ± 1.34 abcde	-
16-0-1.5-55	71.71 ± 6.08 ab	-
16-11-1.5-14	55.61 ± 2.26 bcdef	457.5
16-11-1.5-55	43.30 ± 6.36 f	153.6
16-22-1.5-14	70.85 ± 0.78 abc	325.2
16-22-1.5-55	58.75 ± 6.29 bcde	113.6
16-33-1.5-14	58.82 ± 0.14 bcde	274
16-33-1.5-55	57.35 ± 8.27 bcdef	101
8-0-3.5-14	72.72 ± 5.88 a	-
8-0-3.5-55	73.31 ± 1.70 a	-
8-11-3.5-14	62.46 ± 2.42 abc	371.5
8-11-3.5-55	62.93 ± 5.43 abc	125.2
8-22-3.5-14	58.15 ± 5.62 abc	387.3
8-22-3.5-55	41.93 ± 8.63 abc	121.6
8-33-3.5-14	50.61 ± 3.25 bc	291.2
8-33-3.5-55	49.65 ± 7.42 c	110.1
16-0-3.5-14	72.06 ± 8.14 a	-
16-0-3.5-55	68.33 ± 4.68 ab	-
16-11-3.5-14	61.84 ± 2.19 abc	711
16-11-3.5-55	48.46 ± 0.92 c	91.2
16-22-3.5-14	54.82 ± 1.13 abc	407.8
16-22-3.5-55	59.37 ± 8.56 abc	77.4
16-33-3.5-14	53.40 ± 0.71 abc	N.D.[b]
16-33-3.5-55	54.07 ± 8.58 abc	66.3

a. The numbers followed by the same letters within the group of same NaCl content are not significantly different.
b. The value was not measured due to operation error.

Table 5.2. Properties of the SLCs measured by a compression test using a texture analyzer[a].

Sample	Serum release[b] ± SD (g)	$Stress_{max}$ ± SD (KPa)	$Strain_{max}$ ± SD (%)
8-0-1.5-14	2.85 ± 0.42 b	69.91 ± 3.25 e	79.90 ± 0.14 ab
8-0-1.5-55	2.47 ± 0.21 c	53.41 ± 8.27 e	79.82 ± 0.35 ab
8-11-1.5-14	0.96 ± 0.07 d	65.26 ± 10.96 e	73.81 ± 1.98 abc
8-11-1.5-55	0.63 ± 0.06 fg	51.58 ± 8.60 e	59.54 ± 1.28 abc
8-22-1.5-14	0.74 ± 0.07 ef	58.90 ± 0.28 e	62.86 ± 0.99 abc
8-22-1.5-55	0.52 ± 0.04 fgh	93.07 ± 9.37 e	55.08 ± 1.86 bc
8-33-1.5-14	0.48 ± 0.04 fghi	100.92 ± 17.98 de	59.78 ± 3.42 abc
8-33-1.5-55	0.30 ± 0.00 hi	169.72 ± 21.49 cd	55.87 ± 3.17 bc
16-0-1.5-14	4.39 ± 0.14 a	293.18 ± 100.13 ab	79.99 ± 0.00 ab
16-0-1.5-55	4.66 ± 0.06 a	256.62 ± 37.48 ab	79.99 ± 0.00 a
16-11-1.5-14	0.77 ± 0.11 e	236.21 ± 20.60 abc	78.06 ± 3.58 ab
16-11-1.5-55	0.45 ± 0.06 ghi	216.36 ± 50.66 abc	67.92 ± 2.04 abc
16-22-1.5-14	0.47 ± 0.00 fghi	309.21 ± 61.90 a	76.92 ± 2.54 ab
16-22-1.5-55	0.25 ± 0.07 hi	270.17 ± 31.73 ab	59.76 ± 4.00 abc
16-33-1.5-14	0.12 ± 0.00 i	192.87 ± 34.65 bcd	48.01 ± 8.77 c
16-33-1.5-55	0.20 ± 0.00 hi	201.60 ± 41.44 abc	73.89 ± 47.66 abc
8-0-3.5-14	3.26 ± 0.31 a	55.40 ± 14.53 d	80.00 ± 0.00 a
8-0-3.5-55	3.39 ± 0.00 a	62.07 ± 2.63 d	79.85 ± 0.29 a
8-11-3.5-14	1.08 ± 0.13 b	76.47 ± 19.57 cd	76.62 ± 2.37 ab
8-11-3.5-55	0.86 ± 0.06 b	59.83 ± 9.05 d	60.55 ± 1.62 cdef
8-22-3.5-14	0.83 ± 0.06 b	71.11 ± 14.09 cd	66.14 ± 2.67 bcde
8-22-3.5-55	0.49 ± 0.10 b	112.25 ± 15.81 bcd	54.08 ± 3.42 efg
8-33-3.5-14	0.47 ± 0.00 b	101.22 ± 3.90 bcd	60.28 ± 1.99 cdef
8-33-3.5-55	0.30 ± 0.10 b	166.29 ± 29.47 bcd	56.41 ± 1.12 defg
16-0-3.5-14	3.83 ± 1.56 a	213.83 ± 37.96 ab	78.68 ± 2.31 a
16-0-3.5-55	3.22 ± 1.12 a	331.76 ± 156.48 a	78.25 ± 2.47 ab
16-11-3.5-14	0.90 ± 0.00 b	142.21 ± 47.96 bcd	64.65 ± 0.78 bcde
16-11-3.5-55	0.47 ± 0.06 b	179.14 ± 16.01 bcd	46.30 ± 2.03 g
16-22-3.5-14	0.42 ± 0.07 b	206.26 ± 42.92 abc	73.60 ± 2.55 abc
16-22-3.5-55	0.22 ± 0.00 b	214.87 ± 53.25 ab	45.06 ± 15.63 g
16-33-3.5-14	0.17 ± 0.00 b	152.86 ± 88.03 bcd	67.99 ± 9.62 abcd
16-33-3.5-55	0.07 ± 0.06 b	322.11 ± 20.73 a	51.72 ± 3.80 fg

a. The numbers followed by the same letters within the group of same NaCl content are not significantly different.

b. Serum release, amount of liquid expelled from the sample during the compression test. $Stress_{max}$, maximum stress measured during the compression test; $Strain_{max}$, strain at the maximum stress.

Table 5.3. Sodium release properties of the SLCs[a].

Sample	R_{max} ± SD[b] (ppm Na/s)	C_{max} ± SD (ppm Na)	AUC ± SD (10^3ppm Na.s)
8-0-1.5-14	4.57 ± 0.35 ab	60.44 ± 1.98 ab	20.26 ± 0.49 bc
8-0-1.5-55	2.99 ± 0.74 bc	50.32 ± 2.95 ab	15.73 ± 1.12 defg
8-11-1.5-14	0.73 ± 0.21 de	45.25 ± 8.98 ab	12.49 ± 2.55 ghi
8-11-1.5-55	0.71 ± 0.14 de	69.35 ± 4.74 ab	15.89 ± 1.27 cdefg
8-22-1.5-14	0.77 ± 0.14 de	64.14 ± 6.43 ab	16.06 ± 0.49 cdefg
8-22-1.5-55	0.74 ± 0.17 de	75.90 ± 3.83 ab	16.58 ± 1.38 cdef
8-33-1.5-14	0.73 ± 0.10 de	76.20 ± 6.49 ab	16.80 ± 1.51 cde
8-33-1.5-55	0.82 ± 0.19 de	79.13 ± 3.86 ab	17.72 ± 0.97 cd
16-0-1.5-14	5.26 ± 2.05 a	79.70 ± 10.89 ab	29.54 ± 0.92 a
16-0-1.5-55	6.25 ± 0.21 a	90.99 ± 2.12 a	31.28 ± 0.14 a
16-11-1.5-14	0.34 ± 0.11 e	33.83 ± 4.39 b	8.02 ± 0.95 ij
16-11-1.5-55	0.36 ± 0.12 e	43.23 ± 7.01 ab	9.68 ± 1.79 hi
16-22-1.5-14	0.34 ± 0.07 de	79.93 ± 65.97 ab	8.10 ± 0.85 ij
16-22-1.5-55	0.60 ± 0.14 de	59.09 ± 0.57 ab	13.20 ± 0.14 efgh
16-33-1.5-14	0.58 ± 0.07 de	73.59 ± 23.41 ab	12.64 ± 0.64 fghi
16-33-1.5-55	1.89 ± 0.42 cd	73.21 ± 40.73 ab	23.21 ± 1.70 b
8-0-3.5-14	10.76 ± 0.87 a	149.01 ± 22.62 abcd	50.07 ± 7.70 ab
8-0-3.5-55	10.01 ± 2.17 a	140.60 ± 8.75 abcd	47.05 ± 2.76 abc
8-11-3.5-14	1.61 ± 0.48 b	87.93 ± 26.09 d	21.38 ± 5.72 e
8-11-3.5-55	2.25 ± 0.12 b	157.34 ± 24.11 abc	37.86 ± 5.86 bcde
8-22-3.5-14	1.80 ± 0.17 b	121.32 ± 10.60 bcd	28.73 ± 2.27 cde
8-22-3.5-55	2.38 ± 0.75 b	181.21 ± 5.88 ab	43.13 ± 1.55 bc
8-33-3.5-14	1.76 ± 0.32 b	150.44 ± 9.71 abcd	35.51 ± 2.42 bcde
8-33-3.5-55	2.59 ± 0.53 b	166.53 ± 10.12 abc	39.54 ± 2.58 bcd
16-0-3.5-14	10.01 ± 0.35 a	193.50 ± 30.97 ab	65.30 ± 12.02 a
16-0-3.5-55	12.34 ± 3.54 a	195.60 ± 31.03 a	63.44 ± 10.41 a
16-11-3.5-14	2.31 ± 0.60 b	95.18 ± 20.09 cd	24.41 ± 5.72 de
16-11-3.5-55	2.90 ± 0.10 b	178.09 ± 17.75 ab	43.39 ± 4.50 bc
16-22-3.5-14	0.63 ± 0.14 b	79.37 ± 1.13 d	17.69 ± 0.07 e
16-22-3.5-55	2.87 ± 1.13 b	168.82 ± 25.67 abc	39.45 ± 3.18 bcde
16-33-3.5-14	1.29 ± 0.71 b	134.34 ± 50.42 abcd	29.96 ± 11.17 bcde
16-33-3.5-55	2.41 ± 0.52 b	157.41 ± 31.69 abc	36.93 ± 7.26 bcde

a. The numbers followed by the same letters within the group of same NaCl content are not significantly different.

b. R_{max}, maximum rate of sodium release; C_{max}, maximum concentration of released sodium; AUC, area under the curve of sodium release.

Table 5.4. Correlation coefficients between treatments, structural, textural properties and sodium release properties of SLCs[a].

	NaCl (%)	P%[b]	W%	F/S	Pressure	$R_{g,f}$	Porosity	R_{max}	C_{max}	AUC	Serum release
$R_{g,f}$	1.5	-0.11	0.28	-0.15	-0.91***						
	3.5	0.09	0.28	-0.32	-0.86***						
Porosity	1.5	-0.08	0.51*	-0.58*	-0.09	0.06					
	3.5	0.00	0.75***	-0.84***	-0.19	0.45					
R_{max}	1.5	0.12	0.59*	-0.82***	0.03	-0.34	0.55*				
	3.5	0.03	0.72***	-0.90***	0.12	-0.52	0.76***				
C_{max}	1.5	0.05	-0.27	0.12	0.11	-0.41	0.24	0.37			
	3.5	0.09	0.11	-0.24	0.60*	-0.84***	-0.02	0.48			
AUC	1.5	0.04	0.28	-0.45	0.19	-0.44	0.30	0.86***	0.62*		
	3.5	0.08	0.48	-0.66**	0.37	-0.80***	0.42	0.84***	0.87***		
Serum	1.5	0.10	0.71***	-0.87***	-0.06	0.68*	0.55*	0.96***	0.26	0.76***	
	3.5	-0.07	0.83***	-0.92***	-0.09	0.62*	0.85***	0.94***	0.28	0.72***	
$Stress_{max}$	1.5	0.91***	-0.34	-0.14	-0.01	-0.17	-0.10	0.14	0.23	0.09	0.15
	3.5	0.78***	-0.38	-0.08	0.32	-0.31	-0.09	0.15	0.36	0.30	-0.04
$Strain_{max}$	1.5	0.23	0.61*	-0.77***	-0.16	0.40	0.49	0.61*	-0.21	0.29	0.65**
	3.5	-0.15	0.61*	-0.64**	-0.51*	0.70*	0.74***	0.60*	-0.29	0.19	0.76***

a. The numbers with the superscripts of one, two, and three asterisks indicate significant correlations for $P < 0.05$, 0.01, and 0.005, respectively.
b. P% and W%, protein and water contents (w/w) in the SLCs, respectively; F/S, weight ratio of fat to solid content of the SLCs; $R_{g,f}$, gyration radius of the fat globules in the SLCs; R_{max}, maximum rate of sodium release; C_{max}, maximum concentration of released sodium; AUC, area under the curve of sodium release. Serum release, amount of liquid expelled from the sample during the compression test. $Stress_{max}$, maximum stress measured during the compression test; $Strain_{max}$, strain at the maximum stress.

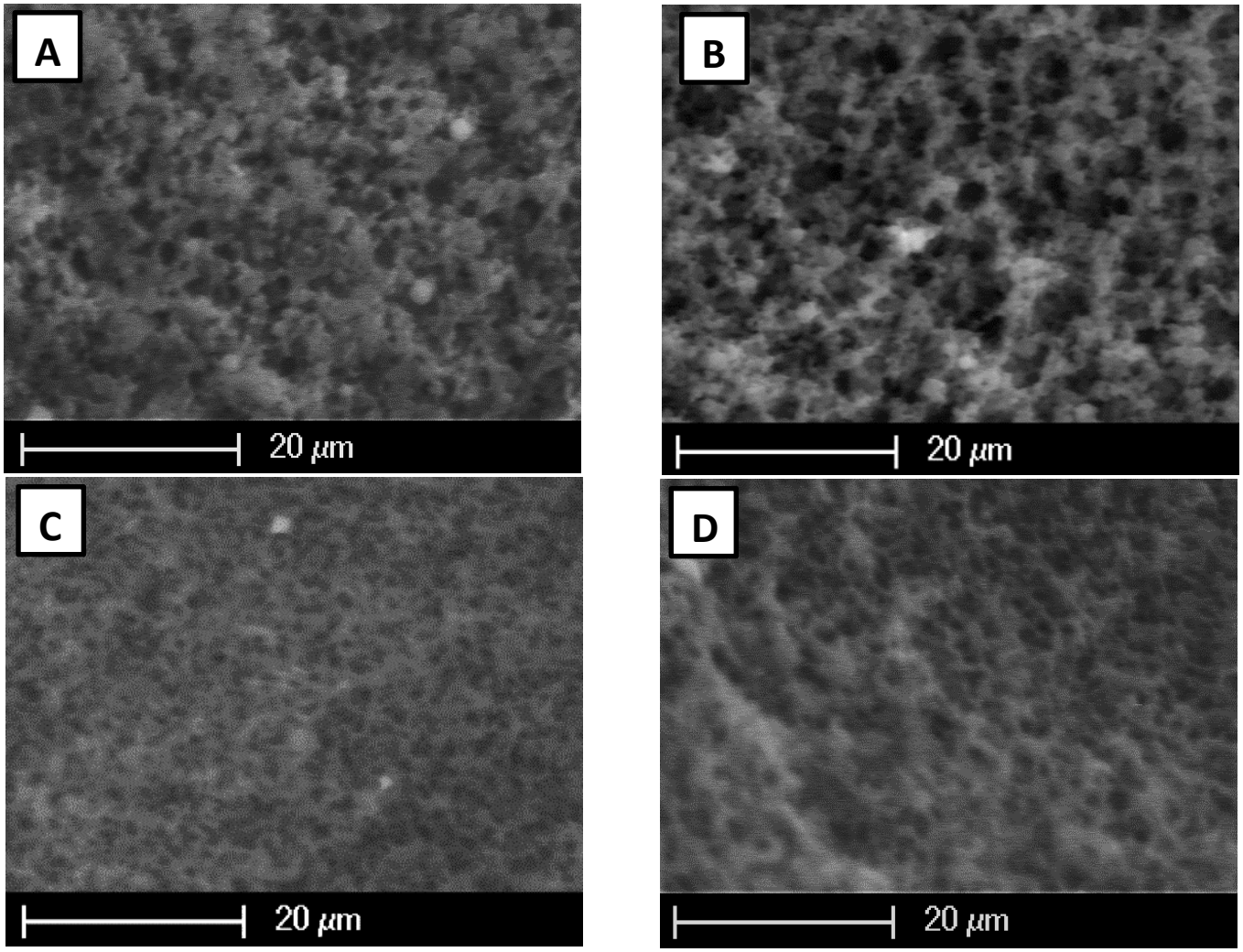

Figure 5.1. ESEM images of the cross-sections of SLCs 8-33-1.5-14 (A), 16-22-1.5-14 (B), 8-33-1.5-55 (C), and 16-22-1.5-55 (D).

CHAPTER 6

Correlating Structural Properties to Saltiness Perception of Model Lipoproteic Gels

6.1 Abstract

Structural engineering for sodium reduction in processed foods is an emerging area of research. Understanding structural effects on saltiness perception is prerequisite to developing appropriate engineering strategies for sodium reduction. In this study, porosity and gyration radius of fat ($R_{g,f}$) were correlated with saltiness perception of model lipoproteic gels. The model solid lipoproteic colloids (SLCs) were made by pressure homogenization of whey protein isolate, anhydrous milk fat, and NaCl, followed by heat-induced gelation. Quantitative descriptive analysis (QDA) was used to profile the sensory properties including the SLC saltiness. Time-intensity (TI) method was used to characterize the temporal saltiness perception properties of the SLCs. Correlation analysis between selected QDA and TI properties, as well as the porosity, $R_{g,f}$ and textural properties, was performed. Saltiness correlated positively with the instrumental properties including porosity and serum release. Saltiness also correlated positively with the QDA syneresis. Besides, saltiness correlated positively with the TI parameters including R_{inc} (the rate of saltiness increment), I_{max} (the maximum saltiness), and negatively with t_{max} (time to reach I_{max}). The above correlations suggested that the expulsion of serum is a major driving factor for sodium release, and increasing porosity can in this way boost saltiness. Saltiness did not correlate to $R_{g,f}$, due to the counteracting effects of $R_{g,f}$ on sodium release. The $R_{g,f}$ correlated negatively with the QDA crumbly, but positively with the QDA gelatinous. Hence, the decrease in $R_{g,f}$ would favor sodium diffusion from the crumbly samples, but would disfavor serum release due to the less gelatinous texture. This study identified porosity as a potential target for structural engineering to reduce sodium in lipoproteic foods. Future directions can focus on optimizing the matrix structure with enhanced sodium release while remaining ideal sensory texture for consumer acceptance.

Keywords

Porosity, gyration radius of fat, quantitative descriptive analysis, time-intensity method, saltiness perception

6.2 Introduction

Sodium reduction in processed lipoproteic foods such as cheese and processed meats has drawn increasing attention in food research and industry (Desmond 2006; Johnson and others 2009; Felicio and others 2016; Yotsuyanagi and others 2016). Engineering food structures to modulate the sensory properties is as a promising strategy to develop healthy food products low in salt, fat or sugar or high in micronutrients (Aguilera 2005; Stieger 2011; Knoop and others 2013; Norton and others 2014). Understanding the structural impact on textural and sensory properties is prerequisite to structural optimization toward ideal sodium release and sensory acceptance. Solid lipoproteic colloid (SLC) composed of lipid and protein, in the oil-in-water emulsion structure, has been used as the model lipoproteic food system to study the matrix effects on sodium release and saltiness perception (Phan and others 2008; Lauverjat and others 2009b; de Loubens and others 2011a; de Loubens and others 2011b; Panouille and others 2011; Kuo and Lee 2014a; Kuo and Lee 2014b; Kuo and others 2016).

Two primary mechanisms between food structure/texture and sodium release have been proposed as potential routes to enhance saltiness perception via structural engineering. First, sodium can be convectively transported by the liquid medium from within the pore region to the exterior of the food matrix (Kuo and Lee 2014b). The outward flow of the liquid medium, i.e., the serum release, occurs when the matrix is subjected to external force (van den Berg and others 2007a). Serum release of a model gel system was found to be positively correlated to “watery” sensory attributes by a descriptive analysis panel (van den Berg and others 2007b). In a series of studies on the protein/polysaccharide mixed gel, serum release was found to be higher in the gels with heterogeneous, bi-continuous, or coarse stranded microstructures, compared to the homogeneous or protein-continuous microstructures (van den Berg and others 2007a; van den Berg and others 2007b; Stieger and van de Velde 2013). It was thus proposed that the gel with higher porosity can give higher serum release, and, in turn, faster sodium release and greater saltiness perception (Stieger and van de Velde 2013). However, the protein/polysaccharide mixed gels in the above studies did not include fat. Therefore, this non-fat model gel system may have limited implications for the structural engineering of lipoproteic products. Furthermore, only descriptive analysis was used to determine the taste qualities of the above protein/polysaccharide mixed gels. Indeed, the time-intensity method to determine the temporal saltiness perception properties would be

helpful to validate the convective mechanisms involving rapid transport of sodium via serum release.

In addition to the convective transport, sodium in food matrix can also be released via spontaneous diffusion (Kuo and Lee 2014b). The driving force for spontaneous diffusion is the concentration gradient across the interior and exterior of the matrix. The rate of diffusion is proportional to the total area of the contacting surfaces between the matrix and the surrounding medium (Kuo and Lee 2014b). Hence, increasing the surface area between the food matrix and the saliva can increase the total sodium release during mastication (de Loubens and others 2011a). Increasing fat content (de Loubens and others 2011a; de Loubens and others 2011b; Panouille and others 2011; Boisard and others 2013; Boisard and others 2014) or decreasing the particle size of fat (Phan and others 2008; Kuo and Lee 2014a; Kuo and others 2016) of lipoproteic gels can lead to greater extent of gel breakdown, and, hence, greater sodium release *in vitro* or in-mouth. Adjusting particle size of fat should be more favorable than increasing fat content as the latter may bring concerns with nutrition labeling. It is worth noticing that, in the study of Phan and others (2008), in-mouth sodium release but not saltiness perception was enhanced by the reduction of fat particle size. Since the above sensory studies on lipoproteic gels did not consider the factor of serum release, it is unknown how particle size of fat can influence serum release and thus affect saltiness perception.

The objective of this study is to correlate porosity and particle size of fat to saltiness perception of the SLCs. Descriptive analysis was used to profile the saltiness and sensory texture, and time-intensity method was used to determine the temporal saltiness perception properties. Correlation analysis was performed on selected sensory and instrumental properties to reveal the relationships between structure, texture and saltiness perception properties of the SLCs. Regression models for the saltiness were constructed to demonstrate the possibility of predicting saltiness by the structural properties of the SLCs.

6.3 Materials and Methods

6.3.1 Preparation of the SLCs

The procedure for making the SLCs for the sensory evaluations was described in Chapter 3 (Kuo and Lee 2014a) with a few modifications as below. The formulation and treatment variables include the contents of protein (8 and 16%, w/w), fat (0, 11, 22, and 33%, w/w), and the homogenization pressure (14 and 55 MPa). The NaCl level of the SLCs was

kept at 1.5%, w/w. All equipment and containers were food grade and sanitized using 200 ppm of the liquid sanitizer XY-12 (Ecolab, St Paul, MN, USA) before the preparation. After the pressure homogenization, 250 g emulsion was heated at 90˚C for 35 min in the polycarbonate jar (2116-0500, Nalgene™, Rochester, NY, USA). Due to syneresis during the storage, 280 g instead of 250 g was weighed and heated in the jars for the non-fat SLCs. After overnight storage at 6-8˚C, the SLCs were cut into 5 g cubes. One hour before serving the panel, the cubes were taken out from the 6-8˚C refrigerator and left at room temperature in the 1 oz. plastic sample cups with lids.

6.3.2 Panelists recruitment

The recruitment, sample preparation, and the session procedures were approved by the University of Illinois Institutional Review Board (IRB) (Protocol No. 16459). The participants submitted a questionnaire to indicate their qualification to this panel. The qualifying criteria included age of 18 or more, no any food allergies, and with availability meeting the session schedule. The participants attended a screening session of identifying basic tastes and ranking the saltiness of NaCl solutions. The concentrations (w/v) of the basic taste solutions were 0.05% citric acid (sour), 0.7% sucrose (sweet), 0.1% NaCl (salty), 0.024% caffeine (bitter) and water (none). The NaCl concentrations for the ranking test were 0, 0.17, 0.3, 0.4, 1, and 1.2%. Twelve panelists, including 10 females and 2 males, were recruited based on their screening results and availabilities.

6.3.3 Training and testing procedures

6.3.3.1 Quantitative descriptive analysis (QDA)

The QDA panel included 16 training sessions and 4 actual test sessions. Each session ran for 1 hour. The first 6 training sessions were used for term generation, including two sessions of initial term generation, two reference refinement sessions, and two term finalization sessions. Table 6.1 lists the finalized attributes and the corresponding definitions, references, evaluations protocols for each modality (aroma, aroma-by-mouth, taste, aftertaste, and texture). The panel also determined the rinsing protocol between each single tasting to be in the order of carbonated, warm and room temperature water.

The term generation was followed by 9 sessions of group scoring practice. During the group scoring for each attribute, the panel identified the sample carrying the strongest intensity. With such sample being 15 on a 15-point scale, they then determined the intensity of the corresponding reference as an anchor. For each attribute, the panelists then evaluated the rest samples and calibrated their own rating against the group average. Initially, the group scoring was focused on a specific modality per session. In the 7^{th}, 8^{th}, and 9^{th} sessions of group scoring, the panelists rated all attributes for all modalities of each sample. Throughout the group training sessions, the panelists also practiced to chew the samples *ad libitum* but conformed their chewing times to be within 3 seconds apart from the group average for each sample.

Following the group scoring was one practice session of individual booth ratings and 4 sessions of actual booth ratings. The booth sessions were carried out under incandescent lighting at 25°C in Bevier Hall at the University of Illinois Campus. The Compusense *five* Plus (Version 5.0: Guelph ON, Canada) data acquisition system was used for the data collection. Prior to each booth session, the panelists re-familiarized themselves with the references with the list of the attribute definitions and evaluation protocols (Table 6.1). Also, they were allowed to re-familiarize with the references and the reference list at any time during the booth rating. In each booth session, the panelists evaluated two replicates of four samples consecutively. The 4 samples within each replicate were given randomly. For each sample, the panelists chew the first cube to evaluate the aroma, aroma-by-mouth, taste and aftertaste. After rinsing, the panelists chew the second cube to evaluate the texture. The panelists submitted the ratings for each attribute on a categorical scale with integral scores ranging from 0 to 15. Before the actual booth tests, the panelists were given their own ratings and the group averages from the booth practice. The actual booth tests were carried out in the same procedure as the practice booth sessions, except that the data from the actual test was not revealed to the panelists.

6.3.3.2 Time-intensity (TI) evaluations

After the completion of all QDA sessions, the same 12 panelists went through 4 sessions of training and 4 sessions of actual test for the TI evaluations. Each session ran for 1 hour. The first two training sessions of TI were group practice, during which the test objectives and protocols were explained. During the group practice, the panelists re-familiarized with the saltiest SLC identified in the QDA results. Throughout chewing of this SLC, the panelists identified the saltiness peak. With this peak intensity being the score of 15,

the panelists determined the scores of three reference NaCl solutions on a 15 points scale. The scores of the three NaCl references, 0.2, 0.4 and 0.6% (w/v) were 3.5, 10 and 13.5, respectively. To practice the TI-evaluation, the panelist placed a sample cube in mouth and chewed naturally for 30 seconds before they expectorated. Throughout the chewing, they write down the saltiness scores every five second. After the expectoration, they continue to note down the saltiness for another 60 seconds. A stopwatch and a metronome were used simultaneously to count the time and to alert the scoring every 5 seconds. The 60 seconds of post expectoration was decided based on the panelists' evaluation on different SLCs. It was the longest time required to have the saltiness to return to zero after spitting out. The rinsing protocol in between tasting of each reference and sample was carbonated, warm and room temperature water. For each sample, the panelists evaluated twice and compared their own peak intensity versus the group average. No further curve calibration among the panelists was performed. The panelists were not informed with any typical shapes of TI curves, either. They were instructed to review if their duplicate ratings were consistent, and if they were differentiating different SLCs with their time-intensity profiles.

Following the group training were two practice sessions of individual booth evaluation and four sessions of actual booth evaluation. The hardware and software for the booth evaluation were the same as described in the QDA method (section 6.3.3.1). In each booth session, the panelists evaluated two replicates of four samples consecutively. The 4 samples within each replicate were given randomly. At the beginning of each booth session, the panelists re-familiarized with the three NaCl references. To evaluate the sample, the panelist placed a sample cube in mouth and click "Start" on the monitor with a mouse. The panelists then chewed naturally while evaluating the saltiness momentarily by dragging the mouse along a linear scale ranging from 0 to 15. The three references and their corresponding scores were marked on the scale. The panelists expectorated at 30 second as reminded by the monitor while continued rating the saltiness for another 60 seconds. After each booth practice session, the panelists received the comparison of the peak intensity from their own evaluations and from the group average for each sample. Each panelist also received the TI curves from his or her own ratings, and was encouraged to improve the consistency within samples and differentiability among samples. The panelists were asked not to communicate their curve information with each other. The actual booth tests were carried out in the same procedure as the practice booth sessions, except that the data from the actual test was not revealed to the panelists.

6.3.4 Data analyses

The data of the instrumental properties are presented in Chapter 5. The data of the sensory properties in this chapter include the QDA attributes and the TI parameters. The following parameters were extracted from each single curve of TI evaluation (Figure 6.1): I_5: saltiness at 5 second; I_{max}, the maximum saltiness; t_{max}, the time in second to reach I_{max}; R_{inc}, the rate of saltiness increment = I_{max}/t_{max}; I_{30}, the saltiness right before expectoration; R_{dec}, the rate of saltiness decrement = $(I_{max}-I_{30})/(30-t_{max})$; $AUC_{<30}$, area under the curve before expectoration; $AUC_{>30}$, area under the curve after expectoration; t_{end}, the time in second the saltiness reaches zero.

The analysis of variance (ANOVA) for each QDA attribute and TI parameter was performed on the Statistical Analysis Software (SAS)® Enterprise Guide® (Version 9.1, SAS Institute Inc., Cary, NC). The PROC GLM function was used for the model including the following factors: sample, panelist, replication, sample*panelist, sample*replication, and panelist*replication. When the sample*panelist factor is significant, the adjusted F value for the sample factor was calculated as F_{adj} = [sample mean square]/[sample*panelist mean square]. For the QDA attributes and the TI parameters with significant sample difference, Fisher's least significant difference (LSD) was used for the mean separation.

The principal component analysis (PCA) and the Pearson's correlation analysis between the sensory and the instrumental properties of the SLCs were performed on the Origin 8.6 (ORIGIN PC Corporation, Miami, FL, USA). The instrumental properties of the SLCs were given in Chapter 5 (Tables 5.1 and 5.2). The PCA and the correlation analysis were firstly performed on the 16 SLCs and then on only the 12 fat-containing SLCs. Hierarchical cluster analysis of each QDA modality was performed on the significant variables using Origin 8.6. Cluster analyses based on the variables included in each PCA of this study were also performed. Euclidean distance and ward method were used for all the cluster analyses.

6.4 Results and Discussion

6.4.1 Sensory profiles of the SLCs by QDA

Table 6.2, 6.3, and 6.4 list the sensory properties of the SLCs profiled using QDA. Figure 6.2 shows the PCA biplot of the QDA properties of the SLCs. Overall, the QDA properties of the SLCs varied by formulation and pressure treatment. The non-fat SLCs were

clustered against the fat-containing SLCs by their aroma properties. The non-fat SLCs shared the aroma of pungent, oxidized oil and egg, while the fat-containing SLCs shared the aroma of sweet milk, mild Cheddar, and buttery (Table 6.2). The sour cream aroma-by-mouth did not differ significantly among the samples while the cheesy aroma-by-mouth was stronger in the SLCs with 22% and 33% fat (Table 6.3). The non-fat SLCs were clustered against the fat-containing SLCs by their astringent and salty aftertastes. The fat-containing SLCs with higher solid contents and prepared with higher pressure were characterized with the grainy aftertaste. In contrast, the fat-containing SLCs with lower solid contents or prepared with lower pressure were characterized with the slippery aftertaste (Table 6.3). The non-fat samples were also clustered against the fat-containing samples by their higher salty and sour tastes. Also, the non-fat samples shared the texture of syneresis, fibrous, and squeaky. With increasing protein or fat content, or increasing pressure, the texture of the fat-containing SLCs shifted from gelatinous to fracturable, and further to crumbly and gritty (Table 6.4).

The present study focused on the relationships between structure, texture, sodium release and saltiness perception properties. Hence, significant QDA attributes of textures and tastes are included in further PCA analyses (Section 6.4.3).

6.4.2 Temporal saltiness perception properties of the SLCs by TI method

Figure 6.3 shows the TI curves for each SLCs averaged across all panelists and replications. Table 6.5 lists the TI parameters extracted from the TI curves. Compared to the SLCs with 8% protein (Figure 6.3A), the SLCs with 16% protein (Figure 6.3B) had lower I_{max} ($P < 0.0001$) and higher t_{max} ($P = 0.0079$) values. Compared to the non-fat SLCs, the fat containing SLCs had lower I_{max} ($P < 0.0001$) and higher t_{max} ($P < 0.0001$) values. Compared to the SLCs treated at low pressure, the SLCs treated at high T had lower I_{max} ($P < 0.001$). The significant TI parameters including I_5, I_{max}, t_{max}, R_{inc}, R_{dec}, $AUC_{<30}$, and I_{30} were selected for further PCA analyses (Section 6.4.3).

6.4.3 Relating sensory properties to instrumental properties of SLCs

The discussion in this section is focused on the following sensory variables: the QDA salty, fracturable, crumbly, gelatinous, and syneresis, and the TI parameters of I_5, I_{max}, t_{max}, and R_{inc}. The above QDA texture attributes were selected due to their relevance with the deformation, breakdown, or moisture withholding properties of the SLCs (Table 6.1). The

I_{max} was selected since it corresponds to the definition of the QDA salty (Table 6.1). The I_5 and R_{inc}, representing the initial and average rate of saltiness increment, respectively, were also selected to understand the dependence of saltiness perception on the rate of saltiness increment.

6.4.3.1 PCA of both non-fat and fat-containing SLCs

Figures 6.4A and B show the principal component biplots of the QDA tastes and textures, TI parameters, and instrumental properties for all of the samples including the non-fat and the fat-containing SLCs. Figure 6.4C shows the dendogram of the cluster analysis corresponding to Figure 6.4. The PC I and PC II explained 58.6% and 14.9% of the total variance, respectively (Figure 6.4A). On the positive side of the PC I, the non-fat SLCs were clustered in the region where the QDA attributes of salty and syneresis located. Also located in this region are the TI parameters of I_{max}, R_{inc}, and I_5, and the instrumental properties of serum, R_{max}, and AUC. On the negative side of the PC I was the cluster of all the fat-containing SLCs. The biplot of PC I and PC III explained 58.6% and 9.7% of the total variance, respectively (Figure 6.4B). On this biplot, three clusters spread along the vector of syneresis. On the positive end of the syneresis vector was the cluster of the non-fat SLCs, whereas, on the negative end was the cluster of the fat-containing SLCs with 16% protein. In between the above two clusters was the cluster of fat-containing SLCs with 8% protein.

The high saltiness of the non-fat SLCs as observed from Figure 6.4A can be explained by the positive correlation between porosity and saltiness (Table 6.6). Porosity correlated positively with serum release, R_{max}, syneresis and salty. Compared to the fat-containing samples, the higher porosity of the non-fat samples led to higher serum release as noticed by instrumental analysis. This trend corresponds to the higher syneresis of the non-fat samples observed by the QDA. The higher serum release resulted in higher rate of *in vitro* sodium release (R_{max}) of the non-fat samples. Correspondingly, syneresis correlated positively with the TI parameters including I_5, R_{inc} and I_{max}. Eventually, the faster sodium release driven by the rapid serum release led to greater saltiness observed by the QDA. This is the first study that quantified the porosity and then showed the numerical correlation between porosity and saltiness.

It is worth noticing that the QDA salty correlated highly positively with the TI parameter I_{max} ($P < 0.005$, Table 6.6). This correlation suggested that the panelists well followed the rating standard of salty, which was decided by the panel to be the peak saltiness

during the chewing. Nevertheless, whether the peak saltiness represents the "salty taste" for general consumers requires further consumer studies. In fact, in a preliminary sensory study where the panelists were given the freedom to rate saltiness by their own criteria, the saltiness of the non-fat SLCs with 8% protein was significantly lower, compared to the non-fat SLCs with 16% protein (data not shown). This lower saltiness of the non-fat SLCs with 8% protein may be due to the faster vanishing of saltiness which influenced the saltiness scoring in the preliminary panel.

The QDA salty in this study also correlated positively with the TI parameters I_5 and R_{inc} with high significance ($P < 0.005$, Table 6.6). However, the correlation coefficient was higher between the salty and I_5 (0.92) than between the salty and R_{inc} (0.82). This difference may be related to the perceptual or scoring effects discussed previously (Busch and others 2009). In the study of Busch (2009), the panelists received a continuous flow of NaCl solution with periodically changing concentrations via a gustometer. The total amount of NaCl delivered was the same among different delivery sequences. However, the overall saltiness in terms of AUC was higher when the delivery sequence started with higher NaCl concentration, compared to the sequence starting with a lower NaCl concentration. It was then hypothesized that the first two seconds of stimulus predominated the following rating, due to perceptual effect (stronger initial perception leading to stronger overall perception), or due to scoring effect (higher initial scoring leading to higher overall scoring). Therefore, the correlation between the QDA salty and the TI parameter I_5 may be due to the initial stimulus which affected on the following perception or rating of peak intensity.

6.4.3.2 PCA of only fat-containing SLCs

Table 6.7 lists the correlation coefficients between the QDA, TI and instrumental properties of only the fat-containing samples. Figure 6.5A shows the principal component biplot of the QDA tastes and textures, TI parameters, and instrumental properties for only the fat-containing SLCs. Figure 6.5B shows the dendogram of the cluster analysis corresponding to Figure 6.5A. The PC I and PC II explained 40.9% and 21.2% of the total variance, respectively. The SLCs were clustered depending on their formulation and pressure treatment. On the positive side of the PC I was the cluster of the SLCs of 8% protein with either lowest level of fat (11%), or with 22% fat but low pressure. These SLCs shared the QDA properties of syneresis and salty (Table 6.4 and 6.3), as well as the TI parameters of I_5 and R_{inc} (Table 6.5). With increasing fat or pressure, the SLCs in this cluster shifted from the gelatinous to fracturable texture, and presented less serum release. On the negative side of the

salty vector located the cluster of the SLCs of 16% protein with either lowest level of fat (11%), or more fat but low pressure. These SLCs shared the TI properties of t_{max}, and the instrumental property $stress_{max}$. Along the positive side of PC II located the cluster of SLCs with comparatively high protein, fat, pressure, or the combination of them. Located in the region of this cluster were the QDA crumbly and the instrumental properties including R_{max} and AUC.

The $R_{g,f}$ did not correlate with the QDA salty or any of the TI parameters. This lack of correlation may result from the counteracting effects of $R_{g,f}$ on sodium release. The $R_{g,f}$ correlated negatively with the QDA crumbly (Table 6.7), which corresponded to the hypothesis that lowering $R_{g,f}$ leads to greater breakdown extent (Phan and others 2008; Kuo and others 2016). In fact, the QDA crumbly also correlated positively with the instrumental properties including R_{max} and AUC, suggesting that the crumblier SLCs presented higher *in vitro* sodium release. However, the $R_{g,f}$ also correlated positively with the QDA gelatinous and the instrumental property serum release. These correlations indicated that the SLCs with larger fat particles are perceived as "firmer and more moist," and tend to release more serum under pressure. Serum release, in turn, correlated positively with the QDA syneresis and the TI parameters including I_5 and I_{max}. Based on Darcy's Law, the volumetric flow rate of liquid through porous media is proportional to the pressure difference acting over a given distance (Walstra 2003). The earlier breakdown would release the pressure acting on the gel, lowering the potential to expel the liquid out from the gel. Plus, during the actual mastication process, crumblier samples may require less chewing work. The less chewing may, therefore, result in a lower chance of liquid expulsion overall. Hence, although lowering $R_{g,f}$ may help to increase the surface area for sodium diffusion, it may also reduce the tendency for serum release. The counteracting effects of $R_{g,f}$ on the spontaneous diffusion and the convective transfer of sodium thus may result in no apparent effect on the saltiness perception in the model SLCs.

The association between chewing work and saltiness perception has been discussed in earlier literature. Phan and others (2008) measured the voltage and work of chewing using electromyography. The mean and maximum voltages and total work of chewing were related to saltiness. This relation suggested that variation in mastication behavior upon different food textures could alter the saltiness perception (Kuo and Lee 2014b). Still it is unclear whether such mastication-texture interaction affects saltiness at the perceptual or physiological level (whether greater chewing work leads to greater saltiness perception or greater in-mouth

sodium release). In the present work, the QDA salty correlated positively with fracturable and syneresis. It is thus postulated that for the fat-containing SLCs, moderate breakdown property would favor sodium release. When the SLC breaks down relatively fast, the crumbled gel debris requires less chewing work, and thus may lead to lower serum release and lower sodium release. When the SLC breaks down in a slower manner, while the required chewing work drives the serum from the gel, the newly created surface area would assist the serum release, thus, leading to greater saltiness.

6.4.4 Modeling saltiness by the structural properties of the SLCs

Figure 6.6 shows the linear regression of the QDA salty by the porosity for all SLCs including the non-fat and fat-containing samples. Given the significant correlation between the QDA salty and the porosity (Table. 6.6), the linear regression only yielded an R^2 of 0.30. The sample 16-22-14 was detected to be an outlier in the linear regression. A second linear regression was applied excluding the sample 16-22-14 and yielded an R^2 of 0.50. The lack of goodness of fit in the above regression suggested that porosity is not sufficient in predicting saltiness of the SLCs. Most samples with 8% protein had the actual salty higher than the predicted values, but most samples with 16% protein had the actual salty lower than the predicted values (Figure 6.6). This trend indicated that other matrix factors such as the ionic interaction between protein and sodium could influence the saltines (Ruusunen and others 2001; Lauverjat and others 2009a; Clariana and others 2011; Boisard and others 2013). Figure 6.7 shows the partial least square regression for the QDA salty by the porosity and $R_{g,f}$ of the fat-containing SLCs. When the regression was performed on all of the fat-containing SLCs (Figure 6.7A), both porosity and $R_{g,f}$ yielded very low coefficients for the regression, due to their lack of correlations with the QDA salty (Table 6.7). The modeling of saltiness may be improved by using the textural instead of the structural properties, since the $R_{g,f}$ exerted counteracting effects on the texture and sodium release (Section 6.4.3.2). The PLS regression was also performed on the fat-containing SLCs with the same levels of protein (Figures 6.7B and C). The regression on the SLCs with 16% protein showed improved result (Figure 6.7C), with greater coefficients for the porosity and $R_{g,f}$ compared to Figures 6.7A or B. The above PLS results suggested that other matrix factors including but not limited to protein content also affect saltiness perception. Overall, identifying other matrix factors with direct influences on the saltiness perception is necessary to developing an acceptable model to predict the saltiness of the SLCs.

6.5 Conclusions

In this study, saltiness perception of model lipoprotein gels was correlated with both porosity and particle size of fat for the first time in literature. Compared to the fat containing samples, the non-fat lipoproteic gels with high porosity showed higher serum release, higher sensory syneresis property, faster saltiness increment, and higher saltiness perception. This trend demonstrated that saltiness may be effectively enhanced via increasing the convective transfer of sodium with modified gel structure. For the fat containing samples, the particle size of fat did not affect the saltiness perception. This lack of the effect of fat particle size was due to the counteracting impacts of the particle size of fat on the sodium release. Decreasing in particle size of fat favors diffusive sodium transfer while disfavors the convective sodium transfer. The porosity and the particle size of fat were insufficient to predict the saltiness of the SLCs. The present study revealed the structural changes critical to sodium release and saltiness perception in a model food system containing both protein and fat. Further studies monitoring the in-mouth sodium release can assist in picturing the overall effects of matrix structure on the saltiness perception. More matrix factors should be identified for constructing the saltiness prediction model. Future development can focus on structural optimization to enhance sodium release while maintaining the acceptable sensory properties of the products.

6.6 References

Aguilera JM. 2005. Why food microstructure? J.Food Eng. 67(1–2):3-11.

Boisard L, Andriot I, Arnould C, Achilleos C, Salles C, Guichard E. 2013. Structure and composition of model cheeses influence sodium NMR mobility, kinetics of sodium release and sodium partition coefficients. Food Chem. 136(2):1070-7.

Boisard L, Andriot I, Martin C, Septier C, Boissard V, Salles C, Guichard E. 2014. The salt and lipid composition of model cheeses modifies in-mouth flavour release and perception related to the free sodium ion content. Food Chem. 145(0):437-44.

Busch JLHC, Tournier C, Knoop JE, Kooyman G, Smit G. 2009. Temporal contrast of salt delivery in mouth increases salt perception. Chem.Senses 34(4):341-8.

Clariana M, Guerrero L, Sárraga C, Díaz I, Valero Á, García-Regueiro JA. 2011. Influence of high pressure application on the nutritional, sensory and microbiological characteristics of sliced skin vacuum packed dry-cured ham. Effects along the storage period. Innovative Food Science & Emerging Technologies 12(4):456-65.

de Loubens C, Panouillé M, Saint-Eve A, Déléris I, Tréléa IC, Souchon I. 2011a. Mechanistic model of in vitro salt release from model dairy gels based on standardized breakdown test simulating mastication. J.Food Eng. 105(1):161-8.

de Loubens C, Saint-Eve A, Deleris I, Panouille M, Doyennette M, Trelea IC, Souchon I. 2011b. Mechanistic model to understand in vivo salt release and perception during the consumption of dairy gels. J.Agric.Food Chem. 59(6):2534-42.

Desmond E. 2006. Reducing salt: A challenge for the meat industry. Meat Sci. 74(1):188-96.

Felicio TL, Esmerino EA, Vidal VAS, Cappato LP, Garcia RKA, Cavalcanti RN, Freitas MQ, Conte Junior CA, Padilha MC, Silva MC, Raices RSL, Arellano DB, Bollini HMA, Pollonio MAR, Cruz AG. 2016. Physico-chemical changes during storage and sensory acceptance of low sodium probiotic Minas cheese added with arginine. Food Chem. 196: 628-37.

Johnson ME, Kapoor R, McMahon DJ, McCoy DR, Narasimmon RG. 2009. Reduction of sodium and fat levels in natural and processed cheeses: scientific and technological aspects. Comprehensive Reviews in Food Science and Food Safety 8(3):252-68.

Knoop JE, Sala G, Smit G, Stieger M. 2013. Combinatory effects of texture and aroma modification on taste perception of model gels. Chemosens.Percept. 6(2):60-9.

Kuo W, Lee Y. 2014a. Temporal sodium release related to gel microstructural properties-implications for sodium reduction. J.Food Sci. 79(11):E2245-52.

Kuo W, Lee Y. 2014b. Effect of food matrix on saltiness perception-implications for sodium reduction. Comprehensive Reviews in Food Science and Food Safety 13(5):906-23.

Kuo W, Ilavsky J, Lee Y. 2016. Structural characterization of solid lipoproteic colloid gels by ultra-small-angle X-ray scattering and the relation with sodium release. Food Hydrocoll. 56: 325-33.

Lauverjat C, Deleris I, Trelea IC, Salles C, Souchon I. 2009a. Salt and aroma compound release in model cheeses in relation to their mobility. J.Agric.Food Chem. 57(21):9878-87.

Lauverjat C, Loubens Cd, Déléris I, Tréléa IC, Souchon I. 2009b. Rapid determination of partition and diffusion properties for salt and aroma compounds in complex food matrices. J.Food Eng. 93(4):407-15.

Norton JE, Wallis GA, Spyropoulos F, Lillford PJ, Norton IT. 2014. Designing Food Structures for Nutrition and Health Benefits. Annual Review of Food Science and Technology, Vol 5 5177-95.

Panouille M, Saint-Eve A, de Loubens C, Deleris I, Souchon I. 2011. Understanding of the influence of composition, structure and texture on salty perception in model dairy products. Food Hydrocoll. 25(4):716-23.
Phan VA, Yven C, Lawrence G, Chabanet C, Reparet JM, Salles C. 2008. *in vivo* sodium release related to salty perception during eating model cheeses of different textures. Int.Dairy J. 18(9):956-63.
Ruusunen M, Simolin M, Puolanne E. 2001. The effect of fat content and flavor enhancers on the perceived saltiness of cooked 'bologna-type' sausages. Journal of Muscle Foods 12(2):107-20.
Stieger M. 2011. Texture-taste interactions: Enhancement of taste intensity by structural modifications of the food matrix. Procedia Food Sci. 1(0):521-7.
Stieger M, van de Velde F. 2013. Microstructure, texture and oral processing: New ways to reduce sugar and salt in foods. Curr. Opin. Colloid. In. 18(4):334-48.
van den Berg L, van Vliet T, van der Linden E, van Boekel MAJS, van de Velde F. 2007a. Serum release: The hidden quality in fracturing composites. Food Hydrocoll. 21(3):420-32.
van den Berg L, van Vliet T, van der Linden E, van Boekel MAJS, van de Velde F. 2007b. Breakdown properties and sensory perception of whey proteins/polysaccharide mixed gels as a function of microstructure. Food Hydrocoll. 21(5–6):961-76.
Walstra P. 2003. Physical chemistry of foods. New York, NY: Marcel Dekker Inc.
Yotsuyanagi SE, Contreras-Castillo CJ, Haguiwara MMH, Cipolli KMVAB, Lemos ALSC, Morgano MA, Yamada EA. 2016. Technological, sensory and microbiological impacts of sodium reduction in frankfurters. Meat Sci. 115: 50-9.

6.7 Tables and Figures

Table 6.1. The QDA attributes generated with model SLCs and their corresponding definitions and references.

Modality	Attribute	Reference		Definition
		Item	Score	
Aroma	Sweet milk	Condensed milk	11.7	The aroma of condensed milk
	Mild cheddar	Mild Cheddar	9.4	The aroma of mild cheddar
	Pungent	Parmesan	11.2	The aroma of parmesan cheese
	Buttery	Butter	9.7	The aroma of butter
	Oxidized oil	Oxidized oil	11.4	The aroma of oxidized oil
	Egg	Egg	11.5	The aroma of hard-boiled egg
Aroma-by-mouth	Sour cream	Sour cream	10.6	The aroma-by-mouth (peak intensity) of sour cream
	Cheesy	Mozzarella string cheese	9.5	The aroma-by-mouth (peak intensity) of Mozzarella string cheese
Taste	Salty	0.4% NaCl	10.2	The salty taste (peak intensity) of NaCl solution
		0.3% NaCl	4.0	
	Sour	0.01% Lactic acid	7.5	The sour taste (peak intensity) of lactic acid solution
Aftertaste	Grainy	Firm tofu	6.9	The grainy mouthfeel left on tongue
	Slippery	Almond milk	10.9	The slippery mouthfeel left on tongue
	Astringent	Greek yogurt	9.2	The astringent mouthfeel on tongue of Greek yogurt
	Salty	0.3% NaCl	7.6	The salty aftertaste of NaCl
Texture	Fracturable	Firm tofu	8.0	Easiness of first bite to fracture (into two or more pieces)
	Crumbly	Feta cheese	9.7	Readily breaks into small pieces with chewing
	Gelatinous	Jell-O	10.7	Firm and moist
	Gritty	Grits	10.8	Feeling of coarse particles like grits during chewing
	Fibrous	Pineapple core	13.3	Lasting fibrous feeling during chewing
	Syneresis	Fresh mozzarella balls	8.3	Expulsion of liquid with chews
	Squeaky	Exploded egg	8.0	The squeaky sounds with chews

Table 6.2. Aroma properties of the SLCs collected via the QDA[a].

Sample	Sweet milk ± SD	Mild Cheddar ± SD	Pungent ± SD	Buttery ± SD	Oxidized oil ± SD	Egg ± SD
8-0-14[b]	7.1 ± 1.7 ef	7.3 ± 2.6 cd	8.9 ± 2.6 ab	8.1 ± 1.9 fgh	8.3 ± 3.5 a	8.7 ± 2.6 a
8-0-55	7.2 ± 2.3 ef	7.4 ± 1.7 bcd	8.5 ± 2.8 ab	7.5 ± 2.1 h	8.4 ± 3.1 a	7.6 ± 3.4 bc
8-11-14	9.3 ± 2.6 abc	8.4 ± 2.2 abc	6.7 ± 2.5 ef	9.6 ± 2.6 abcde	6.5 ± 2.8 b	5.6 ± 2.2 ghi
8-11-55	9.2 ± 2.6 bc	9.0 ± 2.2 a	7.2 ± 2.8 cde	9.0 ± 2.5 cdef	6.0 ± 2.6 b	6.5 ± 2.3 def
8-22-14	9.8 ± 2.6 abc	8.3 ± 2.4 abc	6.4 ± 2.7 ef	9.7 ± 2.3 abcde	6.1 ± 2.7 b	5.8 ± 2.3 fghi
8-22-55	9.0 ± 2.5 cd	9.1 ± 2.1 a	7.1 ± 3.2 cdef	9.3 ± 2.5 bcde	6.1 ± 2.8 b	6.3 ± 2.7 efg
8-33-14	9.6 ± 3.0 abc	9.4 ± 2.4 a	6.4 ± 3.2 ef	9.7 ± 2.6 abcde	6.1 ± 2.5 b	5.4 ± 2.6 h
8-33-55	10.3 ± 2.2 ab	9.3 ± 1.5 a	6.1 ± 2.4 ef	10.0 ± 2.4 abc	5.5 ± 2.3 b	6.0 ± 2.4 efghi
16-0-14	6.9 ± 2.2 ef	7.0 ± 1.7 d	8.8 ± 2.5 ab	7.9 ± 1.8 gh	8.7 ± 3.6 a	8.8 ± 2.8 a
16-0-55	6.7 ± 2.2 f	7.4 ± 1.9 bcd	9.3 ± 3.1 a	7.4 ± 1.9 h	8.1 ± 3.2 a	7.3 ± 3.3 cd
16-11-14	8.0 ± 2.4 de	8.5 ± 2.6 ab	8.1 ± 2.7 bc	9.0 ± 2.6 def	8.3 ± 3.0 a	8.4 ± 2.4 ab
16-11-55	8.8 ± 2.6 cd	8.7 ± 2.6 a	8.0 ± 3.1 bcd	8.8 ± 2.1 efg	6.2 ± 2.6 b	6.8 ± 3.4 cde
16-22-14	10.3 ± 2.1 ab	9.2 ± 2.0 a	6.9 ± 2.9 def	9.8 ± 1.9 abcd	6.4 ± 3.0 b	6.2 ± 2.4 efghi
16-22-55	10.5 ± 2.3 a	9.3 ± 1.8 a	6.1 ± 3.0 f	10.4 ± 2.0 a	6.1 ± 3.0 b	6.3 ± 2.3 efghi
16-33-14	9.8 ± 2.2 abc	8.9 ± 1.5 a	6.7 ± 3.0 ef	9.3 ± 2.4 bcde	6.1 ± 3.1 b	5.3 ± 2.7 i
16-33-55	10.3 ± 2.6 ab	9.0 ± 2.2 a	6.7 ± 2.7 ef	10.1 ± 1.8 ab	6.2 ± 2.4 b	5.9 ± 2.2 efghi

a. The values followed by the same letters are not significantly different ($\alpha = 0.05$).
b. Sample code: protein(%, w/w)-fat(%, w/w)-homogenization pressure(MPa). All samples contained 1.5% (w/w) NaCl.

Table 6.3. Aroma-by-mouth, taste and aftertaste properties of the SLCs collected via the QDA[a].

Sample	Aroma-by-mouth		Taste		Aftertaste			
	Sour cream ± SD	Cheesy ± SD	Salty ± SD	Sour ± SD	Grainy ± SD	Slippery ± SD	Astringent ± SD	Salty ± SD
8-0-14[b]	8.7 ± 3.4 a	5.7 ± 1.2 f	11.9 ± 3.2 a	7.8 ± 3.8 a	6.4 ± 3.1 e	4.4 ± 2.8 gh	9.2 ± 2.7 a	8.3 ± 2.7 ab
8-0-55	8.6 ± 3.7 a	5.8 ± 1.4 f	11.9 ± 2.7 a	8.0 ± 3.6 a	6.8 ± 2.6 de	4.2 ± 2.8 gh	9.1 ± 2.0 a	8.5 ± 1.8 a
8-11-14	8.1 ± 3.2 a	7.8 ± 2.6 e	8.9 ± 3.1 cd	5.5 ± 2.5 bc	5.2 ± 1.7 f	7.8 ± 3.6 a	5.0 ± 2.2 ef	6.5 ± 2.1 e
8-11-55	8.4 ± 2.8 a	8.7 ± 1.9 cd	9.2 ± 2.3 cd	5.7 ± 1.6 bc	6.3 ± 1.6 e	7.9 ± 3.2 a	5.6 ± 2.6 de	6.8 ± 2.2 cde
8-22-14	8.1 ± 2.7 a	9.4 ± 2.2 abcd	9.3 ± 2.6 cd	5.6 ± 1.6 bc	6.6 ± 1.8 e	7.6 ± 3.0 ab	5.1 ± 2.2 def	7.5 ± 1.7 bcd
8-22-55	7.2 ± 2.0 a	9.4 ± 2.4 abcd	9.3 ± 2.4 cd	5.1 ± 1.7 cde	7.2 ± 1.7 de	6.0 ± 3.3 de	6.0 ± 2.7 cd	6.6 ± 2.1 e
8-33-14	6.8 ± 2.5 a	9.6 ± 2.1 ab	9.5 ± 2.3 c	5.6 ± 1.7 bc	8.5 ± 2.2 c	6.3 ± 2.8 cde	5.5 ± 2.6 def	7.6 ± 1.9 bc
8-33-55	6.8 ± 2.4 a	9.9 ± 1.8 ab	9.1 ± 1.9 cd	5.6 ± 1.6 bc	9.4 ± 2.6 ab	5.7 ± 2.3 ef	6.0 ± 1.8 cde	6.7 ± 1.7 de
16-0-14	8.2 ± 3.1 a	6.4 ± 1.7 f	11.1 ± 2.3 ab	7.3 ± 3.1 a	7.6 ± 2.3 de	4.2 ± 2.3 fh	9.0 ± 2.2 a	8.6 ± 1.9 a
16-0-55	8.4 ± 3.5 a	6.3 ± 1.3 f	10.9 ± 2.8 b	7.6 ± 3.2 a	8.5 ± 2.6 bc	3.4 ± 2.2 h	10.1 ± 2.8 a	8.0 ± 2.3 ab
16-11-14	7.6 ± 3.3 a	9.1 ± 2.5 bcd	8.4 ± 2.9 de	6.0 ± 2.6 b	6.4 ± 1.8 e	7.0 ± 2.8 abc	5.9 ± 2.2 cde	6.4 ± 2.7 ef
16-11-55	6.9 ± 2.9 a	8.6 ± 2.0 de	6.2 ± 2.4 g	4.3 ± 1.6 e	7.2 ± 2.1 de	5.9 ± 3.5 de	5.4 ± 2.2 def	5.3 ± 2.2 g
16-22-14	7.2 ± 2.3 a	10.3 ± 2.5 a	6.8 ± 1.9 fg	4.5 ± 1.6 de	6.4 ± 1.7 e	6.7 ± 2.8 bcd	5.5 ± 2.7 def	6.8 ± 1.8 de
16-22-55	7.1 ± 3.0 a	9.9 ± 2.2 ab	6.5 ± 2.2 g	5.3 ± 2.4 bcd	9.1 ± 2.3 abc	4.5 ± 2.7 g	7.3 ± 3.2 b	5.7 ± 2.4 fg
16-33-14	7.0 ± 3.1 a	9.7 ± 3.1 ab	6.7 ± 2.6 fg	4.4 ± 1.8 e	6.4 ± 2.2 e	7.8 ± 2.7 a	4.5 ± 2.6 f	6.2 ± 1.9 ef
16-33-55	6.6 ± 2.6 a	9.5 ± 2.2 abc	7.5 ± 2.4 ef	5.4 ± 1.9 bcd	9.7 ± 2.9 a	4.8 ± 3.0 fg	6.9 ± 3.5 bc	6.5 ± 1.7 e

a. The values followed by the same letters are not significantly different ($\alpha = 0.05$).
b. Sample code: protein(%, w/w)-fat(%, w/w)-homogenization pressure(MPa). All samples contained 1.5% (w/w) NaCl.

Table 6.4. Textural properties of the SLCs collected via the QDA[a].

Sample	Fracturable ± SD	Crumbly ± SD	Syneresis ± SD	Gelatinous ± SD	Gritty ± SD	Fibrous ± SD	Squeaky ± SD
8-0-14[b]	5.4 ± 2.7 ef	6.4 ± 2.9 fg	13.8 ± 1.6 a	7.0 ± 2.5 f	7.0 ± 3.1 efgh	11.2 ± 2.3 a	7.2 ± 4.0 c
8-0-55	4.8 ± 3.4 f	6.3 ± 3.3 fg	13.8 ± 1.8 a	5.8 ± 2.0 g	6.8 ± 2.6 fghi	11.3 ± 3.7 a	6.2 ± 3.6 d
8-11-14	9.0 ± 2.3 c	7.3 ± 2.5 de	9.7 ± 2.5 c	10.5 ± 2.9 ab	4.9 ± 2.3 k	2.5 ± 2.5 efg	4.6 ± 2.9 ef
8-11-55	10.5 ± 2.7 a	8.6 ± 2.3 c	9.2 ± 1.8 c	11.0 ± 2.4 ab	6.7 ± 1.8 ghi	2.9 ± 2.4 def	5.3 ± 2.4 e
8-22-14	9.5 ± 2.2 bc	8.6 ± 2.3 c	8.3 ± 1.6 d	9.8 ± 2.6 c	6.3 ± 2.3 hij	2.8 ± 2.7 def	4.1 ± 2.7 fg
8-22-55	10.2 ± 2.2 ab	9.5 ± 2.3 b	6.8 ± 2.6 e	8.7 ± 2.7 de	8.8 ± 2.7 d	3.4 ± 2.8 cd	4.0 ± 2.4 fg
8-33-14	9.7 ± 1.9 abc	9.6 ± 2.5 b	8.0 ± 2.4 d	9.4 ± 2.8 cd	7.8 ± 2.0 efgh	2.3 ± 2.6 fg	3.8 ± 2.4 gh
8-33-55	9.8 ± 3.2 abc	11.0 ± 2.9 a	5.9 ± 2.5 f	7.4 ± 2.9 f	9.9 ± 1.8 bc	3.1 ± 3.0 cde	6.3 ± 2.9 d
16-0-14	5.4 ± 2.6 ef	6.9 ± 2.8 efg	12.5 ± 1.9 b	6.7 ± 2.2 f	7.6 ± 3.0 ef	11.2 ± 3.2 a	12.0 ± 2.9 a
16-0-55	4.8 ± 2.2 f	6.2 ± 2.8 g	12.8 ± 2.1 b	5.5 ± 2.2 g	9.1 ± 3.2 cd	11.5 ± 3.2 a	10.2 ± 4.3 b
16-11-14	8.0 ± 2.0 d	8.0 ± 2.0 cd	7.0 ± 1.9 e	9.9 ± 2.8 bc	6.5 ± 2.3 hij	4.8 ± 3.6 b	5.1 ± 2.9 e
16-11-55	7.6 ± 2.5 d	7.7 ± 2.3 de	5.8 ± 2.2 f	8.2 ± 2.5 e	7.5 ± 2.2 efg	3.3 ± 2.7 cd	5.3 ± 3.0 e
16-22-14	8.1 ± 1.8 d	7.2 ± 1.8 def	5.3 ± 1.9 fg	9.9 ± 2.7 bc	5.7 ± 2.0 jk	3.5 ± 2.9 cd	5.2 ± 2.7 e
16-22-55	9.4 ± 2.9 bc	11.5 ± 2.5 a	4.5 ± 2.6 h	5.5 ± 2.4 g	10.6 ± 2.2 ab	3.9 ± 3.4 c	4.1 ± 2.8 fg
16-33-14	6.1 ± 2.1 e	7.4 ± 2.5 de	4.8 ± 1.3 gh	8.3 ± 2.6 e	6.0 ± 2.3 ij	1.8 ± 1.9 g	3.4 ± 2.3 gh
16-33-55	7.4 ± 3.0 d	11.4 ± 3.3 a	4.4 ± 2.1 h	5.7 ± 1.9 g	11.0 ± 2.9 a	3.1 ± 2.9 def	3.1 ± 2.5 h

a. The values followed by the same letters are not significantly different ($\alpha = 0.05$).
b. Sample code: protein(%, w/w)-fat(%, w/w)-homogenization pressure(MPa). All samples contained 1.5% (w/w) NaCl.

Table 6.5. Time-intensity parameters for the saltiness perception of the SLCs[a].

Sample	I_5 ± SD[c]	R_{inc} ± SD (sec^{-1})	t_{max} ± SD (sec)	I_{max} ± SD	R_{dec} ± SD (sec^{-1})	I_{30} ± SD	$AUC_{<30}$ ± SD (sec)	t_{end} ± SD (sec)	$AUC_{>30}$ ± SD (sec)
8-0-14[b]	12.5 ±3.2 a	3.5 ±3.0 a	6.1±3.7 e	14.3±1.2 a	0.2±0.1 abcd	10.3 ±2.9ab	337.1 ±62.4a	59.8±9.2 a	195.9±98.4 a
8-0-55	12.1 ±2.4 ab	2.6 ±2.0 b	8.0±5.2 de	13.5±2.0 b	0.2±0.1 ab	9.1 ±3.4def	317.9 ±73.8b	60.1±13.6a	177.3±98.6 a
8-11-14	8.0 ±3.4 c	1.2 ±0.7 def	14.2±6.4 bc	13.1±1.5 b	0.1±0.1 def	10.8 ±2.9a	308.4 ±49.8b	64.1±7.6 a	233.4±79.9 a
8-11-55	7.3 ±2.9 cde	1.4 ±1.6 d	12.9±6.2 c	11.1±2.1 de	0.2±0.1 bcd	8.3 ±2.8fg	248.9 ±61.1d	59.8±7.9 a	150.1±75.1 a
8-22-14	7.7 ±3.3 cd	1.2 ±0.6 de	13.2±5.9 c	12.4±1.9 c	0.1±0.1 cde	9.8 ±2.5bcd	280.2 ±47.9c	66.0±6.7 a	219.2±87.3 a
8-22-55	6.1 ±2.3 efg	0.8 ±0.3 ef	15.6±5.3 abc	11.2±2.0 d	0.2±0.2 bcd	9.0 ±2.6def	250.6 ±46.2d	60.9±6.4 a	183.8±87.5 a
8-33-14	6.8 ±2.4 efg	0.9 ±0.7 ef	16.5±6.2 ab	12.0±2.1 c	0.1±0.2 cde	10.1 ±2.6abc	278.3 ±54.5c	65.2±9.4 a	223.4±79.2 a
8-33-55	6.1 ±2.3 fg	0.8 ±0.4 ef	17.4±7.2 a	11.1±2.2 de	0.1±0.2 cde	9.2 ±2.8cde	252.2 ±54.8d	62.6±6.2 a	199.2±74.9 a
16-0-14	11.0 ±3.4 b	1.9 ±1.4 c	9.0±4.3 de	13.5±2.2 b	0.2±0.1 a	9.0 ±3.6def	310.0 ±79.6b	60.5±9.8 a	177.0±99.9 a
16-0-55	11.5 ±3.1 ab	2.2 ±1.5 bc	9.0±5.7 de	13.7±1.9 ab	0.2±0.1 abc	9.4 ±3.5cde	321.2 ±61.5ab	60.8±8.9 a	190.0±93.3 a
16-11-14	5.4 ±2.1 fg	0.9 ±0.9 ef	17.0±7.8 a	10.4±2.0 ef	0.1±0.2 defg	8.6 ±2.7ef	227.9 ±35.5e	58.7±9.0 a	170.0±81.0 a
16-11-55	4.8 ±1.7 h	0.7 ±0.6 f	17.2±7.1 a	8.7±1.2 g	0.1±0.1 fg	7.4 ±2.1gh	197.4 ±33.2f	58.4±6.5 a	151.7±65.1 a
16-22-14	4.8 ±2.2 h	0.9 ±0.8 ef	16.5±7.7 ab	9.1±2.1 g	0.1±0.2 def	7.2 ±2.2h	198.4 ±47.6f	60.6±9.0 a	156.6±71.7 a
16-22-55	5.5 ±2.7 gh	1.0 ±0.9 def	15.1±7.6 abc	10.0±2.9 f	0.1±0.1 efg	8.6 ±2.9ef	222.8 ±59.5e	62.3±8.2 a	178.5±76.8 a
16-33-14	5.1 ±1.9 gh	0.9 ±0.9 ef	16.8±7.2 ab	9.9±2.4 f	0.1±0.1 g	8.8 ±2.6ef	222.7 ±44.4e	63.5±11.7a	212.4±116.8a
16-33-55	4.6 ±2.0 h	0.8 ±1.0 ef	17.3±7.7 a	9.0±2.1 g	0.1±0.1 defg	7.3 ±2.6h	189.4 ±40.8f	58.8±9.2 a	156.3±84.2 a

a. The values followed by the same letters are not significantly different ($\alpha = 0.05$).
b. Sample code: protein(%, w/w)-fat(%, w/w)-homogenization pressure(MPa). All samples contained 1.5% (w/w) NaCl.
c. I_5: saltiness at 5 second; I_{max}: the maximum saltiness; t_{max}: the time in second to reach I_{max}; R_{inc}, the rate of saltiness increment = I_{max}/t_{max}; I_{30}, the saltiness right before expectoration; R_{dec}, the rate of saltiness decrement = $(I_{max}-I_{30})/(30-t_{max})$; $AUC_{<30}$: area under the curve before expectoration; $AUC_{>30}$: area under the curve after expectoration; t_{end}: the time in second the saltiness reaches zero.

Table 6.6. Pearson's correlation coefficient between the instrumental and sensory properties of the SLCs including both non-fat and fat-containing samples[a].

	Porosity	R_{max}	C_{max}	AUC	Serum	$Stress_{max}$
R_{max}[b]	0.55 *					
C_{max}	0.24	0.37				
AUC	0.30	0.86 ***	0.62 *			
Serum	0.55 *	0.96 ***	0.26	0.76 ***		
$Stress_{max}$	-0.10	0.14	0.23	0.09	0.15	
$Strain_{max}$	0.49	0.61 *	-0.21	0.29	0.65 **	0.22

a. The correlation is significant at $\alpha = 0.05$, 0.01, and 0.005 for the values followed by 1, 2, and 3 asterisk(s).
b. R_{max}, maximum rate of sodium release; C_{max}, maximum concentration of released sodium; AUC, area under the curve of sodium release; Serum, amount of liquid expelled from the sample during the compression test. $Stress_{max}$, maximum stress measured during the compression test; $Strain_{max}$, strain at the maximum stress. Refer to Chapter 5 for the data of the instrumental properties.

Table 6.6 (cont.).

	Porosity	R_{max}	C_{max}	AUC	Serum	$Stress_{max}$	$Strain_{max}$	Salty	Sour	Fracturable	Crumbly	Syneresis	Gelatinous	Gritty	Fibrous
Salty	0.54 *	0.73 ***	0.15	0.61 *	0.75 ***	-0.43	0.45								
Sour	0.64 **	0.84 ***	0.05	0.63 **	0.84 ***	-0.18	0.64 **	0.91 ***							
Fracturable	-0.52 *	-0.77 ***	-0.04	-0.45	-0.74 ***	-0.27	-0.62 *	-0.42	-0.62 *						
Crumbly	-0.53 *	-0.50 *	0.13	-0.10	-0.64 **	0.05	-0.56 *	-0.46	-0.47	0.67 ***					
Syneresis	0.61 **	0.78 ***	0.01	0.53	0.85 ***	-0.34	0.60	0.92 ***	0.91 ***	-0.57	-0.70 ***				
Gelatinous	-0.22	-0.61 *	-0.24	-0.58 *	-0.46	-0.34	-0.26	-0.22	-0.47	0.60 *	-0.10	-0.20			
Gritty	-0.23	0.17	0.36	0.44	-0.02	0.30	-0.16	-0.10	0.04	0.09	0.71 ***	-0.28	-0.69 ***		
Fibrous	0.64 **	0.91 ***	0.10	0.62 *	0.93 ***	0.10	0.70 ***	0.77 ***	0.91 ***	-0.80 ***	-0.60 *	0.85 ***	-0.59 *	0.04	
Squeaky	0.35	0.84 ***	0.30	0.69	0.92 ***	0.33	0.56 *	0.62 *	0.69 ***	-0.59 *	-0.53 *	0.70 ***	-0.37	0.03	0.82 ***

a. The correlation is significant at $\alpha = 0.05$, 0.01, and 0.005 for the values followed by 1, 2, and 3 asterisk(s).

b. R_{max}, maximum rate of sodium release; C_{max}, maximum concentration of released sodium; AUC, area under the curve of sodium release; Serum, amount of liquid expelled from the sample during the compression test. $Stress_{max}$, maximum stress measured during the compression test; $Strain_{max}$, strain at the maximum stress. Refer to Chapter 5 for the data of the instrumental properties.

Table 6.6 (cont.).

	Porosity	R_{max}[b]	C_{max}	AUC	Serum	$Stress_{max}$	$Strain_{max}$	Salty	Sour	Fracturable	Crumbly	Syneresis	Gelatinous	Gritty	Fibrous	Squeaky
I_5	0.65 **	0.84 ***	0.10	0.61 *	0.87 ***	-0.29	0.55 *	0.92 ***	0.93 ***	-0.62 **	-0.63 **	0.98 ***	-0.35	-0.15	0.89 ***	0.71 ***
R_{inc}	0.73 ***	0.79 ***	0.02	0.49	0.77 ***	-0.27	0.58 *	0.82 ***	0.89 ***	-0.67 ***	-0.60 *	0.89 ***	-0.4	-0.13	0.88 ***	0.59 *
t_{max}	-0.73 ***	-0.83 ***	-0.08	-0.57 *	-0.85 ***	0.25	-0.56 *	-0.84 ***	-0.9 ***	0.63 **	0.62 **	-0.94 ***	0.37	0.16	-0.89 ***	-0.68 ***
I_{max}	0.50	0.70 ***	0.10	0.56 *	0.75 ***	-0.43	0.39	0.92 ***	0.84 ***	-0.38	-0.51 *	0.91 ***	-0.15	-0.21	0.70 ***	0.59 *
R_{dec}	0.59 *	0.73 ***	0.32	0.66 **	0.79 ***	-0.19	0.53 *	0.90 ***	0.83 ***	-0.37	-0.43	0.84 ***	-0.21	-0.04	0.75 ***	0.73 ***
I_{30}	0.10	0.26	-0.06	0.23	0.31	-0.56 *	0.00	0.60 *	0.44	-0.01	-0.23	0.55 *	0.11	-0.26	0.22	0.16
$AUC_{<30}$	0.48	0.69 ***	0.07	0.53 *	0.75 ***	-0.44	0.39	0.91 ***	0.83 ***	-0.40	-0.54 *	0.92 ***	-0.16	-0.23	0.70 ***	0.59 *

a. The correlation is significant at α = 0.05, 0.01, and 0.005 for the values followed by 1, 2, and 3 asterisk(s).

b. R_{max}, maximum rate of sodium release; C_{max}, maximum concentration of released sodium; AUC, area under the curve of sodium release; Serum, amount of liquid expelled from the sample during the compression test. $Stress_{max}$, maximum stress measured during the compression test; $Strain_{max}$, strain at the maximum stress; I_5: saltiness at 5 second; I_{max}: the maximum saltiness; t_{max}: the time in second to reach I_{max}; R_{inc}, the rate of saltiness increment = I_{max}/t_{max}; I_{30}, the saltiness right before expectoration; R_{dec}, the rate of saltiness decrement = $(I_{max}-I_{30})/(30-t_{max})$; $AUC_{<30}$: area under the curve before expectoration. Refer to Chapter 5 for the data of the instrumental properties.

Table 6.6 (cont.).

	I_5[b]	R_{inc}	t_{max}	I_{max}	R_{dec}	I_{30}
R_{inc}	0.93 ***					
t_{max}	-0.97 ***	-0.96 ***				
I_{max}	0.92 ***	0.78 ***	-0.84 ***			
R_{dec}	0.83 ***	0.67 ***	-0.77 ***	0.79 ***		
I_{30}	0.56 *	0.42	-0.44	0.81 ***	0.36	
$AUC_{<30}$	0.93 ***	0.79 ***	-0.84 ***	1.00 ***	0.77 ***	0.81 ***

a. The correlation is significant at α = 0.05, 0.01, and 0.005 for the values followed by 1, 2, and 3 asterisk(s).
b. I_5: saltiness at 5 second; I_{max}: the maximum saltiness; t_{max}: the time in second to reach I_{max}; R_{inc}, the rate of saltiness increment = I_{max}/t_{max}; I_{30}, the saltiness right before expectoration; R_{dec}, the rate of saltiness decrement = $(I_{max}-I_{30})/(30-t_{max})$; $AUC_{<30}$: area under the curve before expectoration.

Table 6.7. Pearson's correlation coefficient between the instrumental and sensory properties of the fat-containing SLCs[a].

	$R_{g,f}$[b]	Porosity	R_{max}	C_{max}	AUC	Serum	$Stress_{max}$
Porosity	0.21						
R_{max}	-0.34	-0.02					
C_{max}	-0.41	0.37	0.35				
AUC	-0.44	-0.08	0.89***	0.54			
Serum	0.68*	0.08	-0.3	-0.54	-0.32		
$Stress_{max}$	-0.17	0.06	-0.21	-0.08	-0.45	-0.51	
$Strain_{max}$	0.4	0.13	0.04	-0.5	-0.32	0.47	0.33

a. The correlation is significant at $\alpha = 0.05$, 0.01, and 0.005 for the values followed by 1, 2, and 3 asterisk(s).
b. $R_{g,f}$, gyration radius of the fat particles; R_{max}, maximum rate of sodium release; C_{max}, maximum concentration of released sodium; AUC, area under the curve of sodium release; Serum, amount of liquid expelled from the sample during the compression test. $Stress_{max}$, maximum stress measured during the compression test; $Strain_{max}$, strain at the maximum stress. Refer to Chapter 5 for the data of the instrumental properties.

Table 6.7 (cont.).

	$R_{g,f}$[b]	Porosity	R_{max}	C_{max}	AUC	Serum	$Stress_{max}$	$Strain_{max}$	Salty	Sour	Fracturable	Crumbly	Syneresis	Gelatinous	Gritty	Fibrous
Salty	0.26	0.01	0.17	0.16	0.41	0.55	-0.80***	-0.14								
Sour	0.23	0.04	0.26	-0.17	0.34	0.47	-0.43	0.17	0.74**							
Fracturable	-0.14	0.07	-0.02	0.2	0.29	0.39	-0.56	-0.20	0.71**	0.58*						
Crumbly	-0.61*	-0.19	0.61*	0.35	0.72**	-0.5	0.06	-0.25	0.1	0.38	0.35					
Syneresis	0.49	0.06	-0.17	-0.25	-0.03	0.86***	-0.82***	0.09	0.76***	0.51	0.57	-0.38				
Gelatinous	0.62*	0.31	-0.49	-0.18	-0.42	0.78***	-0.49	0.19	0.5	0.17	0.25	-0.76***	0.82***			
Gritty	-0.74**	-0.32	0.57	0.29	0.62*	-0.62*	0.24	-0.21	-0.11	0.16	0.17	0.95***	-0.57	-0.87***		
Fibrous	-0.03	-0.01	-0.24	-0.46	-0.37	0.17	0.51	0.51	-0.17	0.27	0.09	0.16	-0.22	-0.15	0.25	
Squeaky	-0.04	-0.18	-0.49	-0.19	-0.4	0.29	0.09	0.16	0.13	0.12	0.34	-0.18	0.22	0.32	-0.16	0.37

a. The correlation is significant at $\alpha = 0.05$, 0.01, and 0.005 for the values followed by 1, 2, and 3 asterisk(s).

b. $R_{g,f}$, gyration radius of the fat particles; R_{max}, maximum rate of sodium release; C_{max}, maximum concentration of released sodium; AUC, area under the curve of sodium release; Serum, amount of liquid expelled from the sample during the compression test. $Stress_{max}$, maximum stress measured during the compression test; $Strain_{max}$, strain at the maximum stress. Refer to Chapter 5 for the data of the instrumental properties.

Table 6.7 (cont.).

	$R_{g,f}$ [b]	Porosity	R_{max}	C_{max}	AUC	Serum	$Stress_{max}$	$Strain_{max}$	Salty	Sour	Fracturable	Crumbly	Syneresis	Gelatinous	Gritty	Fibrous	Squeaky
I_5	0.42	0.10	-0.04	-0.06	0.17	0.07 *	-0.87 ***	-0.16	0.78 ***	0.55	0.66 *	-0.14	0.90 ***	0.60 *	-0.39	-0.36	0.10
R_{inc}	0.25	0.53	0.03	-0.06	0.11	0.51	-0.60 *	-0.02	0.45	0.49	0.48	-0.12	0.69 *	0.50	-0.36	-0.21	0.00
t_{max}	-0.24	-0.47	0.07	0.07	-0.07	-0.56	0.65 *	0.11	-0.43	-0.35	-0.57	0.15	-0.69 *	-0.49	0.35	0.18	0.02
I_{max}	0.50	0.01	-0.03	-0.04	0.19	0.65 *	-0.80 ***	-0.18	0.83 ***	0.60 *	0.60 *	-0.07	0.82 ***	0.51	-0.33	-0.33	0.02
R_{dec}	0.13	0.30	0.16	0.33	0.34	0.52	-0.59 *	0.08	0.86 ***	0.61 *	0.79 ***	0.10	0.65 *	0.51	-0.09	0.00	0.27
I_{30}	0.51	-0.17	-0.08	-0.10	0.12	0.50	-0.67 *	-0.27	0.66 *	0.47	0.41	-0.06	0.65 *	0.35	-0.28	-0.4	-0.08
$AUC_{<30}$	0.49	-0.06	-0.09	-0.06	0.14	0.64 *	-0.80 ***	-0.20	0.78 ***	0.53	0.58 *	-0.12	0.82 ***	0.52	-0.36	-0.38	0.05

a. The correlation is significant at $\alpha = 0.05$, 0.01, and 0.005 for the values followed by 1, 2, and 3 asterisk(s).

b. $R_{g,f}$, gyration radius of the fat particles; R_{max}, maximum rate of sodium release; C_{max}, maximum concentration of released sodium; AUC, area under the curve of sodium release; Serum, amount of liquid expelled from the sample during the compression test. $Stress_{max}$, maximum stress measured during the compression test; $Strain_{max}$, strain at the maximum stress; I_5: saltiness at 5 second; I_{max}: the maximum saltiness; t_{max}: the time in second to reach I_{max}; R_{inc}, the rate of saltiness increment = I_{max}/t_{max}; I_{30}, the saltiness right before expectoration; R_{dec}, the rate of saltiness decrement = $(I_{max}-I_{30})/(30-t_{max})$; $AUC_{<30}$: area under the curve before expectoration. Refer to Chapter 5 for the data of the instrumental properties.

Table 6.7 (cont.).

	I_5[b]	R_{inc}	t_{max}	I_{max}	R_{dec}	I_{30}
R_{inc}	0.74 **					
t_{max}	-0.79 ***	-0.91 ***				
I_{max}	0.94 ***	0.56	-0.61 *			
R_{dec}	0.63 *	0.44	-0.44	0.62 *		
I_{30}	0.82 ***	0.37	-0.42	0.94 ***	0.35	
$AUC_{<30}$	0.94 ***	0.53	-0.59 *	0.99 ***	0.56	0.95 ***

a. The correlation is significant at $\alpha = 0.05$, 0.01, and 0.005 for the values followed by 1, 2, and 3 asterisk(s).
b. I_5: saltiness at 5 second; I_{max}: the maximum saltiness; t_{max}: the time in second to reach I_{max}; R_{inc}, the rate of saltiness increment = I_{max}/t_{max}; I_{30}, the saltiness right before expectoration; R_{dec}, the rate of saltiness decrement = $(I_{max}-I_{30})/(30-t_{max})$; $AUC_{<30}$: area under the curve before expectoration.

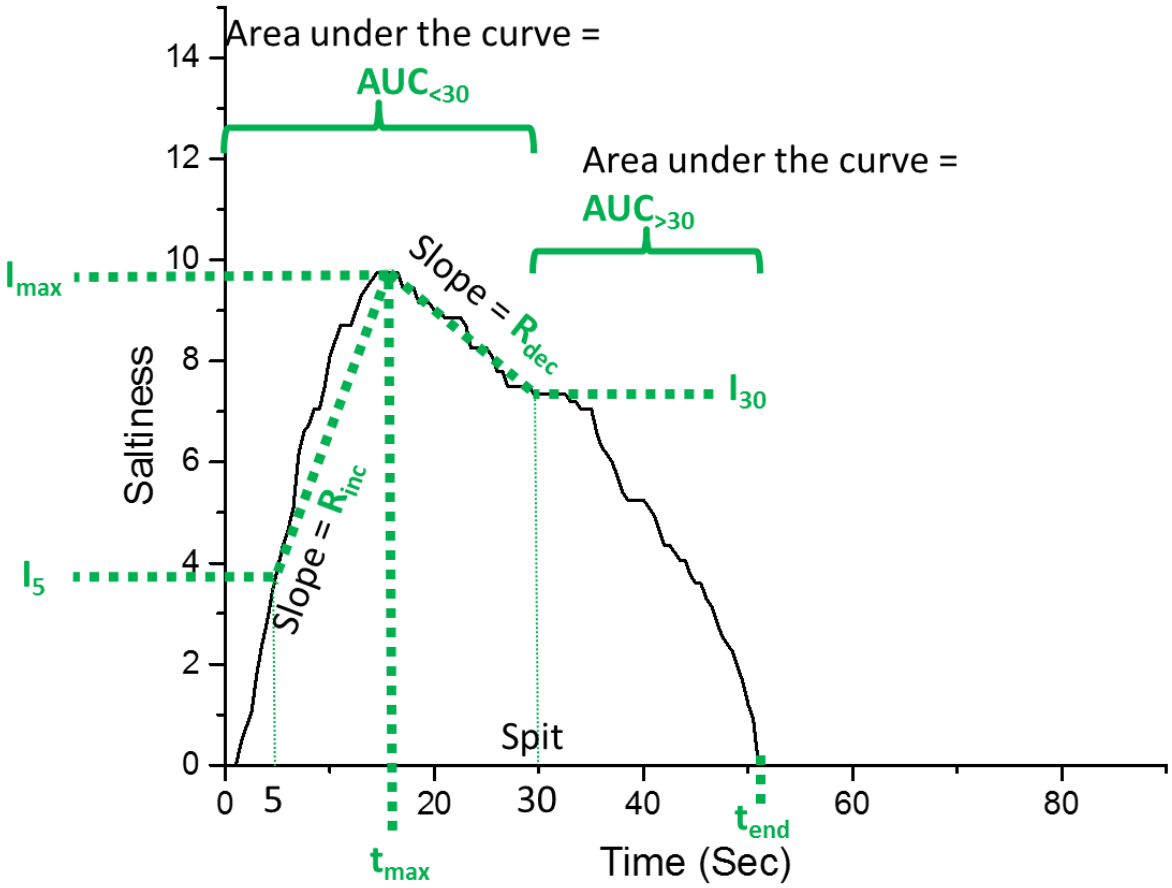

Figure 6.1. Extraction of the time-intensity parameters from individual ratings using the replication 1 of sample 8-22-55 evaluated by panelist 4 as an example. I_5: saltiness at 5 second; I_{max}: the maximum saltiness; t_{max}: the time in second to reach I_{max}; R_{inc}, the rate of saltiness increment = I_{max}/t_{max}; I_{30}, the saltiness right before expectoration; R_{dec}, the rate of saltiness decrement = $(I_{max}-I_{30})/(30-t_{max})$; $AUC_{<30}$: area under the curve before expectoration; $AUC_{>30}$, area under the curve after expectoration; t_{end}, the time in second the saltiness reaches zero.

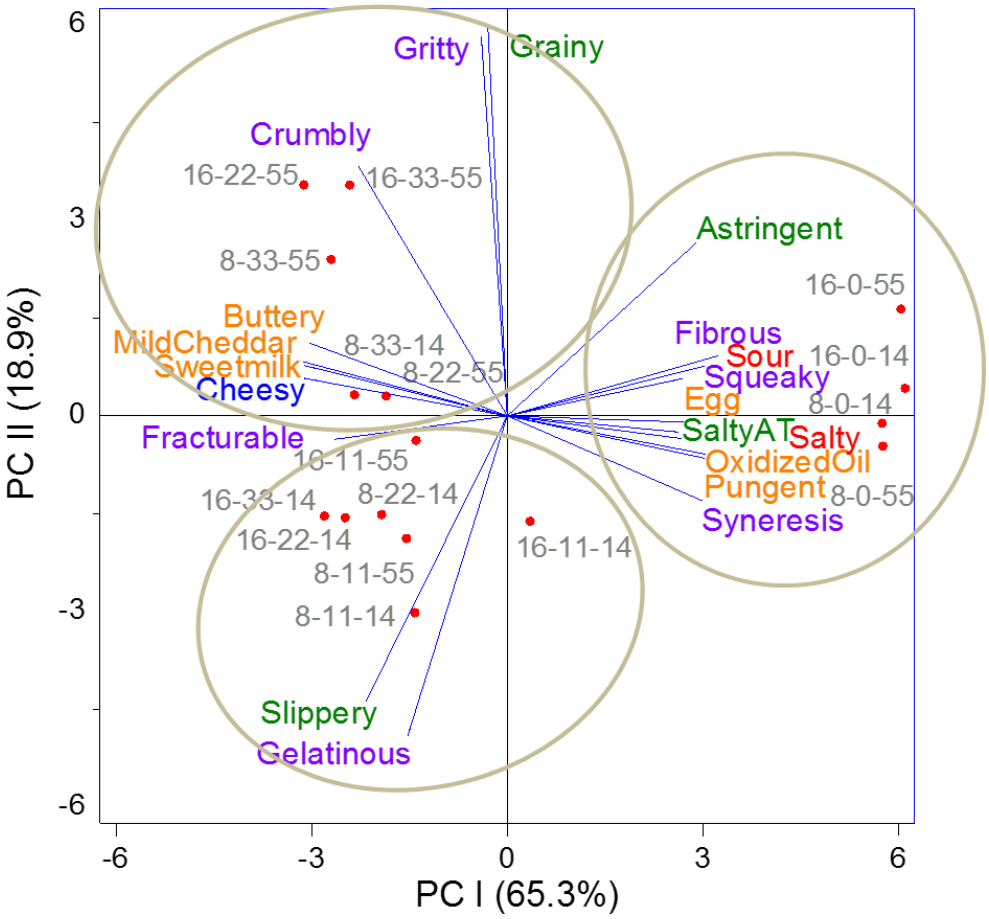

Figure 6.2. Principal component biplot by PC I and II of the QDA properties of the SLCs including non-fat and fat-containing samples. Sample code: protein(%, w/w)-fat(%, w/w)-homogenization pressure(MPa). All samples contained 1.5% (w/w) NaCl. The circles indicate the clusters. Color code for each modality: aroma – orange, aroma-by-mouth – blue, taste – red, aftertaste – green, texture – purple.

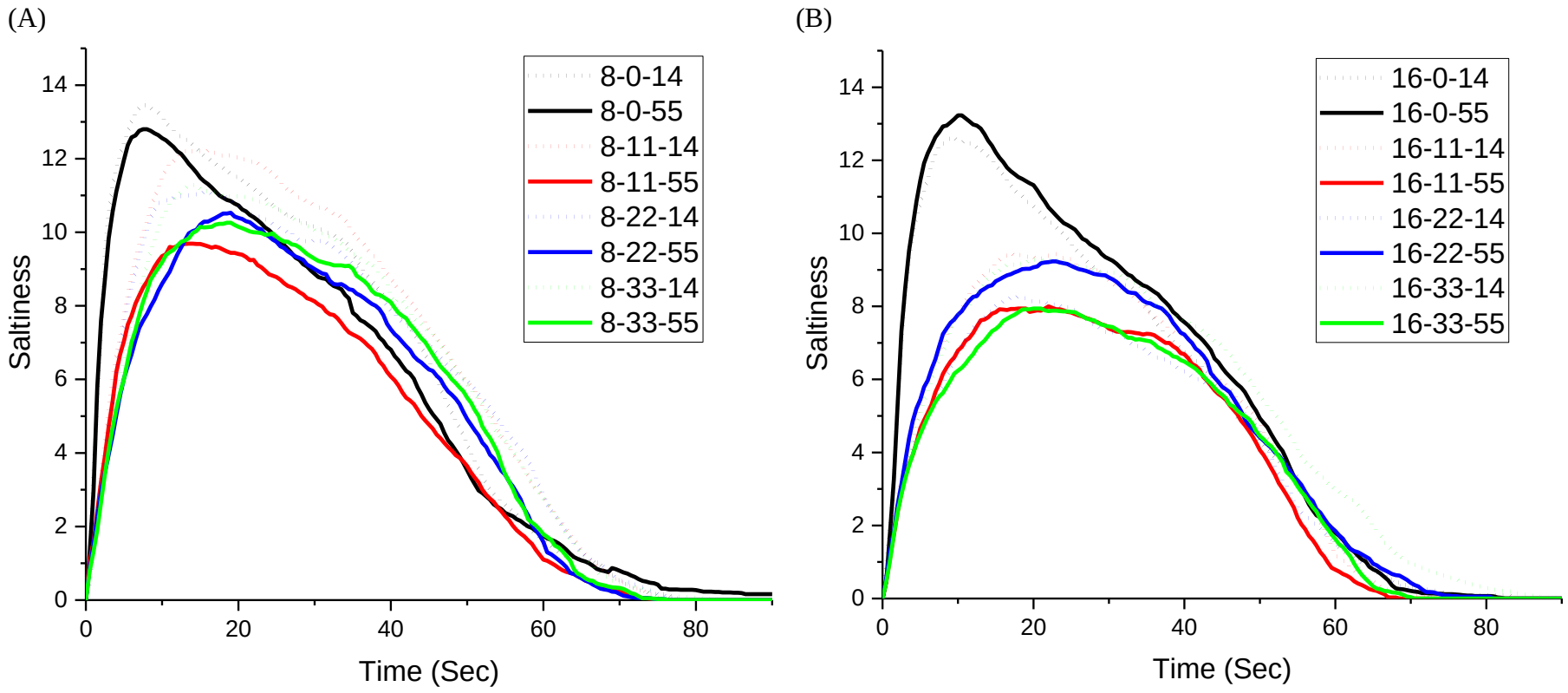

Figure 6.3. Time-intensity curves of saltiness perception of the SLCs with 8% (A) and 16% protein (B). Sample code: protein(%, w/w)-fat(%, w/w)-homogenization pressure(MPa). All samples contained 1.5% (w/w) NaCl.

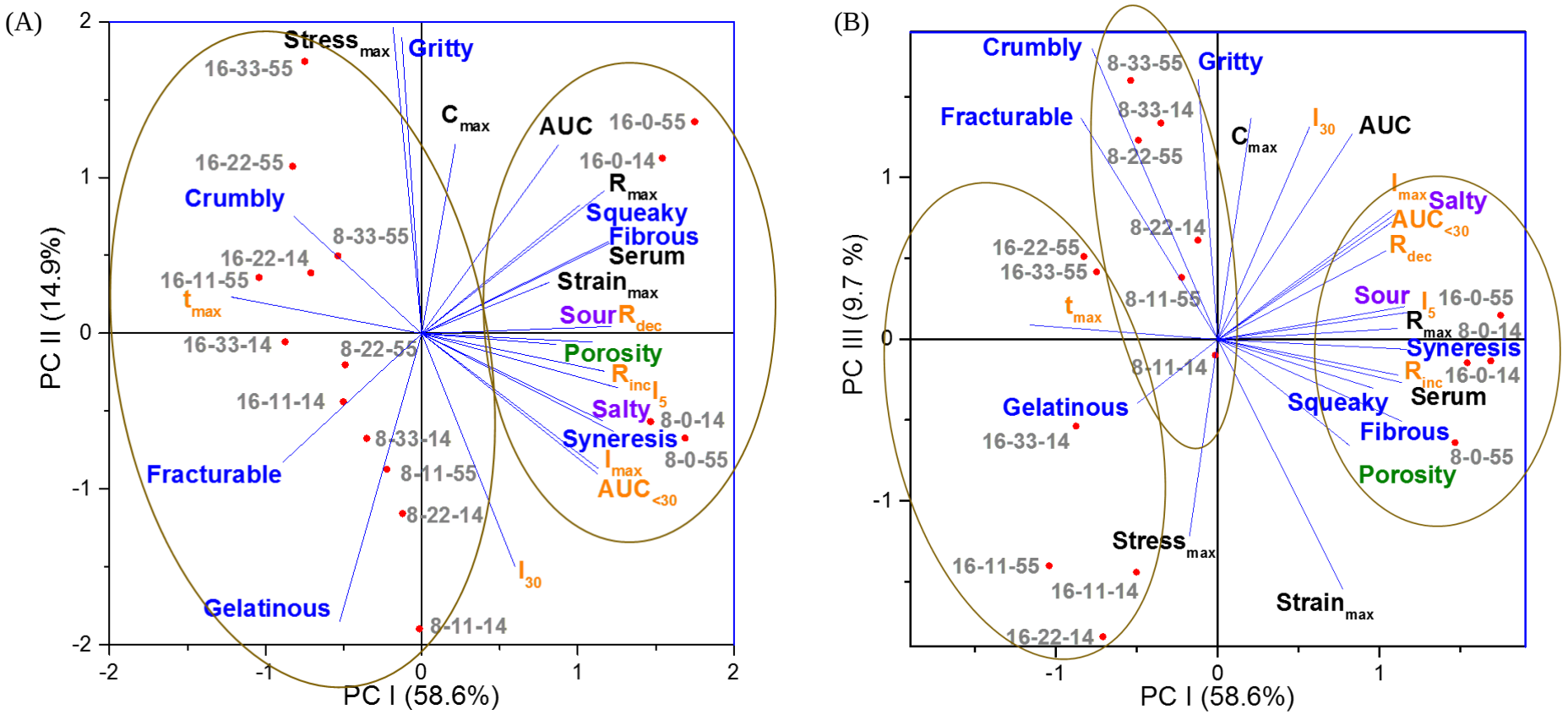

Figure 6.4. Principal component biplots by PC I and II (A), PC I and III (B) and the corresponding dendogram of the cluster analysis (C) for the instrumental and sensory properties of the SLCs including non-fat and fat-containing samples. Sample code: protein(%, w/w)-fat(%, w/w)-homogenization pressure(MPa). All samples contained 1.5% (w/w) NaCl. The circles in (a) and (b) indicate the clusters. Color codes and abbreviations: instrumental properties (black): R_{max}, maximum rate of sodium release; C_{max}, maximum concentration of released sodium; AUC, area under the curve of sodium release; Serum, amount of liquid expelled from the sample during the compression test. $Stress_{max}$, maximum stress measured during the compression test; $Strain_{max}$, strain at the maximum stress; TI parameters (orange): I_5: saltiness at 5 second; I_{max}: the maximum saltiness; t_{max}: the time in second to reach I_{max}; R_{inc}, the rate of saltiness increment = I_{max}/t_{max}; I_{30}, the saltiness right before expectoration; R_{dec}, the rate of saltiness decrement = $(I_{max}-I_{30})/(30-t_{max})$; $AUC_{<30}$: area under the curve before expectoration; QDA textures (blue); QDA tastes (purple).

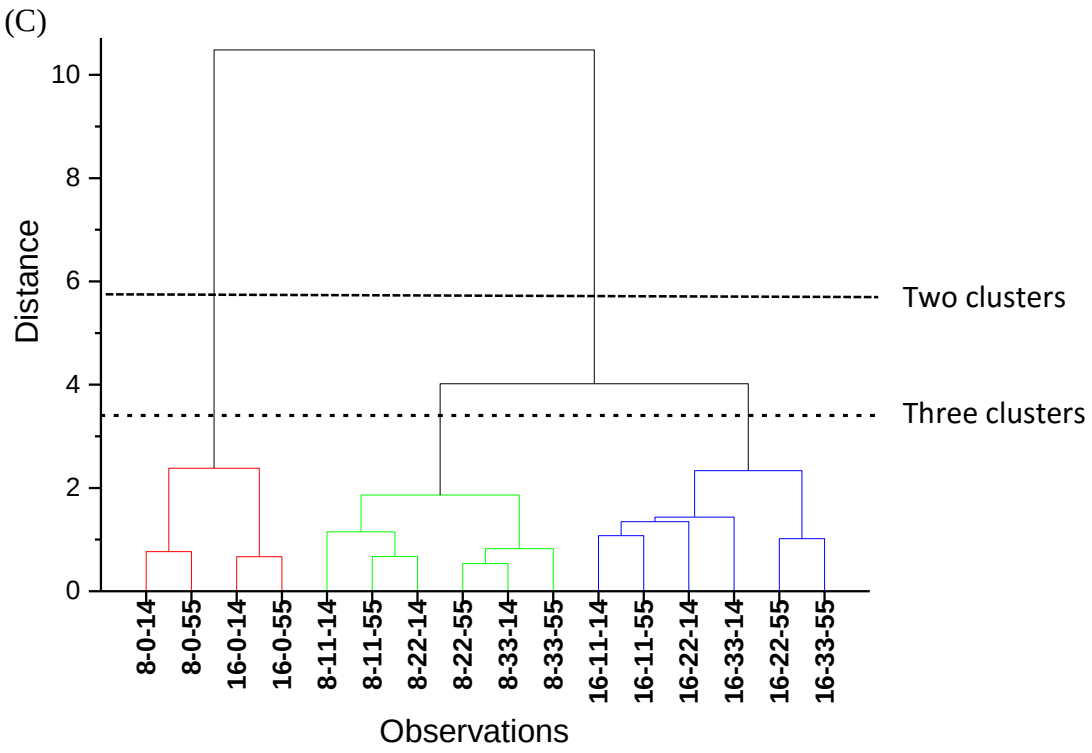

Figure 6.4 (cont.). (C) The dendogram of the cluster analysis for the instrumental and sensory properties of the SLCs including non-fat and fat-containing samples.

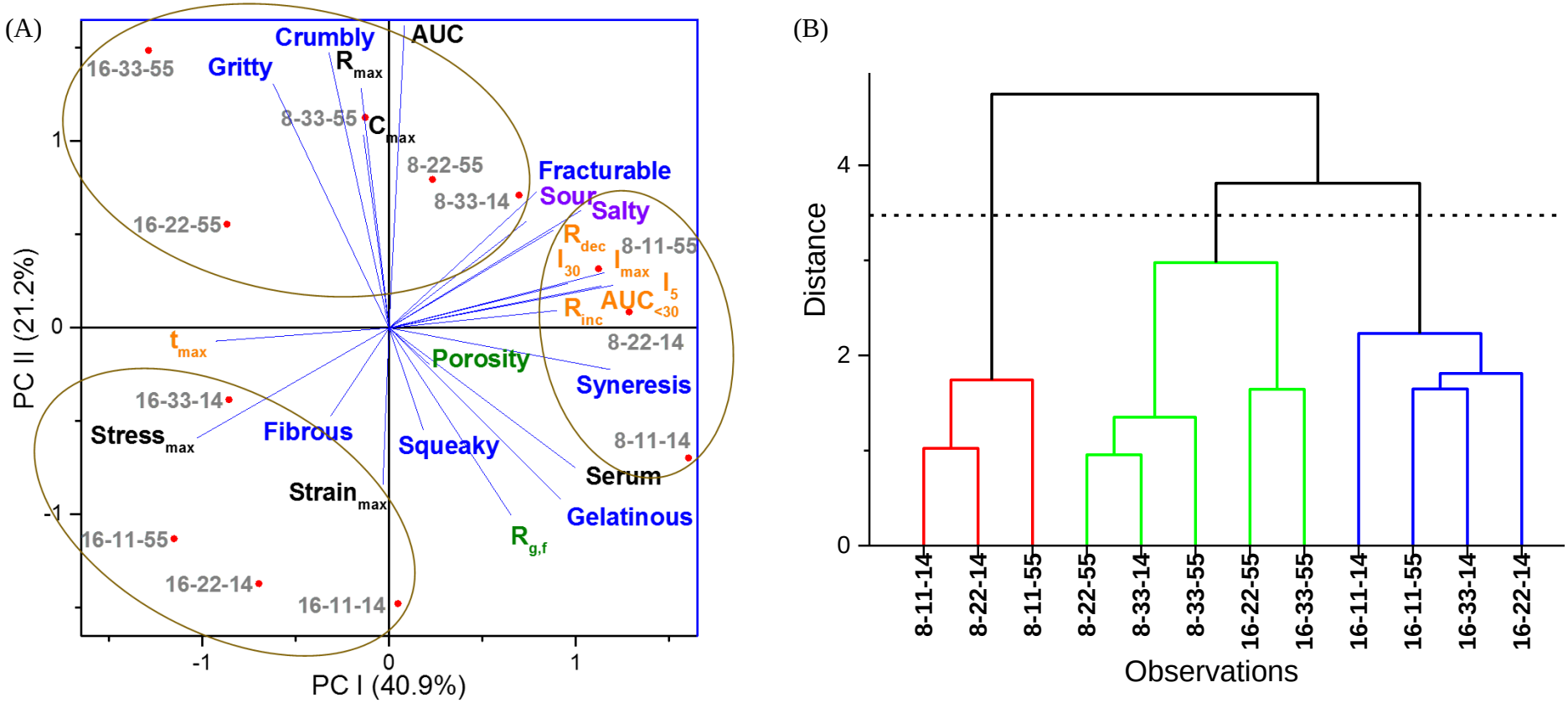

Figure 6.5. Principal component biplots by PC I and II (A) and the corresponding dendogram of the cluster analysis (B) for the instrumental and sensory properties of the fat-containing SLCs. Sample code: protein(%, w/w)-fat(%, w/w)-homogenization pressure(MPa). All samples contained 1.5% (w/w) NaCl. The circles indicate the clusters. Color codes and abbreviations: $R_{g,f}$ (green), gyration radius of fat particles; instrumental properties (black): R_{max}, maximum rate of sodium release; C_{max}, maximum concentration of released sodium; AUC, area under the curve of sodium release; Serum, amount of liquid expelled from the sample during the compression test; $Stress_{max}$, maximum stress measured during the compression test; $Strain_{max}$, strain at the maximum stress; TI parameters (orange): I_5: saltiness at 5 second; I_{max}: the maximum saltiness; t_{max}: the time in second to reach I_{max}; R_{inc}, the rate of saltiness increment = I_{max}/t_{max}; I_{30}, the saltiness right before expectoration; R_{dec}, the rate of saltiness decrement = $(I_{max}-I_{30})/(30-t_{max})$; $AUC_{<30}$: area under the curve before expectoration; QDA textures (blue); QDA tastes (purple).

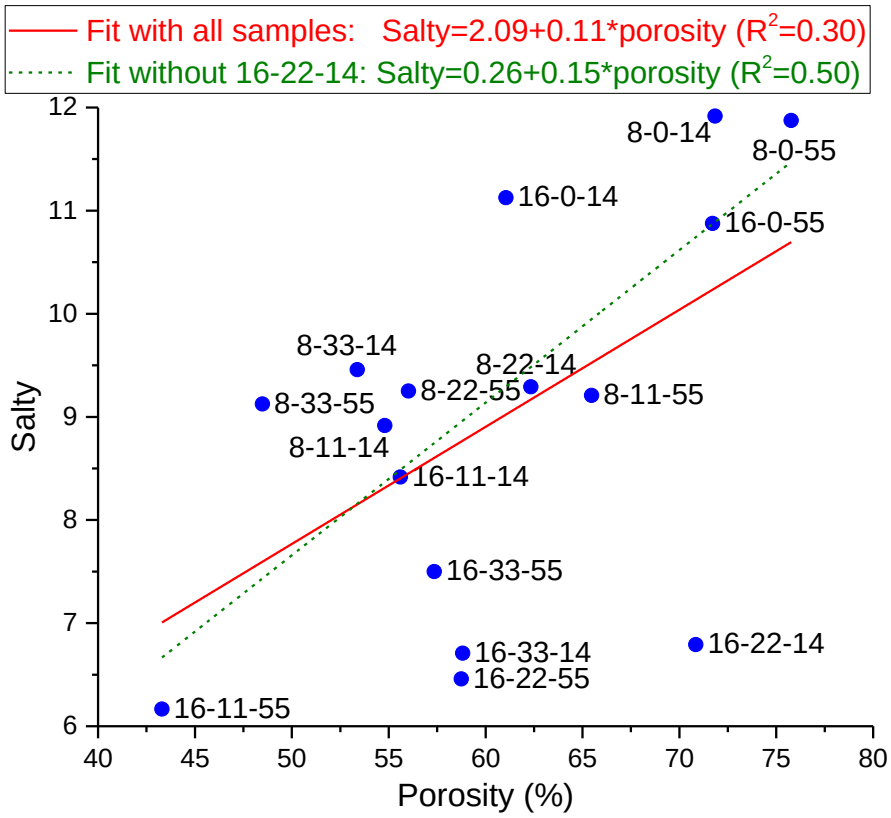

Figure 6.6. Linear regression of the QDA salty by porosity for all SLCs including or not including the outlier 16-22-14. Sample code: protein(%, w/w)-fat(%, w/w)-homogenization pressure(MPa). All samples contained 1.5% (w/w) NaCl.

(A)

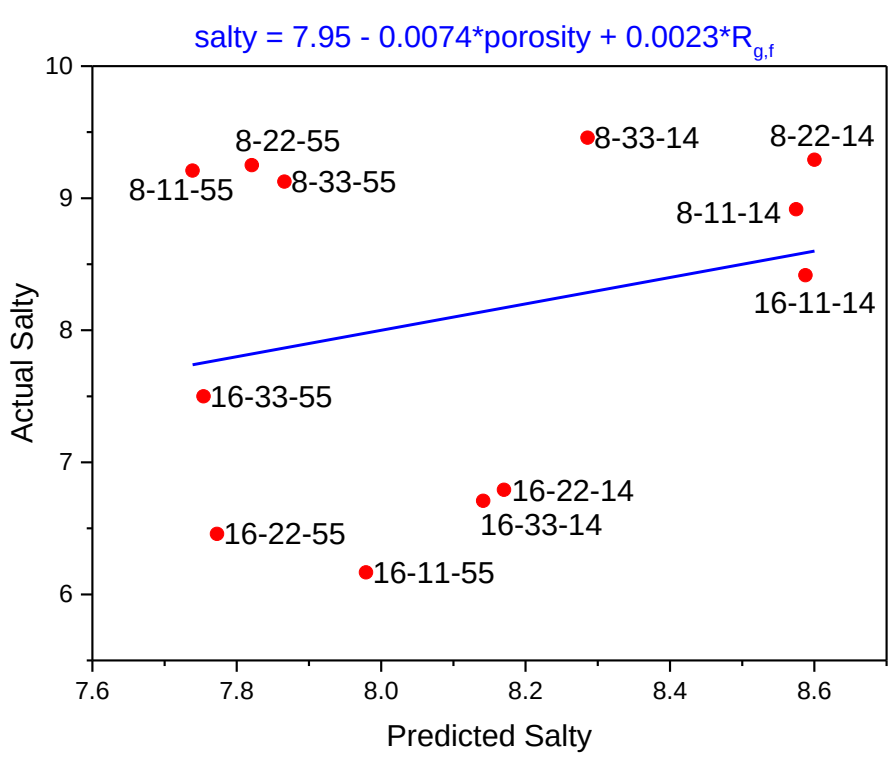

(B)

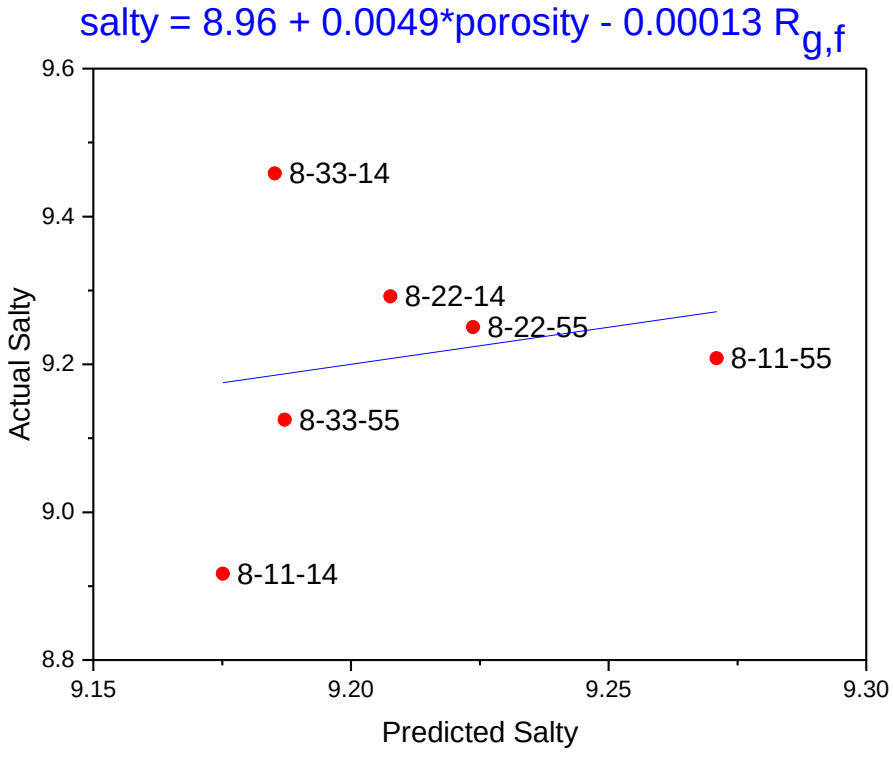

Figure 6.7. Partial least square regression for the QDA salty by the porosity and gyration radius of fat ($R_{g,f}$) of the fat-containing SLCs. (A) Based on all the fat-containing SLCs, (B) based on the fat-containing SLCs with 8% protein, and (C) based on the fat-containing SLCs with 16% protein. Sample code: protein(%, w/w)-fat(%, w/w)-homogenization pressure(MPa). All samples contained 1.5% (w/w) NaCl.

(C)

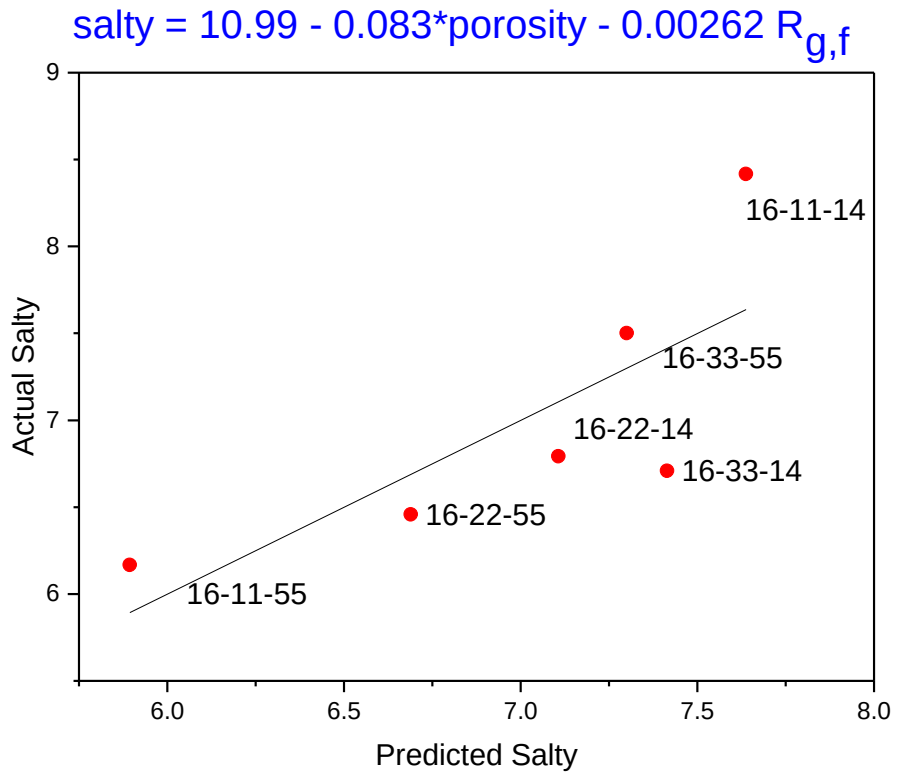

Figure 6.7 (cont.). (C) Partial least square regression for the QDA salty by the porosity and gyration radius of fat ($R_{g,f}$) based on the fat-containing SLCs with 16% protein.

CHAPTER 7

Conclusion and Future Directions

This study aimed at relating the structural properties to the saltiness perception of model lipoproteic foods. The overall conclusion is that porosity rather than particle size of fat affects the saltiness perception of the model lipoproteic foods. The findings from this study demonstrated the potential of sodium reduction via structural engineering of processed foods.

Varying structural properties were created in the model food system, solid lipoproteic colloids (SLCs). An image analysis method was developed to quantify the porosity of the SLCs. The ultra-small-angle X-ray scattering was utilized as a novel technique to quantify the particle size of fat in the SLCs.

Overall, the *in vitro* sodium release properties correlated stronger to the structural properties than to the treatment variables. For the SLCs with both 1.5%, w/w and 3.5%, w/w NaCl, the positive correlations between the porosity and the maximum rate of sodium release (R_{max}) were as strong as the positive correlations between the water content and the R_{max}. For the SLCs with 3.5% NaCl, the maximum concentration of the released sodium (C_{max}) correlated positively with the homogenization pressure and negatively with the gyration radius of fat ($R_{g,f}$). The correlation between the C_{max} and the $R_{g,f}$ was stronger than the correlation between the C_{max} and the homogenization pressure. Also, for the SLCs with 3.5% NaCl, the negative correlation between the area under the curve of sodium release (AUC) and the $R_{g,f}$ was stronger than the negative correlation between the AUC and the ratio of fat to solid content (F/S).

The correlations between the instrumental and sensory properties revealed the effects of structure on texture and sodium release, and hence on saltiness perception of the SLCs. Saltiness perception of the SLCs increased with increasing porosity. This positive correlation was associated with the convective mechanism of sodium transport, where porosity plays a significant role in the rapid serum release to enhance the saltiness perception. The $R_{g,f}$ did not impact saltiness perception, due to counteracting effects on different sodium release mechanisms. The decrease in $R_{g,f}$ resulted in an increased extent of SLC breakdown and increased sodium diffusion. However, the decrease in $R_{g,f}$ resulted in decreased serum release and decreased rate of the convective transport of sodium.

The present study indicated porosity as a target of structural modification to enhance the saltiness of lipoproteic food products. Future studies can be focused on three directions – sodium release, perception fundamentals, and product development.

In the research of sodium release, the aim will be to identify additional matrix properties that affect sodium release. Two potential matrix properties are ionic interaction and matrix tortuosity. The ionic interaction between sodium ion and the polyelectrolyte molecules in the matrix can be evaluated by using NMR and by measuring the partition coefficient of sodium. The matrix tortuosity can be evaluated by using an image analysis of the matrix microstructure. In addition, the porosity quantification may be improved by image analysis of the open-pore porosity and the close-pore porosity, or by using the pycnometer. Sodium release properties of the lipoproteic food may be explained and modeled by using the matrix properties identified to be critical to the sodium release.

In the research of perception fundamentals, the aim will be to identify the factors in sensory testing that affect the saltiness perception of lipoproteic foods. The potential sensory factors include the interactions between the matrix texture and the oral processing behaviors, and the cognitive effects. Comparing the *in vitro* sodium release versus the in-mouth sodium release can help determine whether different matrix texture induced different oral processing behaviors, which further modified the breakdown properties and thus the sodium release of the lipoproteic matrix. Comparing the time-intensity properties of saltiness perception versus in-mouth sodium release can help determining whether the change in saltiness perception corresponded to the sodium level in the mouth, or involved other cognitive factors.

In the direction of product development, the aim will be to engineer the matrix structure to create lipoproteic products with less sodium but acceptable sensory properties. By using different processing techniques, the structure of the lipoproteic matrix may be modified toward enhanced sodium release and saltiness perception. Additional formulation adjustments may be required to ensure that the texture and flavor qualities of the product remain in consumer acceptable range.

In the long term, the improved understanding of the matrix factors involved with saltiness perception will aid in developing ideal sodium reduction techniques for processed foods, and, benefit human health.

APPENDIX A-1 The permission and the publication reprint for the contents of CHAPTER 2

JOHN WILEY AND SONS LICENSE TERMS AND CONDITIONS

Mar 19, 2016

This Agreement between Wan ("You") and John Wiley and Sons ("John Wiley and Sons") consists of your license details and the terms and conditions provided by John Wiley and Sons and Copyright Clearance Center.

License Number	3832731206890
License date	Mar 19, 2016
Licensed Content Publisher	John Wiley and Sons
Licensed Content Publication	Comprehensive Reviews in Food Science and Food Safety
Licensed Content Title	Effect of Food Matrix on Saltiness Perception—Implications for Sodium Reduction
Licensed Content Author	Wan-Yuan Kuo,Youngsoo Lee
Licensed Content Date	Aug 19, 2014
Pages	18
Type of use	Dissertation/Thesis
Requestor type	Author of this Wiley article
Format	Print and electronic
Portion	Full article
Will you be translating?	No
Title of your thesis / dissertation	RELATING STRUCTURAL PROPERTIES TO SALTINESS PERCEPTION OF MODEL LIPOPROTEIC GELS
Expected completion date	Apr 2016
Expected size (number of pages)	250
Requestor Location	Wan-Yuan Kuo 1304 W Pennsylvania Ave Rm 382 E URBANA, IL 61801 United States Attn: Wan-Yuan Kuo
Billing Type	Invoice
Billing Address	Wan-Yuan Kuo 1304 W Pennsylvania Ave Rm 382 E URBANA, IL 61801 United States Attn: Wan-Yuan Kuo
Total	0.00 USD
Terms and Conditions	

Comprehensive REVIEWS in Food Science and Food Safety

Effect of Food Matrix on Saltiness Perception—Implications for Sodium Reduction

Wan-Yuan Kuo and Youngsoo Lee

Abstract: Enhancing sodium release from the food matrix, thus increasing saltiness perception, is a promising strategy to reduce the amount of salt needed in foods. However, the complex nature of the effect of the food matrix on saltiness perception makes it difficult to control saltiness perception when designing food products. The aim of this review is to provide an overview of the food matrix effects on saltiness perception of sodium chloride. The effects are discussed in the order of 3 stages in saltiness perception: release of sodium from food matrix into oral cavity (1st stage), delivery of sodium within oral cavity (2nd stage), and detection of sodium by the taste receptor cells (TRCs) (3rd stage). In the 1st stage, the food matrix affects the initial availability of sodium to be released, and also affects the spontaneous and facilitated migration of sodium from the matrix into the oral cavity. In the 2nd stage, the food matrix affects the availability of sodium and the mixing efficiency of sodium with saliva. The relationship between food matrix and oral processing of food that may affect the sodium release (1st stage) and the delivery (2nd stage) is also discussed. In the 3rd stage, the food matrix affects the physical availability of sodium for the TRCs, the physiological activity of TRCs, and the central activities involved in the perception process. Based on the understanding of complex nature of the matrix effects on saltiness perception discussed in this review, the properties of food matrix may be controlled effectively to enhance saltiness perception and achieve sodium reduction.

Keywords: sodium reduction, microstructure, texture, saltiness perception, oral processing

Introduction

In 2009, the U.S. Institute of Medicine (IOM) suggested that the Food and Drug Administration (FDA) should set clear regulations on the amount of sodium that could be added into foods by manufacturers or suppliers (Henney and others 2010a). While such a strict proposal received some adverse responses from the general population, policy makers argued that mild strategies such as educational efforts on low-sodium diet for the past 40 y had been shown to be ineffective (Henney and others 2010b). The adequate intake (AI) and upper intake level (UL) of sodium for young adults recommended by the IOM are 1500 mg and 2300 mg per day, respectively (IOM 2005). However, from 1988 to 2010, the mean dietary sodium intake by U.S. males and females stayed stable around 4000 and 3000 mg per day, respectively (Henney and others 2010c; Anand and others 2012; Cogswell and others 2012). According to the 2003–2008 NHANES (National Health and Nutrition Examination Survey), 99% of U.S. adults have daily sodium intake exceeding the AI (Cogswell and others 2012). Diet high in sodium is the second highest dietary risk factor for the global "burden of disease" (Lim and others 2012). In the United States, overconsumption of sodium was estimated to be the cause of 65% hypertension or prehypertension rate of the adults, leading to $73.4 billion of medical costs in 2009, and about 100000 annual deaths (Danaei and others 2009; Henney and others 2010b). It is estimated that annual savings of up to $7 billion in health care can be achieved by reducing the average dietary sodium intake by 400 mg/day (DGAC 2005; DGAC 2010).

In response to the urgent appeal for sodium reduction, several strategies have been proposed to reduce sodium while maintaining the perceptibility of processed foods. These include stealth reduction, saltiness potentiation, multisensory application, physical modification of salt crystals, and sodium replacement. The stealth reduction refers to reducing the sodium amount in processed foods gradually so that consumers are unaware of the change. However, products with low sodium may eventually get adverse consumer reaction (Phelps and others 2006). Saltiness can be enhanced by biochemical potentiation of saltiness perception using compounds such as potassium lactate (Brewer and others 1995) and amino acids (Yamaguchi and Takahashi 1984). Nonetheless, the strong flavors of these compounds may limit their uses in mildly flavored products (Heidolph and others 2011). Multisensory application refers to the use of other flavoring agents such as yeast extracts, spices, herbs, and aroma compounds to compensate for the reduced saltiness (Dotsch and others 2009). However, usually only the attributes congruent with salty taste can enhance saltiness (Djordjevic and others 2004). Physical modification refers to the use of NaCl with smaller crystal size or specific crystallography

MS 20140315 Submitted 2/25/2014, Accepted 4/30/2014. *Authors are with Dept. of Food Science and Human Nutrition, Univ. of Illinois at Urbana-Champaign, 382K, Agricultural Engineering and Sciences Building, 1304 W. Pennsylvania Ave, Urbana, IL 61801, USA. Direct inquiries to author Lee (E-mail: leeys@illinois.edu).*

doi: 10.1111/1541-4337.12094

APPENDIX A-1

that dissolves faster in saliva. However, it works mostly for surface-salted foods such as French fries and potato chips (Heidolph and others 2011). Sodium replacement is a method partially substituting sodium with other salty-taste substances, among which potassium chloride (KCl) is the most commonly used. However, some people reported off-tastes, including metallic, chemical, and bitter associated with potassium (Sinopoli 2012). Thus this application is often limited to less than 50% of substitution (Eoin 2006). Another strategy for sodium reduction which could be promising, but has not yet drawn much attention, is promoting the efficiency of sodium release and saltiness perception. This strategy is based on the fact that up to 95% of sodium could still remain in the food matrix before being swallowed (Phan and others 2008), and thus is not utilized in terms of generating saltiness.

A series of studies has been carried out to monitor sodium release using model systems, to understand how saltiness perception may be promoted via adjusting the matrix properties (Phan and others 2008; de Loubens and others 2011b; Panouille and others 2011). In the study led by Panouille and others (2011), several factors, such as protein and fat contents, affecting sodium release have been identified using model dairy gels as cheese analogs. Nevertheless, there was lack of direct relationship between the sodium release from the food and saltiness perception. In other words, the highest amount of released sodium did not necessarily generate highest saltiness perceived (Phan and others 2008; de Loubens and others 2011b). This lack of correlation makes it difficult to predict the saltiness of a food product. Thus, it is still challenging to enhance saltiness perception directly through formulation or process adjustments.

The inconsistency between sodium release and saltiness perception implies that the food matrix may play a significant role on sodium release and saltiness perception. To prove this hypothesis, several studies have been conducted to observe the saltiness perception of food samples prepared with various formulations and processes. Among these studies, increased dry matter and protein contents were found to reasonably decrease saltiness as they slow down the release of sodium from the matrix (Colmenero and others 2005; Ruusunen and Puolanne 2005; Lauverjat and others 2009; Panouille and others 2011). Surprisingly, when comparing the effects of fat content on saltiness, about one-third of the studies claimed that increased fat content increased sodium release or saltiness (Shamil and others 1991–1992; Wendin and others 2000; Ruusunen and others 2001; Colmenero and others 2005; Ruusunen and Puolanne 2005; Phan and others 2008; Lauverjat and others 2009; Ventanas and others 2010; Panouille and others 2011), while another one-third revealed that increased fat content decreased sodium release or saltiness (Eymery and Pangborn 1988; Wirth 1988; Paneras and others 1996; Hughes and others 1997; Romeih and others 2002; Phan and others 2008; Panouille and others 2011), and the rest found no correlations (Stampanoni and Noble 1991; Kähkönen and Tuorila 1998; Ruusunen and others 2001; Lteif and others 2009; Saint-Eve and others 2009; Drake and others 2010). These contradictory findings indicate the multiple ways that a single component could contribute to saltiness perception. For example, from the perspective of the matrix nature, fat as a hydrophobic substance acts as a barrier against sodium migration, thus disfavors its release (Hughes and others 1997). From the perspective of sodium availability in the oral cavity, fat was found to coat the tongue surface, thus preventing the taste buds from accessing sodium (Lynch and others 1993). From the perspective of perception, studies showed that certain components of fat may sensitize the taste receptor cells (TRCs), resulting in their higher response toward sodium (Gilbertson and others 2005). Likewise, other food components may alter saltiness perception in different ways, yet most studies only considered limited aspects. Hence, the relationships among the properties of matrix, sodium release, and saltiness perception are still not well understood.

The purpose of this review is to provide an up-to-date research database of the matrix effect on saltiness perception of foods. The matrix effects include multiple aspects from physicochemical, physiological, to cognitive levels, for example, sodium diffusion in foods, stimulation of taste receptors and cross-modal interactions, respectively. By considering the multiple aspects of matrix effects provided in this review, studies evaluating certain matrix effects on saltiness perception can be designed to better control the variables related to matrix. Ultimately, well-controlled studies to understand the matrix effect on saltiness perception will provide useful references for enhancing saltiness via adjusting formulations or processing. Food products low in sodium, while satisfying consumers' desire of saltiness, can therefore be developed.

Reviews of the fundamental saltiness perception mechanisms at molecular and anatomical levels (Sugita 2006; Kilcast and den Ridder 2007; Frings 2009; Kubale 2010) and reviews of strategies for reducing sodium (Desmond 2006; Doyle and Glass 2010; Drake and others 2011; Heidolph and others 2011) are available. However, to the best of the authors' knowledge, there has not been a review of the fundamental matrix effect on the saltiness of foods. In 2013, Busch and others (2013) published a review article covering 3 major principles to enhance saltiness perception—chemical stimulation, cognitive mechanisms, and structural optimization. Stieger and van de Velde (2013) published a review article about the relationships between food microstructure and oral processing, and strategies to reduce sodium and sugar based on such relationships. Both review articles focus on advances in controlling food structure to enhance sodium release. However, both articles are mainly strategy-orientated, and selectively address the underlying principles of the strategies provided. In this review, the more fundamental principles related to saltiness perception of solid foods, such as the effect of tortuosity on sodium diffusion, are discussed. Hence, this review will merge the information gap between the theories of saltiness perception at the molecular level and the strategies of sodium reduction in practical food systems.

For a clear illustration, the process of saltiness perception in this review is described by 3 distinct consecutive stages (Figure 1). The 1st stage designates the migration of sodium from the solid foods to surroundings, from the moment when food is placed in the mouth until sodium is released into oral cavity. Following the 1st stage, the 2nd stage covers the traveling of sodium in the oral cavity, from the moment when it is released from food matrix, till it reaches the surface of tongue. The 3rd stage refers to the influx of sodium from the tongue surface into the TRCs and subsequent cognitive transduction of signal responsible for saltiness generation. For solid foods such as cheeses and sausages, sodium must first be released from the matrix during masticatory breakdown. Hence, the saltiness perception includes the overall 3-stage process. In contrast, for liquid-like foods such as sauces and soups, sodium is relatively mobile and more readily mixed with saliva as compared to sodium in solid foods. Hence, the saltiness perception would be primarily determined by the last 2 stages.

The central hypothesis of this review is that the saltiness perception is governed by sodium migration during oral processing of food. And 2 main factors affecting sodium migration are the concentration gradient of sodium and the resistance to sodium

APPENDIX A-1

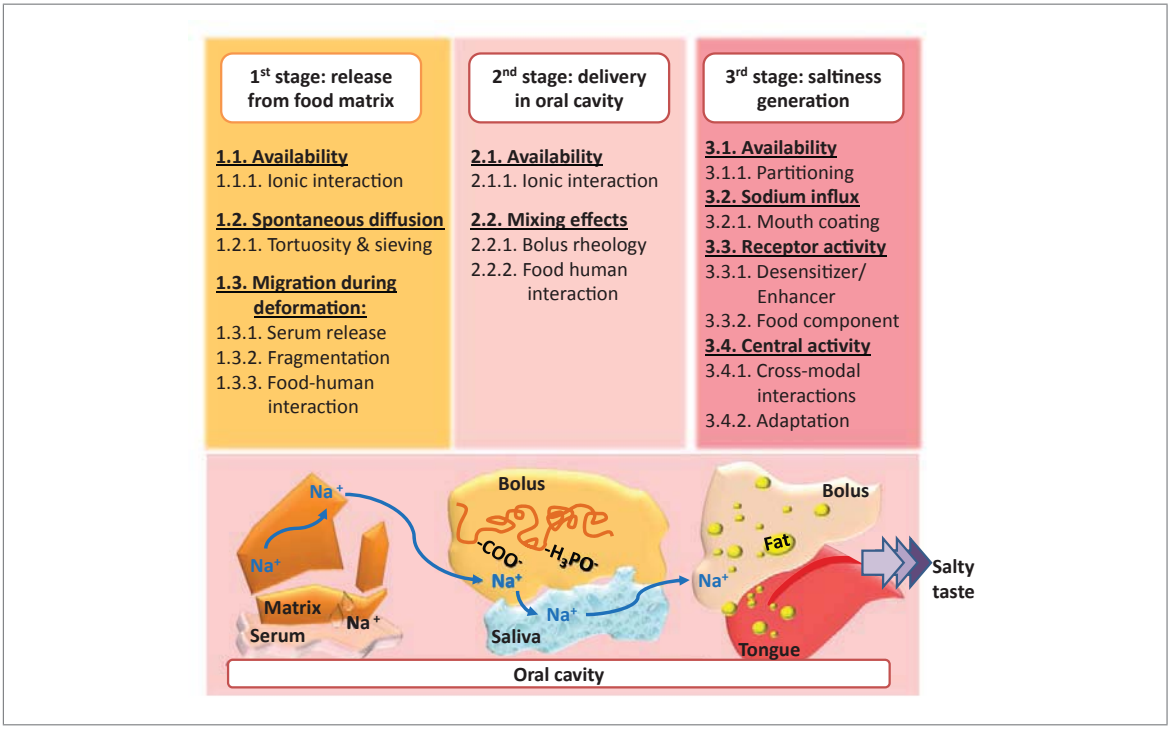

Figure 1–Schematic illustration of the matrix effects during the 3 stages of saltiness perception. The numbers preceding each effect indicate the respective section numbers in the text.

migration. For the 1st and the 2nd stages, the role of the 2 factors affecting sodium migration is based on the principles of mass transfer (Geankoplis 2003). For the 3rd stage, the role of the 2 factors affecting sodium migration is based on the principles of ion transport across the ion channel (Gilbertson and Zhang 1998). In this review, the matrix effects, either on the concentration gradient of sodium or on the resistance to sodium migration, are systematically elaborated in each stage. Additionally, the effects of matrix on the TRC activity and the central activity, such as cross-modal interaction, are discussed.

Sodium Release from Food Matrix—1st Stage

The sodium release from the food matrix in the 1st stage is via diffusive and/or convective transports. The diffusive transport is driven by the difference in sodium concentration across the matrix boundary. The convective transport is driven by the outward liquid flow during the matrix compression. Both diffusive and convective transports depend on the concentration gradient of sodium and the resistance to sodium migration. At given sodium contents of the food, the concentration gradient of sodium is affected by the sodium availability as a result of ionic interaction (Section 1.1). The resistance to sodium diffusion is governed by the tortuosity and sieving effects of the matrix (Section 2.1), whereas the resistance to the convective transport of sodium is reflected by the velocity of the serum flow during the matrix compression (Section 3.1). In addition, the rate of both diffusive and convective transport increase with increased surface area, as a result of the matrix fragmentation during the mastication (Section 3.2). Furthermore, the oral processing parameters may vary in response to different matrix properties. This may additionally modify the food breakdown and thus sodium release (Section 3.3).

Initial availability of sodium

Sodium–polymer interaction in the matrix. The frequent use of NaCl to adjust texture of many food products reflects its nature to interact with ionic polymers such as protein and polysaccharides. Such interaction, though is favored for processing, usually lowers the availability of sodium ion for perception (Rosett and others 1994; Doyle and Glass 2010). NaCl is commonly added to processed meat to enhance water-binding capacity, and thus tenderness and juiciness of the product. The actual process includes swelling of the myofilaments, as a result of Cl^- penetration, and surrounding the filaments with Na^+Cl^- (Ruusunen and Puolanne 2005). In addition to meat protein, NaCl is often used to interact with gluten and milk proteins to achieve the desired texture of bakery and dairy products.

Table 1 summarizes the studies of the effects of sodium–protein interaction on sodium release or saltiness perception of some solid food systems. Ruusunen and others (2001) studied the effect of replacing 71% (w/w) of fat content on the saltiness of "Bologna-type" sausages. When the fat was replaced with lean meat, the saltiness of the sausage was significantly reduced ($P < 0.05$), but when the fat was replaced with water, the saltiness did not change. They, thus, concluded that the ionic interaction between sodium and the lean meat limited the availability of sodium for saltiness perception. Clariana and others (2011) studied the effects of high-pressure processing (HPP) on the saltiness of dry-cured ham. The saltiness of the sample treated at 600 MPa for 360 s

APPENDIX A-1

Table 1–Effects of sodium–protein interaction on the initial availability of sodium in the 1st stage of saltiness perception (release from food matrix)[a].

System	Treatment	Result	Explanation	Source
Model cheese[b]	Content variation: F ↑ (0.07 to 0.15 kg/kg; DM fixed; P ↓ accordingly) or DM ↑ (0.25 to 0.37 or 0.37 to 0.44 kg/kg; F/P mass ratio fixed)	For all samples, $K_{NaCl} < 1$	Sodium-casein (phosphoserine residue) electrostatic interaction reduced amount of sodium available for outward migration.	(Lauverjat and others 2009)
Model cheese[c]	F/P mass ratio ↑ (20/28 to 28/20; DM content fixed)	In-mouth sodium release and saltiness ↑; ^{23}Na-NMR determined bound fraction of sodium ↓; transverse relaxation time ↑	Cations were retained mainly by proteins via electrostatic interactions with its phosphoserine and carboxyl residues.	(Boisard and others 2014)
"Bologna-type" sausage	F content ↓ (0.28 to 0.08 kg/kg; replaced with H_2O or lean meat)	Total NaCl content unchanged; saltiness ↓ only in lean-meat replacing sample	Sodium–meat protein interaction reduced amount of sodium available for perception.	(Ruusunen and others 2001)
Dry-cured ham	High-pressure processing (HPP, 600 MPa, 360 s)	Total NaCl content unchanged; saltiness ↑	HPP weakened the sodium–meat protein interaction, thus yielded more sodium available for perception.	(Clariana and others 2011)

[a] DM: dry matter, F: fat, K_{NaCl}: partition coefficient of NaCl, P: protein.
[b] Made by renneting the mixtures of anhydrous milk fat (AMF), ultrafiltered skim milk retentate powder, NaCl, and water.
[c] Made with AMF, rennet casein, acid casein, melting salts, NaCl, and water.

was higher than that of the control sample. They explained that the HPP weakened the sodium–protein interaction and, thus, led to a higher concentration of free sodium in the product than in the control. Similar results were reported in other studies of dry-cured ham but translated differently. Saccani and others (2004), Serra and others (2007), and Fulladosa and others (2009, 2012) suggested that the poorer water-holding capacity (WHC) after HPP treatment facilitated sodium release with the liquid from the matrix (see Section 3.1 for more discussion). These findings suggested that sodium–polymer interaction apparently is not the only factor that determines saltiness. Indeed, altering formulation or processing parameters often leads to multiple changes in product properties such as moisture content and texture (Ruusunen and others 2001). These changes could affect saltiness through physical (sodium diffusion in matrix) or perceptual (texture–taste interaction) mechanisms (see Sections 2 and 4, respectively, for more discussion). Therefore, controlled model food systems, coupled with instrumental analyses of sodium release, would also be needed to study the impact of sodium–polymer interaction on saltiness perception.

Lauverjat and others (2009) measured sodium release from the model cheese to the surrounding water and obtained the partition coefficient of NaCl (K_{NaCl}). The K_{NaCl} values of all of their cheese samples were below 1, implying a significant portion of NaCl was retained in the model cheese than in the water. This was ascribed to the ionic interaction between sodium ions and the phosphoserine residues of casein. The ionic interaction between sodium and protein was evaluated in terms of sodium mobility in model cheese by measuring the bound fraction and the longitudinal relaxation time (T_1) of sodium with ^{23}Na-NMR (Boisard and others 2014). The cheeses with higher weight ratios of fat/protein had lower bound fractions of sodium and greater T_1, indicating greater sodium mobility. This was attributed to the lower protein content in these cheeses which rendered lower ionic interaction between sodium and casein molecules. The resulting higher sodium mobility thus led to higher sodium availability in these cheeses, which also presented greater degree of in-mouth sodium release.

It should be noted that during oral processing, the structure and texture of the matrix may change instantaneously. Hence, the sodium availability and migration rate may also change dynamically with the evolution of the matrix properties. However, since the chewing period is relatively short compared to the time required to reach partition equilibrium, the K_{NaCl} of a matrix could be considered constant throughout oral processing (de Loubens and others 2011b).

Spontaneous diffusion of sodium

Tortuosity and sieving effects of the matrix. The tortuosity and sieving effect are the intrinsic structural properties of the matrix that predominantly lower the rate of the spontaneous diffusion of sodium. These properties were studied initially for cheese-salting, where sodium migrates from brine into unsalted cheese. More recently these properties have been used to explain sodium release from matrices made of lipid and protein. The tortuosity refers to the obstruction by fat globules or protein aggregates which make the ions travel tortuously with extra length. The sieving effect refers to the friction the ions encounter when passing through the matrix with the lowest pore size comparable to that of the ions (Guinee 2004). Geurts (1974) had reported that the diffusion coefficient of NaCl (D_{NaCl}) in the liquid phase of cheese ($1.2^{**}10^{-10}$–$3^{*}10^{-10}$ m^2/s) was much lower than in water at 12.5 °C (about $1.2^{*}10^{-9}$ m^2/s). Indeed, the D_{NaCl} in cheese products was mainly determined by the volume fractions of fat and protein due to the tortuosity and sieving effects. First, the presence of fat and protein in cheese directly forms a physical barrier which accounts for the tortuosity. Second, the network formed via protein–protein interaction presents small pores which directly exert a sieving effect. Third, the water-binding property of protein indirectly contributes to the sieving effect by increased friction. Besides, the water bound to protein also indirectly contributes to tortuosity by increased occupation of available pore space.

Table 2 lists the studies of the tortuosity or sieving effects on the spontaneous diffusion of sodium in food systems. Hughes and others (1997) observed increased saltiness in frankfurters when the fat content was reduced from 0.3 to 0.05 kg/kg sample by replacing it with water. The authors related this saltiness increase to the removal of the hydrophobic barrier, fat, which impeded sodium diffusion. Phan and others (2008) measured the in-mouth sodium release from model cheese by sampling the saliva of subjects during their chewing processes. It was also claimed that the NaCl diffusion was boosted with a decreased amount of fat working as the hydrophobic barrier. The barrier property in the above 2 studies could indeed be considered as the tortuosity effect of fat. Instrumental analyses would be preferred to evaluate the extent of sodium diffusion as a more direct evidence of the matrix effects.

APPENDIX A-1

Table 2–Effects of tortuosity or sieving on the spontaneous diffusion of sodium in the 1st stage of saltiness perception (release from food matrix)[a].

System	Treatment	Result	Explanation	Source
Chicken sausage	F/P mass ratio ↓ (2.5 to 1)	Sodium release and saltiness ↑	Lowering F content led to less masking to sodium release.	(Chabanet and others 2013)
Franks	F content ↓ (0.3 to 0.05 kg/kg; replaced with H_2O)	Saltines ↑	Lowering fat content decreased hydrophobic barriers that impeded sodium migration in the gel, and thus enhanced sodium release.	(Hughes and others 1997)
Model cheese[b]	F content ↓ (0.3 to 0.2 kg/kg; DM content ↓ accordingly)	Sodium release rate ↑		(Phan and others 2008)
Model cheese[c]	Renneting	$^{*}D_{NaCl}$ ↓	Renneting induced network development by protein, resulting in gelation.	(Panouille and others 2011)
	DM content ↑ (0.26 to 0.43 kg/kg)	$^{*}D_{NaCl}$ ↓	Increased DM content gave higher volume occupation by protein and fat, and higher viscoelasticity (in renneted samples).	
Model cheese[c]	DM content ↑ (0.25 to 0.37 or 0.37 to 0.4 kg/kg) or F content ↓ (0.15 to 0.07 kg/kg; replaced with P)	$^{*}D_{NaCl}$ ↓	Higher DM content led to higher firmness, lower amount of available water and a more pronounced sieving effect of protein network; protein impeded sodium more effectively than fat did.	(Lauverjat and others 2009)
	NaCl content ↓ (0.015 to 0.005 kg/kg)	$^{*}D_{NaCl}$ ↓	NaCl content reduction limited the modification of gel structure, and in turn altered the sodium migration.	
Model cheese[c]	DM content ↑ (0.37 to 0.44 kg/kg)	$^{*}D_{NaCl}$ ↓	DM content increment resulted in a more crosslinked, less fluffier network, and thus generated higher friction against sodium migration.	(Floury and others 2009)
	NaCl content ↓ (0.005 to 0.015 kg/kg)	$^{*}D_{NaCl}$ ↓	Sodium content reduction led to tighter casein network structure, and thus impeded sodium migration.	
	pH ↓ (6.5 to 6.2)	$^{*}D_{NaCl}$ ↓	pH reduction led to poorer hydration of casein micelle, and hence lower solubility of the protein, disfavoring sodium migration.	

[a] DM: dry matter, F: fat, P: protein, $^{*}D_{NaCl}$: apparent diffusion coefficient of sodium.
[a] Made with anhydrous milk fat, rennet casein, melting salts, and water.
[b] Made by renneting mixtures of anhydrous milk fat, ultrafiltered skim milk retentate powder, NaCl, and water.

Lauverjat and others (2009), Floury and others (2009), and Panouille and others (2011) examined the effects of composition on the apparent diffusion coefficient of NaCl ($^{*}D_{NaCl}$) in model cheese. The $^{*}D_{NaCl}$ was obtained by measuring sodium release with a conductivity probe and calculating the mass transfer based on Fick's 2nd law. Overall, all 3 studies observed a decrease in $^{*}D_{NaCl}$ with increased dry matter content, which was explained by the increase in viscoelasticity and decrease in void volume. At constant dry matter content, the $^{*}D_{NaCl}$ was lower in the sample with higher protein content, suggesting that protein is more influential than fat in restricting sodium diffusion (Lauverjat and others 2009). It was explained by the contributions of protein to tortuosity and sieving effect via multiple routes as previously discussed. By contrast, fat only contributed to tortuosity. Furthermore, with given sample composition, the $^{*}D_{NaCl}$ dropped with renneting of the sample (Panouille and others 2011), decreased NaCl content (Floury and others 2009; Lauverjat and others 2009), or decreased pH (Floury and others 2009), which was mainly due to the alteration of casein arrangement and thus the network structure formed with the protein by these treatments. It also implies that the effective volume fraction of protein, which varies with the network structure, is more indicative than the protein content in determining sodium diffusion.

It should be noticed that most solid or gel-like foods undergo deformation during oral processing. Since the matrix structure may be changed simultaneously during the deformation, the tortuosity and sieving effects, and hence, the apparent diffusion coefficient of NaCl ($^{*}D_{NaCl}$) may also change dynamically. However, the changes in geometry and surface area due to matrix deformation and breakdown should have more significant impacts on sodium release. Thus, the $^{*}D_{NaCl}$ could still be considered constant regardless of the product deformation (de Loubens and others 2011b).

Facilitated migration of sodium under matrix deformation

Serum release of the matrix. Table 3 lists the studies on the effects of serum release on the migration of sodium under matrix deformation. As mentioned in Section 1, both Clariana and others (2011) and Fulladosa and others (2009) observed increased saltiness of the dry-cured ham after high-pressure treatments, and attributed this to a decrease in sodium–protein interaction and poorer WHC, respectively. In the study by Fulladosa and others (2009), the transglutaminase-restructured dry-cured hams were treated with 600 MPa for 360 s. The high pressure-treated samples showed a higher percentage of water loss, implying poorer WHC than the control. Therefore, it was concluded that the HPP boosted the sodium release by creating more expressible water that efficiently carried sodium out from the food matrix during oral processing. This hypothesis was also proposed in similar studies by Fulladosa and others (2012) and Clariana and others (2012). Still, without measuring the sodium–polymer interaction, it was not clear whether the saltiness increment was partly due to dissociation of the bound sodium after HPP treatments.

The serum release of fruits, vegetables, and meat products could be related to their juiciness perception (Stieger 2011). While saltiness was positively related with sensory juiciness in some meat products (Ruusunen and others 2005; Ventanas and others 2010), such relationship was not observed by Matulis and others (1995), Crehan and others (2000), or Moeller and others (2010). This inconsistency again reflects the multiple matrix effects on saltiness perception. Thus, it is necessary to obtain a sodium release profile as the baseline to study saltiness perception.

APPENDIX A-1

Table 3–Effects of serum release on the migration of sodium under matrix deformation in the 1st stage of saltiness perception (release from food matrix).

System	Treatment	Result	Explanation	Source
Transglutaminase restructured dry-cured hams with reduced sodium	High-pressure processing (HPP, 600 MPa, 360 s)	Poorer water-holding capacity (WHC), and saltiness ↑, but sodium content unchanged	HPP led to poorer WHC of muscle proteins, resulting in higher serum release during sample deformation, which carried out more sodium available for perception.	(Fulladosa and others 2009)
Restructured dry-cured ham	HPP (600 MPa, 360 s)	Saltiness ↑		(Fulladosa and others 2012)
Sliced and vacuum-packaged commercial dry-cured ham	HPP (400 MPa, 360 s)	Saltiness ↑		(Clariana and others 2012)
Gellan/whey protein isolate gel made by acid-induced cold gelation	Gellan content ↑ (dry matter content adjusted to reach similar large-scale deformation property)	Serum release ↑ Sensory juiciness↑ Saltiness ↑	Gellan increment changed the gel morphology from protein-continuous to bi-continuous, leading to higher gel permeability which carried out sodium faster.	(Stieger 2011)

Jack and others (1995) examined the effects of texture in terms of hardness on sodium release of commercial cheeses using in-mouth conductivity probes. The cheese samples showed a positive correlation between the rate of sodium release and the hardness of cheese. The authors postulated that the cheese with higher hardness had lower moisture content and consequently higher NaCl concentration in the aqueous phase. Thus, the concentrated NaCl solution, when being expressed during oral processing, resulted in a higher release rate of sodium. Nevertheless, as the sodium release was measured in-mouth, the effects of oral processing on the matrix breakdown could not be excluded. The authors indeed mentioned that the greater chewing force required for the harder gel could also contribute to the higher release rate of sodium. Stieger (2011) studied the effects of microstructure on serum release and sodium release of model gels made by acid-induced cold-gelation of gellan/whey protein isolate mixtures. By adjusting the total solid content and the gellan amount, they prepared a series of gels with identical large deformation properties but different serum release under instrumental compression. With the increased gellan ratio, the gel microstructure changed from a protein-continuous to a bi-continuous structure. The change from a protein-continuous to a bi-continuous structure increased the amount of serum release and, consequently, resulted in higher juiciness and saltiness in sensory evaluation. More convincing conclusion could have been drawn if the sodium release during the instrumental compression was also measured and compared with the serum release and saltiness.

During the mastication process, the serum release behavior may change momentarily with the evolution of food microstructure (van den Berg and others 2007). However, it is still assumed that the differences in original structures between samples are much greater than the differences in structures generated during oral processing. Hence, only the changes in surface area would need to be discussed for the effect of fragmentation on serum release.

Matrix fragmentation. Oral processing of solid foods typically includes mastication that breaks down food into pieces smaller than 2 mm, the particle size threshold for swallowing (Prinz and Lucas 1995). Table 4 lists the studies on the effects of fragmentation tendency on the migration of sodium during matrix deformation. In the study with commercial cheeses (Jack and others 1995), the half-fat Cheddar, which presented slow sodium release, was found to be more rubbery by the sensory test. It was hypothesized that the rubbery nature of the sample lowered the extent of disintegration on each chew stroke, which disfavored sodium release. Instrumental analyses for texture and sodium release using model food systems would be a great addition to support the above statement.

Koliandris and others (2008) investigated the effect of matrix texture on sodium release of 2 model gels consisting of low-/high-acetyl gellan and κ-carrageenan/locust bean gum. When the concentration of low-acetyl gellan or κ-carrageenan was increased, the instrumental brittleness and the rate of *in vitro* sodium release increased correspondingly. Thus, they suggested that brittle samples yielded higher surface area after compression, and released more sodium in a given time period. However, the surface area was not measured to confirm this statement.

The research group of Souchon I. (Saint-Eve and others 2009; Loubens and others 2011; Panouille and others 2011) has also investigated the dependency of sodium release or saltiness on breakdown properties of model cheeses. Their earlier study concluded that texture had no effect on saltiness, despite the "fragmentable" score by sensory evaluation increased with the fat content (Saint-Eve and others 2009). The lack of saltiness-texture correlation might be due to the comparatively narrow range of variations in the formulation of cheese samples, where the dry matter (DM) was 0.37 to 0.44 kg/kg cheese and the fat content was 0.2 to 0.4 kg/kg DM. In 2 of their later studies (Loubens and others 2011; Panouille and others 2011), the DM and fat contents varied in greater ranges of 0.15 to 0.43 kg/kg sample and 0 to 0.4 kg/kg DM, respectively. Panouille and others (2011) observed decreased saltiness with increased protein content, and attributed this to the densely formed protein network with more rubbery and less brittle texture. However, their instrumental texture analysis did not confirm this trend. de Loubens and others (2011a) established a real-time measurement of sodium release during gel compression using a texture analyzer. Based on a mass transfer model that includes the surface area of the broken gel as the main parameter, they fitted the release data to obtain the surface area. By comparing with their sensory evaluation results, they hypothesized that the gel with higher fat content was fragmented faster due to the disruption of the protein network by fat. This could be evidenced by the larger breakdown surface area, earlier perception of crumbliness, and longer perception of saltiness of the high-fat sample. Nonetheless, this hypothesis only applied to the samples with milk retentate of 0.25 kg/kg gel. Their previous study (Panouille and others 2011) showed that the saltiest sample (retentate 0.15 kg/kg gel, fat 0.4 kg/kg DM) had a fairly small breakdown surface area.

APPENDIX A-1

Table 4–Effects of fragmentation tendency on the migration of sodium under matrix deformation in the 1st stage of saltiness perception (release from food matrix)[a].

System	Treatment[a]	Result	Explanation[a]	Source
Commercial cheeses	Varying textural characteristics	Sensory rubbery ↑, in-mouth sodium release rate ↓	Rubbery samples disintegrated less extensively on each chew stroke, and thus gave slower sodium release.	(Jack and others 1995)
Gels made of LAG, HAG, KC, LBG	LAG or KC content ↑ (DM content fixed)	Fracture strain ↓; textural brittleness and sodium release rate ↑	Increase in LAG or KC content resulted in more brittle gels, yielding larger surface area after chewing, and thus boosted sodium release.	(Koliandris and others 2008)
Model cheese[b]	F content↑ (0 to 0.17 kg/kg; DM content ↑ accordingly)	Breakdown surface area and sodium release rate ↑; start time ↓ and duration of saltiness dominance ↑	Increased F content weakened the protein network of the gel, which broke down more easily and generated larger surface area beneficial to sodium release.	(de Loubens and others 2011a)
Model cheese[b]	P content ↓ (0.15 to 0.09 kg/kg; DM content fixed or ↓ accordingly)	Saltiness ↑	P content decrement led to higher brittleness and lower rubbery of the gel, which fragmented more easily and yield larger surface area.	(Panouille and others 2011)

[a] DM: dry matter, F: fat, LAG: low acetyl-gellan, HAG: high acetyl-gellan, KC: κ-carrageenan, LBG: locust bean gum, P: protein.
[b] Made by renneting mixtures of anhydrous milk fat, ultrafiltered skim milk retentate powder, sodium, and water.

In addition, the high saltiness was not attributed to the high fragmentation tendency, but to the partitioning effect (Panouille and others 2011). The partitioning effect refers to the concentrating of sodium in the aqueous phase upon incorporation of fat due to the stronger partitioning of sodium in the aqueous compared with the fat phase in the emulsion (discussed more in Section 1.1). The discrepancy between the above 2 parallel studies implies that the fragmentation tendency, expressed by the surface area, may not be the universal predictor for sodium release and saltiness. Other variables such as tortuosity and serum release may need to be incorporated when explaining the saltiness of a product.

In the study of in-mouth sodium release by Phan and others (2008), the sodium release at 20 s and 60 s of chewing increased, respectively, with increased water-to-protein ratio and fat-to-protein ratio. This means that the matrix effects dominating sodium release depended on the duration of mastication. For the initial 20 s of chewing, the authors suggested that water in the matrix was most helpful for sodium release, which indeed was a consequence of serum release. By contrast, when the chewing was prolonged to 60 s, the effect of fragmentation might become prominent. Thus high fat content would make the matrix more fragmentable and lead to greater sodium release. Yet, none of the studies in Section 3.2 considered both serum release and fragmentation in the design of the experiments and the interpretation of the results. In fact, when 2 samples bear the similar fragmentation tendency, but different amounts of serum release, then the sodium release would still be different. This means that to describe sodium release accurately, a more comprehensive model incorporating individual matrix effects may be required.

Interactions between matrix properties and oral processing. So far, the discussions about the matrix effects on sodium release or saltiness perception only include the direct impact from the matrix. In fact, the matrix properties and the oral processing could be interactive. In other words, the mastication and/or salivary functions during oral processing may vary from product to product. Such interaction between matrix and oral processing may lead to a different sodium release profile which could not be revealed by instrumental analyses. Ideally, it will provide a more comprehensive picture of saltiness perception by incorporating all the interactions between matrix properties and oral processing. However, the variety and complexity of such interactions may require another article for discussion. Hence, only limited studies from the literature are discussed in this section to illustrate the concept of such interaction and its potential influences on saltiness perception.

During typical oral processing, mastication and salivary properties are the major 2 oral parameters related to flavor release (Salles and others 2011; Lawrence and others 2012). Tarrega and others (2011) studied the relationship between compositional/textural properties of model cheeses and panelists' mastication activities. The samples with lower fat content had more hardness and required greater chewing work per cycle, number of chewing strokes, and higher amount of total incorporated saliva. However, chewing rate was independent of the fat content or texture of the samples. Similar results were also reported by Mioche and others (2002) and Gaviao and others (2004).

Apart from eating foods, salivary flow may be modulated by certain medicines (Mattes and others 1994), physiological activity (such as chewing paraffin film [Mackie and Pangborn 1990], wax, or rubber [Kerr 1961]), environment (temperature, illumination, and sound), or higher-order cognitive factors (attention, mental imagery, and labeling [Spence 2011]). During eating, saliva flow rate can be elevated from $5^{\star}10^{-9}$ m^3/s (Christensen and others 1984) to beyond $1.67^{\star}10^{-8}$ m^3/s (Navazesh and Christensen 1982) by chemosensory (taste, smell, and chemical irritancy) (Neyraud and others 2003; Harthoorn and others 2009) or tactile factors (Mattes 1997). Among the different chemosensory and tactile factors taste is the most dominating stimulus. Among the different tastes, sourness increases salivary flow rate the most, followed by umami, salty, sweet, and bitter tastes (Froehlich and others 1987; Hodson and Linden 2006). In addition, certain fatty acids were also shown to stimulate saliva secretion (Koriyama and others 2002; Hodson and Linden 2004). Chewing foods with different physicochemical features could also change saliva flow (Mackie and Pangborn 1990).

The matrix effects on oral processing have been widely investigated. However, effects of the consequently altered oral processing on sodium release have been rarely studied, and discussions found in the literature provide only limited valid evidence. Lawrence and others (2012) discovered that, for the model cheese with highest sodium level in their study, the in-mouth sodium release increased with the moisture content of the cheese. This was attributed partly to the facilitated sodium extraction from the matrix due to high moisture content of the sample and high salivation induced by the high sodium concentration (Chabanet and others 2013). Still, as discussed in their article, other factors such as higher amount of noncomplexed sodium might also contribute to sodium release in the mouth, and thus this need further investigation. Phan and others (2008) observed that individuals with higher salivary flow

APPENDIX A-1

rate or masticatory performance produced a bolus with higher sodium release from model cheeses. They ascribed this to high efficiency of sodium extraction by saliva and more extensive food breakdown. Interestingly, saltiness remained the same, and this was hypothesized to be due to receptor saturation or adaption (see Section 4.2 for more discussion). Pionnier and others (2004) observed that the in-mouth sodium release, expressed by area under the curve (AUC) of concentration compared with time plot, was correlated positively with chewing time but negatively with salivary flow rates, chewing rates, masticatory performances, and swallowing rates. While the findings from Phan and others (2008) and Pionnier and others (2004) were based on inter-individual differences, their implications on the interaction between the matrix properties and oral processing are limited.

An overview of the studies in the 1st stage implies that future research on sodium release from the food matrix should address the following. First, direct measures of sodium–polymer interaction such as ^{23}Na-NMR relaxation time should be assessed. This will help to identify whether a change in sodium release is due to its change in concentration gradient and/or the change in resistance to sodium migration. Second, model food gels with well-controlled emulsion structures should be used. Both serum release and fragmentation degree should be assessed and correlated to the *in vitro* sodium release parameters. This will help to identify the matrix effects on the diffusive and/or convective transport of sodium, and the corresponding changes in the temporal sodium release. Third, the comparison between the *in vitro* and in-mouth sodium release should be conducted. This will help to identify the interactions between the matrix and the oral processing properties.

Sodium Delivery in Oral Cavity—2nd Stage

During the oral processing of solid foods, size reduction and lubrication of matrix are 2 major processes to prepare the food bolus ready and safe for swallowing. The fragmented food particulates and released serum are mixed and glued by saliva to form a more cohesive bolus (Stieger and van de Velde 2013). Meanwhile, fat may also be released from the food matrix to the bolus and aid in the lubrication (de Wijk and Prinz 2005). Once being released from the food matrix, the delivery of sodium in the oral cavity is mainly via convective mixing between the food bolus and the saliva (Ferry and others 2006a; Le Reverend and others 2013). Though sodium also migrates via diffusion in the bolus, the diffusive barrier in the semisolid material is comparatively low and thus less influential (Panouille and others 2011). The convective transport of sodium in this stage depends on the concentration gradient of sodium across the bolus and the saliva, and the resistance to the bolus-saliva mixing. At given sodium contents in the food bolus, the concentration gradient depends on sodium availability as a result of ionic interaction (Section 1.1). The resistance to the bolus–saliva mixing is affected by the bolus rheology (Section 2.1). In addition, the varying oral processing parameters in response to different bolus properties can additionally modify the bolus–saliva mixing and thus sodium delivery (Section 2.2).

Sodium availability

Sodium–polymer interaction. The studies on the effects of sodium–hydrocolloid interaction on the availability of sodium during its delivery in the oral cavity are listed in Table 5. In a series of studies done by Rosett and others (1994, 1995, 1996), ^{23}Na-NMR was used to monitor the mobility of sodium and to predict the availability of sodium within certain hydrocolloid solutions. The authors hypothesized that electrostatic interaction between sodium and polymer would restrain sodium mobility, which could be identified by higher values of transverse relaxation rates (R_2, s^{-1}). In the 1st study, NaCl solutions were added with either ionic gums (xanthan gum or κ-carrageenan) or nonionic gums (locust beam gum or guar gum) (Rosett and others 1994). Compared to the solutions with nonionic gums, the ionic gum solutions had higher R_2 values of sodium and lower saltiness scores. The viscosities and pH values, which might also affect the R_2 values, were similar across all samples. Thus, the authors postulated that the higher R_2 values resulted from interaction of the ionic gums with sodium, which limited its availability for saltiness perception. In the 2nd study, the influences of other cations on the sodium–gum interaction were evaluated (Rosett and others 1995). Upon addition of potassium or calcium ions, the R_2 value of sodium in the ionic xanthan gum solution decreased, whereas no changes were found when the gum was a nonionic locust bean gum or guar gum. The authors suggested that potassium and calcium ions could compete with sodium ion for the binding sites of ionic gums and, thus, release more sodium ions, thereby lowering the average R_2 value. The liberation of sodium ion also partly explained the increased saltiness when potassium was added into the sodium/xanthan solution. In the 3rd study, chicken broths were added with thickeners to verify the hypothesis of reduced sodium availability due to electrostatic interaction (Rosett and others 1996). Regardless of viscosity, the saltiness of the broth was lowest when ionic xanthan gum was added, as compared to when the nonionic starches and locust bean gum were added. These studies revealed the correlation between the ionic properties of gums, their effects on the R_2 values of sodium, and the saltiness of the corresponding solutions. Still, other factors potentially influencing the saltiness were not clarified. First, the authors mentioned that viscosity of the xanthan gum solution at higher concentration was not measured due to its elastic feature. This could suggest a gel-like state that largely restrained sodium migration and, therefore, also contributed to the high R_2 and low saltiness of such sample (Schmidt and Ayya 1989). Second, although saltiness increment upon potassium addition was ascribed to the release of sodium from the binding sites of gum, potassium might simply contribute to saltiness by the salty-taste itself.

Mixing of food bolus with saliva

Rheology of food bolus. Among various food ingredients, food thickeners are most frequently studied for their predominant effect on food rheology and the consequent effect on sodium delivery in the oral cavity. The studies on the effects of viscosity or concentration and the effects of flow behavior of thickeners on mixing of sodium with saliva are listed in Table 6 and 7, respectively. Some earlier studies aimed to discover the relationship between thickener concentration and saltiness of thickener solutions, as increase in viscosity with thickener concentration was hypothesized to reduce mixing efficiency of sodium. For instance, Moskowitz and Arabie (1970) prepared a series of sodium carboxymethylcellulose (Na-CMC) solutions with varying concentrations giving apparent viscosity of 0.001 to 1 Pa·s at a shear rate of 0.95 s^{-1}. The saltiness obtained, by the sensory magnitude estimation method, was found to decrease with increasing the viscosity of Na-CMC solution following the power law function. However, a relatively large logarithmic increase in viscosity was required to cause an observable reduction in saltiness, and this was partly ascribed to the restricted range of saltiness scores reported by the panelists.

APPENDIX A-1

Table 5–Effects of sodium–hydrocolloid interaction on the initial availability of sodium in the 2nd stage of saltiness perception (delivery in oral cavity)[a].

System	Treatment	Result	Explanation	Source
Thickener solutions (ionic: XG, KC; nonionic: LBG, GG)	Ionic compared with nonionic thickeners	Higher rate of ^{23}Na-NMR transverse relaxation (R_2) and lower saltiness for ionic thickeners	Electrostatic interaction between ionic thickeners and sodium restricted mobility of sodium, lowering its availability for saltiness perception.	(Rosett and others 1994)
	Sodium concentration ↑ (1 to 2 kg/m^3) or thickener concentration ↑ (1 to 3 kg/m^3)	Viscosity and pH nearly unchanged		
Thickener solutions (ionic: XG, KC; nonionic: LBG, GG)	Molar percentage of added potassium or calcium ↑ (total molality fixed)	R_2 of sodium ↓ for ionic thickener solution	Competitive binding to ionic thickener by potassium compared with sodium released more sodium into salivary phase, increasing its availability for saltiness perception.	(Rosett and others 1995)
	Potassium molality ↑ (sodium molality fixed)	Saltiness ↑ (in all types of thickener solutions)		
	Thickener concentration ↑ (1 to 3 kg/m^3)	Sensory thickness ↑; saltiness not correspondingly changed		
Low sodium chicken broth with thickeners (ionic: XG, Na-CMC; nonionic: LBG, corn starch, potato starch, whole wheat flour)	Different thickeners (concentration adjusted to match thickness)	Saltiness: XG < corn, potato starch, LBG, Na-CMC; R_2 of sodium: XG < Na-CMC	Ionic XG interacted with sodium and lowered its availability for saltiness perception; ionic Na-CMC presented high amount of endogenous sodium which resulted in highest saltiness.	(Rosett and others 1996)
	Added sodium concentration ↑ (0.6 to 1.2 kg/m^3)	R_2 of sodium ↓ for XG solution; thickness unaffected and saltiness not correlated with thickness for all types of thickeners		

[a]LBG: locust bean gum, GG: guar gum; KC: κ-carrageenan, Na-CMC: sodium carboxymethylcellulose, XG: xanthan gum.

Table 6–Effects of thickener viscosity and concentration on the mixing of sodium with saliva in the 2nd stage of saltiness perception (delivery in oral cavity)[a].

Solutions	Treatment	Result	Explanation	Source
Na-CMC	Viscosity ↑ (0.001 to 1 Pa.s; thickener concentration ↑ accordingly)	Saltiness ↓ (intensity $T = kV^n$, k: constant, V: apparent viscosity in cp, n: negative; for almost all sodium concentrations)	Viscosity increment caused a masking effect for saltiness.	(Moskowitz and Arabie 1970)
CSF, TSF, GSF, MC	Viscosity ↑ (0.001 to 1 Pa.s; thickener concentration ↑ accordingly)	Increment of sodium recognition threshold: CSF > TSF > GSF > MC	Effects of thickener viscosity on saltiness reduction depended on thickener types.	(Paulus and Haas 1980)
Ionic: CMC-L, CMC-M, NaA, XG; Nonionic: HPC	Thickener addition	Decrement of taste intensity: citric acid > sucrose, caffeine > sodium; intensity ↑: saccharin	Taste modification by thickener depended more on tastant/thickener combination than on viscosity.	(Pangborn and others 1973)
	Thickener concentration ↑ (viscosity ↑ accordingly)	Similar trend as the thickener addition, but different significant levels; saltiness: increased only by CMC-L		
CMC-L, CMC-M, CMC-H	Viscosity of CMC-H ↑ (1^*10^{-6} to 0.002 m^2/s, thickener concentration ↑ accordingly)	Saltiness ↓ (for 50 mol/m^3 sodium at any viscosity or for 100 mol/m^3 sodium at highest viscosity; no ↓ for higher sodium concentration)	Neither concentration nor viscosity of thickener solely determined saltiness (chain length related to local movement of sodium, mouth coating and more might affect).	(Christensen 1980)
	Different CMC (different molality accordingly; fixed viscosity)	Saltiness: CMC-L > CMC-M, CMC-H (only at higher viscosity (2.2^*10^{-4} to 13^*10^{-4} m^2/s))		
HPMC	Thickener concentration ↑ (0.002 to 0.01 kg/kg)	> coil-overlap concentration (c^*), saltiness ↓	Abrupt increase in viscosity caused insufficient mixing in solutions.	(Cook and others 2002)
Ionic: IC; nonionic: HPMC	Thickener concentration ↑	> c^*, saltiness ↓		(Cook and others 2003)

[a]CSF: carob seed flour, CMC-L, CMC-M, and CMC-H: sodium carboxymethylcellulose with low, medium, and high molecular weight, GSF: guar seed flour, HPC: hydroxypropyl cellulose, HPMC: hydroxylpropyl-methyl-cellulose, IC: ι-carrageenan, MC: methyl cellulose, NaA: sodium-alginate, Na-CMC: sodium carboxymethylcellulose, TSF: tara seed flour, XG: xanthan gum.

In another study of 4 different thickener solutions, with rising apparent viscosity from 0.001 to 1 Pa·s, the saltiness recognition threshold increased with a descending extent of carob seed flour, tara seed flour, guar seed flour, and methyl cellulose. The authors, thus, suggested that effect of thickener viscosity on saltiness reduction depended on thickener types (Paulus and Haas 1980).

Pangborn and others (1973) compared the changes in basic tastes by the addition and increment of several thickeners, distinguished by their ionic properties or flow behaviors. They concluded that the taste-modification depended more on the tastant/thickener combination than on viscosity alone. In the case of NaCl, the saltiness was even increased by the Na-CMC of low viscosity type (shorter chain length). Since concentration of Na-CMC was

APPENDIX A-1

Table 7–Effects of flow behavior of thickeners on the mixing of sodium with saliva in the 2nd stage of saltiness perception (delivery in oral cavity)[a].

Solutions	Treatment	Result	Explanation	Source
LBG and gelatin	LBG concentration ↑ (0.1% to 1.0%[b])	$> c^*$ (0.5%), mixing efficiency with water ↓	The compact coil conformation of gelatin lowered chance of molecular entanglement, resulting in Newtonian behavior upon stirring.	(Koliandris and others 2008)
	Gelatin concentration ↑ (1% to 30%[b])	$> c^*$ (8%), up to 30%, mixing effect remained good		
Nonionic, $> c^*$: GG (shear-thinning), dextran (Newtonian)	MW of GG ↑ (420 to 2660 kg/mol; fixed zero-shear viscosity at 0.03 or 0.09 Pa·s; viscosity at high-shear ↓ accordingly)	Saltiness unchanged	Saltiness was affected by viscosity at zero or low shear (constant viscosity region, explained by the degree of space occupancy), not affected by the viscosity at high shear.	(Koliandris and others 2010)
	MW of GG ↑ (420 to 2660 kg/mol; fixed high-shear (3000 s^{-1}) viscosity at 0.03 Pa·s; zero-shear viscosity ↑ accordingly)	Saltiness ↓		
	Thickener concentration ↑ (viscosity ↑ accordingly)	Saltiness ↓		

[a] c^*: the coil-overlap concentration, LBG: locust bean gum, GG: guar gum.
Mass or volume concentration or mass fraction not specified.

adjusted to increase solution viscosity, it remained uncertain whether concentration or viscosity of the Na-CMC solution was the more dominant factor in changing saltiness. In order to distinguish the 2 effects, Christensen (1980) compared solutions made of 3 types of Na-CMC differing in molecular weight (MW) and intrinsic viscosity. At the same viscosity level, the Na-CMC solution with the lowest MW, and thus the highest molality, was perceived as saltier than the other 2. Hence, the authors concluded that neither viscosity nor concentration was solely responsible for the changes in saltiness. In fact, owing to the physicochemical nature of Na-CMC, other factors such as electrostatic interaction, endogenous sodium (Section 1.1), mouth-coating (Section 2.1), and osmolality (Section 3.2) may interfere with the saltiness perception as well.

Another perspective of viscosity/concentration effects was considered in the studies of Cook and others (2002, 2003). Significant reduction in saltiness occurred when the concentrations of ι-carrageenan or hydroxypropyl-methyl-cellulose exceeded c^*, the coil-overlap concentration. The authors explained that when the thickener concentration reached c^*, an abrupt increase in viscosity led to poor mixing and, thus, a lower transportation rate of sodium toward the receptor. However, Koliandris and others (2008) stated that a concentration beyond c^* may not necessarily reduce saltiness of the thickener solution. In their study, the extent of *in vitro* mixing was revealed by the migration of red ink from the thickener solution to the water being mixed in. At concentrations above c^*, while locust beam gum solution showed evident reduction in mixing, the gelatin solution remained well mixed. The authors explained that the compact coil conformation of gelatin ensured minimum entanglement between molecules, and thus yielded Newtonian behavior upon stirring (Wulansari and others 1998).

The importance of flow behavior in determining the mixing efficiency of the thickener was further explored by Koliandris and others (2010). In their study, shear-thinning solutions were made by 2 types of guar gum differing in MW, and the concentrations were adjusted to match the same viscosity at certain shear rates. There was no difference in saltiness between the 2 guar gum solutions when being matched to the same viscosity at zero shear. The high-MW guar gum solution experienced significantly lower viscosity at higher shear condition than the low-MW guar gum solution. By contrast, when being matched to the same viscosity at high shear, the high-MW guar gum solution had higher viscosity at zero shear and resulted in lower saltiness than the low-MW guar gum solution. The authors concluded that viscosity at zero or low shear was more relevant than at high shear in determining the saltiness of a shear-thinning solution, yet it remains unclear whether changes in viscosity at the low-shear region would alter saltiness. For future studies, the significance of flow behavior in the mixing of thickener solutions and, hence, the sodium delivery in the oral cavity requires more attention.

Interactions between matrix properties and oral processing. Salivary properties, including flow rate and saliva composition, are the major oral parameters that affect sodium delivery in the 2nd stage.

Some of the gustatory or masticatory stimulations mentioned in Section 1.3.3 that enhance salivary secretion may change the composition of saliva as well. For instance, some basic tastants (such as citric acid, NaCl, and sucrose) were found to stimulate the secretion of salivary protein from $2.5^{\star}10^{-9}$ to $1.3^{\star}10^{-8}$ kg/s and alpha-amylase from 0.167 to 1 unit/s, and to increase alpha-amylase activity by 18% (Froehlich and others 1987; Harthoorn and others 2009). Mastication, particularly chewing larger pieces of food products, also elevated the salivary protein and amylase amounts and amylase activity (Mackie and Pangborn 1990). Sucrose intake increased the salivary pH from 6 to 7.2 (as opposed to 6.7 with the control water intake) (Harthoorn and others 2009), and NaCl intake or chewing also caused similar pH increment (Neyraud and others 2003). Furthermore, Froehlich and others (1987) reported that citric acid enhanced the salivary concentration of sodium, but did not change the potassium, calcium, or magnesium concentration.

Since the interaction between matrix properties and oral processing is complex, there are hardly any generalized rules describing how such interaction could alter the sodium delivery in the oral cavity. Hence, only 2 case studies are discussed below to demonstrate the possible influences. Heinzerling and others (2011) investigated the effect of saliva flow rate on taste perception. They used a modified Lashley cup to drain out the natural saliva and deliver artificial saliva to the panelists. The panelists with the controlled artificial saliva flow rates evaluated saltiness, sourness, bitterness, and sweetness of solutions containing NaCl, citric acid, magnesium

APPENDIX A-1

sulfate, and sucrose, respectively. The increased saliva flow rate lowered the saltiness and sourness, but did not change bitterness and sweetness. The authors concluded that higher saliva flow rate would be needed for bitterness and sweetness than for saltiness and sourness to sufficiently dilute the tastants to lower the perceived intensities. However, since the artificially controlled saliva flow rate was 2 times faster than normal, such dilution effects may not occur in typical consumption processes. Besides, factors such as bolus mixing efficiency and swallowing rate may change accordingly with the saliva flow rate, but were not considered. Ferry and others (2006a, 2006b) studied the effects of thickener morphology and amylase on the mixing efficiency and saltiness of NaCl dispersions. At comparable viscosities, the granular dispersions of wheat and modified waxy maize starches mixed with the saliva faster than the dispersions of hydroxypropyl-methyl-cellulose and fully gelatinized waxy maize starch. However, for the dispersions of granular starches, addition of amylase reduced the mixing efficiency, and the panelists with higher amylase activity reported lower saltiness and thickness of the dispersions. The authors proposed that the transformation of granular structure into molecular chains by amylase disfavored the mixing of starch solution with saliva, resulting in lower saltiness.

An overview of the studies in the 2nd stage implies that the future research on sodium delivery in the oral cavity should address the followings. First, the instrumental measurements of the *in vitro* mixing efficiency and delivery of sodium should be correlated with the instrumental measurements of the *in vitro* formation and rheology of the food bolus. Second, instrumental measurements of the in-mouth sodium delivery and bolus rheology should be developed and correlated with the oral processing parameters. The above correlations will help to identify the key rheological features of the food bolus and the food–human interactions that determine sodium delivery in the oral cavity.

Saltiness Generation—3rd Stage

Though not yet fully elucidated, mechanisms of saltiness perception in humans have been proposed in many studies (Simon and others 1993; Smith and Ossebaard 1995) and reviewed (Sugita 2006; McCaughey 2007; Frings 2009; Kubale 2010). It is generally believed that in a human, both specific (epithelial Na^+ channels, ENaC) (Lin and others 1999) and nonspecific (taste variant of the transient receptor potential vanilloid 1, TRPV1t) (Lyall and others 2004) ion channels serve as the receptors for salty stimuli (Kubale 2010). In the 3rd stage, sodium enters the TRC via passive diffusion through the ion channels (Gilbertson and Zhang 1998). The flux of passive diffusion depends on the concentration gradient of sodium across the ion channels and the resistance to sodium migration. At given sodium contents near the receptor sites, the concentration gradient is affected by the partitioning of sodium in the hydrophilic phase due to the presence of emulsions (Section 1.1, Table 8). The resistance to sodium migration into the TRCs is due to mouth-coating on the tongue surface (Section 2.1, Table 8). The membrane depolarization, as a result of sodium influx, initiates a subsequent signal transduction cascade, which eventually produces the saltiness signal (Sugita 2006). The saltiness perception can be further modulated at the cellular level (Section 3, Table 9) or the cognitive level (Section 4.1, Table 10). The saltiness perception in the 3rd stage largely depends on the physiological status and central activity of the human subject. Since the focus of this review is mainly on the factors originating from the food matrix, only selected studies will be discussed below to demonstrate the possible mechanisms that could contribute to saltiness perception at this stage.

Sodium availability for the TRCs

Partitioning of sodium in an emulsion matrix. The emulsifying of foods may facilitate sodium passage via a promoted concentration gradient. When a hydrophobic phase is present in a food mixture, it occupies the volume but does not contain NaCl, since the partition ratio of NaCl in aqueous compared with oil phase is 1 (Koriyama and others 2002). In foods with a higher volume percentage of the hydrophobic phase, sodium concentration in the aqueous phase is higher than in the foods with lower percentage of hydrophobic phase. This results in larger apparent gradient of sodium ions across the aqueous phase of the oral cavity and the TRCs and, thus, facilitates sodium passage (Yamamoto and Nakabayashi 1999; Metcalf and Vickers 2002). This partitioning effect was used to explain the enhanced saltiness with increased fat content in cream cheese (Wendin and others 2000), model cheese (Phan and others 2008; Panouille and others 2011), and salad cream (Shamil and others 1991–1992).

Malone and others (2003) used different formulation designs to study the effects of fat contents on saltiness in iso-viscous oil-in-water (o/w) hydrocolloid emulsions. When the NaCl concentration in the overall emulsion was fixed, saltiness increased with rising fat content (higher NaCl concentration in the aqueous phase).When the NaCl concentration in the aqueous phase was fixed, saltiness decreased with rising fat content (lower NaCl concentration in the overall emulsion). The authors suggested that saltiness may be positively related to both the NaCl concentration in the aqueous phase and the volume of the aqueous phase. Goh and others (2010) made air/water emulsion gels of hydrocolloids with a formulation design similar to that of Malon and others (2003). At constant NaCl concentration in the overall product, saltiness also increased with elevated air volume percentage. While at constant NaCl concentration in the aqueous phase, saltiness was not affected by air volume percentage. The authors explained that in the o/w emulsion, fat might reduce the saltiness by impeding sodium migration or by coating the tongue. While in the air/water emulsion, air cells are destroyed upon chewing and, thus, do not bring the same effect as fat does.

Barylkopikielna and others (1994) compared saltiness between o/w and water-in-oil (w/o) emulsions both with fat of 0.5 m^3/m^3. The o/w emulsion had the aqueous phase directly in contact with the oral cavity and thus, was presumed to give greater saltiness than its w/o counterpart. However, the authors found equal saltiness between the o/w and the w/o emulsions. They ascribed this to the incorporation of saliva during the mastication process of the sensory test, which caused immediate phase reversion of w/o to o/w. Nevertheless, since the o/w emulsion was found to be more viscous, it might have caused slower migration of sodium in the oral cavity (Section 2.1). This could have counteracted the effect of direct contact between the aqueous phase and the oral cavity. Rietberg and others (2012) studied the effect of emulsion stability on saltiness of w/o dispersions. At constant NaCl concentration in the aqueous phase, saltiness correlated positively with the water/fat ratio, but negatively with emulsifier concentration (Rietberg and others 2012). The authors explained that a high water/fat ratio or low emulsifier concentration could increase the probability of droplet–droplet collisions and coalescence. This would facilitate the release of sodium during oral processing. Additionally, the high water/fat ratio also alleviated the mouth-coating by fat and, thus, increased the availability of sodium to TRCs.

APPENDIX A-1

Food matrix effect on saltiness . . .

Table 8–Matrix effects on the availability and migration of sodium to the taste receptor cells (TRCs) in the 3rd stage of saltiness perception (saltiness generation).

Effect	System	Treatment	Result	Explanation	Source
Partitioning of sodium in emulsions	Iso-viscous oil in water (o/w) emulsions of hydrocolloids	Fat content ↑ (0 to 0.6 kg/kg) (sodium content in overall product fixed, but ↑ in aqueous phase (0.05 to 0.125 kg/kg) accordingly)	Saltiness ↑	Saltiness may depend on aqueous phase volume and the sodium concentration in the aqueous phase.	(Malone and others 2003)
		Fat mass fraction ↑ (mass fraction of sodium in aqueous phase fixed, but ↓ in overall product accordingly)	Saltiness ↓		
	o/w or water in oil (w/o) system emulsified with sucrose stearate	o/w compared with w/o emulsions (fat content fixed at 0.5 m^3/m^3)	Saltiness unchanged; viscosity was higher in o/w one	Dilution with saliva caused phase reversion of w/o to o/w and thus led to same saltiness of the 2.	(Barylkopikielna and others 1994)
	Air/water emulsion gels of hydrocolloids	Air content ↑ (0 to 0.4 m^3/m^3) (mass concentration of sodium in overall product fixed, but ↑ in aqueous phase accordingly)	Saltiness ↑	Unlike fat which coated on mouth or solids which impeded sodium migration, air was destroyed upon chewing and thus had no negative effects on saltiness perception.	(Goh and others 2010)
		Air content ↑ (0 to 0.4 m^3/m^3) (mass concentration of sodium in aqueous phase fixed, but ↓ in overall product accordingly)	Saltiness unchanged		
Mouth coating	Gelatin gels tasted (without chewing) after applying oil on tongue	Applying oil compared with water control (sodium fixed at 40 or 150 mol/m^3)	Maximum saltiness and area under the curve (in time-intensity profile): oils < water	Fat coatings physically interfered with sodium access to receptors. Higher viscosity of coconut oil led to larger extent of mouth-coating.	(Lynch and others 1993)
		Applying coconut oil compared with sunflower oil	Saltiness ↓: coconut oil > sunflower oil		

Table 9–Matrix effects on activity of taste receptor cells (TRCs) in the 3rd stage of saltiness perception (saltiness generation).

Effect	System	Treatment	Result	Explanation	Source
Chemical desensitizers and enhancers	Synthesized Maillard-reacted peptides (MRPs) from purified soy protein hydrolysates	MRPs concentration ↑ (sodium concentration fixed, epithelial Na^+ channels blocked by benzamil)	Both saltiness (human) and chorda tympani (CT) responses to sodium (wild-type rats) ↑ and then ↓; no effects on transient receptor potential vanilloid 1 (TRPV1) knockout mice	MRPs exerted biphasic effects on saltiness by interacting with TRPV1.	(Katsumata and others 2008)
Activation of TRCs by common food components	Hyperosmotic solutions of dextrans	Osmolality ↑ (238 to 680 $mOsm\text{-}kg^{-1}$; MW ↓ (500 to 10 kg/mol) and concentration ↑ (103 to 300 kg/m^3) accordingly; viscosity fixed at 30 mPa.s)	Saltiness ↑	Osmolality increment reduced the cell volume, thereby increasing the TRCs activity.	(Koliandris and others 2011)
	Polyunsaturated, monounsaturated, saturated fatty acid (PUFA, MUFA, SFA), triglyceride	Presence of FA compared with control	Currents of delayed rectifying potassium (DRK) channels in taste cells of rats ↓ only by PUFA; MUFA, SFA, triglycerides had no effects	PUFA blocked DRK channels, lowering TRC threshold and potentiating their responses.	(Gilbertson and others 2005)

Sodium flux into the TRCs

Mouth-coating by the matrix. The pathway of sodium ions into TRCs could be physically blocked due to mouth- or tongue-coating by foods. Fat is often assumed as the major ingredient that possesses such barrier property (Lynch and others 1993; Rietberg and others 2012). Lynch and others (1993) studied the effects of applying oil on the tongue on the subsequent saltiness evaluation of gelatin gels. The maximum saltiness intensity and AUC drawn from the time-intensity profile of saltiness were both lowered by the application of oil prior to sensory tests. They have also reported that coconut oil resulted in greater saltiness reduction than sunflower oil. The authors explained that mouth-coating by fat interfered with the accessibility of sodium by TRCs, and that coconut oil exerted larger interference due to higher viscosity. However, Valentova and Pokorny (1998) observed that the prior ingestion of sunflower oil only reduced the bitter, sweet, and astringent intensities, but not the salty or sour intensities. They hypothesized that the sodium ions and protons which are responsible for the saltiness

APPENDIX A-1

Food matrix effect on saltiness . . .

Table 10–Matrix effects on central activities in the 3rd stage of saltiness perception (saltiness generation).

Effect	System	Treatment	Result	Explanation	Source
Cross-modal interaction	Sodium solutions added with sardine or carrot flavors	Presence of flavors compared with control (not flavored) (sodium fixed at 10 or 20 mol/m^3)	Saltiness ↑ only by sardine flavors	Sardine flavor caused odor-induced saltiness enhancement (OISE), while carrot aroma did not due to its nonsalty-related attribute.	(Nasri and others 2011)
Adaptation	Sodium solutions delivered with periodical concentration variation	Amplitude of variation in sodium concentration ↑ (from constant to variation between 5.6 and 9.1 kg/m^3; average delivered sodium fixed at 6.3 kg/m^3)	Area under the curve (AUC) of time-intensity profile of saltiness ↑	Concentration variation reduced adaptation of taste receptor cells (TRCs).	(Busch and others 2009)
		Initial sodium concentration high compared with low (average delivered sodium fixed at 6.3 kg/m^3)	Higher AUC from high initial sodium concentration	High initial sodium concentration bore stronger perceptual and/or scoring effects.	
	Bread with nonhomogeneous sodium distribution	Difference in sodium contents between neighboring layers ↑ (from 0 to 0.0346 kg/kg flour; total sodium in bread fixed)	Saltiness ↑	Sensory contrast of heterogeneously distributed sodium removed taste adaptation or induced trains of phasic receptor responses, with an overall stronger perception.	(Noort and others 2010)

and sourness, respectively, were small enough to penetrate the oil layer. While the molecules responsible for the other 3 tastes were too large to penetrate. In addition to fat, Na-CMC was also believed to cause mouth-coating effects (Christensen 1980). Still, it is worth validating whether the lowered saltiness by mouth-coating was simply due to a physical barrier or possibly due to interaction between mouthfeel and saltiness at a higher perceptual level (Section 4.1).

Activity of the TRCs

Chemical desensitizers and enhancers in the matrix. Certain compounds such as amiloride (Anand and Zuniga 1997), benzamil (Brandsma 2006; Katsumata and others 2008), and miraculin (Capitanio and others 2011) are saltiness desensitizers. On the other hand, some saltiness enhancers now being commercialized or investigated can potentiate the response of TRCs at a given NaCl concentration (Brandsma 2006). These chemical enhancers include amino acid-based molecules such as Maillard-reacted peptides (Brandsma 2006; Katsumata and others 2008), monosodium glutamate (Fuke and Ueda 1996), or pyridinium compounds (Soldo and others 2004) such as alapyridaine (Soldo and others 2003). Except for monosodium glutamate, these chemical enhancers may not exist naturally in a broad category of food products and, thus, are more likely to be incorporated as food additives. In contrast, hydrocolloids and fat, which appear frequently as common food components, are found to possibly activate TRCs as well.

Activation of the TRCs by common food components in the matrix. Koliandris and others (2011) proposed that the hyperosmotic solutions made by hydrocolloids may be used to enhance saltiness perception. For iso-viscous dextran solutions, the one with lower-MW dextran and higher osmolality was perceived as saltier. This was ascribed to the high osmotic pressure which led to cell shrinkage and, therefore, activation of the TRCs (Lyall and others 1999).

In addition to osmolality, the presence of fatty acids may also change the activity of TRCs, and intensify tastes such as sweetness and saltiness. Based on the characterization of fungiform TRCs in rats, Gilbertson and others (2005) revealed that polyunsaturated fatty acids (such as linoleic, linolenic, and arachidonic acid) could block delayed rectifying potassium (DRK) channels, while triglycerides, saturated fatty acids, and monounsaturated fatty acids had no such an effect. The blocking of DRK channels could lower the threshold of TRCs and, in turn, potentiate their responses to other tastants such as sugars and salts (Spector and Glendinning 2009). However, based on sensory studies conducted on human subjects, Mattes (2007) concluded that linoleic acid had a negative correlation with saltiness, and Reckmeyer and others (2010) found no effect of linoleic acid on saltiness ratings. In addition, the lower saltiness perception at an increased fat/protein ratio in a study of chicken sausage was also postulated to be due to the negative modulation of taste receptors by fat (Chabanet and others 2013). This suggested that the human gustatory system may not comply with the mechanism where blocking of the DRK with fatty acids enhances saltiness. In fact, since fat exists predominantly as triglycerides in foods, the effectiveness of such receptor modulation by fat in foods remains undiscovered (Tucker and Mattes 2012).

Process involving central activities of perception

Cross-modal interactions. Cross-modal interactions refer to interactions between at least 2 different sensory modalities (Xiao and others 2011). The odor–taste interaction has recently been utilized in a multisensory approach for a sodium reduction. For example, Nasri and others (2011) showed that the saltiness ratings of a NaCl solution were significantly raised by the addition of sardine flavor. Such odor-induced saltiness enhancement (OISE) was also demonstrated in chicken bouillons flavored with savory aroma compounds (Batenburg and van der Velden 2011), in soup and meat flavored with naturally brewed soy sauce (Kremer and others 2009), and in a model cheese flavored with comté cheese and sardine odors (Lawrence and others 2011). Other types of cross-modal interactions such as taste–taste (Keast and Breslin 2003), texture–taste (Burseg and others 2011; Chabanet and others 2013), and interference from visual, sound, or verbal cues are likely to influence saltiness perception as well (Spence 2011).

Adaptation. Adaptation refers to the decrease in sensations, either of gustatory or other senses as well, with prolonged stimulation (Wark and others 2007). Research has identified taste

APPENDIX A-1

Table 11–Summary of the effects of food matrix on saltiness perception.

Stage	Concentration gradient	Resistance to sodium migration		Food–human interaction or cellular/central activity	
1st	Sodium–polymer interaction reduces the sodium availability and thus the concentration gradient.	Spontaneous diffusion	The tortuosity and sieving effects from the matrix structure impedes sodium diffusion.	The varying properties of foods can modify the oral processing parameters such as mastication force and saliva flow rate differently, and thus lead to different sodium release.	
		Migration during food deformation	The serum compressed out from the matrix carries sodium via convective transport. The matrix fragmentation during mastication generates new surface area for the diffusive and convective transport of sodium.		
2nd	Sodium–polymer interaction reduces the sodium availability.	Mixing of sodium with the saliva	The high concentration or viscosity of the thickeners reduces the mixing efficiency between the food bolus and the salvia. The different flow behaviors of the thickeners may lead to different mixing behaviors.	The varying properties of foods can modify the oral processing parameters and lead to different mixing effects of the bolus with the saliva. Hence, the sodium delivery rate may be altered.	
3rd	The presence of fat leads to concentrating of sodium in the water phase, and thus increases the local concentration gradient of sodium.	Sodium flux into the taste receptor cells (TRCs)	The fatty ingredients may form a barrier on the tongue surface, impeding sodium from entering the TRCs.	Receptor activity	Some taste enhancers, desensitizers, or food components may modify response of the TRCs to the salty stimuli.
				Central activity	The cross-modal interaction between saltiness perception and some sensory modalities may enhance saltiness. The contrasted delivery of sodium removes the taste adaption effect, resulting in higher saltiness perception.

adaptation as a peripheral process, since the chorda tympani activity and sensory rating both are reduced with continuous taste stimulation (Diamant and Zotterman 1969; Zotterman 1971). Still others suggested that the central process which occurs in the brain and spinal cord also participates in taste adaptation, due to habituation or decreased attention (Gillan 1984; Bujas and others 1995). Several studies have been carried out to test the hypothesis of adaption removal and its effects on saltiness perception (Stevens 1969; Meiselma and Halpern 1973; Halpern and Meiselman 1980; Halpern and others 1986; Busch and others 2009; Morris and others 2009).

To propose a novel strategy of sodium reduction, Busch and others (2009) studied the effectiveness of intermittent NaCl delivery on adaptation removal. Sodium chloride solution was delivered to the panelists' oral cavities with a gustometer at controlled flow rate and concentration variation. The AUC was obtained from the time-saltiness intensity recorded by the panelists. Compared to the control (constant NaCl concentration), the delivery with fluctuated NaCl concentration yielded higher AUC, given the same average NaCl concentration. The authors explained that the constant NaCl concentration in the control led to adaptation of the TRCs and, thus, decreased saltiness sensation with time, while the pulsed stimuli of NaCl eliminated such adaptation. Additionally, the delivery sequence, started with high concentration of NaCl, resulted in higher AUC than the one started with low concentration, given the same average concentration of the 2. This was ascribed to perceptual (stronger beginning saltiness induced stronger overall saltiness perception) and/or scoring (higher beginning scores induced higher overall rating) effect managed by the central process. The higher ratings for the sequence of high-low stimuli were also found in the study on the bitterness of the ice-cream bars (Le Berrre and others 2013). This was attributed to a top-down expectation effect that activated the primary cortex, instead of a simply bias-driven manner.

For sodium reduction in foods, it may not be feasible to implement temporal variation in real food products. To apply the concept of contrast delivery, Noort and others (2010) made breads using alternating layers of dough with varying NaCl concentrations. They achieved 28% reduction of sodium with no loss in saltiness scores as compared to the control bread. In addition to adaptation removal, the authors also postulated that the spatially interchanging NaCl concentration also caused an accumulation of serial phasic responses of the receptor that led to a higher overall saltiness. While the o/w and w/o emulsions discussed in Section 1.1 might also be taken as spatially nonhomogeneous systems at a micro-scale, they are unlikely to generate the contrast delivery effect. This is due to the inability of humans to perceptually distinguish size difference of the emulsion droplets, especially when their diameters are below 5 micrometer (Akhtar and others 2005; Dresselhuis and others 2008).

An overview of the studies in the 3rd stage implied that future research needs to address the following. First, model emulsions made of controlled formulations of lipid and hydrocolloid should be used. Measuring the sodium influx to the TRCs, the sodium diffusion in the surface layer on the tongue, and the TRC response to the sodium influx will help understand the effects of the model emulsion on sodium partitioning, mouth-coating, and TRC activation, respectively. Second, more studies on the texture–saltiness interaction should be carried out. This will help exploring the potential of saltiness enhancement via cross-modal interaction, in addition to the more frequently studied OISE. Third, more studies on the adaptation in solid food systems are needed. This will help develop sodium reduction strategies via adaptation removal in commercial food products.

APPENDIX A-1

Conclusions

This review provides a systematic and stepwise discussion of food matrix effect on saltiness perception. Saltiness perception of any food product is a multistep and complex process, where various mechanisms coexist to determine the final saltiness. As summarized in Table 11, 2 common factors affecting saltiness perception in the 3 stages are the concentration gradient of sodium and the resistance to sodium migration. Therefore, any matrix effects on the saltiness perception should be considered as the effects on either or both of the 2 factors. Additionally, the matrix effects on the oral processing, the taste receptor activity and central activity, which could alter the saltiness perception, should also be considered. Studies testing a hypothesis regarding a single matrix effect on saltiness perception should contain designs that consider other factors potentially involved. Eventually, studies with hypotheses based on this review could lead to generalized models describing saltiness using food matrix parameters. Such models can provide implications to enhance saltiness perception and achieve sodium reduction in foods.

Acknowledgments

The authors thank Dr. Soo-Yeun Lee for her valuable comments on this article.

References

Akhtar M, Stenzel J, Murray BS, Dickinson E. 2005. Factors affecting the perception of creaminess of oil-in-water emulsions. Food Hydrocoll 19(3):521–6.

Anand J, Goldman JD, Steinfeldt LC, Montville JB, Heendeniya KY, Omolewa-Tomobi G, Enns CW, Ahuja JK, Martin CL, LaComb RP, Moshfegh AJ. 2012. What we eat in America, NHANES 2009–2010: documentation and data files. Worldwide Web Site: Food Surveys Research Group. Available from: http://www.ars.usda.gov/Services/docs.htm?docid=18349. Accessed 2014 February 25.

Anand K, Zuniga J. 1997. Effect of amiloride on suprathreshold NaCl, LiCl, and KCl salt taste in humans. Physiol Behav 62(4):925–9.

Barylkopikielna N, Martin A, Mela DJ. 1994. Perception of taste and viscosity of oil-in-water and water-in-oil emulsions. J Food Sci 59(6):1318–21.

Batenburg M, van der Velden R. 2011. Saltiness enhancement by savory aroma compounds. J Food Sci 76(5):S280–8.

Le Berrre E, Boucon C, Knoop M, Dijksterhuis G. 2013. Reducing bitter taste through perceptual constancy created by an expectation. Food Qual Prefer 28(1):370–4.

Boisard L, Andriot I, Martin C, Septier C, Boissard V, Salles C, Guichard E. 2014. The salt and lipid composition of model cheeses modifies in-mouth flavour release and perception related to the free sodium ion content. Food Chem 145(0):437–44.

Brandsma I. 2006. Reducing sodium – a European perspective. Food Technol 60(3):24–9.

Brewer MS, Gills LA, Vega JD. 1995. Sensory characteristics of potassium lactate and sodium chloride in a model system. J Sens Stud 10(1):73–87.

Bujas Z, Ajduković D, Szabo S, Mayer D, Vodanović M. 1995. Central processes in gustatory adaptation. Physiol Behav 57(5):875–80.

Burseg KMM, Camacho S, Bult JHF. 2011. Effects of pulsation rate and viscosity on pulsation-induced taste enhancement: new insights into texture-taste interactions. J Agric Food Chem 59(10):5548–53.

Busch JLHC, Tournier C, Knoop JE, Kooyman G, Smit G. 2009. Temporal contrast of salt delivery in mouth increases salt perception. Chem Senses 34(4):341–8.

Busch JLHC, Yong FYS, Goh SM. 2013. Sodium reduction: optimizing product composition and structure towards increasing saltiness perception. Trends Food Sci Technol 29(1):21–34.

Capitanio A, Lucci G, Tommasi L. 2011. Mixing taste illusions: the effect of miraculin on binary and trinary mixtures. J Sens Stud 26(1):54–61.

Chabanet C, Tarrega A, Septier C, Siret F, Salles C. 2013. Fat and salt contents affect the in-mouth temporal sodium release and saltiness perception of chicken sausages. Meat Sci 94(2):253–61.

Christensen C. 1980. Effects of solution viscosity on perceived saltiness and sweetness. Atten Percept Psychophys 28(4):347–53.

Christensen CM, Navazesh M, Brightman VJ. 1984. Effects of pharmacologic reductions in salivary flow on taste thresholds in man. Arch Oral Biol 29(1):17–23.

Clariana M, Guerrero L, Sárraga C, Díaz I, Valero Á, García-Regueiro JA. 2011. Influence of high pressure application on the nutritional, sensory and microbiological characteristics of sliced skin vacuum packed dry-cured ham. Effects along the storage period. Innov Food Sci Emerg Technol 12(4):456–65.

Clariana M, Guerrero L, Sarraga C, Garcia-Regueiro JA. 2012. Effects of high pressure application (400 and 900 MPa) and refrigerated storage time on the oxidative stability of sliced skin vacuum packed dry-cured ham. Meat Sci 90(2):323–9.

Cogswell ME, Zhang Z, Carriquiry AL, Gunn JP, Kuklina EV, Saydah SH, Yang Q, Moshfegh AJ. 2012. Sodium and potassium intakes among US adults: NHANES 2003–2008. Am J Clin Nutr 96(3):647–57.

Colmenero FJ, Ayo MJ, Carballo J. 2005. Physicochemical properties of low sodium frankfurter with added walnut: effect of transglutaminase combined with caseinate, KCl and dietary fibre as salt replacers. Meat Sci 69(4):781–8.

Cook DJ, Hollowood TA, Linforth RST, Taylor AJ. 2002. Perception of taste intensity in solutions of random-coil polysaccharides above and below c∗. Food Qual Prefer 13(7–8):473–80.

Cook DJ, Linforth RST, Taylor AJ. 2003. Effects of hydrocolloid thickeners on the perception of savory flavors. J Agric Food Chem 51(10):3067–72.

Crehan CM, Hughes E, Troy DJ, Buckley DJ. 2000. Effects of fat level and maltodextrin on the functional properties of frankfurters formulated with 5, 12 and 30% fat. Meat Sci 55(4):463–9.

Danaei G, Ding EL, Mozaffarian D, Taylor B, Rehm J, Murray CJL, Ezzati M. 2009. The preventable causes of death in the United States: comparative risk assessment of dietary, lifestyle, and metabolic risk factors. Plos Med 6(4):e1000058.

de Loubens C, Panouillé M, Saint-Eve A, Déléris I, Tréléa IC, Souchon I. 2011a. Mechanistic model of *in vitro* salt release from model dairy gels based on standardized breakdown test simulating mastication. J Food Eng 105(1):161–8.

de Loubens C, Saint-Eve A, Deleris I, Panouille M, Doyennette M, Trelea IC, Souchon I. 2011b. Mechanistic model to understand *in vivo* salt release and perception during the consumption of dairy gels. J Agric Food Chem 59(6):2534–42.

Desmond E. 2006. Reducing salt: a challenge for the meat industry. Meat Sci 74(1):188–96.

DGAC. 2005. Report of the Dietary Guidelines Advisory Committee on the Dietary Guidelines for Americans, 2005, to the Secretary of Agriculture and the Secretary of Health and Human Services. U.S. Dept. of Agriculture, Agricultural Research Service, Washington, DC.

DGAC. 2010. Report of the Dietary Guidelines Advisory Committee on the Dietary Guidelines for Americans, 2010, to the Secretary of Agriculture and the Secretary of Health and Human Services. U.S. Dept. of Agriculture, Agricultural Research Service, Washington, DC.

Diamant H, Zotterman Y. 1969. A comparative study of the neural and psychophysical response to taste stimuli. In: Pfaffman C, editor. Olfaction and taste III. New York: Rockefeller Univ. Press.

Djordjevic J, Zatorre RJ, Jones-Gotman M. 2004. Odor-induced changes in taste perception. Exp Brain Res 159(3):405–8.

Dotsch M, Busch J, Batenburg M, Liem G, Tareilus E, Mueller R, Meijer G. 2009. Strategies to reduce Sodium consumption: a food industry perspective. Crit Rev Food Sci Nutr 49(10):841–51.

Doyle ME, Glass KA. 2010. Sodium reduction and its effect on food safety, food quality, and human health. Compr Rev Food Sci Foods Safety 9(1):44–56.

Drake MA, Miracle RE, McMahon DJ. 2010. Impact of fat reduction on flavor and flavor chemistry of Cheddar cheeses. J Dairy Sci 93(11):5069–81.

Drake SL, Lopetcharat K, Drake MA. 2011. Salty taste in dairy foods: can we reduce the salt? J Dairy Sci 94(2):636–45.

Dresselhuis DM, de Hoog EHA, Cohen Stuart MA, Vingerhoeds MH, van Aken GA. 2008. The occurrence of in-mouth coalescence of emulsion droplets in relation to perception of fat. Food Hydrocoll 22(6):1170–83.

Eoin D. 2006. Reducing salt: a challenge for the meat industry. Meat Sci 74(1):188–96.

Eymery O, Pangborn RM. 1988. Influence of fat, citric-acid and sodium-chloride on texture and taste of a cheese analog. Sci Aliments 8(1):381–92.

APPENDIX A-1

Ferry A, Hort J, Mitchell JR, Cook DJ, Lagarrigue S, Valles Pamies B. 2006a. Viscosity and flavour perception: why is starch different from hydrocolloids? Food Hydrocoll 20(6):855–62.

Ferry AS, Mitchell JR, Hort J, Hill SE, Taylor AJ, Lagarrigue S, Valles-Pamies B. 2006b. In-mouth amylase activity can reduce perception of saltiness in starch-thickened foods. J Agric Food Chem 54(23):8869–73.

Floury J, Rouaud O, Le Poullennec M, Famelart M. 2009. Reducing salt level in food: Part 2. Modelling salt diffusion in model cheese systems with regards to their composition. LWT-Food Sci Technol 42(10):1621–8.

Frings S. 2009. Primary processes in sensory cells: current advances. J Comp Physiol A Neuroethol Sens Neural Behav Physiol 195(1):1–19.

Froehlich DA, Pangborn RM, Whitaker JR. 1987. The effect of oral stimulation on human parotid salivary flow rate and alpha-amylase secretion. Physiol Behav 41(3):209–17.

Fuke S, Ueda Y. 1996. Interactions between umami and other flavor characteristics. Trends Food Sci Technol 7(12):407–11.

Fulladosa E, Serra X, Gou P, Arnau J. 2009. Effects of potassium lactate and high pressure on transglutaminase restructured dry-cured hams with reduced salt content. Meat Sci 82(2):213–8.

Fulladosa E, Sala X, Gou P, Garriga M, Arnau J. 2012. K-lactate and high pressure effects on the safety and quality of restructured hams. Meat Sci 91(1):56–61.

Gaviao MBD, Engelen L, van der Bilt A. 2004. Chewing behavior and salivary secretion. Eur J Oral Sci 112(1):19–24.

Geankoplis CJ. 2003. Principles of unsteady-state and convective mass transfer. In: Geankoplis CJ, editor. Transport processes and separation process principles. 4th ed. Upper Saddle River, N.J.: Prentice Hall. p 459–512.

Geurts TJ. 1974. Transport of salt and water during salting of cheese. I. Analysis of the processes involved. Nederlands Melk- en Zuiveltijdschrift 28(2):102–29.

Gilbertson T, Liu L, Kim I, Burks C, Hansen D. 2005. Fatty acid responses in taste cells from obesity-prone and -resistant rats RID G-7147-2011. Physiol Behav 86(5):681–90.

Gilbertson T, Zhang H. 1998. Characterization of sodium transport in gustatory epithelia from the hamster and rat. Chem Senses 23(3): 283–93.

Gillan DJ. 1984. Evidence for peripheral and central processes in taste adaptation. Percept Psychophys 35(1):1–4.

Goh SM, Leroux B, Groeneschild CAG, Busch JLHC. 2010. On the effect of tastant excluded fillers on sweetness and saltiness of a model food. J Food Sci 75(4):S245–9.

Guinee TP. 2004. Salting and the role of salt in cheese. Int J Dairy Technol 57(2–3):99–109.

Halpern BP, Meiselman HL. 1980. Taste psychophysics based on a simulation of human drinking. Chem Senses 5(4):279–94.

Halpern BP, Kelling ST, Meiselman HL. 1986. An analysis of the role of stimulus removal in taste adaptation by means of simulated drinking. Physiol Behav 36(5):925–8.

Harthoorn LF, Brattinga C, Van Kekem K, Neyraud E, Dransfield E. 2009. Effects of sucrose on salivary flow and composition: differences between real and sham intake. Int J Food Sci Nutr 60(8):637–46.

Heidolph BB, Ray DK, Roller S, Koehler P, Weber J, Slocum S, Noort MWJ. 2011. Looking for my lost shaker of salt . . . replacer: flavor, function, future. Cereal Foods World 56(1):5–19.

Heinzerling CI, Stieger M, Bult JHF, Smit G. 2011. Individually modified saliva delivery changes the perceived intensity of saltiness and sourness. Chemosens Percept 4(4):145–53.

Henney JE, Taylor CL, Boon CS. 2010a. Recommended strategies to reduce sodium intake and to monitor their effectiveness. In: Henney JE, Taylor CL, Boon CS, editors. Strategies to reduce sodium intake in the United States. Washington, DC: The Natl. Academies Press. p 285–96.

Henney JE, Taylor CL, Boon CS. 2010b. Preface. In: Henney JE, Taylor CL, Boon CS, editors. Strategies to reduce sodium intake in the United States. Washington, DC: The Natl. Academies Press. p ix.

Henney JE, Taylor CL, Boon CS. 2010c. Sodium intake reduction: An Important but elusive public health goal. In: Henney JE, Taylor CL, Boon CS, editors. Strategies to reduce sodium intake in the United States. Washington, DC: The Natl. Academies Press. p 29–66.

Hodson NA, Linden RWA. 2004. Is there a parotid-salivary reflex response to fat stimulation in humans? Physiol Behav 82(5):805–13.

Hodson NA, Linden RWA. 2006. The effect of monosodium glutamate on parotid salivary flow in comparison to the response to representatives of the other four basic tastes. Physiol Behav 89(5):711–7.

Hughes E, Cofrades S, Troy DJ. 1997. Effects of fat level, oat fibre and carrageenan on frankfurters formulated with 5, 12 and 30% fat. Meat Sci 45(3):273–81.

IOM. 2005. Sodium and chloride. In: IOM, editor. Dietary reference intakes for water, potassium, sodium, chloride, and sulfate. Washington, DC: Natl. Academies Press. p 269–423.

Jack FR, Piggott JR, Paterson A. 1995. Cheddar cheese texture related to salt release during chewing, measured by conductivity – preliminary-study. J Food Sci 60(2):213–7.

Kähkönen P, Tuorila H. 1998. Effect of reduced-fat information on expected and actual hedonic and sensory ratings of sausage. Appetite 30(1):13–23.

Katsumata T, Nakakuki H, Tokunaga C, Fujii N, Egi M, Phan TT, Mummalaneni S, DeSimone JA, Lyall V. 2008. Effect of Maillard reacted peptides on human salt taste and the amiloride-insensitive salt taste receptor (TRPV1t). Chem Senses 33(7):665–80.

Keast RSJ, Breslin PAS. 2003. An overview of binary taste–taste interactions. Food Qual Prefer 14(2):111–24.

Kerr AC. 1961. The physiological regulation of salivary secretion in man: a study of the response of human salivary glands to reflex stimulation. New York: Pergamon Press. p 24–7; 48–59.

Kilcast D, den Ridder C. 2007. Sensory issues in reducing salt in food products. In: Kilcast D, Angus F, editors. Reducing salt in foods – practical strategies. Cambridge, UK: Woodhead Publishing. p 208–9.

Koliandris A, Lee A, Ferry A, Hill S, Mitchell J. 2008. Relationship between structure of hydrocolloid gels and solutions and flavour release. Food Hydrocoll 22(4):623–30.

Koliandris A, Morris C, Hewson L, Hort J, Taylor AJ, Wolf B. 2010. Correlation between saltiness perception and shear flow behaviour for viscous solutions. Food Hydrocoll 24(8):792–9.

Koliandris A, Michon C, Morris C, Hewson L, Hort J, Taylor AJ, Wolf B. 2011. Enhancement of saltiness perception in hyperosmotic solutions. Chemosens Percept 4(1–2):9–15.

Koriyama T, Wongso S, Watanabe K, Abe H. 2002. Fatty acid compositions of oil species affect the 5 basic taste perceptions. J Food Sci 67(2):868–73.

Kremer S, Mojet J, Shimojo R. 2009. Salt reduction in foods using naturally brewed soy sauce. J Food Sci 74(6):S255–62.

Kubale V. 2010. Taste perception: from anatomical to molecular level. Slovenian Vet Res 47(3):107–27.

Lauverjat C, Deleris I, Trelea IC, Salles C, Souchon I. 2009. Salt and aroma compound release in model cheeses in relation to their mobility. J Agric Food Chem 57(21):9878–87.

Lawrence G, Salles C, Palicki O, Septier C, Busch J, Thomas-Danguin T. 2011. Using cross-modal interactions to counterbalance salt reduction in solid foods. Int Dairy J 21(2):103–10.

Lawrence G, Buchin S, Achilleos C, Berodier F, Septier C, Courcoux P, Salles C. 2012. In vivo sodium release and saltiness perception in solid lipoprotein matrices. 1. effect of composition and texture. J Agric Food Chem 60(21):5287–98.

Lim SS, Vos T, Flaxman AD, Danaei G, Shibuya K, Adair-Rohani H, AlMazroa MA, Amann M, Anderson HR, Andrews KG, Aryee M, Atkinson C, Bacchus LJ, Bahalim AN, Balakrishnan K, Balmes J, Barker-Collo S, Baxter A, Bell ML, Blore JD, Blyth F, Bonner C, Borges G, Bourne R, Boussinesq M, Brauer M, Brooks P, Bruce NG, Brunekreef B, Bryan-Hancock C, Bucello C, Buchbinder R, Bull F, Burnett RT, Byers TE, Calabria B, Carapetis J, Carnahan E, Chafe Z, Charlson F, Chen H, Chen JS, Cheng AT, Child JC, Cohen A, Colson KE, Cowie BC, Darby S, Darling S, Davis A, Degenhardt L, Dentener F, Des Jarlais DC, Devries K, Dherani M, Ding EL, Dorsey ER, Driscoll T, Edmond K, Ali SE, Engell RE, Erwin PJ, Fahimi S, Falder G, Farzadfar F, Ferrari A, Finucane MM, Flaxman S, Fowkes FGR, Freedman G, Freeman MK, Gakidou E, Ghosh S, Giovannucci E, Gmel G, Graham K, Grainger R, Grant B, Gunnell D, Gutierrez HR, Hall W, Hoek HW, Hogan A, Hosgood III HD, Hoy D, Hu H, Hubbell BJ, Hutchings SJ, Ibeanusi SE, Jacklyn GL, Jasrasaria R, Jonas JB, Kan H, Kanis JA, Kassebaum N, Kawakami N, Khang Y, Khatibzadeh S, Khoo J, Kok C, Laden F, Lalloo R, Lan Q, Lathlean T, Leasher JL, Leigh J, Li Y, Lin JK, Lipshultz SE, London S, Lozano R, Lu Y, Mak J, Malekzadeh R, Mallinger L, Marcenes W, March L, Marks R, Martin R, McGale P, McGrath J, Mehta S, Memish ZA, Mensah GA, Merriman TR, Micha R, Michaud C, Mishra V, Hanafiah KM, Mokdad AA, Morawska L, Mozaffarian D, Murphy T, Naghavi M, Neal B, Nelson PK, Nolla JM, Norman R, Olives C, Omer SB, Orchard J, Osborne R,

APPENDIX A-1

Ostro B, Page A, Pandey KD, Parry CD, Passmore E, Patra J, Pearce N, Pelizzari PM, Petzold M, Phillips MR, Pope D, Pope III CA, Powles J, Rao M, Razavi H, Rehfuess EA, Rehm JT, Ritz B, Rivara FP, Roberts T, Robinson C, Rodriguez-Portales JA, Romieu I, Room R, Rosenfeld LC, Roy A, Rushton L, Salomon JA, Sampson U, Sanchez-Riera L, Sanman E, Sapkota A, Seedat S, Shi P, Shield K, Shivakoti R, Singh GM, Sleet DA, Smith E, Smith KR, Stapelberg NJ, Steenland K, Stöckl H, Stovner LJ, Straif K, Straney L, Thurston GD, Tran JH, Van Dingenen R, van Donkelaar A, Veerman JL, Vijayakumar L, Weintraub R, Weissman MM, White RA, Whiteford H, Wiersma ST, Wilkinson JD, Williams HC, Williams W, Wilson N, Woolf AD, Yip P, Zielinski JM, Lopez AD, Murray CJ, Ezzati M. 2012. A comparative risk assessment of burden of disease and injury attributable to 67 risk factors and risk factor clusters in 21 regions, 1990–2010: a systematic analysis for the global burden of disease study 2010. Lancet 380(9859):2224–60.

Lin W, Finger TE, Rossier BC, Kinnamon SC. 1999. Epithelial Na^+ channel subuints in rat taste cells: localization and regulation by aldosterone. J Compar Neurol 405:406–420.

Loubens Cd, Saint-Eve A, Deleris I, Panouille M, Doyennette M, Trelea IC, Souchon I. 2011. Mechanistic model to understand *in vivo* salt release and perception during the consumption of dairy gels. J Agric Food Chem 59(6):2534–42.

Lteif L, Olabi A, Baghdadi OK, Toufeili I. 2009. The characterization of the physicochemical and sensory properties of full-fat, reduced-fat, and low-fat ovine and bovine halloumi. J Dairy Sci 92(9):4135–45.

Lyall V, Heck GL, DeSimone JA, Feldman GM. 1999. Effects of osmolarity on taste receptor cell size and function. Am J Physiol-Cell Ph 277(4):C800–13.

Lyall V, Heck GL, Vinnikova AK, Ghosh S, Phan TH, Alam RI, Russell OF, Malik SA, Bigbee JW, DeSimone JA. 2004. The mammalian amilorideinsensitive non-specific salt taste receptor is a vanilloid receptor-1 variant. J Physiol 558:147–59.

Lynch J, Liu Y, Mela D, Macfie H. 1993. A time intensity study of the effect of oil mouthcoatings on taste perception. Chem Senses 18(2):121–9.

Mackie DA, Pangborn RM. 1990. Mastication and its influence on human salivary flow and alpha-amylase secretion. Physiol Behav 47(3):593–5.

Malone ME, Appelqvist IAM, Norton IT. 2003. Oral behaviour of food hydrocolloids and emulsions. part 2. Taste and aroma release. Food Hydrocoll 17(6):775–84.

Mattes RD. 1997. Physiologic responses to sensory stimulation by food: nutritional implications. J Am Diet Assoc 97(4):406–13.

Mattes RD. 2007. Effects of linoleic acid on sweet, sour, salty, and bitter taste thresholds and intensity ratings of adults. Am J Physiol-Gastr L 292(5):G1243–8.

Mattes RD, Shaw LM, Engelman K. 1994. Effects of cannabinoids (marijuana) on taste intensity and hedonic ratings and salivary flow of adults. Chem Senses 19(2):125–40.

Matulis RJ, Mckeith FK, Sutherland JW, Brewer MS. 1995. Sensory characteristics of frankfurters as affected by fat, salt, and pH. J Food Sci 60(1):42–7.

McCaughey S. 2007. Dietary salt and flavor: mechanisms of taste perception and physiological controls. In: Kilcast D, Angus F, editors. Reducing salt in foods – practical strategies. Cambridge, UK: Woodhead Publishing. p 77–98.

Meiselma Hl, Halpern BP. 1973. Enhancement of taste intensity through pulsatile stimulation. Physiol Behav 11(5):713–6.

Metcalf K, Vickers Z. 2002. Taste intensities of oil-in-water emulsions with varying fat content. J Sens Stud 17(5):379–90.

Mioche L, Bourdiol P, Monier S, Martin J. 2002. The relationship between chewing activity and food bolus properties obtained from different meat textures. Food Qual Prefer 13(7–8):583–8.

Moeller SJ, Miller RK, Aldredge TL, Logan KE, Edwards KK, Zerby HN, Boggess M, Box-Steffensmeier JM, Stahl CA. 2010. Trained sensory perception of pork eating quality as affected by fresh and cooked pork quality attributes and end-point cooked temperature. Meat Sci 85(1):96–103.

Morris C, Koliandris A, Wolf B, Hort J, Taylor AJ. 2009. Effect of pulsed or continuous delivery of salt on sensory perception over short time intervals. Chemosens Percept 2(1):1–8.

Moskowitz HR, Arabie P. 1970. Taste intensity as a function of stimulus concentration and solvent viscosity. J Texture Stud 1(4):502–10.

Nasri N, Beno N, Septier C, Salles C, Thomas-Danguin T. 2011. Cross-modal interactions between taste and smell: odour-induced saltiness enhancement depends on salt level. Food Qual Prefer 22(7):678–82.

Navazesh M, Christensen CM. 1982. A comparison of whole mouth resting and stimulated salivary measurement procedures. J Dent Res 61(10):1158–62.

Neyraud E, Prinz J, Dransfield E. 2003. NaCl and sugar release, salivation and taste during mastication of salted chewing gum. Physiol Behav 79(4–5):731–7.

Noort MWJ, Bult JHF, Stieger M, Hamer RJ. 2010. Saltiness enhancement in bread by inhomogeneous spatial distribution of sodium chloride. J Cereal Sci 52(3):378–86.

Paneras ED, Bloukas JG, Papadima SN. 1996. Effect of meat source and fat level on processing and quality characteristics of frankfurters. LWT-Food Sci Technol 29(5–6):507–14.

Pangborn RM, Trabue IM, Szczesniak AS. 1973. Effect of hydrocolloids on oral viscosity and basic taste intensities. J Texture Stud 4(2):224–41.

Panouille M, Saint-Eve A, de Loubens C, Deleris I, Souchon I. 2011. Understanding of the influence of composition, structure and texture on salty perception in model dairy products. Food Hydrocoll 25(4): 716–23.

Paulus K, Haas EM. 1980. The influence of solvent viscosity on the threshold values of primary tastes. Chem Senses 5(1):23–32.

Phan VA, Yven C, Lawrence G, Chabanet C, Reparet JM, Salles C. 2008. *In vivo* sodium release related to salty perception during eating model cheeses of different textures. Int Dairy J 18(9):956–63.

Phelps T, Angus F, Clegg S, Kilcast D, Narain C, den Ridder C. 2006. Sensory issues in salt reduction. Food Qual Prefer 17(7–8):633–4.

Pionnier E, Chabanet C, Mioche L, Taylor AJ, Le Quere JL, Salles C. 2004. *In vivo* nonvolatile release during eating of a model cheese: relationships with oral parameters. J Agric Food Chem 52(3):565–71.

Prinz JF, Lucas PW. 1995. Swallow thresholds in human mastication. Arch Oral Biol 40(5):401–3.

Reckmeyer NM, Vickers ZM, Csallany AS. 2010. Effect of free fatty acids on sweet, salty, sour and umami tastes. J Sens Stud 25(5):751–60.

Le Reverend BJD, Norton IT, Bakalis S. 2013. Modelling the human response to saltiness. Food Function 4(6):880–8.

Rietberg MR, Rousseau D, Duizer L. 2012. Sensory evaluation of sodium chloride-containing water-in-oil emulsions. J Agric Food Chem 60(16):4005–11.

Romeih EA, Michaelidou A, Biliaderis CG, Zerfiridis GK. 2002. Low-fat white-brined cheese made from bovine milk and two commercial fat mimetics: chemical, physical and sensory attributes. Int Dairy J 12(6):525–40.

Rosett TR, Shirley L, Schmidt SJ, Klein BP. 1994. Na^+ binding as measured by ^{23}Na nuclear magnetic resonance spectroscopy influences the perception of saltiness in gum solutions. J Food Sci 59(1):206–10.

Rosett TR, Wu Z, Schmidt SJ, Ennis DM, Klein BP. 1995. KCl, $CaCl_2$, Na^+ binding, and salt taste of gum systems. J Food Sci 60(4): 849–53.

Rosett TR, Kendregan SL, Gao Y, Schmidt SJ, Klein BP. 1996. Thickening agents effects on sodium binding and other taste qualities of soup systems. J Food Sci 61(5):1099–104.

Ruusunen M, Puolanne E. 2005. Reducing sodium intake from meat products. Meat Sci 70(3):531–41.

Ruusunen M, Simolin M, Puolanne E. 2001. The effect of fat content and flavor enhancers on the perceived saltiness of cooked 'Bologna-type' sausages. J Muscle Foods 12(2):107–20.

Ruusunen M, Vainionpää J, Lyly M, Lähteenmäki L, Niemistö M, Ahvenainen R, Puolanne E. 2005. Reducing the sodium content in meat products: The effect of the formulation in low-sodium ground meat patties. Meat Sci 69(1):53–60.

Saccani G, Parolari G, Tanzi E, Rabbuti S. 2004. Sensory and microbiological properties of dried hams treated with high hydrostatic pressure. Report of the 50th International Congress of Meat Science and Technology; Helsinki, Finland, 8–13 August 2004. p 726–9.

Saint-Eve A, Lauverjat C, Magnan C, Déléris I, Souchon I. 2009. Reducing salt and fat content: impact of composition, texture and cognitive interactions on the perception of flavoured model cheeses. Food Chem 116(1):167–75.

Salles C, Chagnon M, Feron G, Guichard E, Laboure H, Morzel M, Semon E, Tarrega A, Yven C. 2011. In-mouth mechanisms leading to flavor release and perception. Crit Rev Food Sci Nutr 51(1):67–90.

Schmidt SJ, Ayya N. 1989. Characterization of sodium binding in polysaccharides using sodium-^{23}NMR. In: Millane RP, BeMiller JN,

APPENDIX A-1

Chandrasekaran R, editors. Frontiers in carbohydrate research— I: Food applications. Essex, England: Elsevier Science Publishers. p 200–14.

Serra X, Grèbol N, Guàrdia MD, Guerrero L, Gou P, Masoliver P, Gassiot M, Sárraga C, Monfort JM, Arnau J. 2007. High pressure applied to frozen ham at different process stages. 2. Effect on the sensory attributes and on the colour characteristics of dry-cured ham. Meat Sci 75(1):21–8.

Shamil S, Wyeth LJ, Kilcast D. 1991–1992. Flavour release and perception in reduced-fat foods. Food Qual Prefer 3(1):51–60.

Simon SA, Holland VF, Benos DJ, Zamphighi GA. 1993. Transcellular and paracellular pathways in lingual epithelia and their influence in taste transduction. Microsc Res Tech 26:196–208.

Sinopoli DA, Lawless HT. 2012. Taste properties of potassium chloride alone and in mixtures with sodium chloride using a check-all-that-apply method. J Food Sci 77(9):S319–22.

Smith DV, Ossebaard CA. 1995. Amiloride suppression of the taste intensity of sodium chloride:evidence from direct magnitude scaling. Physiol Behav 57:773–7.

Soldo T, Blank I, Hofmann T. 2003. (+)-(S)-Alapyridaine—a general taste enhancer? Chem Senses 28(5):371–9.

Soldo T, Frank O, Ottinger H, Hofmann T. 2004. Systematic studies of structure and physiological activity of alapyridaine. A novel food-born taste enhancer. Mol Nutr Food Res 48(4):270–81.

Spector AC, Glendinning JI. 2009. Linking peripheral taste processes to behavior. Curr Opin Neurobiol 19(4):370–7.

Spence C. 2011. Mouth-watering: the influence of environmental and cognitive factors on salivation and gustatory/flavor perception. J Texture Stud 42(2):157–71.

Stampanoni C, Noble A. 1991. The influence of fat, acid, and salt on the temporal perception of firmness, saltiness, and sourness of cheese analogs. J Texture Stud 22(4):381–92.

Stevens SS. 1969. Sensory scales of taste intensity. Percept Psychophys 6(5):302–8.

Stieger M. 2011. Texture-taste interactions: enhancement of taste intensity by structural modifications of the food matrix. Procedia Food Sci 1(0):521–7.

Stieger M, van de Velde F. 2013. Microstructure, texture and oral processing: new ways to reduce sugar and salt in foods. Curr Opin Colloid In 18(4):334–48.

Sugita M. 2006. Taste perception and coding in the periphery. Cell Mol Life Sci 63(17):2000–15.

Tarrega A, Yven C, Sémon E, Salles C. 2011. In-mouth aroma compound release during cheese consumption: relationship with food bolus formation. Int Dairy J 21(5):358–64.

Tucker RM, Mattes RD. 2012. Are free fatty acids effective taste stimuli in humans? J Food Sci 77(3):S148–51.

Valentova H, Pokorny J. 1998. Effect of edible oils and oil emulsions on the perception of basic tastes. Nahrung-Food 42(6):406–8.

van den Berg L, van Vliet T, van der Linden E, van Boekel MAJS, van de Velde F. 2007. Serum release: the hidden quality in fracturing composites. Food Hydrocoll 21(3):420–32.

Ventanas S, Puolanne E, Tuorila H. 2010. Temporal changes of flavour and texture in cooked Bologna type sausages as affected by fat and salt content. Meat Sci 85(3):410–9.

Wark B, Lundstrom BN, Fairhall A. 2007. Sensory adaptation. Curr Opin Neurobiol 17(4):423–9.

Wendin K, Langton M, Caous L, Hall G. 2000. Dynamic analyses of sensory and microstructural properties of cream cheese. Food Chem 71(3): 363–78.

de Wijk RA, Prinz JF. 2005. The role of friction in perceived oral texture. Food Qual Prefer 16(2):121–9.

Wirth F. 1988. [Reduction of the NaCl content and the action of salt substitutes in meat products]. Mitteilungsblatt der Bundesanstalt fuer Fleischforschung, Kulmbach (Nr. 100):7940–5.

Wulansari R, Mitchell JR, Blanshard JMV, Paterson JL. 1998. Why are gelatin solutions Newtonian? Food Hydrocoll 12(2): 245–9.

Xiao X, Dupuis-Roy N, Luo JL, Zhang Y, Chen AT, Zhang QL. 2011. The event-related potential elicited by taste-visual cross-modal interference. Neuroscience 199(0):187–92.

Yamaguchi S, Takahashi C. 1984. Interactions of monosodium glutamate and sodium chloride on saltiness and palatability of a clear soup. J Food Sci 49(1):82–5.

Yamamoto Y, Nakabayashi M. 1999. Enhancing effect of an oil phase on the sensory intensity of salt taste of NaCl in oil/water emulsions. J Texture Stud 30(5):581–90.

Zotterman Y. 1971. The recording of the electrical response from human taste nerves. In: Beidler, L editor. Handbook of sensory physiology. Berlin: Springer-Verlag. p 102–15.

APPENDIX A-2 The permission and the publication reprint for the contents of CHAPTER 3

JOHN WILEY AND SONS LICENSE TERMS AND CONDITIONS

Mar 19, 2016

This Agreement between Wan ("You") and John Wiley and Sons ("John Wiley and Sons") consists of your license details and the terms and conditions provided by John Wiley and Sons and Copyright Clearance Center.

License Number	3832831193023
License date	Mar 19, 2016
Licensed Content Publisher	John Wiley and Sons
Licensed Content Publication	Journal of Food Science
Licensed Content Title	Temporal Sodium Release Related to Gel Microstructural Properties —Implications for Sodium Reduction
Licensed Content Author	Wan-Yuan Kuo,Youngsoo Lee
Licensed Content Date	Oct 8, 2014
Pages	1
Type of use	Dissertation/Thesis
Requestor type	Author of this Wiley article
Format	Print and electronic
Portion	Full article
Will you be translating?	No
Title of your thesis / dissertation	RELATING STRUCTURAL PROPERTIES TO SALTINESS PERCEPTION OF MODEL LIPOPROTEIC GELS
Expected completion date	Apr 2016
Expected size (number of pages)	250
Requestor Location	Wan-Yuan Kuo 1304 W Pennsylvania Ave Rm 382 K URBANA, IL 61801 United States Attn: Wan-Yuan Kuo
Billing Type	Invoice
Billing Address	Wan-Yuan Kuo 1304 W Pennsylvania Ave Rm 382 K URBANA, IL 61801 United States Attn: Wan-Yuan Kuo
Total	0.00 USD
Terms and Conditions	

Temporal Sodium Release Related to Gel Microstructural Properties—Implications for Sodium Reduction

Wan-Yuan Kuo and Youngsoo Lee

Abstract: The microstructure of food can be engineered to enhance sodium release during mastication, which may be used as a strategy to reduce sodium content in foods. This study aimed to relate sodium release to microstructural properties of solid lipoproteic colloid (SLC) foods. The SLC gels with 1.5% (w/w) NaCl were prepared by homogenization of whey protein isolate and anhydrous milk fat, followed by heat-induced gelation. The gels varied in protein content (8% or 16%), fat content (0%, 11%, 22%, or 33%), and homogenization pressures (14 or 55 MPa). The maximum rate of sodium release during the initial gel compression increased with increasing gel porosity and pore size. This was due to more releasable serum in the gels with larger pore volume and larger pores. The maximum concentration of sodium at the end of sodium release increased with reduced size of the fat particles in the gels. The smaller fat particles were dispersed more uniformly and interrupted the protein network more, and facilitated the gel breakdown. The above findings suggested that, during the breakdown of the SLC gels, the major mechanisms of sodium release are via serum release followed by sodium diffusion, which are governed by the gel porosity and the particle size of fat, respectively. This study demonstrated the dependence of temporal sodium release properties on the microstructural properties of an SLC food system. The findings from this study could lay the foundation for further investigation of the dependence of saltiness perception on SLC microstructure, which can provide insight for sodium reduction in SLC products.

Keywords: particle size, porosity, serum release, sodium reduction, sodium release

Practical Application: The dependency of sodium release on the food microstructures discussed in this study can be useful for optimizing the formulation and the manufacturing process toward an optimum food microstructure to enhance sodium release during mastication. Consequently, with enhanced sodium release, a lower amount of sodium will be needed in the product, and thus consumers will be able to reduce sodium intake.

Introduction

Sodium overconsumption is an alarming health problem around the world. The global mean sodium intake in 2010 was 3950 mg/d, nearly doubling the limit of 2000 mg/d recommended by the World Health Organization (WHO; Powles and others 2013). Diet high in sodium is the 2nd highest dietary risk factor attributable to the global burden of disease in 2010 (Lim and others 2012). Evidences from multiple randomized trials have indicated the positive relationship between sodium intake and blood pressure (Aaron and Sanders 2013). Overconsumption of sodium has been associated with the development or severity of several chronic diseases such as cardiovascular diseases (Cook and others 2014), bone diseases, kidney stones, gastric cancer, and asthma (Doyle and Glass 2010). Though there have been mixed findings on the association between health and sodium reduction at further lower level (2300 to 1500 mg/d), the health benefits of lowering excessive sodium intake to 2300 mg/d are widely agreed and advised by the most recent report of the Inst. of Medicine (Committee on the Consequences of Sodium Reduction in Populations 2013). Based on the U.S. Natl. Health and Nutrition Examination Survey (NHANES) 2003 to 2008, 91% of U.S. adults consume more than 2300 mg of sodium per day, (Cogswell and others 2012). Overconsumption of sodium is believed to be a major cause of the 65% incidence rate of hypertension or prehypertension of the U.S. adults, leading to 100000 annual deaths and $73.4 billion medical costs in 2009 (Danaei and others 2009; Henney and others 2010a). An estimate of $7 billion annual savings in health care can be achieved by reducing the average dietary sodium intake by 400 mg/d (DGAC 2005, 2010). Nevertheless, given the initiation of sodium reduction act early in the 1960s, from 1988 to 2010, the mean dietary sodium intake by the U.S. males and females stayed stable around 4000 and 3000 mg/d, respectively (Henney and others 2010a, 2010b; Anand and others 2012; Cogswell and others 2012).

More than 70% of dietary sodium comes from processed foods (Mattes and Donnelly 1991; Anderson and others 2010). Among the processed foods, solid lipoproteic colloid (SLC) foods such as cheese and sausage, which bear fat/protein emulsion structure, are significant sources of sodium (DGAC 2010). A recent study on SLC model foods revealed that, depending on the chewing behavior of individuals, 70% to 95% sodium is not released before swallowing (Phan and others 2008). Thus, engineering the matrix microstructure to enhance sodium release is a promising solution for sodium reduction in processed SLC foods (Stieger and van de

MS 20140741 Submitted 5/1/2014, Accepted 8/21/2014. *Authors are with Dept. of Food Science and Human Nutrition, Univ. of Illinois at Urbana-Champaign 382K, Agricultural Engineering and Sciences Building, 1304 W. Pennsylvania Ave., Urbana, IL 61801, U.S.A. Direct inquiries to author Lee (E-mail: leeys@illinois.edu).*

doi: 10.1111/1750-3841.12669

Journal of Food Science A Publication of the Institute of Food Technologists

APPENDIX A-2 (Cont.)

Velde 2013). The reduction of sodium content in SLC foods may cause safety issues or alter the product quality such as flavor and texture attributes. Nevertheless, with combined techniques, the microbiological and sensory properties of reduced-sodium foods can be ensured to meet the standards (Grummer and others 2013; Juneja and others 2013).

Previous studies showed that sodium release is affected by several microstructural properties of the food matrix (Stieger and van de Velde 2013). The porosity, which is defined as the volume fraction of voids occupied with fluids in the gel, is positively correlated with serum release during the gel compression (van den Berg and others 2007a). Besides, the gels with bicontinuous network structure yielded higher serum release than the gels with homogeneous structure (van den Berg and others 2008). Increase in serum release of food products can boost the release and perception intensity of tastants such as sucrose (Sala and others 2010) or sodium chloride (Stieger 2011; van de Velde and Adamse 2013). Nevertheless, the above studies were based on protein/polysaccharide mixture systems without the incorporation of emulsion structures, and thus the implications may not be extended to the SLC foods.

In another series of studies, the effects of emulsion structures on sodium release of SLC model gels were assessed. Increase in fat content or decrease in particle size of fat was found to cause greater extent of gel breakdown and thus more sodium release (de Loubens and others 2011a, 2011b; Panouille and others 2011; Boisard and others 2013, 2014). However, little is known regarding the dependence of sodium release on serum release in SLC gels with varying emulsion structures. Lawrence and others (2012a) reported a positive correlation between the in-mouth sodium release and the water content of the SLC gels. Phan and others (2008) observed that the factors dominating the in-mouth sodium release of model SLC gels changed with chewing time. In the initial 20 s of chewing, the samples with higher water content had higher sodium release, whereas after 60 s of chewing, the samples with higher fat content had higher sodium release. This could infer that the sodium release depends more on serum release in the initial stage of chewing, but depends more on gel fragmentation with prolonged chewing. However, the suggested hypothesis above was not confirmed by the instrumental analyses of serum release and sodium release. To construct a more comprehensive picture of temporal sodium release as a function of the SLC gel microstructures, studies with standardized measurements of sodium release and sufficient characterization of gel microstructures and textures are needed.

To the best of our knowledge, there has not yet been any study that examined the relationship between sodium release and multiple microstructural properties in the same SLC system. The objective of this study is to relate temporal sodium release to critical microstructural properties, including porosity, pore size, and particle size of fat of the SLC gels. Effects of these microstructural properties on the temporal sodium release properties, including the maximum rate of sodium release, the maximum concentration of released sodium, and the area under the sodium concentration–time curve, are discussed. To help explain the microstructural influences on sodium release, the serum release and textural properties related to the microstructures and sodium release of the SLC gels were also analyzed.

Materials and Methods

Preparation of the SLC gels

Table 1 lists the formulas and homogenization pressures of the SLC gels. Whey protein isolate (WPI, Hilmar 9000, Hilmar Ingredients, Hilmar, Calif., U.S.A.) and anhydrous milk fat (AMF, Berkshire Dairy & Food Products, LLC, Wyomissing, Pa., U.S.A.) were used to prepare the 6 SLC gels. The SLC gels in this study contained 1.5% (w/w) NaCl and 2 levels of protein (8% and 16%, w/w). For the gels with 8% protein, the fat levels varied from 0%, 22% to 33% (w/w) to evaluate the effects of direct increment of fat contents on the gel microstructures and sodium release. For the gels with 16% protein, the fat level was 11% so as the solid content to be similar to the gels of 8% protein and 22% fat. In addition, for the gels with the highest fat content (33%) and the gels with highest protein content (16%), 2 different homogenization pressures (14 and 55 MPa) were used to observe the effects of pressure on the structures in the gels. The SLC gel codes represent their formulas and homogenization pressures as follows: protein (%)–fat (%)–NaCl (%)–pressure (MPa). When making the SLC gels, WPI was 1st suspended in the NaCl solution by stirring for 10 min at room temperature. Then, the WPI suspension was incubated at 45 °C for 20 min, followed by storage at 6 to 8 °C for 16 h to ensure complete hydration of the WPI powder. Before the prehomogenization, the WPI suspension was incubated at 45 °C for 20 min. The WPI suspension was prehomogenized with the 45 °C prewarmed AMF at 11600 rpm for 3 min using an IKA T-25 Digital High-Speed Homogenizer (IKA Works Inc., Wilmington, N.C., U.S.A.). The prehomogenized emulsion was then incubated at 45 °C for 40 min. Afterward, the prehomogenized emulsion was pressure homogenized for 3 min using the APV 2 stage homogenizer (SPX Flow Technology, Soeborg, Denmark) with 1st stage at 14 or 55 MPa and 2nd stage at 3.4 MPa. The pressure-homogenized emulsion was then subjected to 170 mm Hg vacuum at room temperature for 20 min to eliminate air bubbles. To make the SLC gel, the emulsion was filled into a Teflon tube (150-mm length, 25.4-mm inner dia.) with both ends sealed with rubber stoppers. The Teflon tube was then heated in 90 °C water bath for 30 min, followed by 16 h storage at 6 to 8 °C. Three to five batches were made for each SLC gel sample.

Table 1–Formula, homogenization pressure of the SLC gels and their compositional properties.

Sample name	Content (% w/w) Protein	Fat	NaCl	Homogenization pressure (MPa)	Dry matter (% w/w)
8–0–1.5–55	8	0	1.5	55	11
8–22–1.5–55	8	22	1.5	55	32
8–33–1.5–55	8	33	1.5	55	45
8–33–1.5–14	8	33	1.5	14	45
16–11–1.5–55	16	11	1.5	55	30
16–11–1.5–14	16	11	1.5	14	30

Characterization of structural properties

Particle size. For the dynamic light scattering (DLS) measurement, the freshly prepared emulsion after vacuum treatment was examined at 25 °C by ZetaPALS ξ potential analyzer (Brookhaven Instruments Co., Holtsville, N.Y., U.S.A.). Intensity-weighted particle size distribution was collected from the average of 3 readings, and the D_{90} values were obtained for each distribution of particle sizes in the intensity profiles. Three to five measurements on the DLS were completed for each sample.

ESEM images

Environmental scanning electron microscopy (ESEM) with a field emission electron gun (FEI Co., Hillsboro, Oreg., U.S.A.) was used to characterize the microstructures of the SLC gels. A 3 × 3 × 7 mm^3 sample stick cut from the cylindrical gel was frozen

APPENDIX A-2 (Cont.)

fractured in liquid N_2, mounted on the stage, immediately put into ESEM to allow ice sublimation at 1 Torr wet mode, and then, observed with accelerating voltage of 20 kV. The gel micrographs were processed using Matlab (Version 7.0.4.356 R14, The Mathworks Inc., Natick, Mass., U.S.A.). A series of functions available in the Matlab Image Processing Toolbox (MathWorks 2014) was used to process the grayscale images of the gel micrographs. First, the "tophat" and the "wiener2" filters were applied to even the background and to smooth the pore morphology, respectively. An improved grayscale thresholding method including the application of 2 thresholds was developed to accurately analyze the porosity and pore size of the samples. The 1st threshold was applied to separate the pore from the matrix. The grayscale intensity of the threshold at which the maximum number of pore could be identified was used (Salvador and others 2009). The 2nd threshold was then applied to remove the foreground regions that protruded from the major plane of the matrix. These foreground regions were believed to be the artifacts made during the freeze-fracture step prior to the ESEM observation. The grayscale intensity of 2nd threshold was determined by multiplying 1.25 to the grayscale intensity of the 1st threshold. At this ratio, the grayscale intensity of the 2nd threshold was approximately the same as that determined by the triangle method (Zack and others 1977) used in previous literature. The binary image obtained after the thresholding was then further processed with the "imclose" filter to dilate narrow breaks and to erode small objects. Then the watershed segmentation was used to separate the connected objects. The porosity was calculated as the percent area with black pixel (pores) versus the total area analyzed. The pore size was expressed as equivalent diameter of a circle. The ESEM characterization and image analysis for each batch preparation of the sample were made triplicates.

Measurement of *in vitro* sodium release

The *in vitro* sodium release was assessed by combining a compression test using a texture analyzer (TA-XT2i, Texture Technologies Corp., Scarsdale, N.Y., U.S.A.) with a conductivity measurement (de Loubens and others 2011a) at room temperature (23 °C). As shown in Figure 1A, a cylindrical SLC gel (25.4-mm dia., 25.4-mm length) was placed in a 500 mL jar, under a TA-25 cylinder probe (50-mm dia., aluminum) of the texture analyzer. Also sitting in the jar was a mechanical stirrer and a conductivity probe (Orion DuraProbe 4-Electrode Conductivity Cells 013005MD) connected with an Orion VERSA STAR Multiparameter Benchtop Meter (Thermo Fisher Scientific Inc. Waltham, Mass, U.S.A.). The measurement was initiated by addition of 400 mL DI water into the jar at time 0 s, and followed by the gel compression at time 25 s. The sample was compressed at the crosshead speed of 1.0 mm/s till 80% of strain. The conductivity was read every 5 s for a total of 365 s, during which the water was stirred at 200 rpm to ensure constant concentration of sodium within the jar. Three parameters were extracted from the concentration–time profiles of the *in vitro* sodium release measurement (Figure 1B). The maximum rate of sodium release, R_{max}, is the greatest slope calculated from any 3 continuous data points alone the concentration–time curve. The maximum concentration of sodium release, I_{max}, is the sodium concentration at the end of the measurement. The area under the curve of sodium release, AUC, is the integrated area under the concentration–time curve.

Serum release and texture analysis

The SLC gels cut into 25.4-mm-long cylinders were hermetically stored at room temperature for 3 h before the texture analysis by the TA-XT2i Texture Analyzer (Texture Technologies Corp.). A combined compression test and serum release measurement was performed with a TA-25 cylinder probe (50-mm dia., aluminum) at room temperature (23 °C). A thin layer of mineral oil (Sigma 330779, Sigma-Aldrich, St. Louis, Mo., U.S.A.) was spread on top of the gel. The gel sample was then placed on the Whatman 42 filter paper (Maidstone, Kent, U.K.) right before the test. The force was measured during compression with the crosshead speed of 1.0 mm/s with the maximum strain of 80%. These compression conditions have been identified to well reflect the sensory texture properties (Xiong and others 2002). To quantify the serum release, the filter paper was removed and weighed right after the compression test.

Table 2–Structural properties of the SLC gels.

Sample	Particle size ± SD (nm)		Porosity ± SD (%)	Pore size ± SD (μm)
	Protein aggregates	Fat globules		
8–0–1.5–55	5.1 ± 0.4^{d} 59.6 ± 15.2^{cd} 240.5 ± 2.4^{a}	–	83.1 ± 1.5^{a}	1.953 ± 0.263^{a}
8–22–1.5–55	84.9 ± 25.7^{c}	289.9 ± 31.2^{b}	67.7 ± 2.2^{b}	0.978 ± 0.194^{b}
8–33–1.5–55	60.5 ± 10.4^{cd}	247.8 ± 18.2^{b}	61.7 ± 1.5^{bc}	0.955 ± 0.082^{b}
8–33–1.5–14	195.4 ± 29.6^{ab}	640.3 ± 69.3^{a}	65.6 ± 1.4^{b}	1.022 ± 0.114^{b}
16–11–1.5–55	94.4 ± 13.3^{c}	254.7 ± 3.7^{b}	57.1 ± 5.7^{c}	0.428 ± 0.060^{c}
16–11–1.5–14	167.6 ± 16.9^{b}	568.7 ± 22.3^{a}	67.2 ± 2.0^{b}	1.150 ± 0.111^{b}

Means within the columns with same letters are not significantly different ($P < 0.05$).

Statistical analysis

The means across the measurement replications for each sample batch were taken, and the results were analyzed using the SAS Software (SAS 9.3, SAS Inst., Inc., Cary, N.C., U.S.A.). The proc glm and the LSMEANS with the adjusted Tukey test were used to analyze the difference between the means of the samples.

Results and Discussion

Microstructural difference between the SLC gels

Figure 2 shows the ESEM images of the frozen fractured SLC gels. Differences in porosity and pore size can be observed between the SLC gels with varying formula and homogenization pressures. These visual differences shown in Figure 2 can be further confirmed by the image analysis results presented in Table 2. The particle sizes of protein aggregates and fat in different SLC emulsions are included in Table 2. For the protein particles, the nonfat sample 8–0–1.5–55 had 3 distributions, whereas the other samples had only 1. The distribution of the smallest protein found in the sample 8–0–1.5–55 was not detected in the fat-containing samples, probably due to its relatively low scattering intensity compared to the fat particles (data not shown). The distribution of the largest protein in the sample 8–0–1.5–55 was not found in the fat-containing samples. It may be due to the presence of fat which used a portion of the protein as the emulsifier, and also interfered with the protein aggregation.

The microstructure of the nonfat sample (8–0–1.5–55, Figure 2A) was especially different from the other 5 samples (Figure 2B–F). The nonfat sample 8–0–1.5–55 was comprised of coarsely aggregated protein particles and had large pores, whereas the other samples were formed by tightly linked, continuous network with relatively lower porosities and pore sizes (Table 2). For

APPENDIX A-2 (Cont.)

the SLC gels with the same protein content (samples 8–0–1.5–55, 8–22–1.5—55, and 8–33–1.5–55; Figure 2A–C), both the porosity and pore size decreased with increasing fat content (Table 2). This was due to the lower moisture contents with increasing amounts of fat. For the SLC gels with similar dry matter contents (samples 8–22–1.5–55 and 16–11–1.5–55; Figure 2B and E), the gel with higher protein but lower fat content (sample 16–11–1.5–55) had lower porosity and smaller pore size (Table 2). This is believed to be caused by the greater structure forming capacity of protein than fat. Both protein and fat occupy the space in the gels and hence reduce the void volume. However, protein can be hydrated and thus entrap water molecules as part of its structure (Geurts 1974). Also, protein can form 3-dimensional network which may embed small voids within its network. Therefore, at similar dry matter contents, the sample with higher fraction of protein showed lower porosity and pore size. When comparing the SLC gels with the same formulation but different homogenization pressures (16–11–1.5–14 vs. 16–11–1.5–55 and 8–33–1.5–14 vs. 8–33–1.5–55), the samples prepared using higher pressure showed lower sizes of the fat globules (Table 2). This was due to more

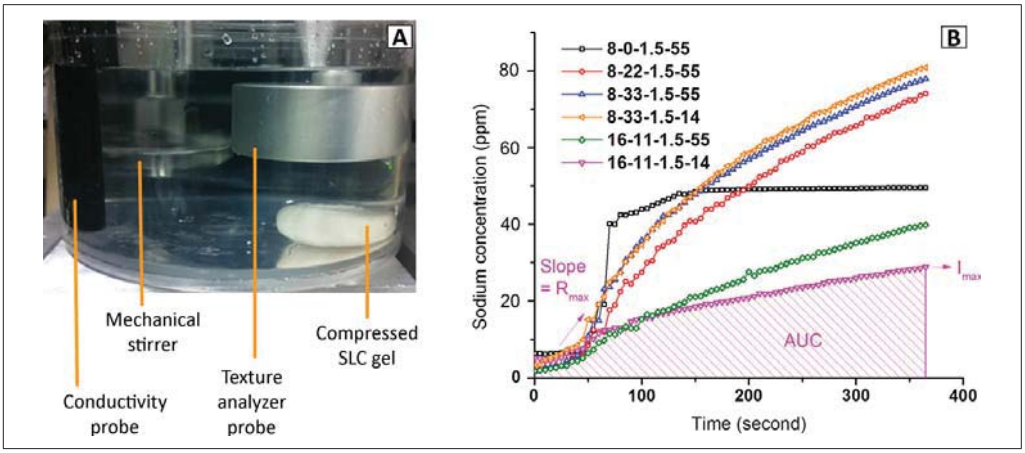

Figure 1–The measurement setting (A) and the representative curves (B) of the *in vitro* sodium release of the SLC gels. The maximum rate of sodium release, R_{max}, the maximum concentration of sodium release, I_{max}, and the area under the curve of sodium release, AUC were derived from each curve as indicated in the graph. Sample code represents protein (%,w/w)–fat (%,w/w)–NaCl (%,w/w)–homogenization pressure (MPa).

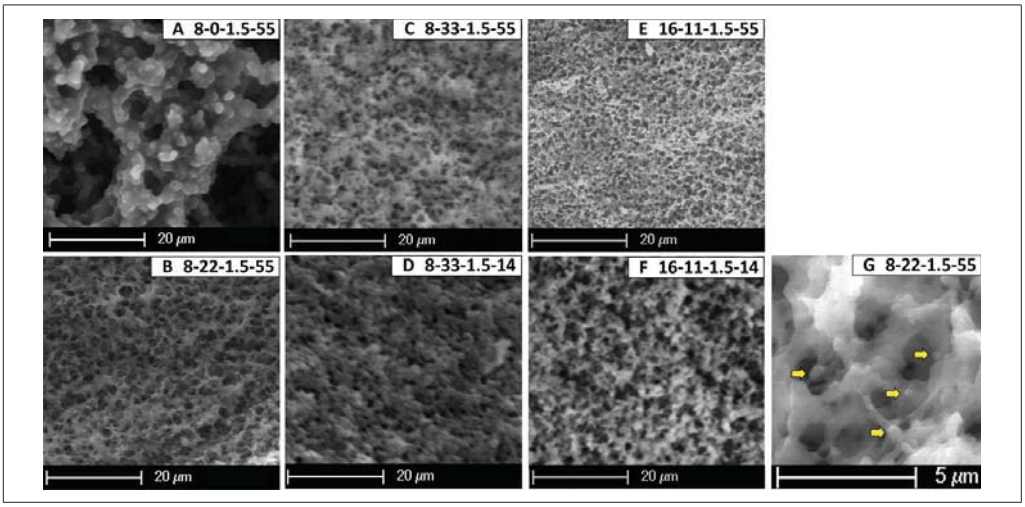

Figure 2–ESEM images of the cross-sections of frozen-fractured lipoproteic emulsion gels. (A) 8–0–1.5–55, (B) 8–22–1.5–55, (C) 8–33–1.5–55, (D) 8–33–1.5–14, (E) 16–11–1.5–55, (F) 16–11–1.5–14, and (G) 8–22–1.5–55 at higher magnification, showing the protein network embedded with fat particles (some pointed by the arrows). Sample code represents protein (%,w/w)–fat (%,w/w)–NaCl (%,w/w)–homogenization pressure (MPa).

APPENDIX A-2 (Cont.)

Table 3–Sodium release properties of the SLC gels.

Sample	R_{max} ± SD (ppm/s)	I_{max} ± SD (ppm)	AUC ± SD (10^3 ppm·s)
8–0–1.5–55	2.99 ± 0.73[a]	50.32 ± 2.95[b]	15.728 ± 1.14[a]
8–22–1.5–55	0.74 ± 0.18[b]	75.90 ± 3.82[a]	16.584 ± 1.36[a]
8–33–1.5–55	0.82 ± 0.20[b]	79.13 ± 3.86[a]	17.72 ± 0.98[a]
8–33–1.5–14	0.73 ± 0.10[b]	76.20 ± 6.49[a]	16.80 ± 1.54[a]
16–11–1.5–55	0.36 ± 0.11[b]	43.23 ± 7.03[b]	9.676 ± 1.81[b]
16–11–1.5–14	0.34 ± 0.10[b]	33.83 ± 4.40[c]	8.024 ± 0.94[b]

Means within the columns with same letters are not significantly different ($P < 0.05$).
R_{max}, maximum rate of sodium release; I_{max}, maximum concentration of sodium release; AUC, area under the curve of sodium release. See Materials and Methods section for the complete description of the 3 sodium release parameters.

Table 4–Textural properties of the SLC gels.

Sample	Serum release ± SD (g)	Maximum stress ± SD (KPa)	Strain at maximum stress ± SD (%)
8–0–1.5–55	2.471 ± 0.166[a]	56.13 ± 9.39[d]	79.85 ± 0.32[a]
8–22–1.5–55	0.524 ± 0.035[c]	93.07 ± 9.37[cd]	55.08 ± 1.86[c]
8–33–1.5–55	0.301 ± 0.015[d]	169.72 ± 21.45[b]	55.87 ± 3.19[c]
8–33–1.5–14	0.485 ± 0.043[c]	100.92 ± 17.97[c]	59.79 ± 3.42[c]
16–11–1.5–55	0.449 ± 0.060[cd]	214.72 ± 51.01[ab]	67.80 ± 1.95[b]
16–11–1.5–14	0.767 ± 0.093[b]	236.21 ± 20.60[a]	78.06 ± 3.58[a]

Means within the columns with same letters are not significantly different ($P < 0.05$).

extensive homogenization at higher pressures, and the similar results were reported in a previous study (Huppertz 2011).

In vitro sodium release properties of the SLC gels

The representative sodium concentration–time curves of the *in vitro* sodium release are illustrated in Figure 1B. Table 3 shows the 3 parameters extracted from the sodium concentration–time curves. During the compression and breakdown of a gel matrix in aqueous media, sodium is released from the gel into the surroundings via either convective or diffusive transfer (Kuo and Lee 2014). In the beginning of the uniaxial compression, the SLC gels dilated along the radial direction and expelled considerable amount of releasable serum. The same manner of gel deformation was also observed by van den Berg and others (2007a) from protein/polysaccharide gels. This fast release of serum transferred relatively large amount of the dissolved sodium from the gel to the surrounding. The sudden release of sodium resulted in the initial abrupt increment of sodium concentration in the surrounding liquid, which accounted for the R_{max}. Therefore, the sodium migration during the gel compression can be considered as primarily through the convective transfer by the serum. After the compression, sodium continued to migrate from the gel into the aqueous phase via diffusion along the concentration gradient between the gel and the aqueous phase. This accounted for the continuing increment of the sodium concentration in the sodium release profile. The total amount of sodium released at the end of measurement was reflected by the I_{max} value, and the cumulative concentration of sodium along the release time was reflected by the AUC.

The profiles of the *in vitro* sodium release of the SLC gels varied with the gel formula and homogenization pressures. The sample 8–0–1.5–55 showed the fastest sodium release (greatest R_{max} value, Table 3) during the gel compression, but the concentration increment reached a plateau earlier than any other gels. Comparing those fat-containing samples, the samples with relatively lower protein but higher fat contents (8–22–1.5–55, 8–33–1.5—55, and 8–33–1.5–14) released more sodium (greater I_{max} and AUC, Table 3) than those gels with relatively higher protein content (16–11–1.5–55 and 16–11–1.5–14). At the same formula, sample 16–11–1.5–55 released more sodium (Table 3) than sample 16–11–1.5–14. The microstructural factors that led to different texture, serum release, and, thus, the different sodium release properties of the SLC gels are discussed further in the following sections.

Effect of fat content on sodium release

Comparing the formula in Table 1 and the sodium release properties in Table 3 implied that the fat content has significant impact on the sodium release of the SLC gels. At constant protein concentration (samples 8–0–1.5–55, 8–22–1.5—55, and 8–33–1.5–55), the increase in the fat content led to increased I_{max} values. This may be attributed to the lowered values of strain at maximum stress (Table 4) with increased fat content. Although for these 3 samples, the maximum stress increased with increasing fat content due to elevated dry matter contents, the decreased values of strain at maximum stress suggested earlier fracture of the gels. The earlier fracture could result in greater extent of gel breakdown and hence create larger surface area of the gel for sodium release (Koliandris and others 2008). The differences in deformation of the gels due to the compression can be seen in Figure 3. The sample 8–0–1.5–55 (Figure 3A) was only compressed but not fractured throughout the tests, whereas the samples 8–22–1.5–55 and 8–33–1.5–55 (Figure 3B and C, respectively) broke into multiple pieces associated with various sizes of small debris. Figure 3(G) shows the internal structure of a representative fat-containing sample (8–22–1.5–55) at higher magnification. Many globular fat particles are embedded in the protein network, and some of the fat particles are indicated by the arrows in Figure 3G. The embedded fat could interfere with the network structure of protein, generating more points of fracture upon compression. This could explain the increased degree of breakdown with increasing fat contents among samples 8–0–1.5–55, 8–22–1.5—55, and 8–33–1.5–55. As a result, the gels with higher fat content yielded greater surface area after fracture, which could lead to greater sodium release. The reduced fracture strain and enhanced sodium release with increasing fat content were also reported by previous literature of model dairy gel made of renneted milk powder (de Loubens and others 2011a; Panouillé and others 2011).

van den Berg and others (2007a, 2007b) corrected the fracture properties of protein/polysaccharide gels for the effect of serum release. In this study, when the textural properties were also corrected for the serum release according to the calculations of van den Berg and others (2007a, 2007b; data not shown), the trends of textural properties among different gels discussed above remain valid.

The effects of fat content on sodium release is more pronounced when comparing the SLC gels with similar dry matter contents (samples 8–22–1.5–55 and 16–11–1.5–55). The sample 8–22–1.5–55 with higher fat content has significantly lower values of maximum stress and strain at maximum stress (Table 4), and significantly higher I_{max} and AUC (Table 3). In addition, the higher I_{max} and AUC values of the samples 8–22–1.5–55 compared to the sample 16–11–1.5–55 could be partly due to the difference in ionic interaction. Previous literature has identified that the sodium-protein interaction in the lipoproteic foods reduces the amount of free sodium available for release (Ruusunen and others 2001; Lauverjat and others 2009; Boisard and others 2013). Thus, the increased interaction between sodium and protein might have decreased the

APPENDIX A-2 (Cont.)

sodium mobility for the sample 16–11–1.5–55, and led to lower sodium release. Boisard and others (2013, 2014) also studied the effects of fat content in model cheese with constant dry matter contents. The *in vitro* sodium release rate, in-mouth sodium release, and saltiness perception increased with increased fat/protein ratio. They ascribed it to the weaker structure of the cheese and higher sodium mobility, evidenced by the lower stress at maximal deformation and the higher NMR relaxation times of sodium, respectively.

However, Lawrence and others (2012a) reported that the maximum sodium concentration released from the lipoproteic matrices in mouth was negatively related with the ratio between fat and dry matter content. They hypothesized that the fat served as the barrier which retarded sodium release. The sample breakdown in their study was done by multiple chews in mouth, and should be more extensive than that in the present study. Also, for the sample with higher fat content and thus lower fracture stress, the panelists may use less work and time to chew (Lawrence and others 2012b). This could ultimately result in similar breakdown degree between the samples with varying fat contents. Hence, it is possible that, in their study, the barrier effect of fat is more pronounced than the gel breakdown effect of fat, and led to the results opposite from our findings.

Effects of emulsion particle sizes on sodium release

In addition to compositional properties such as fat content, emulsion particle size also affected the I_{max} of the SLC gels. When comparing the 2 SLC gels with same formula but different homogenization pressures (16–11–1.5–14 and 16–11–1.5–55), sample 16–11–1.5–55 has lower size of the fat globules (Table 2) and higher I_{max} (Table 3). This is again related to the lower value of strain at maximum stress (Table 4) of sample 16–11–1.5–55, which implied greater surface area of the broken pieces and thus enhanced sodium release. The similar relationship in particle size, I_{max}, and strain at maximum stress was noticed from the samples 8–33–1.5–55 and 8–33–1.5–14, although statistically not significant. At constant fat content, the SLC gel with smaller fat globules has a higher number of fat globules randomly dispersed in the protein network. These highly dispersed fat globules interfere with the formation of protein network, and thus accounted for earlier and greater extent of breakdown upon compression. The greater extent of breakdown of the sample 16–11–1.5–55 (Figure 3E) than sample 16–11–1.5–14 (Figure 3F) can also be identified from the images of the broken gels. The side view image of the sample 16–11–1.5–55 (Figure 3E) shows more broken pieces than that of the sample 16–11–1.5–14 (Figure 3F). A previous study on the model cheese made of rennet casein also found that lower size of fat globules was associated with reduced fracture stress and fracture energy and higher concentration of sodium release (Phan and others 2008). The relationship described above, however, was not significant between the samples 8–33–1.5–55 and 8–33–1.5–14. This is possibly because of the high fat content relative to protein leading to weak gels. Thus, the size of fat globules showed less impact on the I_{max} and the strain at maximum stress for the samples 8–33–1.5–55 and 8–33–1.5–14 than for the samples 16–11–1.5–55 and 16–11–1.5–14.

Effect of porosity and pore size on sodium release

Although the I_{max} values of the sodium release were closely associated with the fat content and the size of the fat globules, the maximum rate of sodium release, R_{max}, depended primarily on the porosity and pore size of the SLC gels.

The sample 8–0–1.5–55 has the highest porosity and pore size (Table 2) and highest R_{max} value among the samples (Table 3). This was attributed to the greatest serum release of this sample (Table 4). As discussed in the previous section, the serum release during gel compression is accounted for the R_{max} values of the *in vitro* sodium release. According to previous studies (van den Berg and others 2007b; Stieger and van de Velde 2013), serum release had a strong positive correlation to gel porosity, and coarse stranded gels had higher serum release. In addition, the hydraulic permeability, which describes the ease of fluid transport through pore spaces, is proportional to the square of pore radius (Sakai 1994). As discussed in the previous section, the sample 8–0–1.5–55 had coarsely aggregated protein particles and considerable void space and large pore size. Therefore, the highest R_{max} and serum release of the sample 8–0–1.5–55 can be attributed to the high porosity and large pore size of this sample. In a study on gellan/WPI gel made by acid induced cold gelation (Stieger 2011), sodium release was boosted by engineering the microstructure of food matrix to enhance serum release. The authors showed that, with the increment in gellan content and the adjustment of dry matter content, the microstructure of the gel changed from protein-continuous to bi-continuous, whereas large deformation properties remained relatively close. The increase in permeability led to higher saltiness perception of the gel.

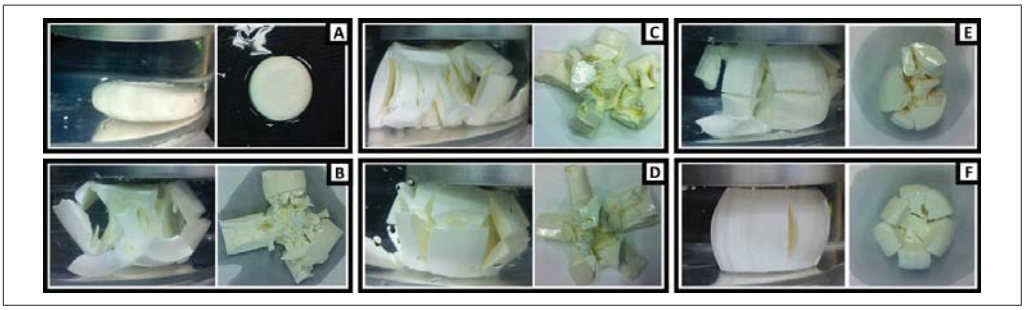

Figure 3–The SLC gels during the *in vitro* sodium release measurement (left of each graph) and after texture analysis (right of each graph). (A) 8–0–1.5–55, (B) 8–22–1.5–55, (C) 8–33–1.5–55, (D) 8–33–1.5–14, (E) 16–11–1.5–55, and (F) 16–11–1.5–14. Sample code represents protein (%,w/w)–fat (%,w/w)–NaCl (%,w/w)–homogenization pressure (MPa).

APPENDIX A-2 (Cont.)

When comparing the 2 samples with similar dry matter contents but different fat content, the impacts of porosity and pore size on the R_{max} values could also be observed. As discussed in previous sections, the porosity and pore size were both significantly lower in sample 16–11–1.5–55 than in sample 8–22–1.5–55 (Table 2), due to the greater structure forming capacity of protein than fat. The serum release (Table 4) and R_{max} (Table 3) values of the sample 16–11–1.5–55 were accordingly lower than those of the sample 8–22–1.5–55. The differences, though, are not significant at $\alpha = 0.05$. Such lack of significance could result from the lower gel integrity of the sample 8–22–1.5–55 due to the greater structural interference by fat. During the compression, the sample 8–22–1.5–55 broke earlier than the sample 16–11–1.5–55. The earlier fracture could release the formal pressure on the gel, and thus lower the chance for the serum to be compressed out. In addition to the formal pressure, the serum release rate also depends on the gel porosity (van den Berg and others 2007a). Loss of porosity during the gel deformation could lead to leveling-off of the serum release. Future studies on the microstructural changes of the SLC gels after compression would help to identify the impact of porosity alteration during the compression on serum release. On the other hand, the lack of significant difference in the R_{max} values may partly be due to the comparatively high R_{max} value of the sample 8–0–1.5–55 than the other samples. In fact, when the adjusted Tukey test was performed on the 5 samples excluding the sample 8–0–1.5–55, the R_{max} value of the sample 8–22–1.5–55 was significantly higher than that of 16–11–1.5–55.

The effect of homogenization pressure on structural properties showed clear trends. The sample 16–11–1.5–55 has significantly lower porosity and pore size as compared to the sample 16–11–1.5–14 (Table 2). This difference can also be observed from Figure 2E and F. The sample 16–11–1.5–55 displays finer network structure with smaller and more evenly distributed pore size than that of the sample 16–11–1.5–14. This indicated that increased pressure of homogenization induced effective dispersion of protein particles and formation of a finer, more crosslinked gel network. The serum release of the sample 16–11–1.5–55 was significantly lower than that of the sample 16–11–1.5–14 (Table 4). This complies with the previous discussion about the impacts of porosity and pore size on serum release. The trend of porosity, pore size, serum release, R_{max} values, and I_{max} values between the samples 8–33–1.5–55 and 8–33–1.5–14 were similar to those between the samples 16–11–1.5–55 and 16–11–1.5–14. However, the differences in porosity and pore size are not significant at $\alpha = 0.05$. This may indicate that the change of homogenization pressure is more effective in creating structural variations of protein-rich gels than in fat-rich gels.

In the study of Lawrence and others (2012a) on the lipoproteic matrices, the maximum sodium concentration during the in-mouth sodium release assessment was positively correlated with the water content of the samples. They related this to the higher solvating capacity of sodium with enhanced water content. If the serum release and sensory juiciness were evaluated, it would help to identify the mechanisms behind the positive relationship between sodium release and water content of the samples in their study.

Conclusion

This study explored the dependence of sodium release on multiple structural properties of the SLC gels using quantitative analyses of *in vitro* sodium release, gel microstructures, and textures. The parameters from the *in vitro* sodium release curves, describing the temporal sodium release properties, were closely related with various microstructural properties and the associated textural properties of the SLC gels. Generally, the R_{max}, maximum rate of sodium release during the gel compression, increased with increasing porosity and pore size of the gels owning to greater serum release. The I_{max}, maximum concentration of sodium released, increased with increasing fat content or decreasing particle size of fat owning to more extensive gel breakdown. The findings from this study provided insights for engineering the microstructure of SLC-based products to modify the temporal properties of sodium release. Optimized food structure can effectively amplify saltiness and achieve the sodium reduction in the SLC-based products with a further understanding of the correlation between the sodium release and saltiness perception.

References

Aaron KJ, Sanders PW. 2013. Role of dietary salt and potassium intake in cardiovascular health and disease: a review of the evidence. Mayo Clin Proc 88(9):987–95.

Anand, J, Goldman, JD, Steinfeldt, LC, Montville, JB, Heendeniya, KY, Omolewa-Tomobi, G, Enns, CW, Ahuja, JK, Martin, CL, LaComb, RP, Moshfegh, AJ. 2012. What we eat in America, NHANES 2009–2010: documentation and data files. Worldwide Web Site: Food Surveys Research Group [Internet]. Available from: http://www.ars.usda.gov/Services/docs.htm?docid=18349. Accessed 2014 Mar 17.

Anderson CAM, Appel LJ, Okuda N, Brown IJ, Chan Q, Zhao L, Ueshima H, Kesteloot H, Miura K, Curb JD, Yoshita K, Elliott P, Yamamoto ME, Stamler J. 2010. Dietary sources of sodium in China, Japan, the United Kingdom, and the United States, women and men aged 40 to 59 years: the INTERMAP study. J Am Diet Assoc 110(5):736–45.

Boisard L, Andriot I, Arnould C, Achilleos C, Salles C, Guichard E. 2013. Structure and composition of model cheeses influence sodium NMR mobility, kinetics of sodium release and sodium partition coefficients. Food Chem 136(2):1070–7.

Boisard L, Andriot I, Martin C, Septier C, Boissard V, Salles C, Guichard E. 2014. The salt and lipid composition of model cheeses modifies in-mouth flavour release and perception related to the free sodium ion content. Food Chem. 145(0):437–44.

Cogswell ME, Zhang Z, Carriquiry AL, Gunn JP, Kuklina EV, Saydah SH, Yang Q, Moshfegh AJ. 2012. Sodium and potassium intakes among US adults: NHANES 2003–2008. Am J Clin Nutr 96(3):647–57.

Committee on the Consequences of Sodium Reduction in Populations. 2013. Findings and conclusions. In: Brian L. Strom, Ann L. Yaktine, and Maria Oria, editors. Sodium intake in populations: assessment of evidence. Washington, D.C.: The National Academies Press. p 119–126.

Cook NR, Appel LJ, Whelton PK. 2014. Lower levels of sodium intake and reduced cardiovascular risk. Circulation 129(9):981–9.

Danaei G, Ding EL, Mozaffarian D, Taylor B, Rehm J, Murray CJL, Ezzati M. 2009. The preventable causes of death in the United States: comparative risk assessment of dietary, lifestyle, and metabolic risk factors. PloS Med 6(4):e1000058.

de Loubens C, Panouillé M, Saint-Eve A, Déléris I, Tréléa IC, Souchon I. 2011a. Mechanistic model of *in vitro* salt release from model dairy gels based on standardized breakdown test simulating mastication. J Food Eng 105(1):161–8.

de Loubens C, Saint-Eve A, Deleris I, Panouille M, Doyennette M, Trelea IC, Souchon I. 2011b. Mechanistic model to understand *in vivo* salt release and perception during the consumption of dairy gels. J Agric Food Chem 59(6):2534–42.

DGAC. 2005. Report of the Dietary Guidelines Advisory Committee on the Dietary Guidelines for Americans, 2005, to the Secretary of Agriculture and the Secretary of Health and Human Services. U.S. Dept. of Agriculture, Agricultural Research Service, Washington, D.C.

DGAC. 2010. Report of the Dietary Guidelines Advisory Committee on the Dietary Guidelines for Americans, 2010, to the Secretary of Agriculture and the Secretary of Health and Human Services. U.S. Dept. of Agriculture, Agricultural Research Service, Washington, D.C.

Doyle ME, Glass KA. 2010. Sodium reduction and its effect on food safety, food quality, and human health. Compr Rev Food Sci F 9(1):44–56.

Geurts TJ. 1974. Transport of salt and water during salting of cheese. I. Analysis of the processes involved. Nederlands melk- en zuiveltijdschrift 28(2):102–29.

Grummer J, Bobowski N, Karalus M, Vickers Z, Schoenfuss T. 2013. Use of potassium chloride and flavor enhancers in low sodium Cheddar cheese. J Dairy Sci 96(3):1401–18.

Henney JE, Taylor CL, Boon CS. 2010a. Preface. In: Committee on Strategies to Reduce Sodium Intake, Inst. of Medicine, editor. Strategies to reduce sodium intake in the United States. Washington, D.C.: The National Academies Press. p ix.

Henney JE, Taylor CL, Boon CS. 2010b. Sodium intake reduction: an important but elusive public health goal. In: Committee on Strategies to Reduce Sodium Intake, Inst. of Medicine, editor. Strategies to reduce sodium intake in the United States. Washington, D.C.: The National Academies Press. p 29–66.

Huppertz T. 2011. Homogenization of milk | high-pressure homogenizers. In: John W. Fuquay, editor. Encyclopedia of dairy sciences. 2nd ed. San Diego, Calif.: Academic Press. p 755–60.

Juneja VK, Altuntaş EG, Ayhan K, Hwang C, Sheen S, Friedman M. 2013. Predictive model for the reduction of heat resistance of Listeria monocytogenes in ground beef by the combined effect of sodium chloride and apple polyphenols. Int J Food Microbiol 164(1):54–9.

Koliandris A, Lee A, Ferry A, Hill S, Mitchell J. 2008. Relationship between structure of hydrocolloid gels and solutions and flavour release. Food Hydrocoll 22(4):623–30.

Kuo W, Lee Y. 2014. Effect of food matrix on saltiness perception—implications for sodium reduction. Compr Rev Food Sci F 13:906–923.

Lawrence G, Buchin S, Achilleos C, Berodier F, Septier C, Courcoux P, Salles C. 2012a. *In vivo* sodium release and saltiness perception in solid lipoprotein matrices. 1. Effect of composition and texture. J Agric Food Chem 60(21):5287–98.

APPENDIX A-2 (Cont.)

Lawrence G, Septier C, Achilleos C, Courcoux P, Salles C. 2012b. *In vivo* sodium release and saltiness perception in solid lipoprotein matrices. 2. Impact of oral parameters. J Agric Food Chem 60(21):5299–306.

Lauverjat C, Deleris I, Trelea IC, Salles C, Souchon I. 2009. Salt and aroma compound release in model cheeses in relation to their mobility. J Agric Food Chem 57(21):9878–87.

Lim SS, Vos T, Flaxman AD, Danaei G, Shibuya K, Adair-Rohani H, AlMazroa MA, Amann M, Anderson HR, Andrews KG, Aryee M, Atkinson C, Bacchus LJ, Bahalim AN, Balakrishnan K, Balmes J, Barker-Collo S, Baxter A, Bell ML, Blore JD, Blyth F, Bonner C, Borges G, Bourne R, Boussinesq M, Brauer M, Brooks P, Bruce NG, Brunekreef B, Bryan-Hancock C, Bucello C, Buchbinder R, Bull F, Burnett RT, Byers TE, Calabria B, Carapetis J, Carnahan E, Chafe Z, Charlson F, Chen H, Chen JS, Cheng AT, Child JC, Cohen A, Colson KE, Cowie BC, Darby S, Darling S, Davis A, Degenhardt L, Dentener F, Des Jarlais DC, Devries K, Dherani M, Ding EL, Dorsey ER, Driscoll T, Edmond K, Ali SE, Engell RE, Erwin PJ, Fahimi S, Falder G, Farzadfar F, Ferrari A, Finucane MM, Flaxman S, Fowkes FGR, Freedman G, Freeman MK, Gakidou E, Ghosh S, Giovannucci E, Gmel G, Graham K, Grainger R, Grant B, Gunnell D, Gutierrez HR, Hall W, Hoek HW, Hogan A, Hosgood III HD, Hoy D, Hu H, Hubbell BJ, Hutchings SJ, Ibeanusi SE, Jacklyn GL, Jasrasaria R, Jonas JB, Kan H, Kanis JA, Kassebaum N, Kawakami N, Khang Y, Khatibzadeh S, Khoo J, Kok C, Laden F, Lalloo R, Lan Q, Lathlean T, Leasher JL, Leigh J, Li Y, Lin JK, Lipshultz SE, London S, Lozano R, Lu Y, Mak J, Malekzadeh R, Mallinger L, Marcenes W, March L, Marks R, Martin R, McGale P, McGrath J, Mehta S, Memish ZA, Mensah GA, Merriman TR, Micha R, Michaud C, Mishra V, Hanafiah KM, Mokdad AA, Morawska L, Mozaffarian D, Murphy T, Naghavi M, Neal B, Nelson PK, Nolla JM, Norman R, Olives C, Omer SB, Orchard J, Osborne R, Ostro B, Page A, Pandey KD, Parry CD, Passmore E, Patra J, Pearce N, Pelizzari PM, Petzold M, Phillips MR, Pope D, Pope III CA, Powles J, Rao M, Razavi H, Rehfuess EA, Rehm JT, Ritz B, Rivara FP, Roberts T, Robinson C, Rodriguez-Portales JA, Romieu I, Room R, Rosenfeld LC, Roy A, Rushton L, Salomon JA, Sampson U, Sanchez-Riera L, Sanman E, Sapkota A, Seedat S, Shi P, Shield K, Shivakoti R, Singh GM, Sleet DA, Smith E, Smith KR, Stapelberg NJ, Steenland K, Stöckl H, Stovner LJ, Straif K, Straney L, Thurston GD, Tran JH, Van Dingenen R, van Donkelaar A, Veerman JL, Vijayakumar L, Weintraub R, Weissman MM, White RA, Whiteford H, Wiersma ST, Wilkinson JD, Williams HC, Williams W, Wilson N, Woolf AD, Yip P, Zielinski JM, Lopez AD, Murray CJ, Ezzati M. 2012. A comparative risk assessment of burden of disease and injury attributable to 67 risk factors and risk factor clusters in 21 regions, 1990–2010: a systematic analysis for the Global Burden of Disease Study 2010. Lancet 380(9859):2224–60.

MathWorks. 2014. Functions in image processing toolbox [Internet]. Available from: http://www.mathworks.com/help/images/functionlist.html. Accessed 2014 Mar 17.

Mattes RD, Donnelly D. 1991. Relative contributions of dietary-sodium sources. J Am Coll Nutr 10(4):383–93.

Panouille M, Saint-Eve A, de Loubens C, Deleris I, Souchon I. 2011. Understanding of the influence of composition, structure and texture on salty perception in model dairy products. Food Hydrocoll 25(4):716–23.

Phan VA, Yven C, Lawrence G, Chabanet C, Reparet JM, Salles C. 2008. *In vivo* sodium release related to salty perception during eating model cheeses of different textures. Int Dairy J 18(9):956–63.

Powles J, Fahimi S, Micha R, Khatibzadeh S, Shi P, Ezzati M, Engell RE, Lim SS, Danaei G, Mozaffarian D, on behalf of the Global Burden of Diseases Nutrition and Chronic Diseases Expert Group (NutriCoDE). 2013. Global, regional and national sodium intakes in 1990 and 2010: a systematic analysis of 24 h urinary sodium excretion and dietary surveys worldwide. BMJ Open 3(12):e003733.

Ruusunen M, Simolin M, Puolanne E. 2001. The effect of fat content and flavor enhancers on the perceived saltiness of cooked 'bologna-type' sausages. J Muscle Foods 12(2): 107–20.

Sakai K. 1994. Determination of pore size and pore size distribution. 2. Dialysis membranes. J Membr Sci 96(1–2):91–130.

Sala G, Stieger M, van de Velde F. 2010. Serum release boosts sweetness intensity in gels. Food Hydrocoll 24(5):494–501.

Salvador P, Toldrà M, Saguer E, Carretero C, Parés D. 2009. Microstructure–function relationships of heat-induced gels of porcine haemoglobin. Food Hydrocoll 23(7): 1654–9.

Stieger M. 2011. Texture-taste interactions: enhancement of taste intensity by structural modifications of the food matrix. Procedia Food Sci 1(0):521–7.

Stieger M, van de Velde F. 2013. Microstructure, texture and oral processing: new ways to reduce sugar and salt in foods. Curr Opin Colloid 18(4):334–48.

van de Velde F, Adamse M. 2013. Juiciness enhances the perceived saltiness of meat products. New Food [Internet]. Available from: http://www.newfoodmagazine.com/10597/new-food-magazine/past-issues/issue-2-2013/juiciness-enhances-the-perceived-saltiness-of-meat-products/. Accessed 2014 Mar 17.

van den Berg L, van Vliet T, van der Linden E, van Boekel MAJS, van de Velde F. 2007a. Serum release: the hidden quality in fracturing composites. Food Hydrocoll 21(3):420–32.

van den Berg L, van Vliet T, van der Linden E, van Boekel MAJS, van de Velde F. 2007b. Breakdown properties and sensory perception of whey proteins/polysaccharide mixed gels as a function of microstructure. Food Hydrocoll 21(5–6):961–76.

van den Berg L, van Vliet T, van der Linden E, van Boekel MAJS, van de Velde F. 2008. Physical properties giving the sensory perception of whey proteins/polysaccharide gels. Food Biophys 3(2):198–206.

Xiong R, Meullenet JF, Hankins JA, Chung WK. 2002. Relationship between sensory and instrumental hardness of commercial cheeses. J Food Sci 67(2):877–83.

Zack G, Rogers W, Latt S. 1977. Automatic-measurement of sister chromatid exchange frequency. J Histochem Cytochem 25(7):741–53.

APPENDIX A-3 The permission and the publication reprint for the contents of CHAPTER 4

ELSEVIER LICENSE
TERMS AND CONDITIONS

Mar 19, 2016

This is a License Agreement between Wan ("You") and Elsevier ("Elsevier") provided by Copyright Clearance Center ("CCC"). The license consists of your order details, the terms and conditions provided by Elsevier, and the payment terms and conditions.

All payments must be made in full to CCC. For payment instructions, please see information listed at the bottom of this form.

Supplier	Elsevier Limited The Boulevard,Langford Lane Kidlington,Oxford,OX5 1GB,UK
Registered Company Number	1982084
Customer name	Wan-Yuan Kuo
Customer address	1304 W Pennsylvania Ave Rm 382 K URBANA, IL 61801
License number	3832821318525
License date	Mar 19, 2016
Licensed content publisher	Elsevier
Licensed content publication	Food Hydrocolloids
Licensed content title	Structural characterization of solid lipoproteic colloid gels by ultra-small-angle X-ray scattering and the relation with sodium release
Licensed content author	Wan-Yuan Kuo,Jan Ilavsky,Youngsoo Lee
Licensed content date	May 2016
Licensed content volume number	56
Licensed content issue number	n/a
Number of pages	9
Start Page	325
End Page	333
Type of Use	reuse in a thesis/dissertation
Portion	full article
Format	both print and electronic
Are you the author of this Elsevier article?	Yes
Will you be translating?	No
Title of your thesis/dissertation	RELATING STRUCTURAL PROPERTIES TO SALTINESS PERCEPTION OF MODEL LIPOPROTEIC GELS
Expected completion date	Apr 2016

APPENDIX A-3 (Cont.)

Food Hydrocolloids 56 (2016) 325–333

Contents lists available at ScienceDirect

Food Hydrocolloids

journal homepage: www.elsevier.com/locate/foodhyd

Structural characterization of solid lipoproteic colloid gels by ultra-small-angle X-ray scattering and the relation with sodium release

Wan-Yuan Kuo [a], Jan Ilavsky [b], Youngsoo Lee [a, *]

[a] Department of Food Science and Human Nutrition, University of Illinois at Urbana-Champaign, 382K, Agricultural Engineering and Sciences Building, 1304 W. Pennsylvania Ave., Urbana, IL 61801, USA
[b] X-Ray Science Division, Argonne National Laboratory, 9700 S. Cass Avenue, Bldg. 401 MS-16, Argonne, IL 60439-4837, USA

ARTICLE INFO

Article history:
Received 18 August 2015
Received in revised form
23 November 2015
Accepted 29 December 2015
Available online 29 December 2015

Keywords:
Ultra-small-angle X-ray scattering (USAXS)
Solid lipoproteic colloid gel
Sodium release
Sodium reduction
Whey protein isolate
Structure

ABSTRACT

Sodium reduction in protein/lipid-based products such as cheese is becoming increasingly important to the food industry. Understanding the structure critical to sodium release is one of the keys to effectively controlling the sensory quality of the product while lowering the sodium content. In this study, ultra-small-angle X-ray scattering (USAXS), novel to food research, was used to characterize the structure of solid lipoproteic colloid (SLC) gels as a model food. The SLC gels were made via heat-induced gelation of emulsions of whey protein isolate and anhydrous milk fat. The gels varied in the contents of protein, fat, and NaCl and homogenization pressures. The gyration radii of the protein aggregates ($r_{g,p}$) and the fat globules ($r_{g,f}$) of the samples before and after the gelation were obtained via fitting the USAXS profiles to inspect the structure formation of the SLC gels. The effects of formulation and processing on the gel $r_{g,p}$ and the gel $r_{g,f}$ were analyzed. In addition, the gel $r_{g,f}$ and the hydrodynamic radius of the droplets ($r_{h,e}$) in the emulsions were correlated with sodium release. The correlation suggested that gel $r_{g,f}$ is a better indicator of sodium release than the emulsion $r_{h,e}$. The findings from this study indicated that USAXS is feasible for the structural investigation of protein/lipid-based foods.

1. Introduction

Reducing the sodium content of food products based on lipid/protein emulsion structures such as cheese and processed meat has gained increasing attention in the food industry (Desmond, 2007, 2006; Johnson, Kapoor, McMahon, McCoy, & Narasimmon, 2009). Currently, industrial and experimental strategies for sodium reduction include stealth reduction (Phelps et al., 2006), sodium replacement (Eoin, 2006; Sinopoli & Lawless, 2012), saltiness potentiation (Brewer, Gills, & Vega, 1995; Heidolph et al., 2011; Yamaguchi & Takahashi, 1984), multisensory application (Djordjevic, Zatorre, & Jones-Gotman, 2004; Dotsch et al., 2009), and physical modification of salt crystals (Heidolph et al., 2011). More recently, the new concept of structural engineering has been proposed to enhance the sodium release and/or saltiness perception of the food matrix (Busch, Yong, & Goh, 2013; Jiménez-Colmenero, 2013; Stieger & van de Velde, 2013). The hypothesis underlying this strategy is that the structure of the food matrix dominates the physicochemical properties of the foods and hence the sodium release and saltiness perception of the food products (Kuo & Lee, 2014a). Therefore, at a given salt level, the sodium release and saltiness perception of the food matrix can potentially be maximized by an optimized food structure.

Various mechanisms have been proposed in the literature to enhance sodium release via food structure modification. Sodium release is greater in foods with more available sodium, with a higher diffusion coefficient of sodium, with more serum release (i.e., the amount of squeezable liquid), or with a higher degree of fragmentation (Kuo & Lee, 2014a). In lipoproteic foods, the availability of sodium has been increased by lowering the protein contents (Boisard et al., 2014; Lauverjat, Deleris, Trelea, Salles, & Souchon, 2009; Ruusunen et al., 2005). Additionally, the diffusion coefficient of sodium in lipoproteic foods has been increased by lowering the fat or dry matter content (Chabanet, Tarrega, Septier, Siret, & Salles, 2013; Floury, Rouaud, Le Poullennec, & Famelart, 2009; Hughes, Cofrades, & Troy, 1997; Lauverjat et al., 2009; Panouille, Saint-Eve, de Loubens, Deleris, & Souchon, 2011; Phan et al., 2008). In addition, lowering the degree of protein crosslinking

* Corresponding author.
E-mail addresses: wkuo7@illinois.edu (W.-Y. Kuo), ilavsky@aps.anl.gov (J. Ilavsky), leeys@illinois.edu (Y. Lee).

http://dx.doi.org/10.1016/j.foodhyd.2015.12.032
0268-005X/

APPENDIX A-3 (Cont.)

lowered the diffusion coefficient of sodium (Panouille et al., 2011). In a model polysaccharide/protein gel, the serum release was found to be higher in a bi-continuous microstructure than in a protein-continuous one (Stieger, 2011). Lastly, the fragmentation degree of lipoproteic foods is greater with higher fat content (de Loubens et al., 2011), lower protein content (Panouille et al., 2011), or smaller particle size of the emulsion droplets (Kuo & Lee, 2014b).

The increased sodium release in lipoproteic foods associated with smaller emulsion droplets was ascribed to the higher surface area after the food breakdown (Kuo & Lee, 2014b). When emulsion gels undergo deformation, the initiation of fracture more likely starts at the interface between fat and protein than between protein and protein. This tendency is because the fat droplets are structural defects, and defects increase the stress concentration of the gel matrix (Sala, van Vliet, Cohen Stuart, Aken, & van de Velde, 2009; van Vliet, Luyten, & Walstra, 1993). This property has been further demonstrated by reductions in the gel fracture strain, stress or energy and by increases in sodium release with higher fat contents or lower emulsion droplet particle sizes in lipoproteic gels (de Loubens et al., 2011; Kuo & Lee, 2014b; Panouille et al., 2011; Phan et al., 2008). Our previous study on model solid lipoproteic colloid (SLC) gels revealed that a higher homogenization pressure led to a lower hydrodynamic radius of the emulsion droplets ($r_{h,e}$), which implied an SLC gel network with more randomly dispersed structural defects. More structural defects thus led to easier fracture and higher surface area of the fractured debris. However, the increase in sodium release with reduced $r_{h,e}$ was not universally significant (Kuo & Lee, 2014b). Because the $r_{h,e}$ was obtained from dynamic light scattering (DLS) of the emulsions prior to the heat-induced gelation, we hypothesized that the particle size of the actual fat globules within the lipoproteic gel correlates better than the emulsion $r_{h,e}$ to the fragmentation degree and thus the release of sodium. An ideal analytical tool to obtain the particle size of fat globules in solid gels is necessary to validate the hypothesis.

Currently, microscopy is the most relevant tool for analyzing the nano- and microstructures of solid foods, and electron microscopy has been extensively used for its suitable characterization range (Dudkiewicz, Luo, Tiede, & Boxall, 2012; Kalab, Allanwojtas, & Miller, 1995). However, electron microscopy usually requires sample pre-treatment, which can take several days and potentially damage the original food structure. In addition, electron microscopy is limited to 2-D imaging a thin layer or a surface (Harada & Matsuoka, 2004) and thus may not represent the bulk sample well.

A small but increasing number of studies have been reported on using ultra-small-angle X-ray scattering (USAXS) to characterize biomaterials (Agrawal, Sanabria-DeLong, Jemian, Tew, & Bhatia, 2007; Nave, Diakun, & Bordas, 1986). Even fewer studies have used USAXS to study food systems (Peyronel, Pink, & Marangoni, 2014a; Peyronel, Quinn, Marangoni, & Pink, 2014b; Väänänen et al., 2003). Depending on the scattering angle, the family of X-ray scattering, including wide-, small-, and ultra-small-angle X-ray scattering, can provide structural information such as chemical composition, crystallography, size, shape and association of particles at different scales (Dudkiewicz et al., 2012). Typical pinhole small-angle X-ray scattering (SAXS) characterizes structures at 1–100 nm. With advanced USAXS instruments, the range can be extended to 1 nm - 1 μm (Ilavsky, Allen, Long, & Jemian, 2002; Ilavsky et al., 2013, 2009). This range ideally covers the wide size range of individual components in foods and the associated structures of the components. Requiring minimal or no pre-treatment, USAXS provides ensemble 3-D structural information from a bulk sample while minimizing the damage of the structure. In addition, USAXS can be applied to turbid systems, such as solid fat and denatured protein, that light scattering is unable to characterize (Harada & Matsuoka, 2004; Peyronel et al., 2014b). Using a synchrotron X-ray radiation source rather than a conventional source provides higher flux and thus higher contrast, so that normally low-contrast biomaterials or foods can be studied more effectively (Harada & Matsuoka, 2004).

The objective of the present study is to use USAXS/pinhole SAXS to investigate the structure of SLC gels and to correlate the USAXS-derived structural properties in the gel with sodium release. The structure formation during the heat-induced gelation of the samples and the effects of formulation and treatment on the gyration radii of the protein aggregates ($r_{g,p}$) and the fat globules ($r_{g,f}$) are discussed. Two radius values, the USAXS-derived gel $r_{g,f}$ and the DLS-derived emulsion $r_{h,e}$, are compared for how well each correlates to sodium release from the SLC gels.

2. Materials and methods

2.1. Materials and sample preparation

Whey protein isolate (WPI, Hilmar 9000, Hilmar Ingredients, Hilmar, CA, USA) and anhydrous milk fat (AMF, Berkshire Dairy & Food Products, LLC, Wyomissing, PA) were used to prepare the SLC gels. The SLC gels are coded according to their formula and homogenization pressure as Protein(%)-Fat(%)-NaCl(%)-pressure (MPa) (Table 1). The SLC gels in this study contained 2 levels of protein (8 and 16%, w/w), 4 levels of fat (0, 11, 22 and 33%, w/w), and 2 levels of NaCl (1.5 and 3.5%, w/w), and they were prepared under 2 different homogenization pressures (14 or 55 MPa). The formula of the samples in this study was chosen to approximate the contents and texture of commercial lipoproteic foods. The two homogenization pressures can result in significantly different emulsion $r_{h,e}$ values (Kuo & Lee, 2014b), which enables investigating the effects of fat globule particle size on the sodium released from the SLC gel. The SLC gel preparation was previously described in detail (Kuo & Lee, 2014b). Briefly, WPI was suspended in a NaCl aqueous solution at 45 °C and incubated at 6–8 °C overnight. Then, the WPI suspension was pre-homogenized with pre-melted AMF at 45 °C using an IKA T-25 Digital High-Speed Homogenizer (IKA-Works Inc., Wilmington, NC, USA). The pre-emulsion was pressure homogenized using an APV 2-stage homogenizer (15 MR, SPX Flow Technology, Soeborg, Denmark) and then heated at 90 °C for 30 min to form the SLC gels. Three to five batches were made for each SLC gel sample.

2.2. USAXS measurement

The USAXS combined with pinhole SAXS was carried out using the Bonse-Hart double-crystal USAXS instrument at beamline 15-ID-D operated by ChemMatCARS at the Advanced Photon Source, Argonne National Laboratory, Argonne, IL, USA (Ilavsky et al., 2009). The 1 mm thick gel sample was sealed in a silicone isolator (JTR20R-A2-1.0-Press-To-Seal, Grace Bio-Labs, Inc., Bend, Oregon, USA). After temperature equilibration for 3 h, the specimen was measured at the scattering vector range $Q = 0.0001$ to 1.35 $Å^{-1}$ at 20 °C, where Q is equal to $4\pi\sin(\theta/2)/\lambda$, and θ and λ are the scattering angle and beam wavelength, respectively. The USAXS measurement was carried out for all samples listed in Table 1 except for one sample due to instrument operational error. Background and absorption corrections for the 1-D profile and subsequent data analyses were performed by IGOR Pro v6.12 with the Irena package (Ilavsky & Jemian, 2009). The Modeling II macro of the Irena package was used to fit the profile of the slit-smeared data (slit length 0.02677 and 0.028503 $Å^{-1}$ for the samples with 1.5% and 3.5% NaCl, respectively). A spheroid with an aspect ratio of one was used as the structure for the fittings of both $r_{g,p}$ and $r_{g,f}$ in this study. Selected SLC emulsions (Fig. 1) were also measured prior to the heating to compare the structural change before and after the gelation.

APPENDIX A-3 (Cont.)

Table 1
Formula and homogenization pressure of the solid lipoproteic colloid (SLC) gels. Sample code represents protein(%,w/w)-fat(%,w/w)-NaCl(%,w/w)-homogenization pressure(MPa).

Protein (%, w/w)	Fat (%, w/w)	Sample code			
		1.5% (w/w) NaCl		3.5% (w/w) NaCl	
		Homogenization at 14 MPa	Homogenization at 14 MPa	Homogenizatio at 14 MPa	Homogenization at 55 MPa
8	0	8-0-1.5-14	8-0-1.5-55	8-0-3.5-14	8-0-3.5-55
8	11	8-11-1.5-14	8-11-1.5-55	8-11-3.5-14	8-11-3.5-55
8	22	8-22-1.5-14	8-22-1.5-55	8-22-3.5-14	8-22-3.5-55
8	33	8-33-1.5-14	8-33-1.5-55	8-33-3.5-14	8-33-3.5-55
16	0	16-0-1.5-14	16-0-1.5-55	16-0-3.5-14	16-0-3.5-55
16	11	16-11-1.5-14	16-11-1.5-55	16-11-3.5-14	16-11-3.5-55
16	22	16-22-1.5-14	16-22-1.5-55	16-22-3.5-14	16-22-3.5-55
16	33	16-33-1.5-14	16-33-1.5-55	16-33-3.5-14	16-33-3.5-55

2.3. Hydrodynamic radius, gel morphology, sodium release and textural properties

To investigate the correlations of the gel $r_{g,f}$ and the emulsion $r_{h,e}$ with sodium release from the gel, ten SLC samples (8-22-1.5-55, 8-33-1.5-55, 8-33-1.5-14, 16-11-1.5-55, 16-11-1.5-14 and their five counterparts with 3.5% NaCl) were selected for characterizations of the emulsion $r_{h,e}$, gel morphology, sodium release and textural properties. Our previous study (Kuo & Lee, 2014b) showed wide variations in sodium release across the SLC gels with 1.5% NaCl listed above. The samples with 3.5% NaCl were also selected to compare the effects of the gel $r_{g,f}$ and the emulsion $r_{h,e}$ at different levels of sodium.

The emulsion $r_{h,e}$ was observed via DLS using a ZetaPALS Zeta potential analyzer (Brookhaven Instruments Co., Holtsville, N.Y., U.S.A.) at 25 °C. After the vacuum procedure, the freshly made emulsions were diluted with DI water to reach the appropriate intensity for the DLS measurement. The rh,e values were collected from the intensity-weighted particle size distribution, which was averaged from 3 instrumental readings. Three to five DLS measurements were completed for each sample.

The internal morphology of the SLC gels was examined using environmental scanning electron microscopy with a field emission electron gun (ESEM, FEI Co., Hillsboro, Oreg., U.S.A.). The gels were cut into $3 \times 3 \times 7$ mm^3 sticks and then freeze fractured in liquid nitrogen. The freeze-fractured gels were immediately mounted on the stage, and ice in the samples was allowed to sublime (i.e., freeze etching) at 1 Torr using the wet mode in the ESEM chamber. The fractured face was then observed with an accelerating voltage of 20 kV.

The sodium release from the SLC gels was measured by simultaneously compressing the gel in DI water and measuring the conductivity of the water at room temperature (23 °C) (de Loubens and others 2011a). The samples were compressed using a texture analyzer (TA-XT2i, Texture Technologies Corp., Scarsdale, N.Y., U.S.A.). The conductivity was measured using a conductivity probe (Orion DuraProbe 4-Electrode Conductivity Cells 013005MD) connected with an Orion VERSA STAR Multiparameter Benchtop Meter (Thermo Fisher Scientific Inc., Waltham, Mass, U.S.A.). A cylindrical sample of SLC gel (25.4-mm dia., 25.4-mm length) was placed in a 500 mL jar under a TA-25 cylinder probe (50-mm dia., aluminum) of the texture analyzer. First, 400 mL of DI water was added into the jar. After 25 s, the texture analyzer began compressing the gel at a crosshead speed of 1.0 mm/s until 80% strain. The conductivity of the DI water was read every 5 s for a total of 365 s while the water was stirred at 200 rpm by a mechanical stirrer. Three parameters were extracted from the curves of the in vitro sodium release (Fig. 2). The maximum rate of sodium release, R_{max}, is the greatest slope calculated from any 3 continuous data points along the concentration–time curve. The maximum concentration of sodium release, C_{max}, is the sodium concentration at the end of the measurement. The area under the curve of sodium release, AUC, is the integrated area under the concentration–time curve.

The textural properties of the SLC gels were measured via a compression test using the texture analyzer (TA-XT2i, Texture Technologies Corp., Scarsdale, N.Y., U.S.A.) at room temperature (23 °C). A thin layer of mineral oil (Sigma 330779, Sigma–Aldrich, St. Louis, Mo., U.S.A.) was spread on top of the gel. The gels were then compressed under the TA-25 cylinder probe (50-mm dia., aluminum) at a speed of 1 mm/s to a maximum strain of 80%. The serum release from the gels during the compression test was collected by a pre-weighed filter paper (Whatman 42, Maidstone, Kent, U.K.) placed underneath the gel. The serum release is the difference in the weight of the filter paper before and after the compression of the gel.

2.4. Statistical analyses

Pearson correlation was used for all the correlation analyses in this study. For all the SLC gels, the gel $r_{g,p}$ and the gel $r_{g,f}$ were correlated with the gel formula and treatment. For the ten further characterized samples (listed in Section 2.2), the USAXS-derived gel $r_{g,f}$ and the DLS-derived emulsion $r_{h,e}$ were correlated with the sodium release and textural properties of the SLC gels.

3. Results and discussion

3.1. Structure of the SLC gels formed via heat-induced gelation

3.1.1. Structural formation of the non-fat gels

Fig. 1A shows the USAXS profiles of the non-fat dispersions before the heat gelation process and their corresponding gels. The non-fat dispersions (Fig. 1A, 8-0-1.5-14, 8-0-1.5-55, and 16-0-1.5-55 dispersions) presented knee-like patterns, with the knee at approximately 0.06 $Å^{-1}$. Based on the Guinier approximation, these curves represented the particles with the gyration radius (r_g) between 1.7 and 2.2 nm. These sizes corresponded to the r_gs of the native beta-lactoglobulin (bLG) monomers or dimers (1.4–1.7 and 2.1–2.3 nm, respectively) (Barteri, Gaudiano, Rotella, Benagiano, & Pala, 2000; Gottschalk, Nilsson, Roos, & Halle, 2003; Moitzi et al., 2011; Verheul, Pedersen, Roefs, & de Kruif, 1999; Witz, Luzzati, & Timasheff, 1964). These sizes also corresponded to the r_g of the native alpha-lactalbumin (aLA) (1.6 nm) (Arai et al., 2002). In WPI, bLG is the most abundant component, followed by aLA (typically ranging from 44 to 70% w/w and 14–22% w/w, respectively) (Farrell et al., 2004; Foegeding, Luck, & Vardhanabhuti, 2011; Lucey, 2014). Therefore, the $r_{g,p}$s of the above non-fat dispersions may be an average of the r_gs of the bLG and the aLA present in the sample.

APPENDIX A-3 (Cont.)

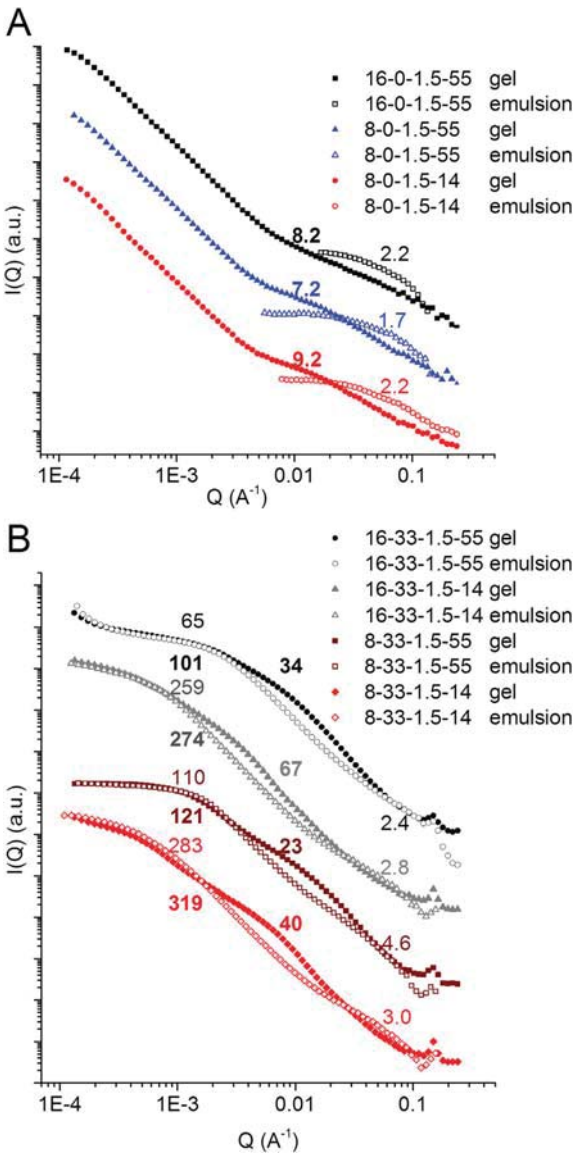

Fig. 1. Slit smeared USAXS profiles of the SLC emulsions and their counterpart gels. A. Non-fat samples and B. Fat-containing samples. The curves are vertically shifted to avoid overlap. The positive numbers are the rg values of the particles in nanometer, with bolded numbers being those of the gels. The negative numbers are the slope of the power law decay exponents.Sample code represents protein(%,w/w)-fat(%,w/w)-NaCl(%,w/w) homogenization pressure(MPa).

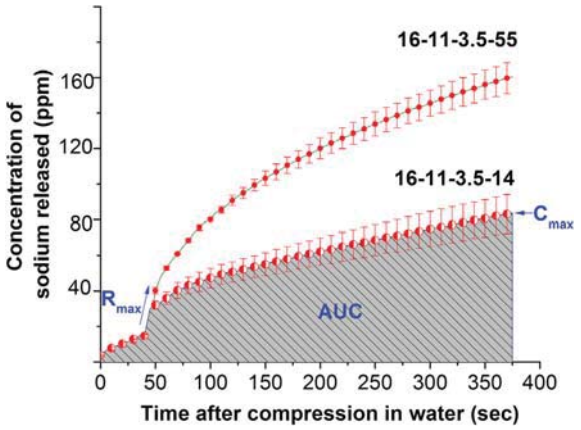

Fig. 2. Representative curves of the in vitro sodium release of two SLC gels. The maximum rate of sodium release, Rmax, the maximum concentration of sodium release, Cmax, and the area under the curve of sodium release, AUC were derived from each curve as indicated in the graph. Sample code represents protein (%,w/w)–fat (%,w/w)–NaCl (%,w/w)–homogenization pressure (MPa).

The USAXS profiles of the non-fat gels (Fig. 1A, 8-0-1.5-14, 8-0-1.5-55, and 16-0-1.5-55 gels) also displayed the knee-like patterns, but they were shifted toward the lower Q range compared with those of their corresponding dispersions. The Guinier approximation resulted in the $r_{g,p}$s of the gels ranging between 7.2 and 9.2 nm, much higher than the corresponding $r_{g,p}$s of the dispersions. These particles in the gels could be aggregates consisting of bLG and aLA. Previous research revealed that bLG formed aggregates with aLA via disulfide bonds and hydrophobic interactions when heated in an aqueous solution (Dalgleish, Senaratne, & Francois, 1997). Protein aggregates with a radius of 29 nm were reported when a WPI solution (3% w/w protein, 54 mM NaCl) was heated at 90 °C for 5 min (Ryan et al., 2012). The much smaller WPI aggregates found in this study as compared with those in previous studies could be due to the homogenization treatment prior to heating. The shearing force of the homogenization may have dispersed the protein particles, disrupting the inter-particle interactions and thus reducing the degree of aggregation. Our previous work has shown that the particle size of protein aggregates decreases with increasing homogenization pressure (Kuo & Lee, 2014b). Additionally, differences in the concentrations of protein and NaCl and in the heating conditions could also lead to the varying particle size of the protein aggregates.

At the lower Q range ($Q < 0.005$ Å^{-1}), the non-fat dispersions (Fig. 1A, 8-0-1.5-14, 8-0-1.5-55, and 16-0-1.5-55 dispersions) did not show any scattering signals, indicating a lack of larger structures at this scale (approximately 100 nm–5 μm). The non-fat gels (Fig. 1A, 8-0-1.5-14, 8-0-1.5-55, and 16-0-1.5-55 gels) showed a linear log–log decay in the Q range of 0.0002–0.002 Å^{-1}. A power law fitting in this Q range on the de-smeared data provided exponents of approximately 4. This power law decay is attributed to Porod scattering by the smooth surfaces of larger scatterers (Feigin & Svergun, 1987; Yoshida, Fukushima, & Yamaguchi, 2014). The Guinier regions of these larger scatterers are beyond the lowest Q (corresponding to 2 μm) in the USAXS measurement in this study. These larger scatterers are believed to be the protein particulates in the SLC gels. These protein particulates, with sizes above 2 μm and smooth surfaces, can be identified in the ESEM image of the SLC gel 8-0-1.5-14 (Fig. 3A).

3.1.2. Structure formation of the fat-containing SLC gels

Fig. 1B shows the USAXS profiles of the fat-containing SLC emulsions before the heat gelation process and their corresponding gels. At $Q = 0.15$ Å^{-1}, a peak was observed in the patterns of the fat-containing samples. This peak is the diffraction of the 2L (bilayered stacking) form of the crystalline AMF within the fat globules in the emulsion structure (Lopez, Lavigne, Lesieur, Bourgaux, & Ollivon, 2001). Similar to the non-fat dispersions (Fig. 1A), the fat-containing emulsions (Fig. 1B, 8-33-1.5-14, 8-33-1.5-55, 16-33-1.5-14 and 16-33-1.5-55 emulsions) exhibited scattering at

APPENDIX A-3 (Cont.)

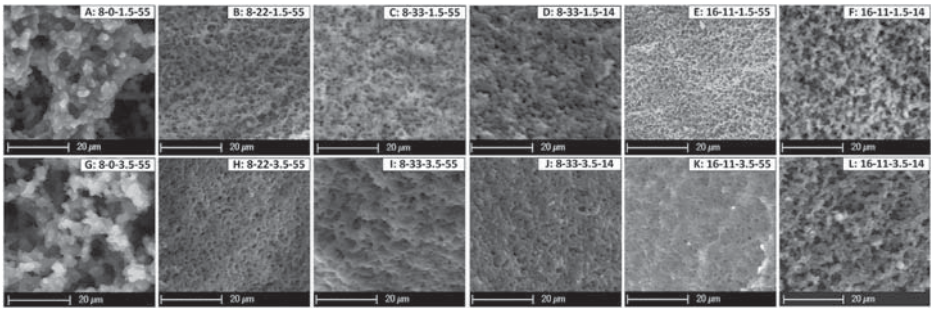

Fig. 3. Environmental scanning electron microscopy (ESEM) images of the cross-sections of frozen-fractured lipoproteic emulsion gels. Sample code represents protein(%,w/w)-fat(%,w/w)-NaCl(%,w/w)-homogenization pressure(MPa).

approximately Q = 0.06 $Å^{-1}$, suggesting that this pattern was from the protein scattering. The $r_{g,p}$s of these particles, however, range between 2.4 and 4.6 nm, slightly higher than those in the non-fat emulsions (1.7–2.2 nm). The higher emulsion $r_{g,p}$s suggests more aggregation of the bLG or the aLA into oligomers. For example, the bLG octamer has an r_g of 3.4 nm (Timasheff & Townend, 1964; Witz et al., 1964). The higher degree of protein aggregation could be attributed to the relatively higher proportion of protein to water in the fat-containing emulsions than in the non-fat dispersions. For example, the proportion of protein to water in the emulsion 8-33-1.5-14 and the dispersion 8-0-1.5-14 are 0.12 and 0.09, respectively.

As in the non-fat samples (Fig. 1A), the protein scattering patterns of the fat-containing samples shifted toward lower Qs after the gelation process (Fig. 1B, 8-33-1.5-14, 8-33-1.5-55, 16-33-1.5-14 and 16-33-1.5-55 gels). The $r_{g,p}$s are again higher than their non-fat counterparts, ranging between 23 and 67 nm. This difference could be the net result from higher concentrations of NaCl and protein in the aqueous phase of the fat-containing samples. Previous studies on heating WPI and bLG solutions showed that the aggregate diameters increased with increasing NaCl concentrations due to lower intermolecular repulsion, enhanced chemical and physical aggregation, and lower protein solubility (Ryan et al., 2012; Verheul, Roefs, & de Kruif, 1998). Additionally, the aggregate association rate increased with increasing concentrations of either NaCl or protein (Bryant & McClements, 2000; Marangoni, Barbut, McGauley, Marcone, & Narine, 2000; Ryan et al., 2012; Wu, Xie, & Morbidelli, 2005).

At a Q of approximately 0.001 $Å^{-1}$, all the fat-containing samples (Fig. 1B) showed clear knees in the scattering profiles, which were used to calculate the $r_{g,f}$. This pattern was attributed to the fat globules for the following reasons. First, this pattern was not observed in the profiles of the non-fat samples. Second, compared with $r_{g,p}$, this pattern showed relatively moderate changes in size after the gelation, which better reflected the status of the fat globules rather than the protein aggregates during heating. Third, as will be discussed in section 3.3.1., ESEM observation of the cross-sectional area of the SLC gels revealed fat particles with a radius of approximately 500 nm, corresponding to the $r_{g,f}$ range between 77 and 711 nm (Table 2).

3.2. Effect of formulation and treatments on the SLC gel structure

Fig. 4 shows the USAXS profiles of the SLC gels made with different formulas and at different homogenizations pressures. All the non-fat gels in Fig. 4 shared similar profile features, including knee-like scattering from the protein aggregates and a power law decay representing the 3-D networking of the aggregates. Likewise, all the fat-containing gels in Fig. 4 shared similar profile features,

Table 2
Radii of gyration of the protein aggregates ($r_{g,p}$) and the fat globules ($r_{g,f}$) in the SLC gels derived from USAXS measurement. Sample code represents protein(%,w/w)-fat(%,w/w)-NaCl(%,w/w)-homogenization pressure(MPa).

Sample (n for NaCl%)	$r_{g,p}$ (nm)		$r_{g,f}$ (nm)	
	n = 1.5	n = 3.5	n = 1.5	n = 3.5
8-0-n-14	9.2	3.1	–	–
8-11-n-14	87.0	59.8	449.3	371.5
8-22-n-14	54.9	53.6	484.6	387.3
8-33-n-14	40.0	37.6	319.3	291.2
16-0-n-14	8.8	2.8	–	–
16-11-n-14	125.1	155.5	457.5	711.0
16-22-n-14	91.5	103.0	325.2	407.8
16-33-n-14	67.0	N.D.[a]	274.0	N.D.[a]
8-0-n-55	7.2	7.5	–	–
8-11-n-55	27.5	24.4	120.5	125.2
8-22-n-55	22.2	21.6	125.8	121.6
8-33-n-55	22.5	31.7	121.2	110.1
16-0-n-55	8.2	20.7	–	–
16-11-n-55	45.5	35.5	153.6	91.2
16-22-n-55	35.0	24.3	113.6	77.4
16-33-n-55	33.5	30.2	101.0	66.3

[a] Sample not measured due to operation error.

including an AMF diffraction peak and two knee-like scatterings from the protein aggregates and the fat globules. The AMF peak intensity increased with the increasing fat content in the formula, implying a successful incorporation of fat into the SLC gels. Additionally, the AMF peaks are broader in the gels made with higher homogenization pressure (Fig. 4, C vs. A and D vs. B, 55 vs. 14 MPa). According to the Scherrer formula, wider diffraction peaks imply smaller crystallites (Patterson, 1939). Hence the broader AMF peaks indicated smaller fat crystals in the fat globules. This finding confirmed that the higher pressure effectively dispersed the emulsion structure. Table 2 lists the values of the gel $r_{g,p}$ and $r_{g,f}$ derived from the Guinier approximation of the USAXS profiles. Overall, both the gel $r_{g,p}$ and $r_{g,f}$ decreased with increasing homogenization pressure ($p < 0.01$). This correlation is much stronger when only the fat-containing gels were analyzed ($p < 0.001$). Higher homogenization pressures have been shown to induce partial denaturation of proteins, improving protein adsorption on the fat globules and thus resulting in a more stable emulsion system (Lee, Lefèvre, Subirade, & Paquin, 2009). Within the group of fat-containing gels made at the low homogenization pressure, the $r_{g,p}$ was positively correlated ($p < 0.01$) with the protein content and negatively correlated ($p < 0.05$) with fat content. A similar positive correlation between the gel $r_{g,p}$ and the protein content was found within the group of fat-containing gels made with the high homogenization pressure ($p < 0.05$). These correlations

APPENDIX A-3 (Cont.)

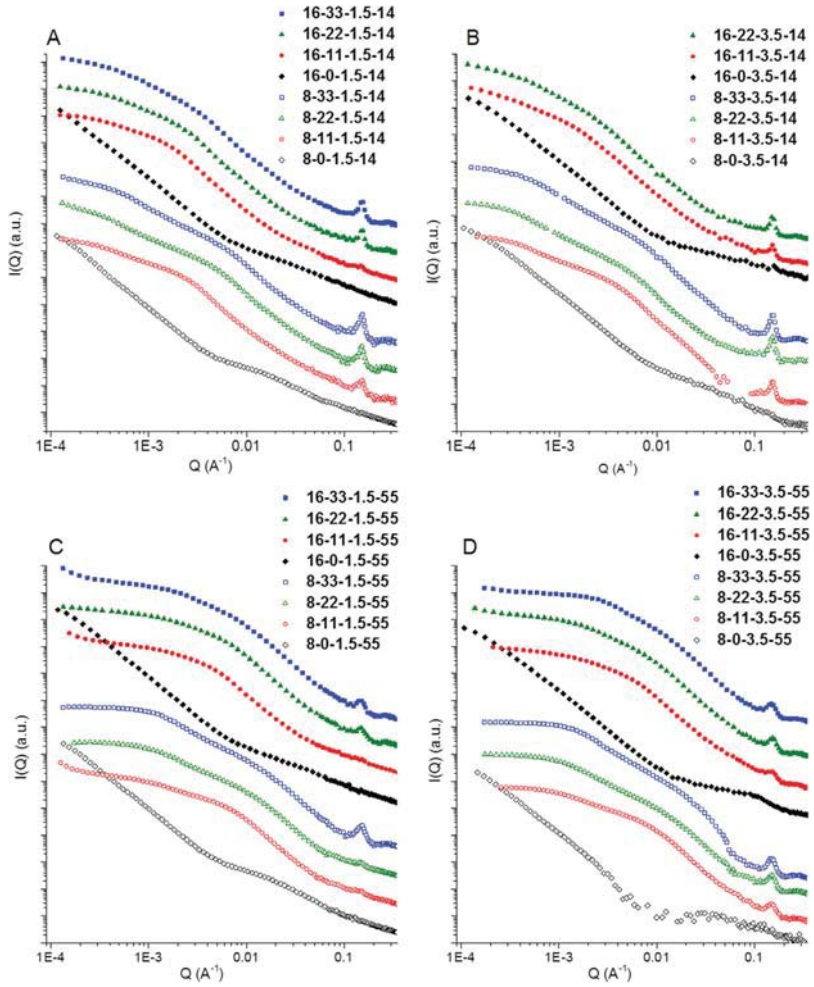

Fig. 4. Slit smeared USAXS profiles of the SLC gels made with 1.5% (A, C) or 3.5% (B, D) NaCl at homogenization pressures of 14 (A, B) or 55 (C, D) MPa. The curves are vertically shifted to avoid overlap. Sample code represents protein(%,w/w)-fat(%,w/w)-NaCl(%,w/w)- homogenization pressure(MPa).

between the $r_{g,p}$s and the protein and fat contents indicated the counteracting behaviors between the protein and fat during the emulsification and gel formation. A higher protein content may promote the probability of protein–protein interaction, leading to larger protein aggregates. A higher fat content may interfere with the protein association, preventing the growth of the protein aggregates. On the other hand, a higher fat content may require a greater fraction of protein for emulsification, reducing the available amount of protein for protein–protein interaction. In the group of fat-containing samples made with the higher homogenization pressure, the gel $r_{g,p}$ did not significantly depend on the fat content. This lack of dependence may be due to the more thorough dispersion of the protein at the higher pressure, which overcame the effect of fat content on the gel $r_{g,p}$.

3.3. Dependence of sodium release on the gel $r_{g,f}$ or emulsion $r_{h,e}$

3.3.1. Correlations between the gel $r_{g,f}$ and sodium release

To understand the influence of the gel $r_{g,f}$ and the emulsion $r_{h,e}$ on sodium release from the SLC gels, ten fat-containing SLC samples (listed in Section 2.2) were further characterized for sodium release, the texture and morphology of the gels, and the emulsion size, $r_{h,e}$. The sodium releaseby the gel as it was compressed by the texture analyzer was measured in water. However, the behavior of the textural properties of the samples acquired during the sodium release measurements was found to be consistent with the behavior observed in the actual textural analysis (data not shown). Hence, the breakdown properties of the gels observed from the textural analysis can be used to explain the differences in their sodium release properties. Table 3 shows the sodium release and textural properties of the SLC gels with 3.5% NaCl and the $r_{h,e}$ values of the corresponding emulsions. The properties of the SLC samples with 1.5% NaCl can be found in our previous study (Kuo & Lee, 2014b). Table 4 shows some of the correlation coefficients between the above properties and the gel $r_{g,f}$ derived from USAXS. For the SLC gels with 3.5% NaCl, the gel $r_{g,f}$ was negatively correlated with the C_{max} (the maximum concentration of released sodium) and the AUC (area under the curve of sodium release vs. time plot) at a highly significant level ($p < 0.005$). These correlations can be attributed to the effect of fat on the breakdown properties of the

APPENDIX A-3 (Cont.)

Table 3
Sodium release and textural properties of the SLC gels with 3.5% NaCl, and the hydrodynamic radius of the droplets in the corresponding emulsions[a]

Sample	R_{max} ± SD[b] (ppm Na/s)	C_{max} ± SD (ppm Na)	AUC ± SD (10^{-3} ppm Na.s)	Serum release ± SD (g)	Max stress ± SD (Kpa)	Strain at maximum stress ± SD (%)	Emulsion $r_{h,e}$ ± SD (nm)
8-22-3.5-55	0.3 ± 0.77 ab[c]	181.21 ± 5.88a	43.13 ± 1.52a	0.49 ± 0.08b	112.25 ± 15.80 ab	54.08 ± 3.42c	127.88 ± 22.42b
8-33-3.5-55	2.59 ± 0.49 ab	166.53 ± 10.15 ab	39.54 ± 2.54 ab	0.30 ± 0.07c	166.29 ± 29.46 ab	56.41 ± 1.12c	134.62 ± 10.40b
8-33-3.5-14	1.76 ± 0.30b	150.44 ± 9.70b	35.51 ± 2.44b	0.47 ± 0.01b	101.22 ± 3.89b	60.28 ± 1.98b	329.18 ± 13.17a
16-11-3.5-55	2.90 ± 0.12a	178.09 ± 17.75a	43.39 ± 4.50a	0.47 ± 0.07b	179.14 ± 16.04a	46.30 ± 2.00d	296.16 ± 3.34b
16-11-3.5-14	2.09 ± 0.31 ab	95.18 ± 20.13c	24.41 ± 5.66c	0.90 ± 0.04a	172.75 ± 83.98a	69.61 ± 2.72a	352.12 ± 33.19a

[a] See Kuo and Lee (2014b) for the properties of the SLC gels with 1.5% NaCl.
[b] R_{max}, maximum rate of sodium release; C_{max}, maximum concentration of sodium release; AUC, area under the curve of sodium release. Serum release, amount of liquid expelled from the sample during the compression test. $r_{h,e}$, hydrodynamic radius of the emulsions particles measured using dynamic light scattering (DLS).
[c] The numbers followed by the same letters are not significantly different.

Table 4
Correlation coefficients between sodium release, textural properties and particle sizes of fat globules of the SLC gels at constant NaCl contents[a]

	C_{max} (ppm Na)		AUC (10^{-3} ppm Na.s)		Strain at maximum stress (%)		Emulsion $r_{h,e}$ from DLS (nm)		Gel $r_{g,f}$ from USAXS (nm)	
NaCl % in SLC gels	1.5	3.5	1.5	3.5	1.5	3.5	1.5	3.5	1.5	3.5
R_{max}[b] (ppm Na/s)	0.989***[c]	0.553	0.994****	0.610	0.924*	−0.749	0.151	−0.412	0.498	−0.578
C_{max} (ppm Na)			0.999****	0.996****	0.957*	−0.913*	0.170	−0.652	0.551	0.987***
AUC (10^{-3} ppm Na.s)					0.948*	−0.940*	0.163	−0.632	0.537	0.979***
Serum release (g)					0.773	0.705	0.599	0.642	0.821	0.923*
Strain at maximum stress (%)							0.415	0.399	0.761	0.902*
Emulsion $r_{h,e}$ from DLS (nm)									0.883*	0.660

[a] Refer to Section 2.2 for the list of the samples. The correlation was carried on each of the five samples with the same NaCl contents.
[b] R_{max}, maximum rate of sodium release; C_{max}, maximum concentration of sodium release; AUC, area under the curve of sodium release. Serum release, amount of liquid expelled from the sample during the compression test. $r_{h,e}$, hydrodynamic radius of the emulsions particles measured using dynamic light scattering (DLS).
[c] The numbers with the superscripts of one, two, three or four asterisks indicate significant correlations for $P < 0.05$, 0.01, 0.005 and 0.001, respectively.

SLC gels. Previous studies on SLC gels showed that, at the same total fat content, smaller fat globules implied a gel network with a higher number of randomly dispersed fat particles (Kuo & Lee, 2014b; Phan et al., 2008). As fat interfered with the integrity of the protein network, the higher number of dispersed fat particles could lead to a greater extent of breakdown and more debris when compressed. This hypothesis can be supported by the positive correlation found between the gel $r_{g,f}$ and the strain at the maximum stress of the SLC gels with 3.5% NaCl (Table 4). In other words, the required strain to break the gels decreased as the gel $r_{g,f}$ decreased. The greater extent of breakdown and more debris, which results in more total surface area for the broken gels, would favor the enhanced release of sodium from the gel in a given period of time (de Loubens et al., 2011). This hypothesis can be supported by the negative correlations of the strain at maximum stress with the C_{max} and with the AUC in the SLC gels with 3.5% NaCl (Table 4). The negative correlation between the gel $r_{g,f}$ and the sodium release, however, was not significant in the SLC gels with 1.5% NaCl. This lack of significance may be due to a difference in the force of inter-protein interaction among the SLC gels with varying NaCl contents. A higher amount of NaCl in the SLC gels implied greater charge screening on the repulsive force between protein molecules. Previous studies showed that this improved screening favored the aggregation, branching, and densification of whey protein particles (Langton & Hermansson, 1996; Pouzot, Nicolai, Durand, & Benyahia, 2004; Verheul et al., 1998). Hence, an overall stronger protein–protein interaction was expected in the protein networks with higher NaCl contents (Hussain, Gaiani, Jeandel, Ghanbaja, & Scher, 2012; Lorenzen & Schrader, 2006). As a result, the SLC gels with 3.5% NaCl exhibited relatively stronger inter-protein interaction than the SLC gels with 1.5% NaCl, and this stronger interaction made the initiation of break upon compression more likely to occur at the protein-fat interface. In other words, the properties of the protein-fat interface dominated the breakdown properties of the SLC gels with 3.5% NaCl. Decreased gel $r_{g,f}$ led to higher sodium release due to increases in the surface area, the probability of break initiation, and the extent of breakdown. In contrast, the protein–-protein interaction in the SLC gels with 1.5% NaCl was weaker than that with 3.5% NaCl, and thus the breakdown at the protein-fat interface might not have been dominant. This difference explained the lack of correlation between the gel $r_{g,f}$, the strain at maximum stress, and the sodium release in the SLC gels with 1.5% NaCl. The above hypothesis can be supported by the ESEM images of the SLC gels shown in Fig. 3. The SLC gels with 3.5% NaCl displayed a denser and more aggregated network morphology than that of the SLC gels with 1.5% NaCl, which suggested greater protein–protein interaction at higher NaCl contents. Furthermore, for the two SLC gels with 3.5% NaCl made with the lower homogenization pressure (8-33-3.5-14 and 16-11-3.5-14, Fig. 3J and L), some bright spherical fat particles stood out from the protein network. In the images of the corresponding 1.5% NaCl gels (8-33-1.5-14 and 16-11-1.5-14, Fig. 3D and F), these fat globules were less visible and more embedded within the protein network. This difference in the appearance of the fat globules among the protein matrix indicated a possibly stronger protein–protein interaction and weaker protein-fat interaction in the SLC gels with the higher NaCl content.

3.3.2. Correlations between the emulsion $r_{h,e}$ and sodium release during compression

No significant correlation was found between the emulsion $r_{h,e}$ and the sodium release from the SLC gels with either 1.5 or 3.5% NaCl (Table 4). This lack of correlation could be because the

APPENDIX A-3 (Cont.)

emulsion $r_{h,e}$ was measured in the SLC emulsions before the heat-induced gelation. Among the 10 samples that underwent the correlation analysis, most of them showed less than ±10% difference between the gel $r_{g,f}$ and the emulsion $r_{h,e}$ values. This consistency implied that the emulsion droplets were relatively stable during the heating process. However, for the samples 16-11-1.5-14 and 16-11-3.5-14, the gel $r_{g,f}$ values were 61% and 101% greater than the emulsion $r_{h,e}$ values. This increase suggested that the emulsion droplets in these two samples were less stable and might have coalesced more drastically during the heating.

According to Fig. 1B showing some selected SLC samples with 1.5% NaCl, the $r_{g,f}$s grew by 10–50% after the gelation. Hence, the fat globules in both SLC gels made with 1.5% and 3.5% NaCl exhibited inconsistent degrees of coalescence as a result of the heating. In the case of 3.5% NaCl, because the gel breakdown and accordingly the sodium release were directly related to the size of the fat globules in the gel, the USAXS-derived gel $r_{g,f}$ proved to be more predictive of sodium release than the DLS-based emulsion $r_{h,e}$.

4. Conclusions

In this study, USAXS was successfully used as a novel technique to investigate the structure of SLC gels and as a demonstration of its potential to predict the sodium release properties of the gels. The protein in the SLC emulsions underwent heat-induced aggregation during the gelation process, resulting in significant increases in the particle sizes of the protein aggregates. Additionally, the fat-containing gels had much larger protein aggregates compared with those in the non-fat gels. The sizes of the fat globules were comparatively more stable than those of the protein aggregates throughout the gelation. The gel $r_{g,p}$ and the gel $r_{g,f}$ were negatively correlated with the homogenization pressure, and the protein and fat contents counteractively affected the protein aggregation. For the SLC gels made with the higher NaCl content, the USAXS-derived gel $r_{g,f}$ predicted the sodium release better than the DLS-based emulsion $r_{h,e}$ did. With sodium being the primary chemical for salty stimuli, present findings in the literature do not agree on whether saltiness perception depends primarily on the maximum rate (de Loubens et al., 2011), maximum intensity or area under the curve (Morris, Koliandris, Wolf, Hort, & Taylor, 2009) of sodium delivery. Future studies evaluating the saltiness perception of the SLC gels with respect to sodium release and gel structures may help identify the governing parameters for saltiness perception. This approach can provide industrial insights and practical strategies for sodium reduction via engineering the structure of lipoproteic foods.

Acknowledgments

This research was funded by the U.S. Department of Agriculture via the National Institute of Food and Agriculture Grant (2015-67017-23089). This research used resources of the Advanced Photon Source, a U.S. Department of Energy (DOE) Office of Science User Facility operated for the DOE Office of Science by Argonne National Laboratory under Contract No. DE-AC02-06CH11357.

References

Agrawal, S. K., Sanabria-DeLong, N., Jemian, P. R., Tew, G. N., & Bhatia, S. R. (2007). Micro- to nanoscale structure of biocompatible PLA-PEO-PLA hydrogels. *Langmuir, 23*(9), 5039–5044.

Arai, M., Ito, K., Inobe, T., Nakao, M., Maki, K., Kamagata, K., et al. (2002). Fast compaction of α-lactalbumin during folding studied by stopped-flow X-ray scattering. *Journal of Molecular Biology, 321*(1), 121–132.

Barteri, M., Gaudiano, M. C., Rotella, S., Benagiano, G., & Pala, A. (2000). Effect of pH on the structure and aggregation of human glycodelin A. A comparison with beta-lactoglobulin A. *Biochimica Et Biophysica Acta-Protein Structure and Molecular Enzymology, 1479*(1–2), 255–264.

Boisard, L., Andriot, I., Martin, C., Septier, C., Boissard, V., Salles, C., et al. (2014). The salt and lipid composition of model cheeses modifies in-mouth flavour release and perception related to the free sodium ion content. *Food Chemistry, 145*(0), 437–444.

Brewer, M. S., Gills, L. A., & Vega, J. D. (1995). Sensory characteristics of potassium lactate and sodium chloride in a model system. *Journal of Sensory Studies, 10*(1), 73–87.

Bryant, C. M., & McClements, D. J. (2000). Influence of NaCl and $CaCl_2$ on cold-set gelation of heat-denatured whey protein. *Journal of Food Science, 65*(5), 801–804.

Busch, J. L. H. C., Yong, F. Y. S., & Goh, S. M. (2013). Sodium reduction: optimizing product composition and structure towards increasing saltiness perception. *Trends in Food Science & Technology, 29*(1), 21–34.

Chabanet, C., Tarrega, A., Septier, C., Siret, F., & Salles, C. (2013). Fat and salt contents affect the in-mouth temporal sodium release and saltiness perception of chicken sausages. *Meat Science, 94*(2), 253–261.

Dalgleish, D. G., Senaratne, V., & Francois, S. (1997). Interactions between alpha-lactalbumin and beta-lactoglobulin in the early stages of heat denaturation. *Journal of Agricultural and Food Chemistry, 45*(9), 3459–3464.

Desmond, E. (2006). Reducing salt: a challenge for the meat industry. *Meat Science, 74*(1), 188–196.

Desmond, E. (2007). Reducing salt in meat and poultry products. In D. Kilcast, & F. Angus (Eds.), *Reducing salt in foods – Practical strategies* (pp. 233–255). Cambridge: Woodhead Publishing.

Djordjevic, J., Zatorre, R. J., & Jones-Gotman, M. (2004). Odor-induced changes in taste perception. *Experimental Brain Research, 159*(3), 405–408.

Dotsch, M., Busch, J., Batenburg, M., Liem, G., Tareilus, E., Mueller, R., et al. (2009). Strategies to reduce sodium consumption: a food industry perspective. *Critical Reviews in Food Science and Nutrition, 49*(10), 841–851.

Dudkiewicz, A., Luo, P., Tiede, K., & Boxall, A. (2012). Detecting and characterizing nanoparticles in food, beverages and nutraceuticals. In Q. Huang (Ed.), *Nanotechnology in the food, beverage and nutraceutical industries* (pp. 53–81). Oxford: Elsevier Ltd.

Eoin, D. (2006). Reducing salt: a challenge for the meat industry. *Meat Science, 74*(1), 188–196.

Farrell, H. M., Jimenez-Flores, R., Bleck, G. T., Brown, E. M., Butler, J. E., Creamer, L. K., et al. (2004). Nomenclature of the proteins of cows' milk-Sixth revision. *Journal of Dairy Science, 87*(6), 1641–1674.

Feigin, L. A., & Svergun, D. I. (1987). *Structure analysis by small-angle X-ray and neutron scattering*. New York: Plenum Press.

Floury, J., Rouaud, O., Le Poullennec, M., & Famelart, M. (2009). Reducing salt level in food: Part 2. Modelling salt diffusion in model cheese systems with regards to their composition. *LWT – Food Science and Technology, 42*(10), 1621–1628.

Foegeding, E. A., Luck, P., & Vardhanabhuti, B. (2011). Whey protein products. In J. W. Fuquay (Ed.), *Encyclopedia of dairy sciences* (2nd ed., pp. 873–878). San Diego: Academic Press.

Gottschalk, M., Nilsson, H., Roos, H., & Halle, B. (2003). Protein self-association in solution: the bovine beta-lactoglobulin dimer and octamer. *Protein Science, 12*(11), 2404–2411.

Harada, T., & Matsuoka, H. (2004). Ultra-small-angle X-ray and neutron scattering study of colloidal dispersions. *Current Opinion in Colloid & Interface Science, 8*(6), 501–506.

Heidolph, B. B., Ray, D. K., Roller, S., Koehler, P., Weber, J., Slocum, S., et al. (2011). Looking for my lost shaker of salt... replacer: flavor, function, future. *Cereal Foods World, 56*(1), 5–19.

Hughes, E., Cofrades, S., & Troy, D. J. (1997). Effects of fat level, oat fibre and carrageenan on frankfurters formulated with 5, 12 and 30% fat. *Meat Science, 45*(3), 273–281.

Hussain, R., Gaiani, C., Jeandel, C., Ghanbaja, J., & Scher, J. (2012). Combined effect of heat treatment and ionic strength on the functionality of whey proteins. *Journal of Dairy Science, 95*(11), 6260–6273.

Ilavsky, J., Allen, A. J., Long, G. G., & Jemian, P. R. (2002). Effective pinhole-collimated ultrasmall-angle x-ray scattering instrument for measuring anisotropic microstructures. *Review of Scientific Instruments, 73*(3), 1660–1662.

Ilavsky, J., & Jemian, P. R. (2009). Irena: tool suite for modeling and analysis of small-angle scattering. *Journal of Applied Crystallography, 42*, 347–353.

Ilavsky, J., Jemian, P. R., Allen, A. J., Zhang, F., Levine, L. E., & Long, G. G. (2009). Ultra-small-angle X-ray scattering at the advanced photon source. *Journal of Applied Crystallography, 42*, 469–479.

Ilavsky, J., Zhang, F., Allen, A. J., Levine, L. E., Jemian, P. R., & Long, G. G. (2013). Ultra-small-angle x-ray scattering instrument at the advanced photon source: history, recent development, and current status. *Metallurgical and Materials Transactions A-Physical Metallurgy and Materials Science, 44A*(1), 68–76.

Jiménez-Colmenero, F. (2013). Potential applications of multiple emulsions in the development of healthy and functional foods. *Food Research International, 52*(1), 64–74.

Johnson, M. E., Kapoor, R., McMahon, D. J., McCoy, D. R., & Narasimmon, R. G. (2009). Reduction of sodium and fat levels in natural and processed cheeses: scientific and technological aspects. *Comprehensive Reviews in Food Science and Food Safety, 8*(3), 252–268.

Kalab, M., Allanwojtas, P., & Miller, S. S. (1995). Microscopy and other imaging techniques in food structure-analysis. *Trends in Food Science & Technology, 6*(6), 177–186.

Kuo, W., & Lee, Y. (2014a). Effect of food matrix on saltiness perception-implications for sodium reduction. *Comprehensive Reviews in Food Science and Food Safety,*

APPENDIX A-3 (Cont.)

13(5), 906–923.
Kuo, W., & Lee, Y. (2014b). Temporal sodium release related to gel microstructural properties-Implications for sodium reduction. *Journal of Food Science, 79*(11), E2245–E2252.
Langton, M., & Hermansson, A. (1996). Image analysis of particulate whey protein gels. *Food Hydrocolloids, 10*(2), 179–191.
Lauverjat, C., Deleris, I., Trelea, I. C., Salles, C., & Souchon, I. (2009). Salt and aroma compound release in model cheeses in relation to their mobility. *Journal of Agricultural and Food Chemistry, 57*(21), 9878–9887.
Lee, S., Lefèvre, T., Subirade, M., & Paquin, P. (2009). Effects of ultra-high pressure homogenization on the properties and structure of interfacial protein layer in whey protein-stabilized emulsion. *Food Chemistry, 113*(1), 191–195.
Lopez, C., Lavigne, F., Lesieur, P., Bourgaux, C., & Ollivon, M. (2001). Thermal and structural behavior of milk fat. 1. Unstable species of anhydrous milk fat. *Journal of Dairy Science, 84*(4), 756–766.
Lorenzen, P. C., & Schrader, K. (2006). A comparative study of the gelation properties of whey protein concentrate and whey protein isolate. *Lait, 86*(4), 259–271.
de Loubens, C., Panouillé, M., Saint-Eve, A., Déléris, I., Tréléa, I. C., & Souchon, I. (2011). Mechanistic model of *in vitro* salt release from model dairy gels based on standardized breakdown test simulating mastication. *Journal of Food Engineering, 105*(1), 161–168.
Lucey, J. A. (2014). Chapter 17-Milk protein gels. In H. Singh, M. Boland, & A. Thompson (Eds.), *Milk proteins* (2nd ed., pp. 493–523). San Diego: Academic Press.
Marangoni, A. G., Barbut, S., McGauley, S. E., Marcone, M., & Narine, S. S. (2000). On the structure of particulate gels – the case of salt-induced cold gelation of heat-denatured whey protein isolate. *Food Hydrocolloids, 14*(1), 61–74.
Moitzi, C., Donato, L., Schmitt, C., Bovetto, L., Gillies, G., & Stradner, A. (2011). Structure of beta-lactoglobulin microgels formed during heating as revealed by small-angle X-ray scattering and light scattering. *Food Hydrocolloids, 25*(7), 1766–1774.
Morris, C., Koliandris, A., Wolf, B., Hort, J., & Taylor, A. J. (2009). Effect of pulsed or continuous delivery of salt on sensory perception over short time intervals. *Chemosensory Perception, 2*(1), 1–8.
Nave, C., Diakun, G. P., & Bordas, J. (1986). Ultra-small angle X-ray diffraction from muscle. Nuclear instruments and methods in physics research section A: accelerators, spectrometers. *Detectors and Associated Equipment, 246*(1–3), 609–612.
Panouille, M., Saint-Eve, A., de Loubens, C., Deleris, I., & Souchon, I. (2011). Understanding of the influence of composition, structure and texture on salty perception in model dairy products. *Food Hydrocolloids, 25*(4), 716–723.
Patterson, A. L. (1939). The Scherrer formula for x-ray particle size determination. *Physical Review, 56*(10), 978–982.
Peyronel, F., Pink, D. A., & Marangoni, A. G. (2014a). Triglyceride nanocrystal aggregation into polycrystalline colloidal networks: ultra-small angle X-ray scattering, models and computer simulation. *Current Opinion in Colloid & Interface Science, 19*(5), 459–470.
Peyronel, F., Quinn, B., Marangoni, A. G., & Pink, D. A. (2014b). Ultra small angle X-ray scattering for pure tristearin and tripalmitin: model predictions and experimental results. *Food Biophysics, 9*(4), 304–313.
Phan, V. A., Yven, C., Lawrence, G., Chabanet, C., Reparet, J. M., & Salles, C. (2008). *in vivo* sodium release related to salty perception during eating model cheeses of different textures. *International Dairy Journal, 18*(9), 956–963.
Phelps, T., Angus, F., Clegg, S., Kilcast, D., Narain, C., & den Ridder, C. (2006). Sensory issues in salt reduction. *Food Quality and Preference, 17*(7–8), 633–634.
Pouzot, M., Nicolai, T., Durand, D., & Benyahia, L. (2004). Structure factor and elasticity of a heat-set globular protein gel. *Macromolecules, 37*(2), 614–620.
Ruusunen, M., Vainionpää, J., Lyly, M., Lähteenmäki, L., Niemistö, M., Ahvenainen, R., et al. (2005). Reducing the sodium content in meat products: the effect of the formulation in low-sodium ground meat patties. *Meat Science, 69*(1), 53–60.
Ryan, K. N., Vardhanabhuti, B., Jaramillo, D. P., van Zanten, J. H., Coupland, J. N., & Foegeding, E. A. (2012). Stability and mechanism of whey protein soluble aggregates thermally treated with salts. *Food Hydrocolloids, 27*(2), 411–420.
Sala, G., van Vliet, T., Cohen Stuart, M. A., Aken, G. A. V., & van de Velde, F. (2009). Deformation and fracture of emulsion-filled gels: effect of oil content and deformation speed. *Food Hydrocolloids, 23*(5), 1381–1393.
Sinopoli, D. A., & Lawless, H. T. (2012). Taste properties of potassium chloride alone and in mixtures with sodium chloride using a check-all-that-apply method. *Journal of Food Science, 77*(9), S319–S322.
Stieger, M. (2011). Texture-taste interactions: enhancement of taste intensity by structural modifications of the food matrix. *Procedia Food Science, 1*(0), 521–527.
Stieger, M., & van de Velde, F. (2013). Microstructure, texture and oral processing: new ways to reduce sugar and salt in foods. *Current Opinion in Colloid & Interface Science, 18*(4), 334–348.
Timasheff, S., & Townend, R. (1964). Structure of the beta-Lactoglobulin tetramer. *Nature, 203*(494), 517–519.
Väänänen, T., Ikonen, T., Jokela, K., Serimaa, R., Pietilä, L., & Pehu, E. (2003). X-ray scattering study on potato (*Solanum tuberosum* L.) cultivars during winter storage. *Carbohydrate Polymers, 54*(4), 499–507.
Verheul, M., Pedersen, J. S., Roefs, S. P. F. M., & de Kruif, K. G. (1999). Association behavior of native beta-lactoglobulin. *Biopolymers, 49*(1), 11–20.
Verheul, M., Roefs, S. P. F. M., & de Kruif, K. G. (1998). Kinetics of heat-induced aggregation of beta-lactoglobulin. *Journal of Agricultural and Food Chemistry, 46*(3), 896–903.
van Vliet, T., Luyten, H., & Walstra, P. (1993). Time-dependent fracture-behavior of food. In E. Dickinson, & P. Walstra (Eds.), *Food colloids and polymers: Stability and mechanical properties* (pp. 175–190). Cambridge: Royal Society of Chemistry.
Witz, J., Luzzati, V., & Timasheff, S. N. (1964). Molecular interactions in beta-lactoglobulin. 8. small-angle X-ray scattering investigation of geometry of beta-lactoglobulin A tetramerization. *Journal of the American Chemical Society, 86*(2), 168. -&.
Wu, H., Xie, J. J., & Morbidelli, M. (2005). Kinetics of cold-set diffusion-limited aggregations of denatured whey protein isolate colloids. *Biomacromolecules, 6*(6), 3189–3197.
Yamaguchi, S., & Takahashi, C. (1984). Interactions of monosodium glutamate and sodium chloride on saltiness and palatability of a clear soup. *Journal of Food Science, 49*(1), 82–85.
Yoshida, K., Fukushima, Y., & Yamaguchi, T. (2014). A study of alcohol and temperature effects on aggregation of β-lactoglobulin by viscosity and small-angle X-ray scattering measurements. *Journal of Molecular Liquids, 189*(0), 1–8.

APPENDIX B-1 The Matlab code for the image analysis of the porosity

```
% This code works with Matlab R2011b Version 7.0.4.356 R14
% copy the code after %1 until before %2
%1==
close all
clear all
clc
imdir = 'C:\Users\wkuo7\Documents\MATLAB\20141022\';
imfile1 = '7R2R1.tif';
Iori = imread([imdir, imfile1]);
imshow(Iori,'border','tight', 'initialMagnification','fit');title('original image')
Icrp = imcrop(Iori,[1 1 1424 845])
imshow(Icrp,'border','tight', 'initialMagnification','fit');title('cropped image')
%manually remove undesired region
Iply = impoly();
Imk3 = Iply.createMask();
% apply tophat filter to even the background
se = strel('disk',100);
Itop = imtophat(Icrp,se);
% average to smooth the edge of pores
Iavg = wiener2(Itop,[2 2]);
% normalize the grayscale intensity to between 0 & 1
Inml = mat2gray(Iavg)
%normalizing intensity to 0~1
[lehist h]=imhist(Inml);
trithres=triangle_th(lehist,256)
% apply lower threshold to Inml with Imk3 as mask
NHOOD=[0,1,0;1,0,1;0,1,0];
se = strel('arbitrary', NHOOD)
I7 = Inml;
I7(~Imk3) = 0;
x=0:0.1:0.8;
y1=zeros(size(x));%pore number of tophat histogram
y2=zeros(size(x));%upper threshold of constant ratio method on tophat histogram
y3=zeros(size(x));%porosity of constant ratio method
for i=1:length(x)
f = @(z) im2bw(z,x(i));
Imbw = roifilt2(Inml,~Imk3,f);
% use imclose to erode trivial objects
Icls = imclose(Imbw,se);
% apply watershed segmentation to separated conjoint pores
Idst = -bwdist(Icls, 'chessboard');
Iwts =watershed(Idst,8);
Icls(Iwts == 0) = 1;
Ilbl = bwlabel(~Icls, 4);
%apply upper threshold of constant ratio method on tophat histogram
y2(i)=1.25*x(i)
Imk1 = im2bw(Inml,y2(i));
I8=I7
```

```
I8(I7>y2(i))=1
I8(I7<y2(i))=0
% calculate number of labeled pores
[Ilbl, y1(i)] = bwlabel(~Icls, 4)
% calculate porosity
line =bwarea(~Ilbl) -bwarea(Imbw)
y3(i) = bwarea(Ilbl)/(bwarea(Ilbl)+(bwarea(~Ilbl)-bwarea(Imk1)-line-(bwarea(Imk3)-
bwarea(I8))))*100
end
plotyy(h,lehist,x,y1)

% copy the code after %2 until before %3
%2===
% apply lower threshold to Inml with Imk3 as mask
% based on the plot of pore number, select a narrower range which covers the lower
threshold that gives the maximum pore number, replace the 0.0186 with the beginning of the
range, replace the 0.3186 with the end of the range
x=0.0186:0.01:0.3186;
y1=zeros(size(x));%pore number of tophat histogram
y2=zeros(size(x));%upper threshold of constant ratio method on tophat histogram
y3=zeros(size(x));%porosity of constant ratio method
for i=1:length(x)
f = @(z) im2bw(z,x(i));
Imbw = roifilt2(Inml,~Imk3,f);
% use imclose to erode trivial objects
Icls = imclose(Imbw,se);
% apply watershed segmentation to separated conjoint pores
Idst = -bwdist(Icls, 'chessboard');
Iwts =watershed(Idst,8);
Icls(Iwts == 0) = 1;
Ilbl = bwlabel(~Icls, 4);
%apply upper threshold of constant ratio method on tophat histogram
y2(i)=1.25*x(i)
Imk1 = im2bw(Inml,y2(i));
I8=I7
I8(I7>y2(i))=1
I8(I7<y2(i))=0
% calculate number of labeled pores
[Ilbl, y1(i)] = bwlabel(~Icls, 4)
% calculate porosity
line =bwarea(~Ilbl) -bwarea(Imbw)
y3(i) = bwarea(Ilbl)/(bwarea(Ilbl)+(bwarea(~Ilbl)-bwarea(Imk1)-line-(bwarea(Imk3)-
bwarea(I8))))*100
end
x2=x
plotyy(x,y1,x2,y3)
fileID = fopen('exp.txt','w');
```

APPENDIX B-1 (Cont.)

```
for i=1:length(x)
fprintf(fileID,'%4.2f %6.0f %5.2f\r\n',x(i),y1(i),y3(i));
end
fclose(fileID);
% copy the code after %3
%3==
f = @(x) im2bw(x, 0.1786);
Imbw = roifilt2(Inml,~Imk3,f);
% use imclose to erode trivial objects
NHOOD=[0,1,0;1,0,1;0,1,0];
se = strel('arbitrary', NHOOD)
Icls = imclose(Imbw,se);
% apply watershed segmentation to separated conjoint pores
I10=Icls
Idst = -bwdist(I10, 'chessboard');
Iwts=watershed(Idst,8);
I10(Iwts == 0) = 1;
Ilbl = bwlabel(~I10, 4);
% calculate number of labeled pores
[Ilbl, num] = bwlabel(~I10, 4)
line=bwarea(~Ilbl)-bwarea(Imbw)

% apply upper threshold to exclude foreground regions
% put upper threshold to replace the 0.22325
Imk1 = im2bw(Inml, 0.22325);
I7 = Inml;
I7(~Imk3) = 0;
I8=I7
I8(I7>0.22325)=1
I8(I7<0.22325)=0
imshow(I8,'border','tight', 'initialMagnification','fit');title('regions above upper threshold in
manual mask')
% calculate porosity
porosity = bwarea(Ilbl)/(bwarea(Ilbl)+(bwarea(~Ilbl)-bwarea(Imk1)-line-(bwarea(Imk3)-
bwarea(I8))))*100
imshow(Ilbl)
S = regionprops(Ilbl,Inml, 'EquivDiameter')
fileID = fopen('exp.txt','w');
numObj = numel(S);
for k = 1 : numObj
fprintf(fileID,'%4.2f\r\n',S(k).EquivDiameter);
end
fclose(fileID);
```

APPENDIX C-1 The IRB approval letter for the QDA and TI panel

UNIVERSITY OF ILLINOIS
AT URBANA-CHAMPAIGN

Office of the Vice Chancellor for Research

Office for the Protection of Research Subjects
528 East Green Street
Suite 203
Champaign, IL 61820

December 28, 2015

Youngsoo Lee
Food Science & Human Nutrition
1304 W. Pennsylvania Ave.
Urbana, IL 61801

RE: *Quantitative Descriptive Analysis and Time-Intensity Evaluation of Model Dairy Gels*
IRB Protocol Number: 16459

Dear Dr. Lee:

Thank you for submitting the completed IRB application form for your project entitled *Quantitative Descriptive Analysis and Time-Intensity Evaluation of Model Dairy Gels*. Your project was assigned Institutional Review Board (IRB) Protocol Number 16459 and reviewed. It has been determined that the research activities described in this application meet the criteria for exemption at 45CFR46.101(b)(6).

This determination of exemption only applies to the research study as submitted. Please note that additional modifications to your project need to be submitted to the IRB for review and exemption determination or approval before the modifications are initiated.

We appreciate your conscientious adherence to the requirements of human subjects research. If you have any questions about the IRB process, or if you need assistance at any time, please feel free to contact me or the IRB Office, or visit our website at http://www.irb.illinois.edu.

Sincerely,

Dustin L. Yocum, Human Subjects Research Specialist, OPRS

c: Wan-Yuan Kuo

telephone (217) 333-2670 • *fax* (217) 333-0405 • *email* IRB@illinois.edu

APPENDIX C-2 The email sent to recruit panelists for the QDA and TI panel

Sensory evaluations on Model Dairy Gels

You are invited to participate in a sensory evaluation on model dairy gels.

To be eligible to participate you must:

- Be available to attend one screening session (1 hour) anytime during 9 am – 4 pm, January 18 – Wednesday January 20.
- Be available to participate in total of 28 hours as below.

Date		Time
Fri	1/22	12 pm – 1 pm ***AND*** 5 pm - 6 pm
Mon	1/25	
Wed	1/27	
Fri	1/29	
Mon	2/1	
Wed	2/3	
Fri	2/5	
Mon	2/8	Any 1 hour between 11 am – 3 pm
Tues	2/9	
Wed	2/10	Any 2, non-consecutive hours between 11 am – 5 pm
Thurs	2/11	
Fri	2/12	12 pm – 1 pm ***AND*** 5 pm - 6 pm
Mon	2/15	Any 1 hour between 11 am – 3 pm
Tues	2/16	
Weds	2/17	Any 2, non-consecutive hours between 11 am – 5 pm
Thurs	2/18	

- Be willing to taste model dairy gels
- Have no food allergies, sensitivities or intolerance
- Be at least 18 years old

At the completion of the study you will receive $280 for your time.

Please complete the attached questionnaire and send to fshnsensory@gmail.com if you are interested in participating in the study.

Feel free to e-mail fshnsensory@gmail.com if you have any question.

Thank you in advance for considering participating in this test.

APPENDIX C-3 The recruitment questionnaire for the QDA and TI panel

Thank you for your interest in participating in this study. To identify if you qualify for the study please provide answers to the following questions. If you have met qualifications for the study, you will be contacted with a testing schedule based on your listed availability. Your answers to these questions will be confidential and will be seen only by the researchers.

Name: _____ Email Address: _____ Cell Phone Number: _____

1. **Do any of the following apply to you?**
   Follow a restricted diet for medical or personal reasons ☐ YES ☐ NO
   Food or beverage allergies/sensitivities/intolerance ☐ YES ☐ NO
2. **Are you at least 18 years old?** ☐ YES ☐ NO
3. **Check *ALL times that you are available***

Screening

- **Must be available at least for one hour in the following time slots**
- ***Individuals with more availabilities are at higher recruiting priority***

	Mon 1/18	Tues 1/19	Wed1/20
9-10a			
10-11a			
11-12a			
12-1p			
1-2p			
2-3p			
3-4p			

Formal panel

- **A: Must be available for all the time slots**
- **B: Must be available for at least 1 hours on each day**
- **C: Must be available for at least two, non-consecutive hours on each day**
- ***Individuals with more availabilities are at higher recruiting priority***

	January				February											
	F 22	M 25	W 27	F 29	M 1	W 3	F 5	M 8	T 9	W 10	R 11	F 12	M 15	T 16	W 17	R 18
11a-12p								B	B	C	C		C	C	C	C
12p- 1p	**A**	**A**	**A**	**A**	**A**	**A**	**A**	B	B	C	C		C	C	C	C
1p- 2p								B	B	C	C		C	C	C	C
2p- 3p								B	B	C	C		C	C	C	C
3p- 4p										C	C				C	C
4p- 5p										C	C				C	C
5p- 6p	**A**	**A**	**A**	**A**	**A**	**A**	**A**									

Please send the survey to fshnsensory@gmail.com

Thank you for taking our survey! Your response is very important to us.

APPENDIX C-4 The screening ballot for the QDA and TI panel

SENSORY EVALUATION ON MODEL DAIRY GELS

SCREENING SESSION
20160118-20

FULL NAME: _____

1. TASTE IDENTIFICATION

1. Rinse your mouth with water before you begin.
2. Take a sip of the sample into your mouth and move it around so it touches all parts of your tongue. ***Do not swallow the sample***; expectorate it into the provided spit cup.
3. Write which of the basic tastes (sweet, salty, sour, bitter, umami or none) you perceive in the sample on the corresponding blank. If you are unsure of the identification, write a "?" after the basic taste name (e.g. "sweet?"). Re-tasting is allowed.
4. Rinse your mouth with water before tasting the next sample.

Sample	Basic Taste	Sample	Basic Taste
735	_____	445	_____
496	_____	704	_____
901	_____		

2. SALTINESS RANKING

1. Rinse your mouth with water before you begin.
2. ***Take the entire shot of the sample*** into your mouth and move it around so it touches all parts of your tongue. ***Do not swallow the sample***; expectorate it into the provided spit cup.
3. Rinse your mouth with water before tasting the next sample.
4. From the two samples, circle the one that tastes saltier. If the saltiness taste the same, write "SAME" after the numbers

Comparison 1: **990 vs 338**

Comparison 2: **732 vs. 382**

Comparison 3: **614 vs. 026**

APPENDIX C-4 (Cont.)

3. DESCRIPTION OF SENSORY TEXTURE TERMS

Find the best description for the following terms

Terms	*Descriptions*
1. Chewiness	_____
2. Creamy	_____
3. Fracturability (Brittleness)	_____
4. Mealy (Grainy)	_____
5. Slimy	_____
6. Soggy	_____

Choice of descriptions:

A. A combination of gumminess and springiness, this is the amount of effort that goes into preparing a solid product for swallowing.
B. Saturated with moisture, heavy and wet, sodden or soaked
C. The sensation of slipperiness on the surfaces of the mouth.
D. The presence of thick, smooth liquid in the mouth.
E. A food's ability to crack or crumble, opposite of cohesiveness.
F. Presence of components of different degrees of firmness or toughness.

You have completed the screening test.

An email will be sent to you soon to notify if you are qualified to participate the panel or not.

Thank you very much!

APPENDIX C-5 The informed consent statement for the QDA and TI panel

INFORMED CONSENT FORM FOR SENSORY EVALUATION PANELISTS

"Time-Intensity Testing on Model Dairy Gels"

You are invited to participate in a study involving descriptive analysis of model dairy gels. The goal of this research is to determine the sensory properties of different model dairy gels. The results will be used to study how to enhance the qualities dairy products. All gels will be tasted and expectorated by the panelists. Panelists will be evaluating the samples with the given software and the results will show the sensory properties in different attributes of the samples.

A complete list of ingredients is available for review. If you have food allergies you should not participate in this study. The University of Illinois does not provide medical or hospitalization insurance coverage for participants in this research study nor will the University of Illinois provide compensation for any injury sustained as a result of participation in this research study, except as required by law. You are free to withdraw from the study at any time for any reason and it will have no effect on your grades at, status at, or future relations with the University of Illinois. The experimenter(s) also reserve the right to terminate the participation of an individual subject at any time when: the subjects were late or missed their scheduled time and could not make up the tests, and (or) the subjects were not willing to comply with the instructions of sample tasting and rating procedure.

You will be participating in 28, 1-hour sessions (2 sessions/day). Upon completion of the study, you will be compensated with $280. You are free to withdraw at any time during the course of the study. If you do not complete the study, you will be compensated for your time at a rate of $10/hour.

Your participation in this study is generally confidential*. The researchers will keep the responses confidential, and any publications or presentations of the results of the research will only include information about group performance. Data gathered from the entire project will be summarized in the aggregate, excluding references to any individual responses. Photos of the panelists participating in this research may be taken and used in oral presentations, in order to give information about the experiment procedure. Names of panelists will not be associated with the photos. Panelists may opt for not having their photographs taken and this option will be included on the consent form. The aggregated results of our analysis will be for journal articles and conference presentations.

APPENDIX C-5 (Cont.)

*The followings state the confidentiality of your participation in further details.

Will my study-related information be kept confidential?
Yes, but not always. In general, we will not tell anyone any information about you. When this research is discussed or published, no one will know that you were in the study. However, laws and university rules might require us to tell certain people about you. For example, your records from this research may be seen or copied by the following people or groups:

- Representatives of the university committee and office that reviews and approves research studies, the Institutional Review Board (IRB) and Office for Protection of Research Subjects;
- Other representatives of the state and university responsible for ethical, regulatory, or financial oversight of research;
- Federal government regulatory agencies such as the Office of Human Research Protections in the Department of Health and Human Services;
- The financial sponsor of the research, USDA

We will ask everyone in the group discussion to respect the privacy of other participants and to treat anything said in the group as confidential. However, please remember there is no guarantee that other participants will cooperate.

You are encouraged to ask any questions about this study before, during, or after your participation. However, specific questions about the samples that could influence the outcome of the study will be deferred to the end of the experiment. Questions can be addressed to Dr. Youngsoo Lee (217-333-9335, leeys@illinois.edu) or Wan-Yuan Kuo (217-898-5128, wkuo7@illinois.edu). You may also contact the IRB Office (217-333-2670, irb@illinois.edu) for any questions about the rights of research subjects or if you have any concerns or complaints.

I understand the above information and voluntarily consent to participate in the study described above.

☐ YES ☐ NO I have been offered a copy of this consent form.

☐ YES ☐ NO I am 18 years of age or older.

☐ YES ☐ NO I agree to have photographs taken of me while participating in this research.

Signature Date

Print Name

APPENDIX C-6 The detailed procedure for the QDA and TI panel

Appendix C-7 summarizes the daily procedure for the QDA and TI panel. Each session was one hour.

QDA panel

Term generation (Session 1-6, day 1-3)

Initial term generation (Sessions 1 and 2, day 1)

In the first session of the QDA panel, the panelists read and signed the consent forms. After the self-introduction of each panelist, a brief introduction to sensory science and QDA method was presented. Afterward, the panelists were instructed to rinse with carbonated, warm and room temperature water. During the sample evaluation, the panelists were instructed to chew the sample cubes naturally, and report the time of chewing to the panel. The average chewing time for each sample was immediately calculated. The panelists were asked to adjust their chewing times to be within ± 3 seconds from the group averages. They were reminded to expectorate all samples and rinses throughout the QDA panel. The term generation was run by each modality. For each modality after evaluating each sample, the panelists wrote down on a term-generation sheet the terms to describe the sensory characteristics of the sample. They were also encouraged to provide reference products for the terms. Then the panelists took turns to share the terms and references they generated. Although focusing on one modality at a time, the panelists were encouraged to provide at any time the additional terms for the modalities that had been run before. A compiled list of 47 terms and 69 references was made at the end of the initial-term-generation session (Appendix C-8). The panelists evaluated 6 samples per session, and each sample was presented at least twice throughout the term generation.

Reference refinement (Sessions 3 and 4, day 2)

The reference refinement was run by each modality. When evaluating each sample, the panelists continued to practice the chewing times to be within ± 3 seconds from the group averages. The panelists also discussed and agreed that the rinsing protocol was sufficient. A list of terms and reference generated from the initial-term-generation session was provided to each panelist. They were encouraged to narrow down the number of terms to 20-30. The panelists followed the list to evaluate the references. Then for each sample, they identified the attributes in the list that they perceived. Afterward, they discussed whether the references represented well the corresponding attributes. They also discussed whether the terms were relatively important to describe and differentiate the samples. For the terms that they agreed to be important, they were instructed to provide definitions and indicate whether the portion size of the reference was appropriate to represent the sample intensity. They were also encouraged to provide new terms and references to sufficiently describe the differences between the samples. At the end of the reference-refinement-session, a list including 23 terms with corresponding references and definitions was generated at the consensus of the panel. A range of the concentration or the portion size was also given for each reference based on the panel recommendation.

Term finalization (Sessions 5 and 6, day 3)

The term finalization was run by each modality. The panelists continued to practice the chewing times to be within ± 3 seconds from the group averages. A list of terms with corresponding references and definitions was given to each panelist. For each term, the panelists first discussed the evaluation protocol. For example, they specified that the

aftertastes of the samples after spitting out should be compared to the perception of the references in the mouth. They also clarify the evaluation standards for each term. For example, the salty taste is the maximum saltiness perceived throughout the chewing. For each reference, 2-3 different portion size or concentrations were provided. The panelists evaluated the samples and exchanged their findings on the attributes perceived. Then they evaluated the references and discussed the appropriate concentration or portion size of the reference that fell within the intensity range of the samples. They were also encouraged to refine and compare the definitions of the terms to avoid redundancy of the terms used. By the end of the term-finalization sessions, a concise list of 21 terms was generated at the consensus of the panelists. For each term on the list, the reference was listed with specified range of the concentration or portion size, and clear definitions, evaluation protocols and standards were given.

Group scoring (Sessions 7-15, days 4-8)

The group scoring was run initially by each modality. In the last three sessions, the group scoring was run by all modalities for each sample. The panelists continued to practice the chewing time and by the end of the group-scoring sessions, all panelists had their chewing times within ± 3 seconds from the group averages. A list of reference including the term, the reference concentration or portion size, the definition and the evaluating protocol and standards was given to each panelist. For each reference, 2 different concentrations or portion sizes were presented to the panelists. The concentrations or portion sizes were chosen based on the panelists' feedback from the reference-refinement sessions. The panelists first reviewed the reference list to refresh themselves with the evaluating protocols and term definitions. For each term, the panelists identified through discussion the sample with the strongest perception. The panelists then selected the appropriate concentrations or portion sizes of the reference so that the reference perception was within the range of sample perception. With the strongest sample being the score of 15 and no perception being the score of 0, the panelists rated the score of the selected reference. The group average of the reference was calculated immediately. Afterward, the panelists practiced rating the other samples based on the anchors of the strongest sample and the reference. The panelists then calibrated their ratings based on the group average. Additional samples and references were available to the panelists who wanted to re-taste. For the salty taste, a lower concentration of NaCl (0.3% w/v) was used as the anchor of score 4, in addition to the 0.4% NaCl (score 10.2). Also, the panelists were instructed to disregard the concept of "zero-salty perception being score 0". This was made to maximize the differences of salty taste between the samples, and to fully utilize the scale. In the last three sessions, the panelists practiced evaluating the aroma, aroma-by-mouth, and taste from chewing one same cube of the sample. Then the panelists evaluated the texture and aftertaste from chewing another cube of the sample. Appendix C-9 listed the preparation and evaluation details of the references.

Booth practice (Session 16, day 9)

A reference tray and a list with the term definitions, the reference scores, evaluating protocols and standards were provided for each panelist. Extra references were provided when the panelists requested to re-taste the references. Before entering the booth, the panelists were instructed to review the reference list and to re-familiarize with all the references. Afterward, the panelists entered the booth and evaluated the samples. Eight samples (four samples * 2

replicates) were presented to the panelists in each session. Each replicate contained two cubes stored in separated 1-oz cups. The panelists took the first cube and evaluated the aroma, aroma-by-mouth, and taste. Then the panelist took the second cube and evaluated texture and aftertaste. The panelists were informed that they can leave the booth to re-familiarize with the references whenever needed. A sample screen shot of the booth program was given in Appendix C-10.

Booth testing (Session 17-20, days 10 and 11)

Before entering the booths, the panelists were instructed to review and re-familiarize with the all the references. They were also instructed to review the result of the booth practice and calibrate their individual ratings with the group average. The booth setup, computer program and sample presentation in each session of the booth testing were the same as the booth practice. The panelists attended two sessions per day, and after the first session, each panelist waited for at least one hour to start the second session. The panelists were encouraged to re-familiarize with the references before entering the booth for the second session. Eight samples were made each day and the panelists evaluated four samples (each duplicated) per session. The order to which the panelists were assigned to the two sessions was random. The booth testing was run for 7 hours on each day.

TI panel

Group training (Sessions 21 and 22, day 12)

In the first session of the TI group training, the concept of TI evaluation and the procedure to operate the recording hardware was presented to the panelists. The difference between the QDA salty and TI salty was clarified. The major difference is that the QDA only evaluated the peak saltiness as the salty while the TI evaluated the saltiness throughout the chewing process. Also, in QDA, the panelists disregarded the concept of "no salty perception being the score of zero". In TI, the zero second which was the moment right before putting the sample in the mouth corresponded to "no salty perception", and thus scored zero. The rinsing protocol in between samples and references was the same as in the QDA. The panelists then evaluated the sample with the highest QDA salty score and were instructed to register the peak saltiness of this sample to be the score of 15 on a linear scale from 0 to 15. Then the panelists were informed to find out appropriate NaCl concentrations that can be the references of low, medium, and medium-high salty perception compared to the peak intensity of the saltiest sample. They evaluated and chose three from four NaCl solutions to be the appropriate references. Then they rate the scores of the three NaCl solutions. The scores of the three NaCl references, 0.2, 0.4 and 0.6% (w/v) were 3.5, 10 and 13.5, respectively. They were instructed to register the saltiness perception of the three references solutions. Afterward, the panelists practice rating the saltiness during chewing of the samples by writing down on paper the saltiness score every 5 seconds. A metronome was used to alert the panelist to rate every 5 seconds. At 25 second the panelists were orally informed to have the spit cup in hand, and at 30 second they were orally informed to spit out while continuing on the rating. The rating lasted for 90 seconds from putting the sample in the mouth. This rating duration was determined by the panelist who took the longest time for the saltiness perception to reach zero for different samples. The panelists were asked not to exchange their rating results.

APPENDIX C-6 (Cont.)

In the second session of the TI group training, a review of the TI rating procedure was presented. The following clarifications were made: the panelists should rate greater saltiness if they perceived increased saltiness after spitting out, the panelist should act normal but consistent as to whether to swallow their saliva after spitting out. The panelists re-tasted the three references and the sample with the highest salty score. They were presented with a linear scale with the references and the saltiest sample anchored at their corresponding scores. In this session, the panelists were informed to be consistent in rating the same samples while being differentiating different samples by their own ratings. They were only asked to calibrate their peak intensity with the averaged peak intensity from the group. They were asked not to exchange their rating results beyond the peak intensity.

Booth practice (Sessions 23 and 24, days 13 and 14)

Before staring the sample evaluation in the booth, the computer screen asked the panelists to re-familiarize with the three NaCl references. The computer screen showed the linear scale with the anchors of the references solutions and the peak saltiness of the saltiest sample. The panelist followed the instructions shown on the computer screen to evaluate the samples (Appendix C-11). The panelists placed the sample in the mouth and click "Start" at the same time. They immediately started chewing while dragging the mouth momentarily to indicate the saltiness. The messages of "Get ready to expectorated" and "Expectorate and continue on rating" appear on the screen during 25-30 and 30-90 seconds, respectively. After 90 seconds the screen instructed the panelists to rinse. Eight cubes (four samples with duplicated ratings), separately stored and labeled in eight cups were presented in one session. Two minutes of waiting were enforced in between the samples.

In the second booth practice in the next day, each panelist was given their own results of TI curves from the first booth practice. Each panelist was informed whether his or her ratings were consistent within the same samples and differentiating different samples. They were also asked to calibrate the peak intensity of their own ratings with the group averages. Then the panelists proceeded to operate the computer program with the same instructions as the first booth practice.

Booth testing (Sessions 25 – 28, days 15 and 16)

The procedure of the booth testing was the same as in the booth practice. Before starting the booth testing, the panelists were given the TI curves of their own rating results from the booth practices and explained whether they improved in the consistency and the ability to differentiate the samples. They were again asked to calibrate the peak intensity of their own ratings with the group averages. For each day, the panelists attended two sessions with at least one hour apart.

APPENDIX C-7 The summarized daily procedure of the QDA and TI panel

Day	Session (1 h)	Activity (total hours)		Modality or attribute focused	Choice of sample	Sample / session
1	1	QDA term generation (6)	Initial (2)	Aroma/Aroma-by-mouth/Taste	Each sample presented at least twice	6
	2			Aftertaste /Texture		
2	3		Refine (2)	Aroma/Aroma-by-mouth/Taste		
	4			Aftertaste /Texture		
3	5		Finalize (2)	Aroma/Aroma-by-mouth/Taste		
	6			Aftertaste /Texture		
4	7	QDA group scoring (9)		Aroma/Aroma-by-mouth	Strongest and weakest samples for each attribute, identified during term generations	6-8
	8					
5	9			Texture		
	10					
6	11			Taste/aftertaste		
	12					
7	13			All	Each sample presented twice	8 (4*2 rep)
	14					
8	15					
9	16	QDA booth practice (1)		All		
10	17	QDA Actual test (4)		All	Duplicate ratings/ sample	
	18					
11	19					
	20					
12	21	TI training (4)	Group (2)	Saltiness	Each sample presented twice	8 (4*2 rep)
	22					
13	23		Booth (2)			
14	24					
15	25	TI actual test (4)		Saltiness	Duplicate ratings/ sample	
	26					
16	27					
	28					

APPENDIX C-8 The compiled list of terms and reference after the initial-term-generation session

Modality	Attribute	Reference
Aroma	Sweet vanilla	Vanilla extract Vanilla pudding
	Fermented dairy	Plain yogurt
	Cream cheese	Cream cheese
	Sour yogurt	Plain Greek yogurt
	Milk	Whole milk
	Eggs	Hardboiled egg
	Soybean milk (rancid)	Soybean milk
	Pungent/musty	Blue cheese Parmesan Gorgonzola
	Chlorine	Dilute oxi-clean
	Moist	Fresh cheese
	Cooked corn	Cooked corn
	Oxidized oil	Crisco Cooked neutral oil
	Mild cheddar	White cheddar
	Buttery	Butter
	Coconut	Coconut oil Unsweetened coconut flakes
Aroma-by-mouth	Dairy	Plain regular yogurt Cream cheese Sour cream
	Aged milk	Buttermilk
	Sour cream	Sour cream
	Cheesy	Mozzarella string cheese
Taste	Sour	Lactic acid solution
	Salty	NaCl solution
Aftertaste	Grainy	Firm tofu Ricotta cheese
	Coating	Greek yogurt Plain yogurt
	Slippery	Almond milk Coconut oil Coconut milk
	Creamy	Cream
	Salty	NaCl solution
	Plastic aroma	Water in plastic cup
	Crumbly Jell-O	Tapioca pudding Rice pudding
	Aged milk	Butter milk
	Metallic	Iron tablets

APPENDIX C-8 (Cont.)

Modality	Attribute	Reference
Texture	Rubbery	Overcooked calamari Off-brand gummy bears
	Squeaky	Fresh cheese curds Pickle spears
	Spongy	Re-thawed frozen tofu Angel food cake
	Tough	Pineapple core Asparagus ends
	Gelatinous	Jell-O
	Grainy/mealy/gritty	Grits Ricotta cheese
	Slippery	Fresh mozzarella balls
	Foamy	Milk froth
	Soft crumbly	Cake base with digestive cookie
	Rubbery outside	Staled tofu
	Fracturable	Firm tofu Gluten-free bread
	Crumbly	Feta cheese
	Porous	Frozen tofu
	Creamy	Pudding Spreadable cheese
	Adhesive	Mochi Milk powder
	Dry	Overcooked chicken breast
	Syneresis	Tres leches Brownies soaked in milk Gulab jamun

APPENDIX C-9 The preparation and evaluation details for the QDA references

Modality	Attribute	Reference	Reference Size	Reference source/preparation	Evaluating protocol
Aroma	Sweet milk	Condensed milk	5 g/ 1 oz. cup	Sweetened Condensed Milk (Eagle Brand, Gahanna, OH)	Sniff from the little openings of the cup
	Mild cheddar	Mild Cheddar	0.1 g/ 5 oz. cup	Natural Cheese Shredded Mild Cheddar Cheese (Kraft Foods, Champaign, IL)	
	Pungent	Parmesan	0.01 g/ 5 oz. cup	Kraft Natural Shredded Cheese Finely Shredded Italian Parmesan	
	Buttery	Butter	0.1 g/ 5 oz. cup	Unsalted Butter (Land O Lakes, Arden Hills, MN)	
	Oxidized oil	Oxidized oil	.005 g/ 5 oz. cup	Pure Vegetable Oil (Crisco, Orrville, Ohio), 1/3 cup microwaved for 6 min	
	Egg	Egg	1/256 egg/ 5 oz. cup	Hardboiled egg, weigh 0.008 g of egg yolk and 0.085 g of egg white	
Aroma-by-mouth	Sour cream	Sour cream	One flat spoon	Arbor Home Mini Food Grade Plastic Coffee Tea Beverage Stirrers Spoon	Compare to the entire servings of the references chewed
	Cheesy	Mozzarella string cheese	1 slice (1 g)	Kraft Mozzarella String Cheese	
Taste	Salty	0.4% NaCl	0.4% (w/v), 5mL	NaCl Granular/USP/FCC (Fisher Chemical, Hampton, NH)	Take entire shot of the references
		0.3% NaCl	0.3% (w/v), 5mL		
	Sour	0.01% Lactic acid	0.01% (w/v), 5 mL	Lactic acid, Adventures in Homebrewing (Ann Arbor, MI)	

APPENDIX C-9 (Cont.)

Modality	Attribute	Reference	Reference Size	Reference source/preparation	Evaluating protocol
Aftertaste	Grainy	Firm tofu	2 g slice	Premium Tofu Firm (House Foods, Garden Grove, CA)	Compared to the entire servings of the references on the tongue (after chewing if necessary)
	Slippery	Almond milk	1 g	Almond Breeze, Unsweetened Original (Blue Diamond Growers, Sacramento, CA)	
	Astringent	Greek yogurt	One flat spoon	Arbor Home Mini Food Grade Plastic Coffee Tea Beverage Stirrers Spoon, Traditional Plain Greek Yogurt (Greek Gods, Seattle, WA)	
	Salty	0.3% NaCl	0.3 % (w/v), 5mL	NaCl Granular/USP/FCC (Fisher Chemical)	
Texture	Fracturable	Firm tofu	5 g cube	Premium Tofu Firm (House Foods)	First bite
	Crumbly	Feta cheese	5 g cube	Athenos Feta Cheese Chunk Traditional (Kraft Foods)	Evaluate the overall property throughout the chewing of the entire pieces of the references
	Gelatinous	Jell-O	5 g cube	Jell-O: Orange Gelatin Dessert (Kraft Foods), 5/4 cup boiling water poured into 88 g powder, stir till dissolved, pour into 5 oz. cups, refrigerated overnight)	
	Gritty	Grits	5 g	Quick-5 Minute Grits (Quaker, Chicago, IL), mix 3/4 cup water and 1/4 cup grits, microwave at high for 3 min	
	Fibrous	Pineapple core	1 cm thick, half disc	Freshly cut and given by County Market (Champaign, IL)	
	Syneresis	Fresh mozzarella balls	1 ball	Fresh Mozzarella Fresca Pearls (Galbani, Buffalo, NY)	
	Squeaky	Exploded egg	One 2.5 g piece	Four egg white microwaved for 4 min, refrigerated overnight	

APPENDIX C-10 The sample screen shots of the booth program for the QDA

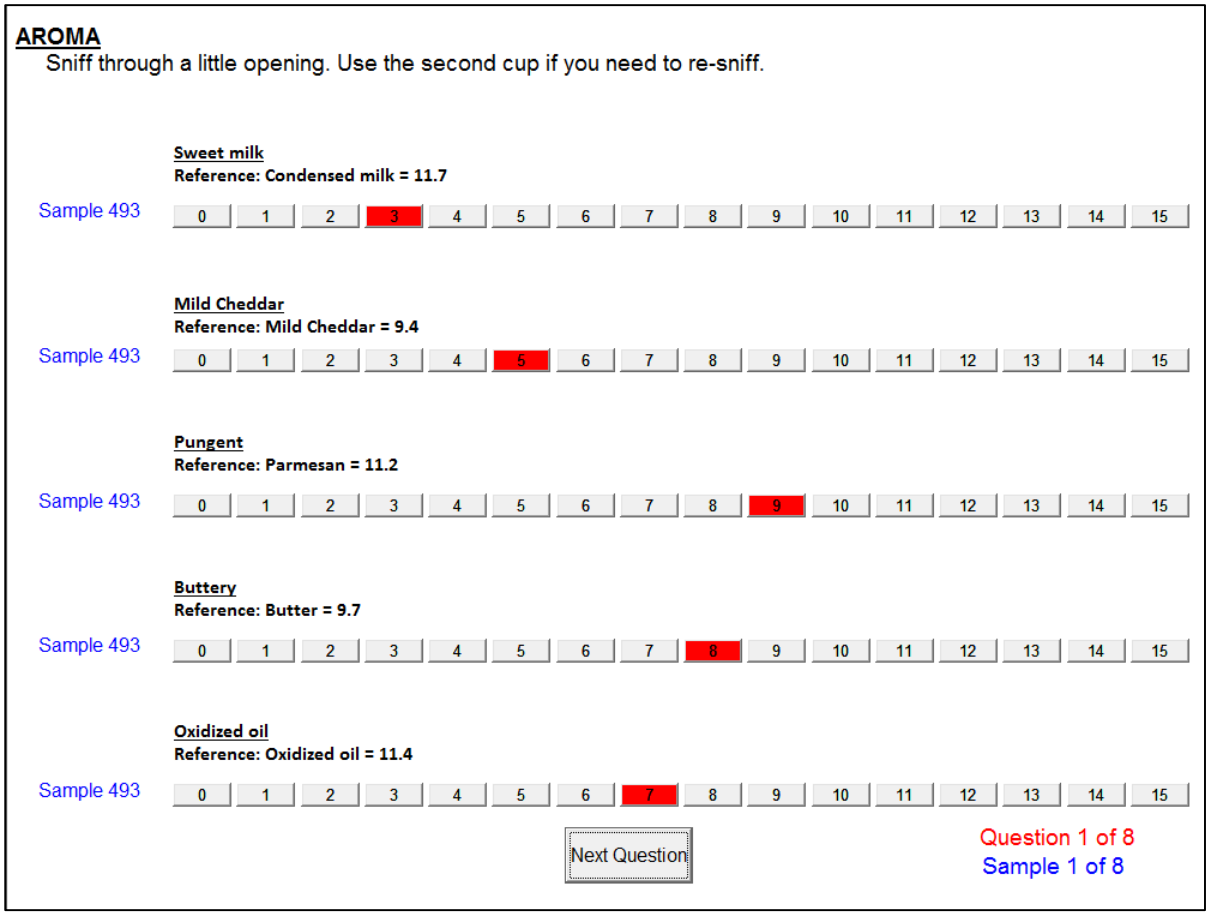

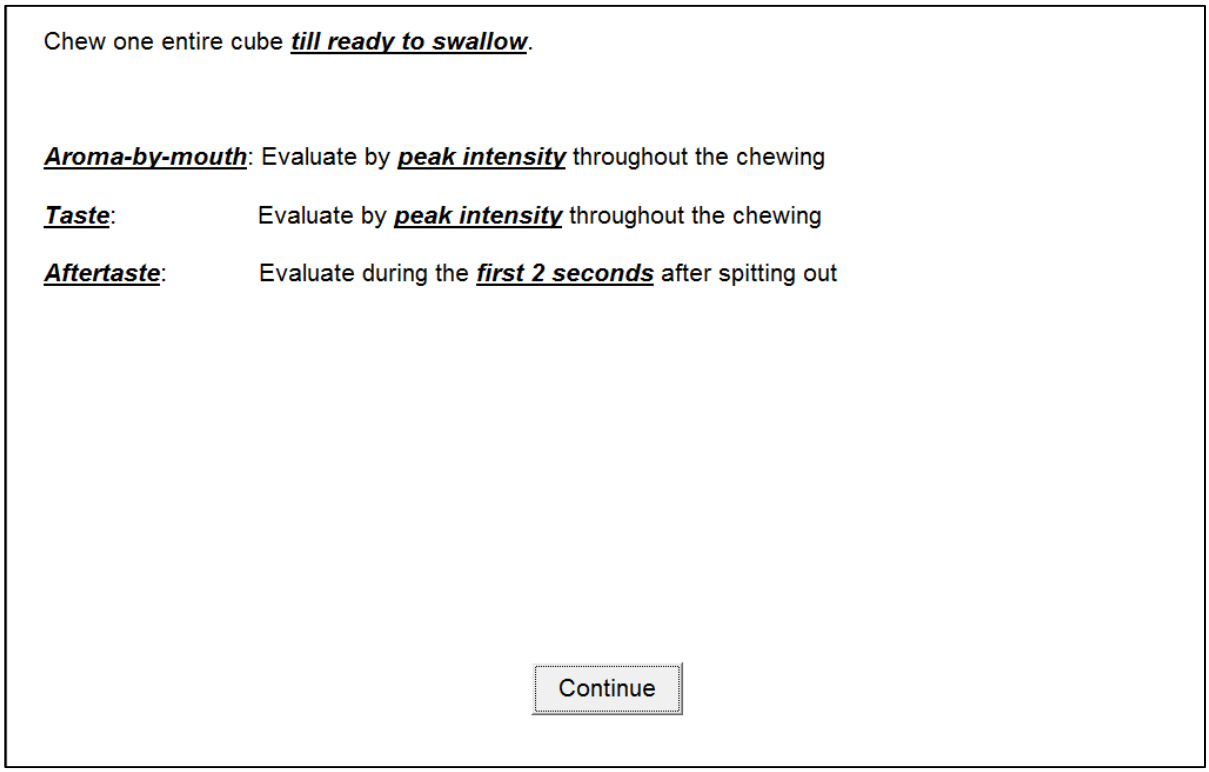

APPENDIX C-10 (cont.)

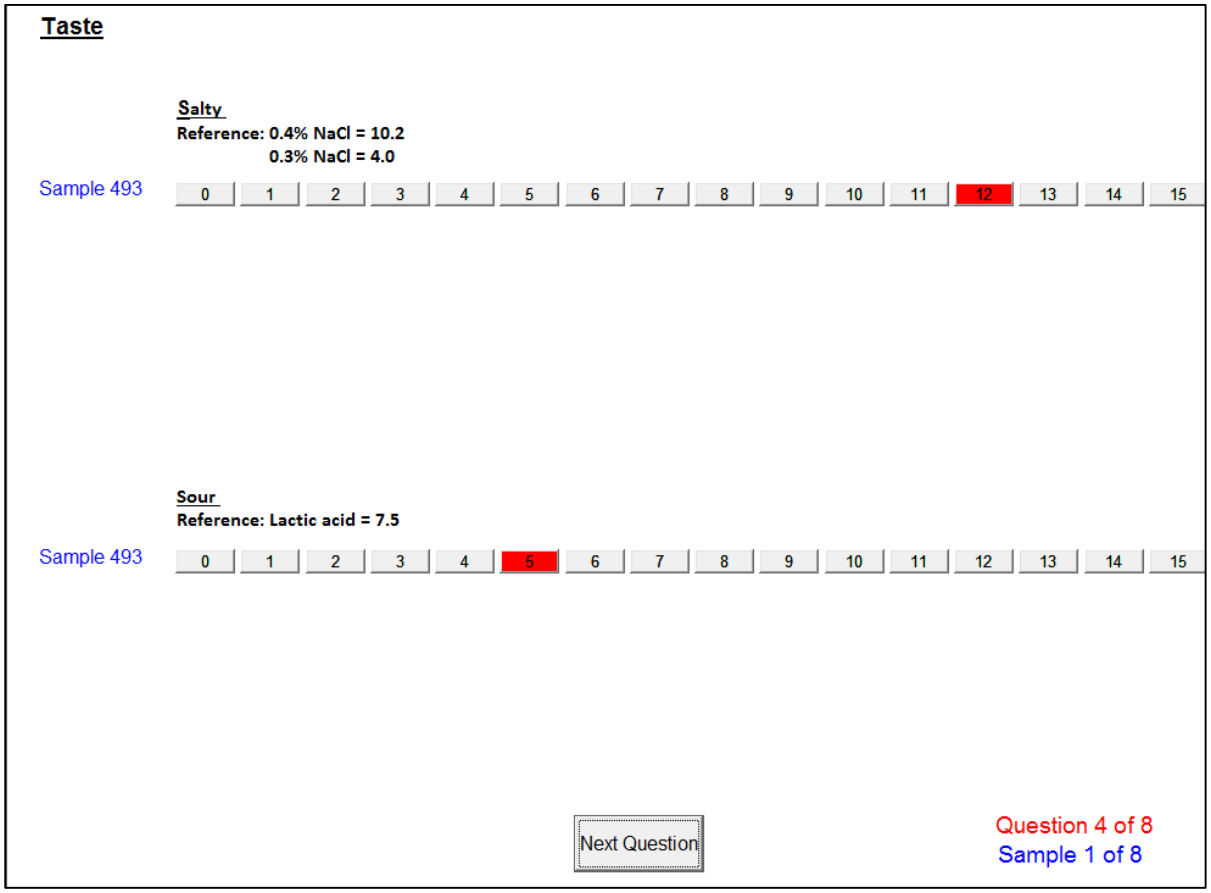

APPENDIX C-10 (cont.)

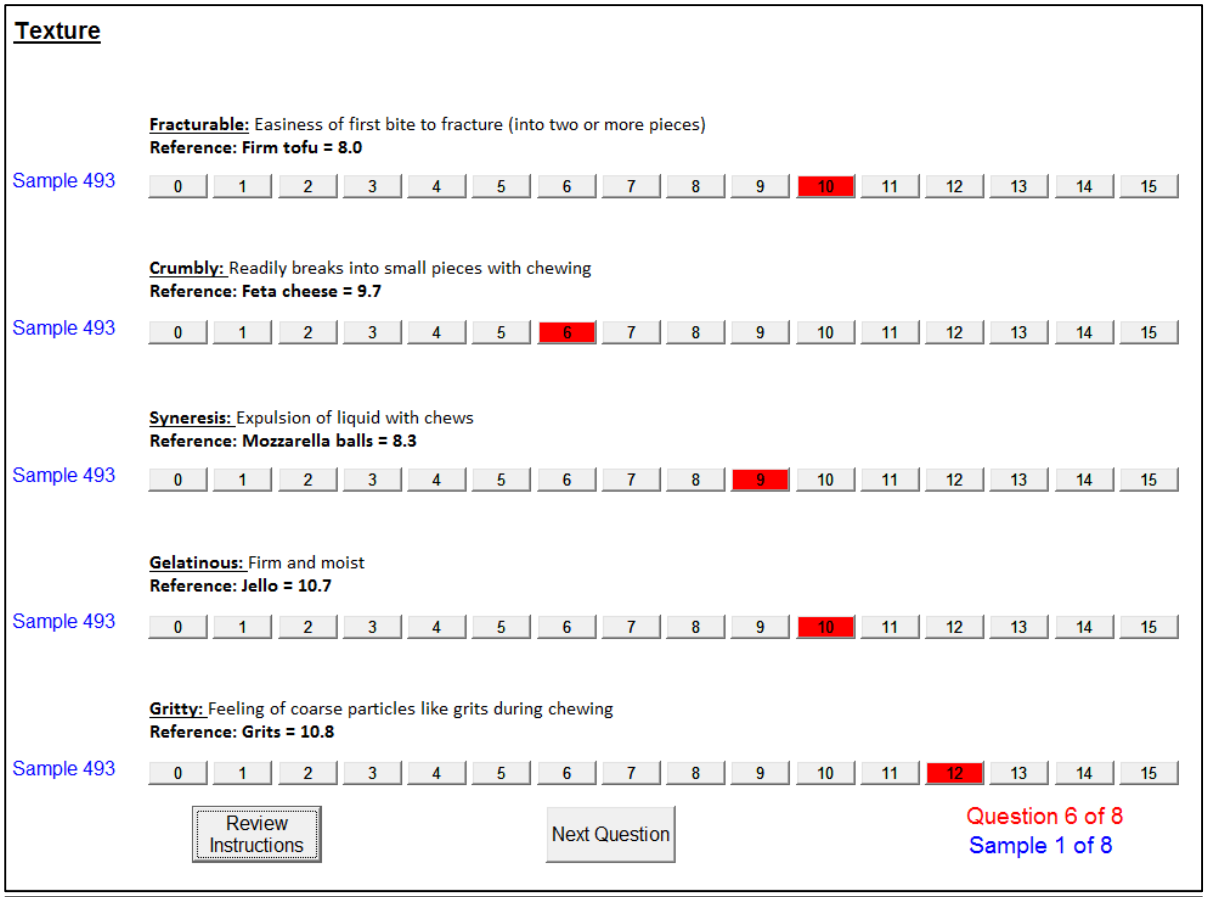

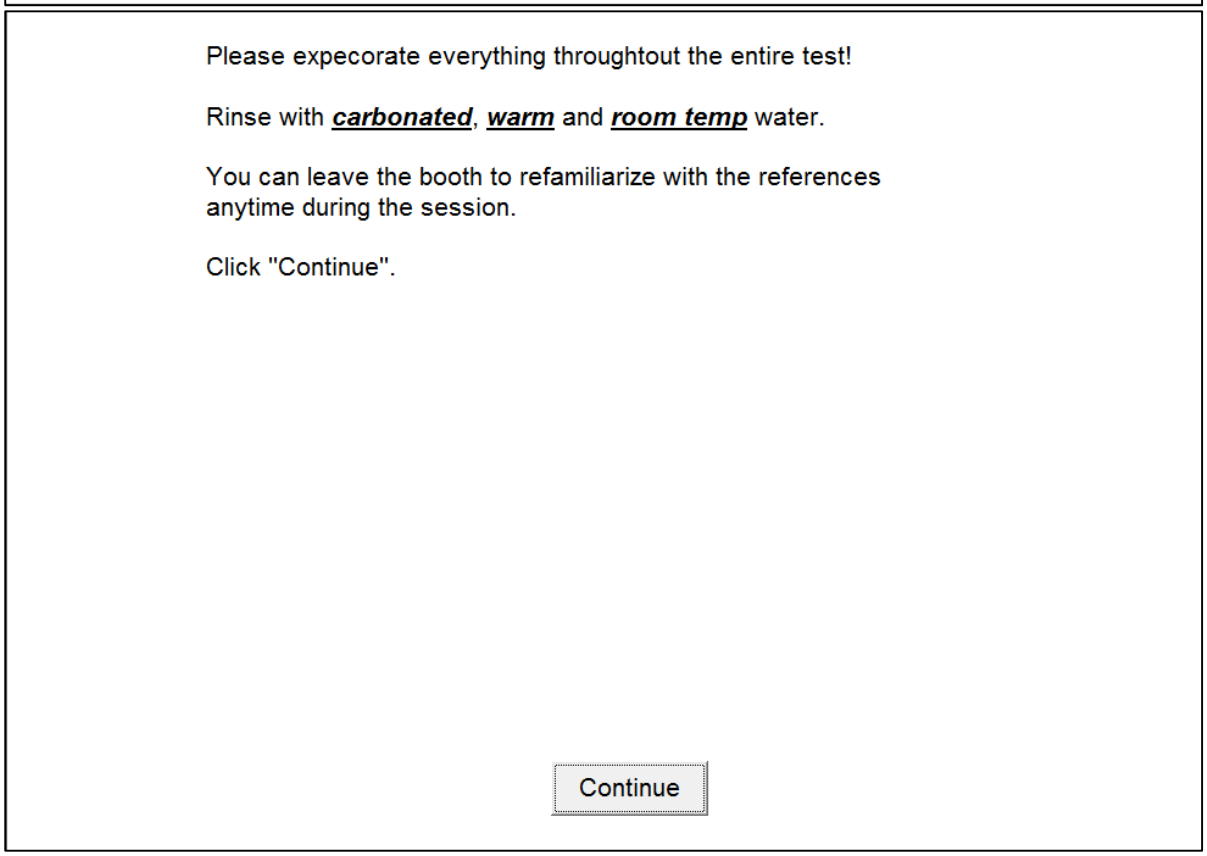

APPENDIX C-11 The sample screen shots of the booth program for the TI evaluation

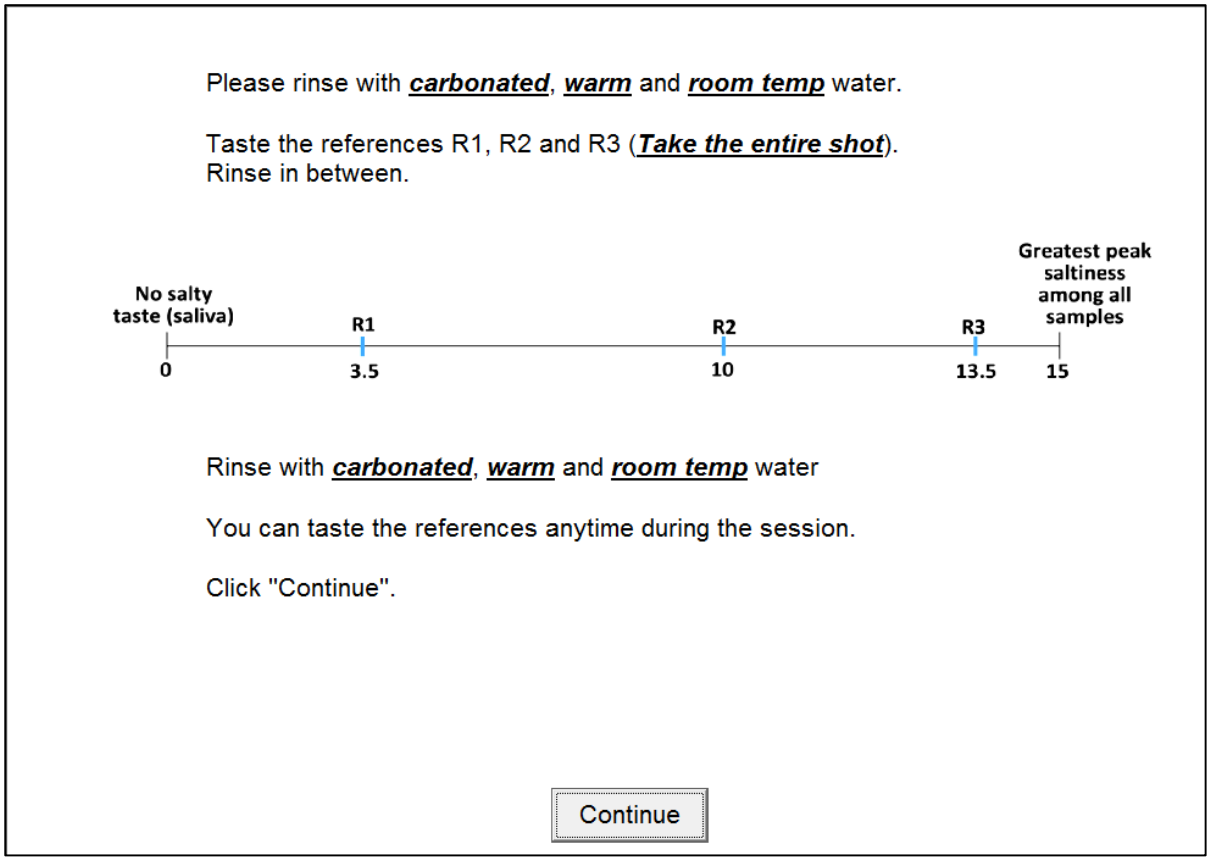

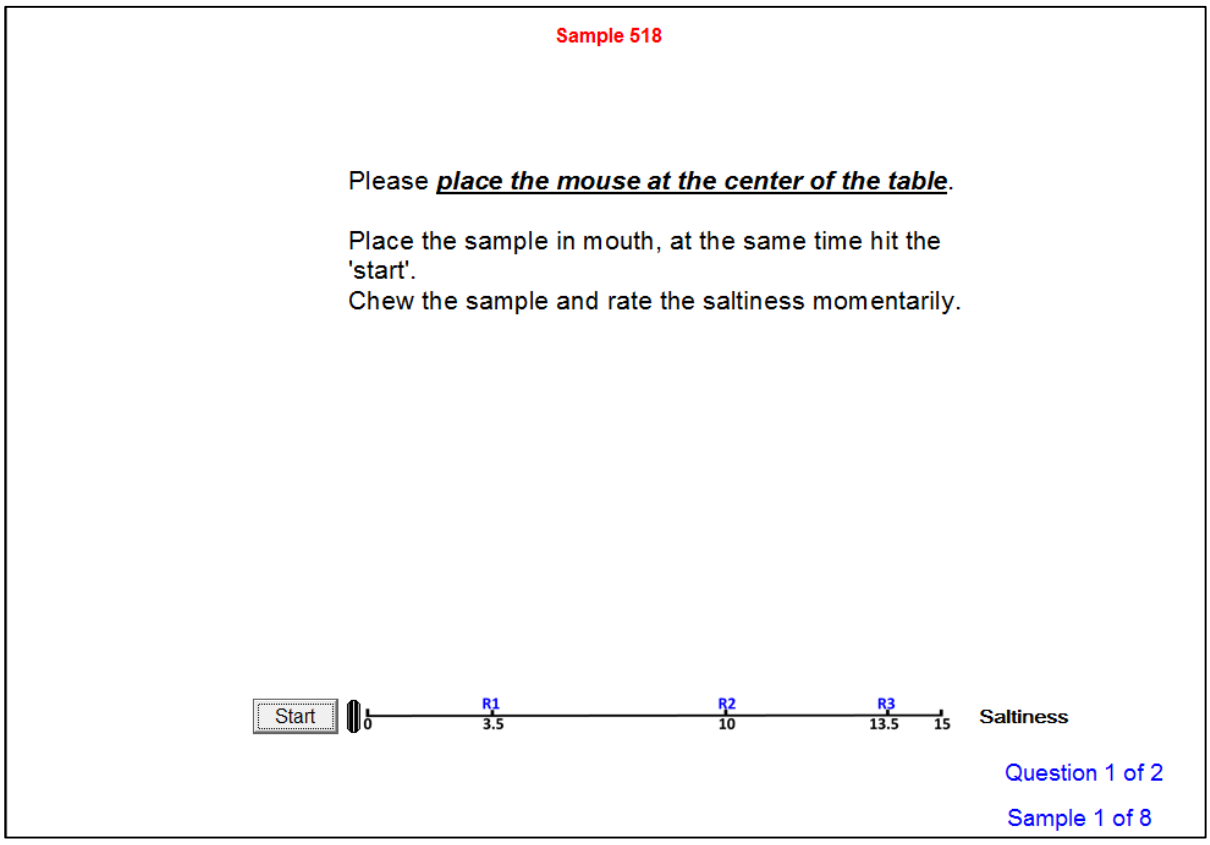

APPENDIX C-11 (cont.)

Sample 518

00:08

Please ***place the mouse at the center of the table***.

Place the sample in mouth, at the same time hit the 'start'.
Chew the sample and rate the saltiness momentarily.

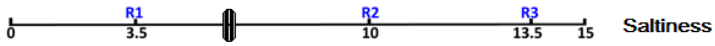

Question 1 of 2

Sample 1 of 8

Sample 052

00:25

Please ***place the mouse at the center of the table***.

Place the sample in mouth, at the same time hit the 'start'.
Chew the sample and rate the saltiness momentarily.

Get ready to expectorate

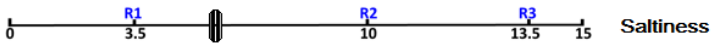

Question 1 of 2

Sample 2 of 8

APPENDIX C-11 (cont.)